



2013

## MODELING BEDROCK MINING HOTSPOTS WITHIN THE OUACHITA NATIONAL FOREST, ARKANSAS

Stephanie H. Mehlhope  
*University of Kentucky*, [smhouc2@uky.edu](mailto:smhouc2@uky.edu)

[Right click to open a feedback form in a new tab to let us know how this document benefits you.](#)

---

### Recommended Citation

Mehlhope, Stephanie H., "MODELING BEDROCK MINING HOTSPOTS WITHIN THE OUACHITA NATIONAL FOREST, ARKANSAS" (2013). *Theses and Dissertations--Geography*. 3.  
[https://uknowledge.uky.edu/geography\\_etds/3](https://uknowledge.uky.edu/geography_etds/3)

This Master's Thesis is brought to you for free and open access by the Geography at UKnowledge. It has been accepted for inclusion in Theses and Dissertations--Geography by an authorized administrator of UKnowledge. For more information, please contact [UKnowledge@lsv.uky.edu](mailto:UKnowledge@lsv.uky.edu).

## **STUDENT AGREEMENT:**

I represent that my thesis or dissertation and abstract are my original work. Proper attribution has been given to all outside sources. I understand that I am solely responsible for obtaining any needed copyright permissions. I have obtained and attached hereto needed written permission statements(s) from the owner(s) of each third-party copyrighted matter to be included in my work, allowing electronic distribution (if such use is not permitted by the fair use doctrine).

I hereby grant to The University of Kentucky and its agents the non-exclusive license to archive and make accessible my work in whole or in part in all forms of media, now or hereafter known. I agree that the document mentioned above may be made available immediately for worldwide access unless a preapproved embargo applies.

I retain all other ownership rights to the copyright of my work. I also retain the right to use in future works (such as articles or books) all or part of my work. I understand that I am free to register the copyright to my work.

## **REVIEW, APPROVAL AND ACCEPTANCE**

The document mentioned above has been reviewed and accepted by the student's advisor, on behalf of the advisory committee, and by the Director of Graduate Studies (DGS), on behalf of the program; we verify that this is the final, approved version of the student's dissertation including all changes required by the advisory committee. The undersigned agree to abide by the statements above.

Stephanie H. Mehlhope, Student

Dr. Alice Turkington, Major Professor

Dr. Anna Secor, Director of Graduate Studies

MODELING BEDROCK MINING HOTSPOTS  
WITHIN THE OUACHITA NATIONAL FOREST, ARKANSAS

---

THESIS

---

A thesis submitted in partial fulfillment of the  
Requirements for the degree of Master of Arts in the  
College of Arts and Sciences  
At the University of Kentucky

By

Stephanie Houck Mehlhope  
Lexington, Kentucky

Director: Dr. Alice Turkington, Professor of Geography  
Lexington, Kentucky

2012

Copyright © Stephanie Houck Mehlhope 2012

MODELING BEDROCK MINING HOTSPOTS  
WITHIN THE OUACHITA NATIONAL FOREST, ARKANSAS

By  
Stephanie Houck Mehlhope

Dr. Alice Turkington

---

Director of Thesis

Dr. Matthew Zook

---

Director of Graduate Studies

01/11/2013

---

I dedicate this thesis to all those that I love – you know who you are.

## ACKNOWLEDGEMENTS

I would like to express my sincere gratitude and heartfelt appreciation to those kind people around me that have supported me in completing this Master's thesis.

It is difficult to overstate my gratitude to my advisor, Dr. Alice Turkington. Her kind supervision, helping hand, and guidance have made my work possible. I am indebted to Dr. Jonathan Phillips for his continued counsel throughout my graduate career and in the field. Through their own various funding sources, Dr. Daniel Marion, Dr. Jonathan Phillips, and Dr. Alice Turkington permitted me to perform my own field research. I would also like to thank all those graduate and undergraduate students that trekked through the mud with me to collect data. Finally, I would like to thank my husband for his continued support of my education and most of all, for his continued support of my dreams.

## TABLE OF CONTENTS

|  |      |
|--|------|
| Acknowledgments.....   | v    |
| List of Tables.....  | viii |
| List of Figures.....   | x    |
| Chapter One: Introduction.....   | 1    |
| Background.....  | 2    |
| Factors Influencing Treethrow and Bedrock Mining.....                    | 5    |
| Topographic Factors.....   | 5    |
| Tree Specific Characteristics.....                                       | 6    |
| Geology and Soils.....   | 10   |
| Chapter Two: Research Design.....  | 12   |
| Environmental Setting.....   | 12   |
| Alum Creek Experimental Forest.....                                      | 15   |
| Rock Creek Tornado Blowdown Area.....                                    | 16   |
| Mena Tornado Blowdown Area.....  | 17   |
| Site Methodology.....  | 18   |
| Alum Creek Experimental Forest.....                                      | 18   |
| Rock Creek Tornado Blowdown Area.....                                    | 22   |
| Mena Tornado Blowdown Area.....  | 24   |
| Chapter Three: Methodology.....  | 27   |
| Statistical determination of variables correlated to bedrock mining..... | 27   |
| Modeling factors using binary logistic regression.....                   | 28   |
| Geospatial Data Compilation.....   | 31   |
| GIS Analysis.....  | 32   |
| Chapter Four: Results.....   | 34   |
| Alum Creek Experimental Forest.....                                      | 35   |
| Constructing the Model.....  | 47   |
| Rock Creek Tornado Blowdown Area.....                                    | 49   |
| Constructing the Model.....  | 55   |
| Mena Tornado Blowdown Area.....  | 57   |
| Constructing the Model.....  | 65   |

|  |     |
|--|-----|
| Map Creation.....                                  | 67  |
| Maps for the Alum Creek Experimental Forest.....   | 69  |
| Maps for the Rock Creek Tornado Blowdown Area..... | 81  |
| Maps for the Mena Tornado Blowdown Area.....       | 90  |
| Chapter Five: Discussion.....                      | 97  |
| Alum Creek Experimental Forest.....                | 97  |
| Rock Creek and Mena Tornado Blowdown.....          | 104 |
| Mapping Results.....                               | 109 |
| Suggestions for Future Studies.....                | 109 |
| Chapter Six: Conclusion.....                       | 111 |
| Appendices.....                                    | 114 |
| A: Unaltered Geospatial Data.....                  | 115 |
| B: Alum Creek Experimental Forest Data .....       | 134 |
| Rootwad Dimensions.....                            | 134 |
| Tree Specific Characteristics.....                 | 135 |
| Geology and Soil.....                              | 137 |
| Topographic Factors.....                           | 138 |
| C: Rock Creek Tornado Blowdown Area Data.....      | 140 |
| Wad Dimensions and Underlying Geology.....         | 140 |
| D: Mena Tornado Blowdown Area Data.....            | 142 |
| Rootwad Dimensions.....                            | 142 |
| Topographic Factors.....                           | 144 |
| E: Other Statistical Data.....                     | 146 |
| Bibliography.....                                  | 153 |
| Vita.....  | 162 |



LIST OF TABLES

Table 2.1, Description of modified decay classes from Spetich et al. (2002).....21

Table 4.1, Descriptive statistics of numerical data in the Alum Creek Experimental Forest.....45

Table 4.2, Pearson’s probabilities from treethrows within the Alum Creek Experimental Forest samples.....46

Table 4.3 Results of Fisher’s Exact Test for the Alum Creek Experimental Forest.....47

Table 4.4, Second round of collinearity testing for the Alum Experimental Forest.....47

Table 4.5, Model summary for the Alum Experimental Forest.....48

Table 4.6, Forward Stepwise (Conditional) output for the Alum Experimental Forest...48

Table 4.7, Descriptive statistics of numerical data for samples within the Rock Creek Tornado Blowdown site.....53

Table 4.8, Pearson’s probabilities for datapoints within the Rock Creek tornado blowdown site.....54

Table 4.9, Fisher’s Exact Test results for the Rock Creek tornado blowdown site.....55

Table 4.10, Second round of collinearity testing for the Rock Creek tornado blowdown.....55

Table 4.11, Model Summary for the Rock Creek tornado blowdown.....56

Table 4.12, Forward Stepwise (Conditional) output for the Rock Creek tornado blowdown area.....56

Table 4.13, Descriptive statistics of numerical data for samples within the Mena tornado blowdown site.....63

Table 4.14, Pearson’s probabilities for samples within the Mena tornado blowdown.....64

Table 4.15, Fisher’s Exact Test results for the Mena tornado blowdown.....65

Table 4.16, Second round of collinearity testing for the Mena tornado blowdown.....65

Table 4.17, Model summary for the Mena tornado blowdown.....66

Table 4.18, Forward Stepwise (Conditional) output for the Mena tornado blowdown....66

|   |     |
|---|-----|
| Table 4.19, Logit coefficients for the Alum Experimental Forest hotspot mapping.....                                | 67  |
| Table 4.20, Logit coefficients for the Rock Creek tornado blowdown.....   | 68  |
| Table 4.21, Logit coefficients for the Mena tornado blowdown.....   | 69  |
| Table 5.1, Mean values of wad dimensions recorded at each of the tornado blowdown study sites.....                  | 151 |
| Table E.1, First round of collinearity testing for the Alum Creek Experimental Forest.....                          | 202 |
| Table E.2, Chi-square testing of the binary logistic regression model for the Alum Creek Experimental Forest.....   | 157 |
| Table E.3, Model summary for the Alum Creek Experimental Forest.....  | 157 |
| Table E.4, Forward Stepwise (Conditional) output for the Alum Creek Experimental Forest.....                        | 158 |
| Table E.5, First round of collinearity testing for the Rock Creek Tornado Blowdown.....                             | 159 |
| Table E.6, Chi-square testing of the binary logistic regression model for the Rock Creek Tornado Blowdown area..... | 159 |
| Table E.7, Model Summary for the Rock Creek Tornado Blowdown.....   | 159 |
| Table E.8, Forward Stepwise (Conditional) output for the Rock Creek Tornado Blowdown area.....                      | 160 |
| Table E.9, First round of collinearity testing for the Mena Tornado Blowdown.....                                   | 160 |
| Table E.10, Chi-square testing of the binary logistic regression model for the Mena Tornado Blowdown.....           | 161 |
| Table E.11, Model summary for the Mena Tornado Blowdown.....  | 161 |
| Table E.12, Forward Stepwise (Conditional) output for the Mena Tornado Blowdown.....                                | 162 |

## LIST OF FIGURES

|  |    |
|--|----|
| Figure 1.1, Bedrock mining diagram.....  | 4  |
| Figure 1.2, Different types of root architecture.....  | 8  |
| Figure 2.1, Location of Ouachita National Forest.....  | 13 |
| Figure 2.2, Map of sampled locations.....  | 14 |
| Figure 2.3, Treethrow in the Alum Creek Experimental Forest.....   | 15 |
| Figure 2.4, Locations of tornado outbreak on November 27, 2005.....                                      | 16 |
| Figure 2.5, An uprooted rootwad at the Mena Blowdown site.....   | 17 |
| Figure 2.6, Sampling locations in the Alum Creek Experimental Forest.....                                | 18 |
| Figure 2.7, Rootwad measurements taken.....  | 19 |
| Figure 2.8, Diagram showing the definitions of the position on slope parameter.....                      | 20 |
| Figure 2.9, Map of areas that were sampled at the Rock Creek blowdown area.....                          | 22 |
| Figure 2.10, Aerial view of the Rock Creek tornado blowdown site.....                                    | 23 |
| Figure 2.11, Drawn hypothetical example of transect for MBA.....   | 24 |
| Figure 2.12, Aerial view of the Mena tornado blowdown site transects.....                                | 25 |
| Figure 4.1, Bedrock presence versus absence for all sites.....   | 34 |
| Figure 4.2, Boxplots of wad dimensions for the Alum Creek Experimental Forest.....                       | 37 |
| Figure 4.3, Boxplots of area and volume wad dimensions for the Alum Creek Experimental Forest.....       | 38 |
| Figure 4.4, Boxplot of DBH for the Alum Creek Experimental Forest.....                                   | 39 |
| Figure 4.5, Boxplot of decay class for the Alum Creek Experimental Forest.....                           | 39 |
| Figure 4.6, Boxplot of aspect and decay class for the Alum Creek Experimental Forest.....                | 40 |
| Figure 4.7, Boxplot of slope angle for the Alum Creek Experimental Forest.....                           | 40 |
| Figure 4.8, Tree type and presence/absence of bedrock mining for the Alum Creek Experimental Forest..... | 41 |

|   |    |
|---|----|
| Figure 4.9, Underlying geology and presence/absence of bedrock mining for the Alum Creek Experimental Forest..... | 41 |
| Figure 4.10, Soil mapping unit and presence/absence of bedrock mining for the Alum Creek Experimental Forest..... | 42 |
| Figure 4.11, Aspect and presence/absence of bedrock mining for the Alum Creek Experimental Forest.....            | 43 |
| Figure 4.12, Type of fall and presence/absence of bedrock mining for the Alum Creek Experimental Forest.....      | 44 |
| Figure 4.13, Position on slope and presence/absence of bedrock mining for the Alum Creek Experimental Forest..... | 44 |
| Figure 4.14, Boxplots of wad dimensions for the Rock Creek tornado blowdown.....                                  | 50 |
| Figure 4.15, Boxplots of area and volume wad dimensions for the Rock Creek tornado blowdown area.....             | 51 |
| Figure 4.16, Boxplot of DBH for the Rock Creek tornado blowdown.....  | 52 |
| Figure 4.17, Boxplot of geology for the Rock Creek tornado blowdown.....  | 52 |
| Figure 4.18, Boxplots of wad dimensions for the Mena tornado blowdown.....  | 58 |
| Figure 4.19, Boxplots of area and volume wad dimensions for the Mena tornado blowdown.....                        | 59 |
| Figure 4.20, Boxplot of DBH for the Mena tornado blowdown.....  | 60 |
| Figure 4.21, Boxplot of slope angle for the Mena tornado blowdown.....  | 60 |
| Figure 4.22, Boxplot of tree type for the Mena tornado blowdown.....  | 61 |
| Figure 4.23, Boxplot of underlying bedrock for the Mena tornado blowdown.....                                     | 61 |
| Figure 4.24, Boxplot of soil mapping unit for the Mena tornado blowdown.....                                      | 62 |
| Figure 4.25, Boxplot of aspect for the Mena tornado blowdown.....   | 62 |
| Maps for the Alum Creek Experimental Forest.....  | 68 |
| Maps for the Rock Creek tornado blowdown.....   | 81 |
| Maps for the Mena tornado blowdown.....   | 90 |

|  |     |
|--|-----|
| Figure 5.1, Dot plot of underlying geology and position on slope for the Alum Creek Experimental Forest site.....                                    | 97  |
| Figure 5.2, Wind rose showing the speed and primary direction of the winds (year-round) and trending direction for the Ouachita National Forest..... | 98  |
| Figure 5.3, Direct insolation map for the Alum Creek Experimental forest area.....   | 99  |
| Figure 5.4, Boxplot of tree type, thickness of wad, and presence of bedrock mining...  | 103 |
| Figure 5.5, Boxplot of decay classification and geology for the Alum Creek forest.....   | 102 |
| Figure 5.6, Dot plot of underlying geology and soil mapping units for the Alum Creek Experimental forest site.....                                   | 103 |
| Figure 5.7, Graph of DBH values for both tornado blowdown sites.....   | 104 |
| Figure 5.8, Comparison of wad area and volume for the tornado blowdown sites.....  | 106 |
| Base geospatial data for the Alum Creek Experimental Forest.....   | 114 |
| Base geospatial data for the Rock Creek tornado blowdown.....  | 122 |
| Base geospatial data for the Mena tornado blowdown.....  | 127 |

## Chapter One

### Introduction

If a tree falls in a forest and no one is around to hear it, does it make a sound? Perhaps, but it certainly will make a geomorphic impact!

There is a vast array of names for treethrow; some call it arboturbation, uprooting, root throw, treefall or tree tip, or even windthrow (blow, fall, or even break), acknowledging the mechanism of fall (Schaetzl et al., 1989). Throughout the globe treethrow has been assumed to be a major factor in the manufacturing of local topography, the modification of population dynamics within an ecosystem, and importantly, in soil formation and alteration through bedrock mining (Gallaway et al., Mena; Roering et al., 2010). For the sake of this paper, bedrock mining refers to any action done by tree roots, either through uprooting or growth, which displaces previously undisturbed bedrock that finds its way to the surface.

Hitherto there have been no attempts to geographically assign areas highly likely to experience bedrock mining by means of treethrow. The critical role that trees play in influencing the characteristics and development of the soil, regolith, and bedrock interface highlights the need for greater understanding of where these processes are most prevalent, which may be termed bedrock mining “hotspots.” Hitherto, the identification of bedrock mining hotspots has not been attempted. This study, concentrating on the Ouachita Mountain Range in west-central Arkansas, extends prior work that has looked at bedrock mining in the region by supplying a method for determining bedrock mining hotspots.

The goals of this study are the following:

1. To determine the abiotic and biotic factors that are highly correlated with the potential for bedrock mining found in treethrows
2. To map areas highly likely to experience bedrock mining by means of treethrow

The current understanding of bedrock mining by treethrow is highly site specific. This is partially due to the impact of varying individual environmental setting factors. However, advancement toward a more comprehensive portrayal of the general process on a regional scale is timely and this study will bring research one step closer toward this end with the addition of further regional information, including data on hotspots of activity as determined by topographic, geologic and pedologic factors, and tree-specific factors such as diameter at breast height and tree type. With increased knowledge of the location of bedrock mining hotspots researchers can better understand and predict local topographic, ecosystem population, and soil characteristic changes.

There are three field study areas for this research. The first, the Alum Creek site, exhibits what I am deeming “cycle-of-life” treethrows. For the purposes of this paper “cycle-of-life” uprootings distinguish non-tornado events (e.g. ice storms or high winds) from uprootings caused by tornados. The second and third study sites, the Rock Creek and Mena Blowdown sites, are the location of two separate tornado blowdowns that occurred in Rock Creek and Mena areas, respectively.

A combination of correlation, chi-squared, and logistic regression statistical techniques were utilized. To complete the first goal of this study, a bivariate statistical analysis will indicate the strength of association between the topographic, environmental, and tree specific variables and the presence of mined bedrock. From these analyses a logistic regression model and an associated map of odds generated using ArcMap software, fulfilling the second goal of this study. Areas of low, moderate, and high odds of bedrock mining activity are highlighted. These maps are intended to be used as a tool for further research.

## **I. Background**

Uprooting events occur when the root structure of a tree is, in some way, pulled from the ground displacing the bole, trunk, and rootwad with ground material. This is distinguished from “snaps,” in which only the bole and a portion of the trunk are damaged, leaving the soil and bedrock below it undisturbed (Schaeztl et al., 1989).

The influence of treethrow in forest dynamics spans from the canopy down to the bedrock interface. The tipping of one (or several) trees can cause mortality in understory plants in the immediate area as they are themselves knocked over in a “domino” fashion or are restricted from sunlight when covered. Likewise, when large canopied trees or groups of trees uproot, gaps form in the canopy allowing increased sunlight to an area that before the fall could only support shrubs, herbs, saplings, and other shade resistant plants. The sudden increase in energy input allows for a rapid change in the opening as surrounding trees increase their branch length, saplings grow quickly, and fast-growing, sun-loving species move into the area (Ulanova, 2000).

On the ground level when a treethrow does occur, coarse woody debris (CWD) adds roughness and biomass to the forest floor. The addition of CWD provides habitat, alters nutrient cycling, and localized geomorphologic processes such as weathering, transport, and deposition of materials (Stevens, 1997). Stevens (1997) illustrates the ways in which small animals, fungi, insects, and bacteria use fallen CWD for protection, nesting, and as a food source. The decaying tree is a clear indication of just one of the ways in which treethrow events affect nutrient cycling in forests. Digestion by earthworms, fungi, and other insects return essential nutrients such as nitrogen, potassium and phosphorus to the assessable nutrient pool (Stevens, 1997). Aside from this simple addition of decayed (or burnt in some cases) mass to the forest floor, uprooting introduces once buried soil, carbon, nutrients, and other biological products to the surface (Lenart et al., 2010). This excavation of material may also increase rates of erosion and weathering through exposure to surficial and atmospheric processes (Lenart et al., 2010). It is also possible that CWD can alter ephemeral streams as well as soil erosion and deposition.

Often a pit-mound arrangement is formed over time at the site of uprooting. This important microtopographic feature evolves from a combination of the hollowed-out pit, which the root system once occupied, and the slow mounding of soil and rock material as it detaches from the root architecture. Pit-mounds have been documented to cover as

much as 40% of total land area of a stand (Ulanova, 2000). These features present slight variances in the temperature, light, and moisture conditions from the surrounding area, providing an important microclimate for new growth and species diversity (Šamonil et al., 2010). Evidence also suggests that differing conditions on the pit and mound can influence species distribution patterns (Lenart et al., 2010, Šamonil et al., 2010, Schaetzl et al., 1989a).

In addition to the creation of pit-mound topography, treethrow events initiate sediment transport, often downslope (Schaetzl and Follmer, 1989; Norman et al., 1995, Gabet et al., 2003). Norman et al. (1995) found that increased slope angle increased the rate of downslope transportation of sediment, the elongation of mounds, and a reduction of pit infilling from mound wasting. Sediment flux ( $q_s$ ) from tree uprooting has been calculated by Gabet and others (2003) as being:

$$q_s = \frac{\text{volume}}{\text{event}} \times \frac{\text{distance}}{\text{event}} \times \frac{\text{events}}{\text{area}} \times \frac{\text{events}}{\text{time}} \quad \text{Equation [1.1]}$$

Considering the terms of the equation for sediment flux, one can imagine that with mass disturbance events such as tornados, fire, hurricanes, ice storms, and other forces, that total sediment flux for a single disturbance from uprooting events can be quite large.

Trees can substantially alter soils within a few generations (Binkley and Giardina, 1998). In fact, even the effect of solitary trees on soil properties is detectable (Boettcher and Kalisz, 1990). New tree growth initially thickens the soil over many hundreds to thousands of years until the soil reaches a depth at which rooting depth does not reach bedrock, in the absence of a mass wasting or soil affecting disturbance event (Gabet and Mudd, 2010). Šamonil et al. (2010) explain that the “synergistic action of erosion-sedimentation and ecological conditions” (p.72) in pit-mound systems affect local soil profile and formation. The O, A, and often lower soil horizons are removed from the pit during the uprooting event, exposing lower layers to be later in-filled with organic debris (Ulanova, 2000). Mound microenvironments are characteristically poorer in nutrients, more acidic, and show a lower bulk-density than adjacent pits (Šamonil et al., 2010). Pits, however, are considered to be at a morphologically more advanced stage of development with greater humus and wood debris content due to infilling, and enhanced leaching (Šamonil et al., 2010).

At the bedrock interface mechanical and chemical disruption occurs from, but is not limited to, root growth and penetration. The very small tips of roots exert enough pressure during growth, both vertically and horizontally, into even the smallest of fractures throughout the bedrock surface to break up bedrock (Gabet et al., 2003). Over time, larger roots can penetrate more deeply and expansively into bedrock, sometimes moving very large, even boulder size, pieces of rock. Observations from uprooted treewads have noted fragments of freshly mined bedrock measuring nearly 2m<sup>3</sup> (Gabet et al., 2003). Figure 1.1 shows how bedrock mining action can increase the surface area available to weathering processes. This increase in surface area and weathering rates is important for soil production within a forest.



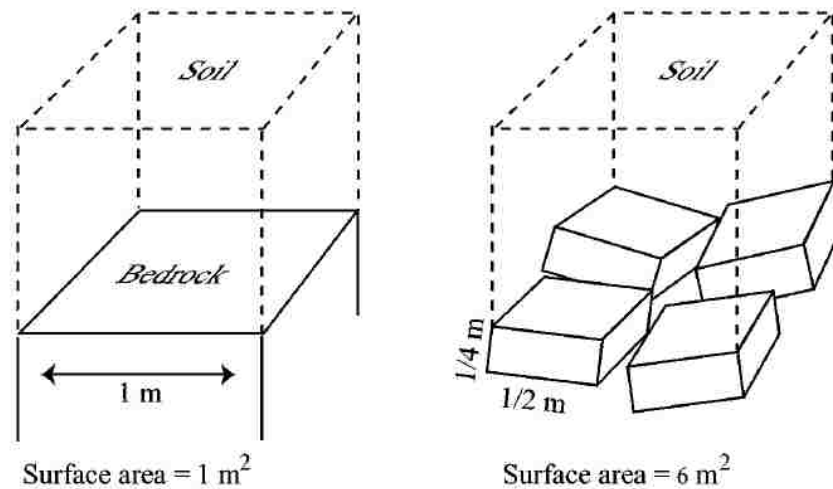


**Figure 1.1** Bedrock mining increases the surface area available to weathering and dislodges fragments of fresh bedrock that may be exhumed during uprooting events (diagram from Gabet et al., 2003)

The causes of uprooting range from simple mortality to exogenous disturbances such, fire, ice storms, and high winds including tornados and hurricanes. Wind damage is the leading cause of abiotic damage to trees (Sellier et al., 2005). When the forcing mechanism for uprooting is strong winds, researchers have often used a range of terms for treethrows including, windthrow, windfall, windbreak, windblow, blowdown, and treefall (Schaetzl et al., 1989). When the vector force of the wind exceeds the tree's bending moment, an incomplete fall or complete uprooting can occur (Sellier et al., 2005). If the aspect of a location bears the brunt of the prevailing wind or storm tracks, the surface topography can greatly influence the susceptibility of a tree to ice or wind damage (LaFon and Speer, 2002, Bragg et al., 2003, Warillow and Mou, 2004, Stueve et al., 2007). Ice storms may cause trees to uproot by increasing the stress on tree roots from the additional weight caused by the accumulation of ice in the tree canopy. Furthermore, a shift in fire regime could have major implications for uprooting likelihood through changes in forest composition and age structure. The results of two studies indicated that prescribed fire could shift the conditions to favor one species, depending on the intensity of the burns (Arthur et al., 1998, Gilbert et al., 2003). Gallaway et al. (2009) examined the effects of wildfire in sediment processes caused by uprooting. Their results suggested that if long periods of time occur between intense fires, then trees will reach a critical diameter at breast height (DBH) necessary for uprooting, while too short of a time span between disturbance events would limit this effect. If a relationship between uprooting and species is reported, then the selection for, and subsequent protection of, specific species could have implications for the likelihood of uprooting.

## **II. Factors Influencing Treethrow and Bedrock Mining**

As early as 1927, deep tree root penetration into seemingly impenetrable granite and sandstone bedrock by as much as roughly 12 m was documented (Vater, 1927). Shortly following in the 1930's, a discussion on the biomechanical role of trees had begun with the recognition of the importance of uprooting trees and the vertical movement of forest soil material (Lutz & Griswold, 1939). By the late 1940's and '50s uprooting was accepted as being caused by both endogenous, in the form of tree weakness or death, and exogenous, through external factors such as high winds, forms of disturbance within the United States (Ruhl, 1952, Schaetzl et al., 1988). Earlier work produced documentation on the exhumation of fresh bedrock by way of tree root penetration into bedrock fractures (Lutz, 1960., Wilford and Wall, 1965). Roering et al. (2010) introduced the use of LIDAR technology to quantify the extent of bioturbation of the bedrock interface by trees so that they might compute curvature values to show that the pit-mound "signature of life" dominates at scales less than 7.5m. From this data the group inferred that many tree-throw datasets "likely underestimate the total volume of bedrock affected by deep rooting (p.189)"

The identification of bedrock mining hotspots by root action is logically undertaken through the analysis of factors influencing mining occurrence. Therefore, discussion will focus on topographic factors, tree specific information including decay class, tree type, and wad measurements, and finally geology and soil characteristics.

### **A. Topographic Factors**

There is a broad range of landscape factors that influence the interaction between topography and uprooting events. Recent efforts to model the factors most significant for catalyzing uprooting events focused on slope angle, moisture saturation, aspect, and solar exposure (e.g. Robert, 2003). Past research indicates that some general rules concerning the ways in which topographic influence manifests in bedrock bioturbation. Broadly, sites that have shallow and rockier soils, are waterlogged, or are exposed to prevailing winds all have an increased likelihood of tree uprooting (Robert, 2003). Instances of windthrow, or uprooting in general, may create an array of microtopographical alterations, including pit-mounds, which can influence future disturbance events and the stability of individual trees (Hart and Grassino-Mayer, 2009, Schaetzl et al. 1989). The shallower a soil is the greater the likelihood of root penetration and subsequent bedrock mining if uprooting does occur (Gabet and Mudd, 2010, Schaetzl et al., 1989).

Aspect, position on slope, and type of fall all affect the rate of uprooting and the potential for bedrock mining activity. Genet et al. (2010) described how a plant's position on slope can greatly influence overall slope stability – thereby influencing potential for uprooting. Ridge tops and the upper reaches of slopes experience higher rates of disturbance compared to other topographic settings due to a variety of reasons (Lorimer and White 2003). For instance, shallow soils on ridges and slopes prevent deep root penetration, increasing the frequency of uprooting as well as increase the frequency of bedrock mining activity, as compared to other topographic settings (Ruel, 2000, Shure et al., 2006). In addition to typically having shallow soils, hilltops are frequently exposed to

higher wind speeds, exacerbating tree vulnerability. Often wind direction and speed varies with elevation; speeds are typically accelerated on ridge tops compared to valley bottoms and slopes. Furthermore, landscape roughness can influence winds at localized scales, producing oscillations that can increase tree vulnerability to toppling. In riparian zones, most treethrows occur downslope due to canopy asymmetries (Kellman and Tackaberry 1993). Belingham and Tanner (2000) found that the best predictor of mortality through uprooting events was a combination of slope angle and the occurrence of recent disturbance.

Foster (1988) observed that topography and aspect serve as major controls on the intensity of wind-forced uprooting and stand damage. Slope aspect not only has a significant effect on heat load (temperature), moisture balance, and vegetation type, it also greatly affects microclimatic variability and weather conditions. Aspect often correlates to wind and weather exposure, thus affecting a tree's potential for uprooting and bedrock mining activity. Slope aspects with a reduced heat load and sun exposure should be expected to retain soil moisture for longer periods, negatively affecting tree stability in many environments. The importance of aspect can also be exhibited when trees fall upslope; this is usually due to the direction of prevailing winds (Kellman and Tackaberry 1993). As wind damage is the leading cause of abiotic damage to trees, it is plain to see how aspect might be an important factor in the force of uprooting (Sellier et al., 2005). This is especially true for catastrophic events, such as hurricanes (Foster, 1988, Ennos, 1997, Lorimer and White, 2003). Within conifer forests in temperate regions, treefall occurs downwind most often (Falinski, 1978). Canopies also exhibit roughness, just as surface topography does. Uneven, rough, stand canopies are generally more resistant to high wind events compared to areas with uniform canopies (Peterson 2007; Rentch, 2010). Indeed, Rentch (2010), following Young and Hubbell (1991) argue that wind speed and direction as well as aspect are the primary factors controlling uprooting; while the importance of these factors changes depending on proximity to the forest edge and the "clumpiness" of tree distributions, two additional elements of canopy roughness.

## **B. Tree specific characteristics**

The extent and magnitude of damage done to a forest stand by wind, fire, ice, and other such exogenic factors are naturally stochastic. However the literature shows that different species have variable resistance to uprooting. Conifers have predominantly been found to be more vulnerable to tree-throw than hardwoods, but several other factors complicate this conclusion (Peterson, 2007, Webb, 1989). Root architecture, wood strength, stem mass, successional position, and crown structure all have influence on the type of tree fall and uprooting resistance. In addition, whether it is a hardwood or conifer appears to affect the rate of uprooting and bedrock mining.

The pattern and depth of rooting has a great amount of influence upon a tree's stability against exogenic uprooting forces. Increased rooting depth increases soil shear strength and thus reduces the likelihood of uprooting (Stokes et al., 1996, Fourcaud et al., 2008). Logically, if rooting depth is greater than soil thickness this would greatly increase the likelihood of bedrock penetration by roots and the likelihood of bedrock mining in

uprooting events. Thick, strong, root buttressing reduces bending and dissipates the center of stress out from the stem base, especially on the windward side of the tree (Nicholl and Ray, 1996). However, one set of simulations found that the role of the tap root in stabilization is negligible if leeward roots grow to a depth greater than the windward roots (Fourcaud et al., 2008).

Serving as a tree's primary mechanism for holding itself upright from the ground, root architecture plays an important role in tree stability. Root architecture typically falls within one of three patterns: plate-like, herringbone, tap, or heart-like (Figure 1.2) (Dupuy et al., 2005). Dupuy et al. (2005) found that the plate-like architecture, exhibiting great lateral growth but only minimal vertical growth, was the least resistant to uprooting. The herringbone root system is typically present in low-nutrient environments and is not very resistant to uprooting due to the absence of strong lateral roots (Gross et al., 1992; Dupuy et al., 2005). The heart-like pattern is accepted as the most effective anchorage type and is commonly found in oak and beech species exhibiting strong roots near the base and dense rooting further away from the tree base (Dupuy et al., 2005; Burns & Honkala, 1990). Finally, tap-like patterns can often be found in both coniferous and deciduous species with deep roots (Dupuy et al., 2005, Burns and Honkala, 1990). The tap-type architecture is the most common type found within the study areas as the majority of trees are conifers or primarily short-leaf pines (*Pinus echinata* Mill.). Dupuy et al. (2005) found that tap root systems had a maximum rooting depth that was more than 0.5 meters deeper than any other architecture type in their study. This would imply a possibility of greater frequency of bedrock disruption and penetration, increasing the potential overall likelihood of bedrock mining activity in the study area.

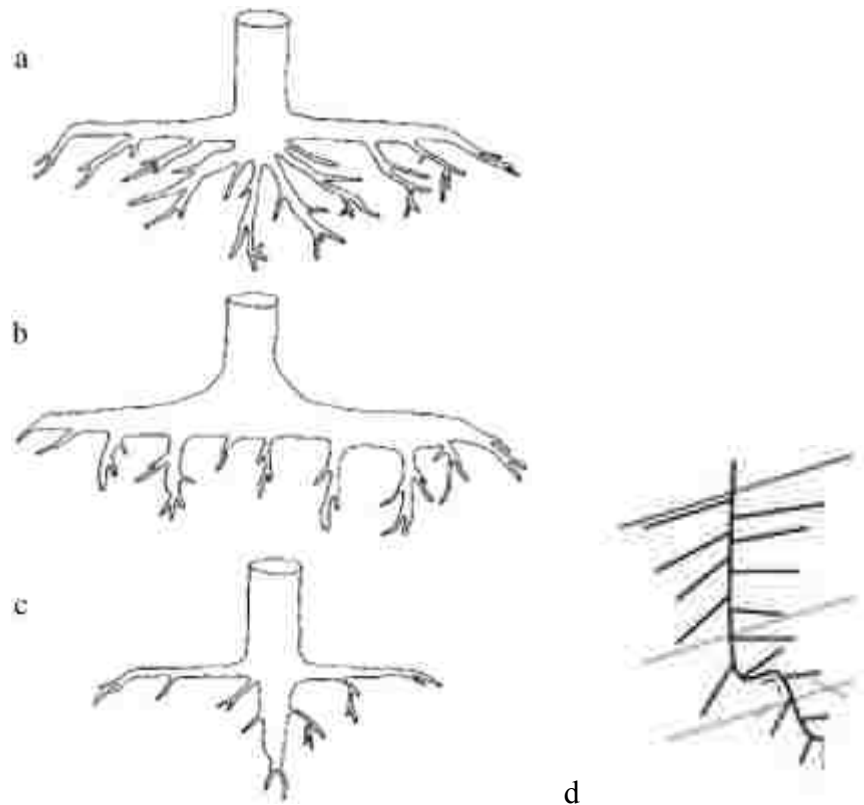


**Figure 1.2.** Different types of root architecture: (a) heart-system roots, (b) plate-root system with vertical sinker roots, and (c) tap-root system (from Stokes and Mattheck, 1996) and (d) herringbone root structure (from Stokes et al., 2009)

Generally, those species with weaker wood are more susceptible to uprooting or breakage (Peterson, 2007). Root tensile strength, or the resistance of the wood to breaking, has been shown to contribute to tree stability (Sellier et al., 2005, Crook and Ennos, 1996). Later-successional species, such as high wood strength deciduous varieties, were found by Peterson (2007) to be more windfirm than their earlier-successional softwood neighbors. This would suggest that with other characteristics being equal, weaker roots would be less likely to mine bedrock as they are more likely to tear or release their hold on bedrock during the uprooting process. This begs the question, if conifers have weaker roots in general than deciduous tree types but have deeper tap-root architecture, which root characteristic is the most important in the study areas?

Studies have also shown that total mass relates negatively with stability - the larger the tree, the less stable it is and more likely it is to uproot. A greater tree diameter (stem mass or diameter at breast height, DBH) yields increased uprooting (Peterson, 2007, Nicholl et al., 2006, Webb, 1989). Nicholl et al. (2006) found stem mass to be the most critical variable in determining the relative strength of a tree's anchorage.

In addition to the roots and trunk, crown structure can also significantly modify overall stability. The branches and leaves almost always have a much greater surface area exposed to the disruptive forces of high winds and heavy ice, than the trunk. The absence

of leaves during the winter in deciduous trees, barring marcescent foliage, reduces the aerial surface area and top-heavy weight of ice in the winter causing them to be somewhat less susceptible to windthrow during the colder months (Peterson, 2007). However, Sellier et al. (2005) found in their model simulations studying the effects of crown architecture on trunk oscillations that leaves and branches can also have a dampening effect upon movement when branches are flexible, decreasing the concentration of strain to the entire network of branches.

It would normally be expected that the larger a tree is in height and DBH that the deeper and more penetrating its roots would be. Early work proposes that root growth is not only determined by species but also by soil environmental characteristics (Biswell, 1935). Yet, current work shows that root penetration and growth is actually more likely to be governed by tree type as well as functional soil space. For trees blown over by a tornado in Arkansas, Phillips et al. (2008) found that tree size (DBH) and age was significantly correlated with rootwad dimensions. However, for cycle-of-life type uprootings, Gabet and Mudd (2010) determined that tree size and age is decoupled from rootwad dimensions. Their observations suggested that thin soils produce shallow pits, and consequently thin root wads, due to root turning against the bedrock interface. With sufficient fractures or weakness in the interface, however, it is quite likely that even trees on the thick soils can mine bedrock when uprooted.

The state of decay of an uprooted tree has no direct bearing on resistance to uprooting or on bedrock penetration by roots. However this is an important factor in site interpretations of uprooting. Decomposition rate varies between species, but typically hardwoods decay more quickly than conifers (Gholz et al., 2000). Decaying boles provide habitat, sustenance, material and nutrients for soil production, and a variety of other functions to an ecosystem (Pyle and Brown, 1999). Logic suggests that there is a positive relationship between the time an uprooted tree has been in situ and disintegration of the root wad. With this in mind, felled boles may remain in place for a relatively long period, ranging from several decades to upward of a century for the largest woody debris, depending upon local climate. Gallaway et al. (2009) looked at sediment detachment and eventual transport away from the root wad and determined that those uprooted trees on steep gradients lost the greatest volume of sediment from the wad. Thus, those oldest wads on the steepest slopes should maintain the least measurable amount of mined bedrock. Even after uprooting and consequent bedrock mining has occurred, rootwads and stumps can fall back into their original pits, decaying over time, leaving displaced bedrock fragments on (baumsteins) or near the surface (Phillips and Marion, 2006).

### C. Geology and Soils

Coherent, structurally sound bedrock is likely to be more resistant to bedrock mining by root action than friable, fragile, bedrock varieties. Phillips et al. (2008b) documented the relationship between roots and bedrock fractures in the Ouachita Mountains, finding that trees consistently penetrated bedrock through fractures, and that such fracturing is more likely to occur in shale than in sandstone as weathering was more rapid in the shale layers. Their findings confirm the idea that easily weathered bedrock is more easily penetrated and broken up by tree roots than tougher or more resistant bedrock varieties. Phillips et al. (2005) suggest that rock fragments produced in situ may be associated with a preferred geologic orientation in that vertical bedding arrangements, as opposed to horizontal, often seen locally in the characteristically folded Ouachita Mountain range allow for easier and more extensive penetration by tree roots into less structurally sound layers.

Soil acts as the primary growing medium for forest systems. Extensive root systems rapidly transfer stress to the surrounding soil when disturbed, inhibiting toppling, but if the area of supporting root coverage is too concentrated in a small space due to impenetrable areas of bedrock or soil plates and overcrowding, it can be detrimental to tree stabilization (Stokes et al., 1996). Areas of soil compaction can inhibit downward or lateral growth, affecting the root growth and thus tree stability (Crossley, 1940). Early work assumed that soil thickness had to be exceptionally thin for uprooting events to mine fresh bedrock but more recent work demonstrates that such is not necessary the case (Lutz, 1960., Phillips and Marion, 2005).

The processes of root penetration and bedrock mining act as important agents in deepening soil and regolith. Gabet et al. (2003) explain that plants can mix and deepen soil through root expansion during growth in even the smallest of fractures in rock, extraction of moisture from the soil causing settling, uprooting, and the eventual infilling of decayed former root channels. Additionally, Phillips et al. (2005) discussed how floralturbation of the regolith is quite frequent within the Ouachita National Forest and that material was very commonly exhumed from as deep as the Cr and R horizons. Of particular interest to this study is the Phillips et al. (2005) group's finding that the local spatial variability in regolith thickness was directly associated with the influence of trees through root action and tree/stump rot followed by infilling of soil.

The relationship between soil thickness and soil production from bedrock weathering was explored through modeling by Gabet and Mudd (2010). This model, designed to simulate physical weathering of bedrock by root growth and tree-throw, includes population dynamics of trees, tree mortality, treethrow frequency, and the relative contribution of uprooting events in the movement of bedrock materials. As soil thickness continues to increase, the model predicts that bedrock erosion by both biomechanical and biophysical means also decreases, thereby decreasing further thickening. The model finally produced a rough and uneven bedrock surface as predicted, as well as pit-and-mound topography associated with forest landscapes. It was found that a positive feedback between soil thickness and tree density manifested itself slowly over the first 1,000 years, and intensified as soil thickened. Soil thickness and biomechanical bedrock disturbance were far less correlated where roots fractured local bedrock, and

where uprooting played a significant role in the exposure of bedrock. Interestingly, it was also found that bedrock erosion rate was not accelerated where soils were thinnest.

This review of previous research suggests that trees play a critical role in influencing the characteristics and development of the soil, regolith, and bedrock interface as well as the overall topography of a forested area. Focus on the topic of bedrock mining has been mainly centered on a discussion of what factors most influence the rate of tree uprooting and bedrock penetration by roots. This research departs from the previous research in that it endeavors to supply a method for the geographic assignment of areas highly likely to experience bedrock mining, hotspots of activity, by means of treethrow.



## **Chapter Two**

### **Research Design**

Prior research has shown that topographic factors such as slope angle, aspect, moisture saturation, position on slope, and depth of soil contribute to the overall stability of trees and their ability to root deeply enough to mine bedrock when overturned (Ennos 1997, Foster, 1988, Hart and Grassino-Mayer, 2009, Kellman and Tackaberry, 1993, Lorimer and White 2003, Rentch, 2010, Robert, 2003, Ruel 2000, Schaetzel et al., 1989, Sellier et al., 2005, Shure et al. 2006, Young and Hubbell, 1991). Rock types with relatively high resistance to stress and fracturing appear to be more resistant to bedrock mining, as fractures act as conduits for water penetration, chemical weathering, and new root growth (Phillips et al. 2005, 2008, Stokes et al., 1996). The literature also shows that soil type, including grain size range characteristics and compaction, as well as soil depth greatly affects tree stability and the rate of bedrock mining done in uprooting events (Crossley, 1940, Gabet and Mudd, 2010). Species characteristics such as the pattern of rooting and crown shape typical of a species, diameter of trunk, and wood strength also contribute to this phenomenon (Burns and Honkala, 1990., Crook and Ennos, 1996., Dupuy et al., 2005., Fourcaud et al., 2008., Gross et al., 1992., Nicholl et al., Rock Creek., Nicholl and Ray, 1996., Peterson, 2007., Sellier et al., 2005., Stokes et al., 1996., Webb, 1989).

Once again, the goals of this study are the following:

1. To determine the abiotic and biotic factors that are highly correlated with the potential of bedrock mining found in treethrows
2. To map areas highly likely to experience bedrock mining by means of treethrow

This study considers the factors identified above in accomplishing its objectives. Data are taken from three field sites in the Ouachita Mountains of Arkansas: the Alum Creek, Rock Creek, and Mena sites. The Alum Creek site exhibits the “cycle-of-life” treethrows. The Rock Creek and Mena sites are locations of two separate tornado blowdowns.

#### **I. Environmental Setting**

Study sites are within the Ouachita National Forest in Garland, Polk, and Saline counties of west-central Arkansas (Figures 2.1 and 2.2). The folded Ouachita Mountain range dominates the landscape, trending east to west, unlike the more familiar Appalachian and Rocky Mountain ranges of the United States that extend north to south, with streams draining the intermontaine valleys (Phillips et al., 2008). Marked by warm summer months, with mean temperatures near 27°C and mild winter months, averaging around 8°C, with more than 140 cm of precipitation roughly evenly spread throughout the year (NWS, 2009). The spring and fall are slightly wetter than the summer and winter and the climate is within the humid subtropical range (NWS, 2009).

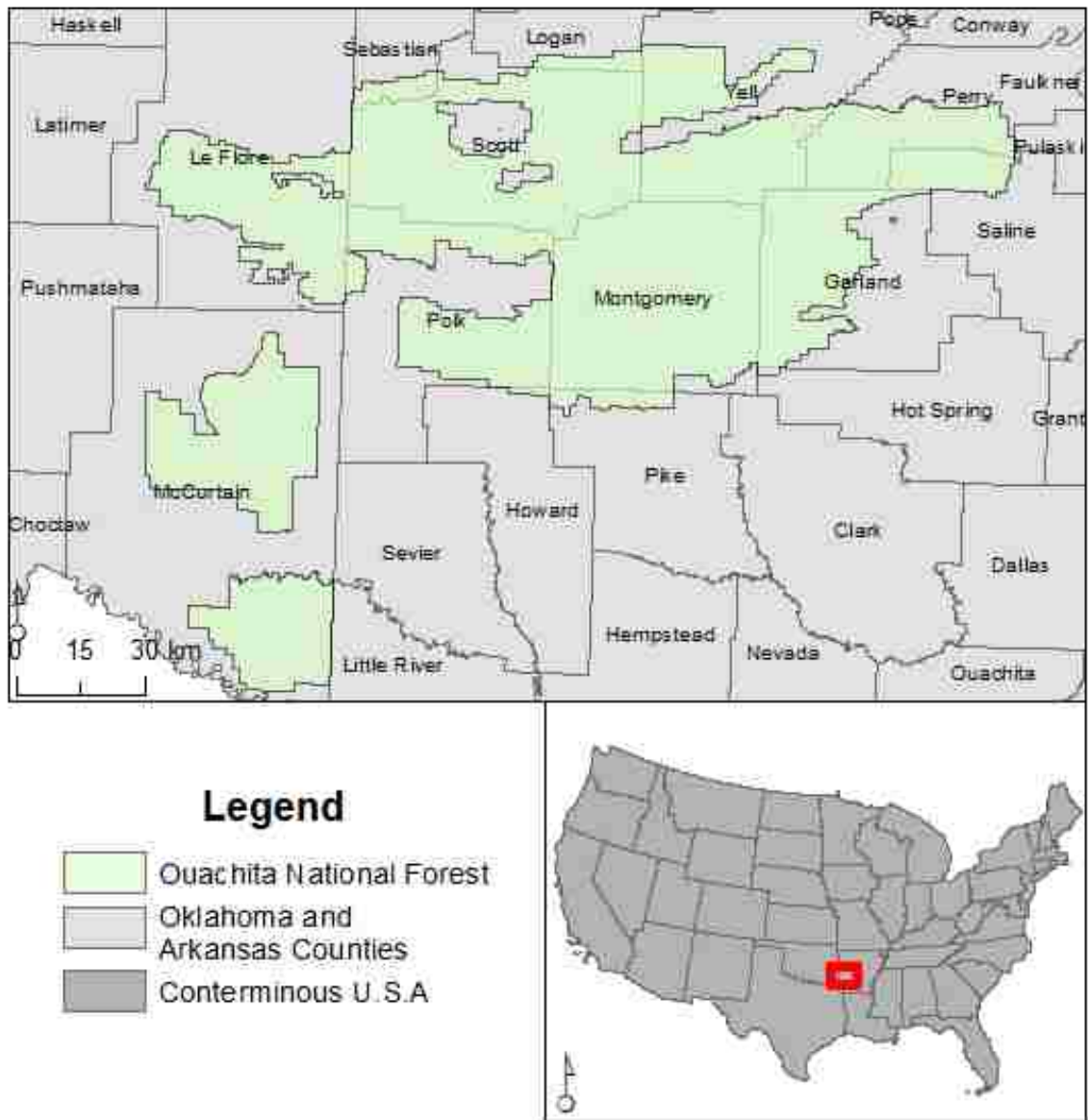


**Figure 2.1.** Location of Ouachita National Forest.

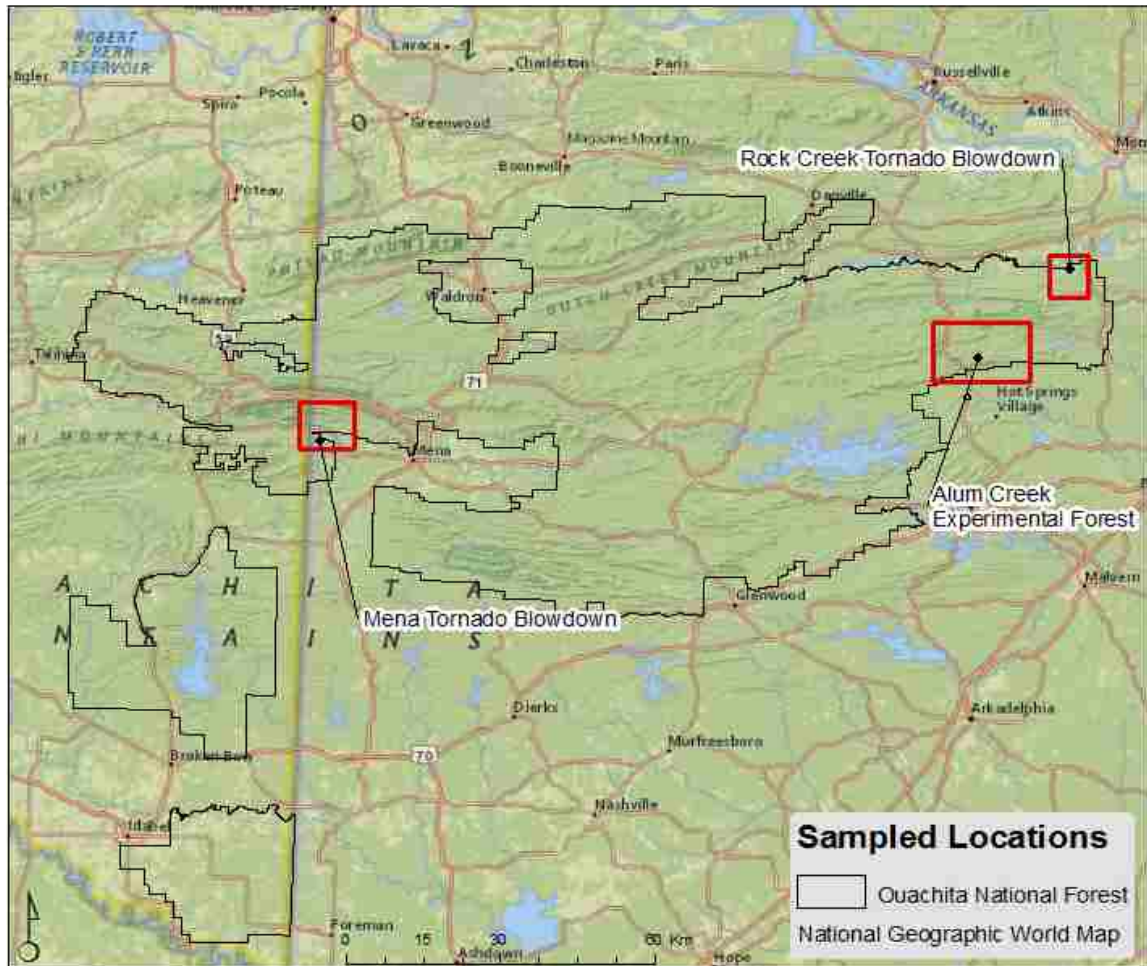


**Figure 2.2** Map of sampled locations including the Alum Creek Experimental Forest, Rock Creek and Mena Tornado Blowdown areas.

The Ouachita Mountain range was formed at about the same time as the Appalachian Range (Richards, 1953). The once flat sedimentary layers were deposited during the Paleozoic era when the area was covered by shallow seas (Peterson et al., 1973). The continental collision that built up the Ouachitas Mountains during the Late Pennsylvanian period is also responsible for the extensive folding and faulting of the stratigraphy. Exposed sedimentary rock types mostly fall within two categories, shale and sandstone. Typically the shales exhibit silty to conglomeratic structure and are highly weathered once uncovered, while the sandstones are coarse grained and more resilient against quick weathering (AGS, 2007). However, areas of novaculite, chert, and even quartzite are also common in certain parts of the region (Stern et al., 1979). With erosion resistant sandstone caps, broad synclines, relatively narrow anticlines, and complex folding, ranging from complete to partial, ridge and valley form and orientation are highly controlled by the structure of the local geology (AGS, 2007).

While Ultisols and Hapludults are dominant soils within the Ouachitas, a high degree of soil variability over small areas has been documented within the forest (Phillips and Marion, 2005). Most areas can be quite rocky, exhibiting colluvial, hillslope clasts, ranging from gravel to small boulder in size.

Tree species makeup in the Ouachita Mountains is dominated by shortleaf pine-oak forest and woodland (approximately 70% of total forest coverage) with significant proportions of mesic hardwood stands, pine savannas, montane oak forest areas, as well as some glade and barrens (USDA, 2005). Riparian areas in the mountainous portions of the forest exhibit seeps rife with sweetgums, black tupelo, and maples (USDA, 2005). Recent restoration efforts by the USDA Forest Service have reintroduced the once common shortleaf pine-bluestem savanna habitat, which was once common in the area before fire suppression efforts began (Hedrick et al., 2007).

### A. Alum Creek Experimental Forest

The Alum Creek Experimental Forest area is situated in the eastern portion of the Ouachita National Forest within Saline County, Arkansas. Established in 1959 with hydrological research in mind, this 1,732 hectare experimental forest features mean daily temperature of -1 to 34° C and 1,321mm of mean annual precipitation (SRS, 2008; Adams et al., 2004). Shortleaf pine dominates the forest which also includes a mixture of white and red oaks, and less frequently, hickories. Soils in the area are generally well-drained, rocky, and loamy Hapludults (SRS, 2008,Phillips et al., 2008). A soil pit dug near a sampled tree-throw was 16 inches to shale bedrock, revealing sandstone and shale clasts both near the surface and on the bedrock interface. A picture of a Shortleaf Pine-Bluestem renewal stand in the Alum Creek Experimental Forest area can be seen in figure 2.3. The Alum Creek Experimental Forest study site is unique in that it is the only study site that is actively managed as a real-world laboratory by the USDA-FS (USDA, 2003).



**Figure 2.3** Treethrow with additional rootwad seen in the background at the Alum Creek Experimental Forest in May, 2011.

## B. Rock Creek Tornado Blowdown Area

On November 27, 2005 twenty-four confirmed tornadoes, ranging from F0 to F3 on the Fujita scale, ripped through central and northern Arkansas (Figure 2.4) (National Weather Service, 2007). Damage to the Ouachita National Forest occurred along an estimated 34km of tornado tracks with hundreds of trees knocked down by winds that were estimated up to 257.5 kph winds (National Weather Service, 2005).

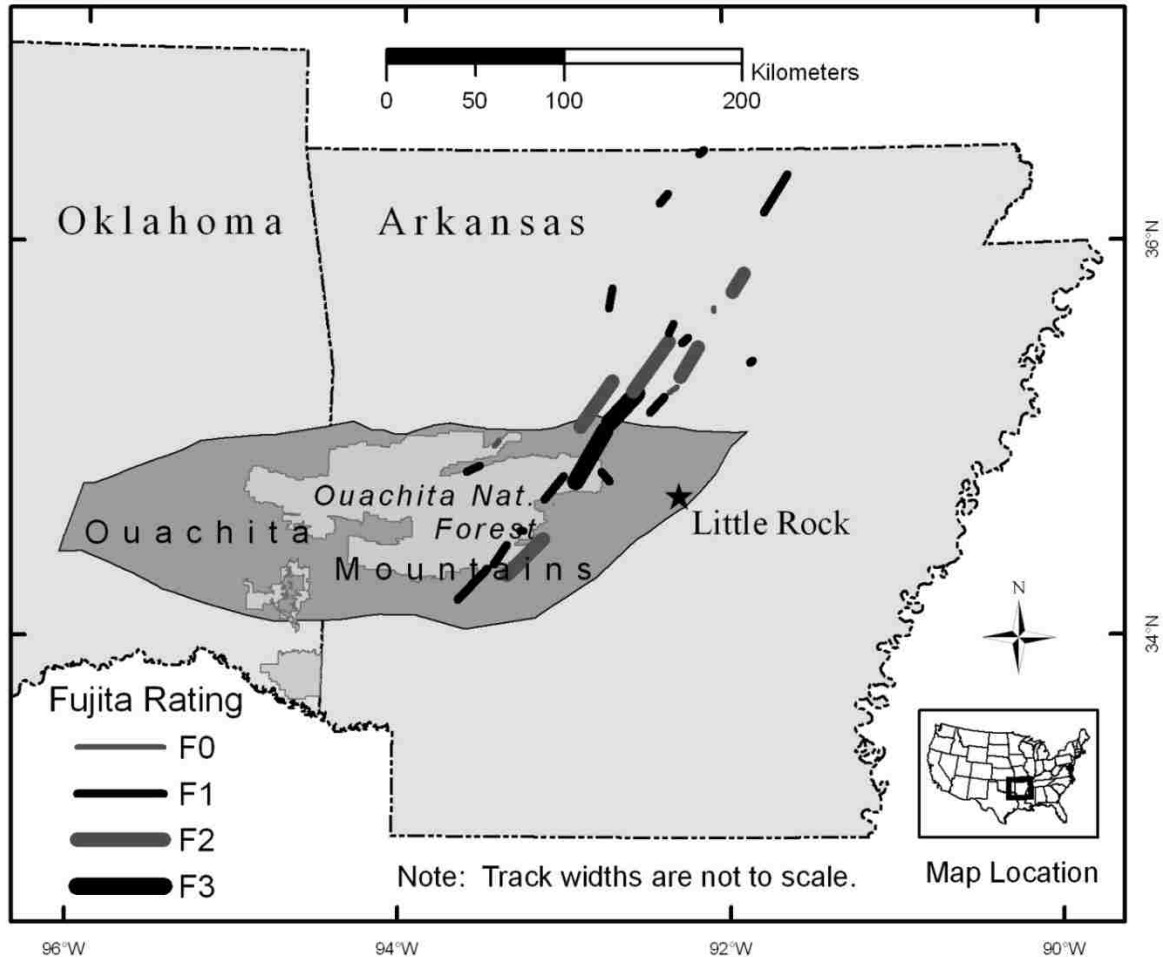


**Figure 2.4** Locations of tornado outbreak on November 27, 2005 (from Phillips et al., 2008a)

This was the first tornado blowdown site sampled. Unlike the mixed forest type found at the Alum Creek Experimental Forest area vegetation cover at the Rock Creek Tornado blowdown site was primarily Shortleaf Pine with a minority component of mixed hardwood species, chiefly oaks with some hickories. All trees sampled at this location (those that were blown over by the winds of the tornado) were Shortleaf Pine.

### C. Mena Tornado Blowdown Area

Polk County, Arkansas in the western portion of the Ouachita National Forest experienced two violent tornadoes in April of 2009 that resulted in three deaths, 30 injuries, and over \$130 million worth of property damage (NCDC, 2011). These storms were part of a tornado outbreak that included at least 12 tornadoes in the southern United States on April 9<sup>th</sup>, Mena (NWS, 2009). The first event, rated an EF1, started its four mile track in La Flore County, Oklahoma at approximately 18:34:00 PM CST and ended its destruction within the Ouachita National Forest, knocking down hundreds of trees in the process (Figure 2.5). The second event, rated an EF3, caused more human impact but less forest damage, started at approximately 19:02:00 PM CST to the southwest of Mena and ended its fifteen mile path of destruction northeast of Ink (NCDC, 2011).



**Figure 2.5.** An uprooted rootwad with several other windthrows in the background at the Mena Blowdown site.

Being the only study site in the west-central portion of the forest, the Mena Tornado Blowdown site is located in the Central Ouachita Mountains. This area is considered to have some of the most rugged terrain within the Ouachita Mountains with shallow, rocky soils, and narrow valleys (The Nature Conservancy, 2003).

## II. Site Methodology

### A. Alum Creek Experimental Forest

Site selection criteria for this study site includes (1) knowledge of the area, based on past research completed in the area in 2005 by Phillips and Marion (2008), (2) the area's accessibility by automobile and hiking (3) the known presence of sufficient numbers of uprooted trees and (4) location within the Ouachita Mountain Range setting similar to that of the Rock Creek and Mena Blowdown areas. It was also important for this study that salvage logging and other timber activities were limited for a favorable data acquisition setting. Areas of salvage logging and other timber activities can potentially disrupt the ability to physically acquire data as well as cause inappropriate assumptions to be made about the forcing mechanism of treethrow or other tree specific factors that are important for this study. Figure 2.6 shows the locations of each of the sampled treethrows.

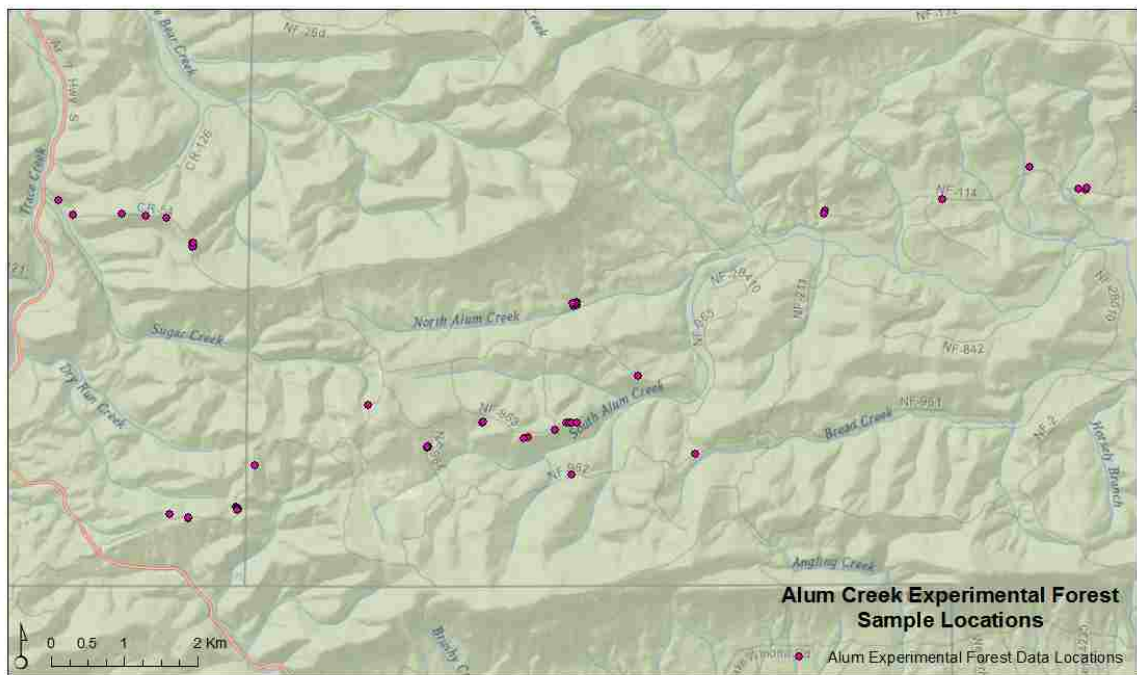


**Figure 2.6** Sampling locations in the Alum Cree Experimental Forest area.

In an effort to maintain a representative subset of the uprooted trees in the area, data was collected on 47 uprooted trees from the Alum Creek Experimental Forest area. The following data were collected for the 47, cycle-of-life type, uprooted trees at the Alum Creek Experimental Forest:

- 1) Latitude and longitude
- 2) Type of Fall (Cross slope, downslope, upslope)
- 3) Position on slope (ridge, top portion of slope, midslope, bottom of slope, flat or valley area) (Figure 2.8)
- 4) Diameter at breast height

- 5) Decay class
- 6) Slope angle
- 7) Tree type (conifer or hardwood)
- 8) Presence or absence of bedrock in rootwad
  - a. Type of bedrock if present
  - b. Estimation of percent of bedrock in wad
- 9) Wad dimensions (width, thickness, height, area, volume) (Figure 2.7)

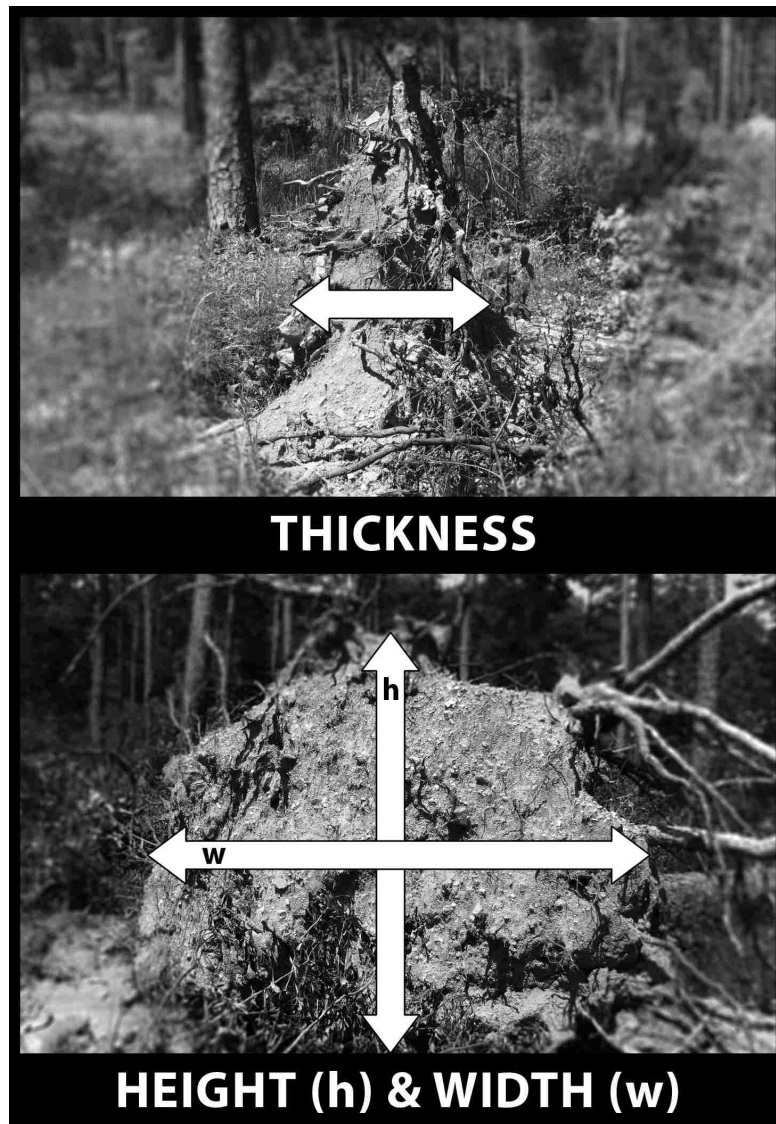


**Figure 2.7** Root wad measurements taken.



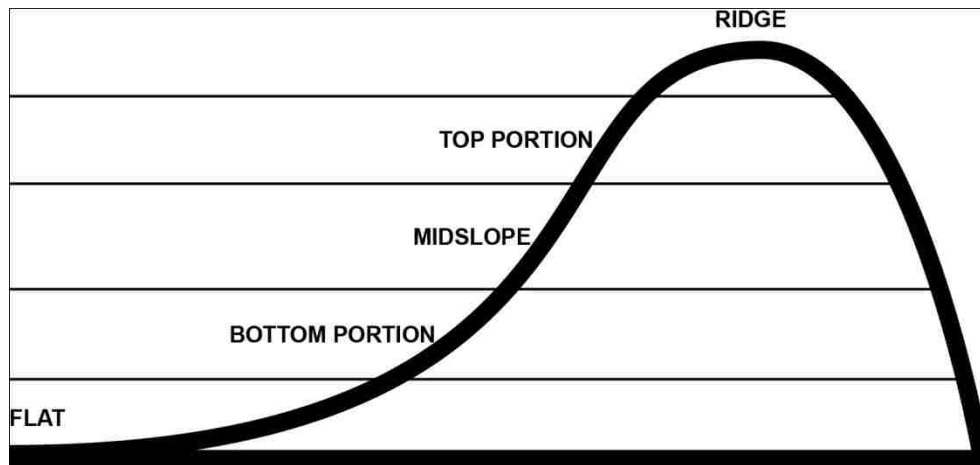


**Figure 2.8**Diagram showing the definitions of the position on slope parameter.

The latitude and longitude of all sampled trees were determined using a GPS unit. Type of fall, position on slope, and species classification were visually addressed and recorded using a digital camera. Diameters at breast height and rootwad dimensions were ascertained using metric unit measurement tape. Multiple width, height, and thickness measurements were taken to accurately represent the dimensions of each root wad. In uprooting sites where the root wad was not present, the dimensions of the pit were measured using similar techniques. The depth of the pit was measured at the deepest point, while multiple measurements were taken for width and height. These measurements were averaged and then used to estimate root wad surface area and volume. The formula used to determine the rootwad surface area was  $Area = height \times width$  and the formula for volume was  $Volume = Area \times thickness$ . The number of measurements taken in the field depended upon the complexity of the geometry of the wad and pit. Slope angle was determined using a compass clinometer. After a sufficient number of photographic records were logged, presence or absence of bedrock, the type of bedrock if present, and percentage of bedrock in the total rootwad mass was visually determined once the wad mass was broken with a mattock.

Decay class (Table 2.1) was modified from Spetich et al. (2002) and recorded for each uprooting site. This parameter will serve as a proxy for obtaining an estimate of time since the tree initially uprooted.

**Table 2.1** Description of modified decay classes from Spetich et al. (2002)

| <b>Class</b> | <b>General Appearance</b>                        | <b>Leaves</b>    | <b>Bark</b>            | <b>Branches/Twigs</b>                    | <b>Wood Condition</b>  |
|--------------|--|------------------|------------------------|--|--|
| <b>1</b>     | Living; some coarse roots still embedded in soil | Present/green    | Tight, intact          | Large and small branches, twigs, present | Hard, intact   |
| <b>2</b>     | Recently dead                                    | Present/green    | Tight, intact          | Large and small branches, twigs, present | Hard, intact   |
| <b>3</b>     | Dead; trunk retains original size and shape      | Sparse to absent | Loose or partly absent | Twigs sparse or absent                   | Hard to partly decayed                                       |
| <b>4</b>     | Dead; trunk retains original size and shape      | Absent           | Trace to absent        | Mostly large branches present            | partly decayed (knife can be inserted)                       |
| <b>5</b>     | Dead; trunk mostly retains size and shape        | Absent           | Absent                 | Absent                                   | Heavily decayed (knife easily inserted 3" or more into wood) |
| <b>6</b>     | Dead; trunk no longer has original shape         | Absent           | Absent                 | Absent                                   | Very heavily decayed (can be excavated with bare hands)      |
| <b>7</b>     | Only approximate trace of downed tree event      | Absent           | Absent                 | Absent                                   | Only sporadic pieces of heavily decayed wood                 |
| <b>8</b>     | No evidence of tree; pit-mound only              | Not applicable   | Not applicable         | Not applicable                           | Not applicable   |
| <b>8A</b>    | No evidence of tree; Probable pit-mound only     | Not applicable   | Not applicable         | Not applicable                           | Not applicable   |

A geographic information system (GIS) was employed to determine the following data for the sample locations within the Alum Creek Experimental Forest site:

- 1) Aspect
- 2) Soil map unit
- 3) Underlying bedrock
- 4) Mean stand DBH

Site aspect was calculated using the Spatial Analyst tool in ArcMap 10.0 from elevation data at the 1/3 arc-second (30 m) resolution available from the United States Geological Survey (2011). Soil data was gathered from National Resources Conservation Service, Soil Survey Staff (2011). The presence of unweathered bedrock disturbed by the tree roots was confirmed by sight. Those appearing “fresh” or lacking in weathered or rounded surfaces were counted as mined bedrock. Lithologic mapping unit data, or geologic formation information, at the 1:24,000 scale was also available through the USGS data repository (USGS, 1993). Mean stand DBH was calculated by taking the

mean of all DBH data available for each USDA-FS delineated stand using USDA-FS stand data (2008).

### B. Rock Creek Blowdown Area

After scouting impacted areas on foot and in aerial photographs, two sample areas with several separate transects each were chosen from areas of severe damage in the far northeastern portion of the forest (Phillips et al., 2008). The Rock Creek (RC) sample area (RC) was originally sampled by Phillips, Marion, and Turkington using three separate transects (2008). This sampling area had two transects (Figure 2.9). All data collected at this site was acquired by Phillips, Marion, and Turkington (2008b).

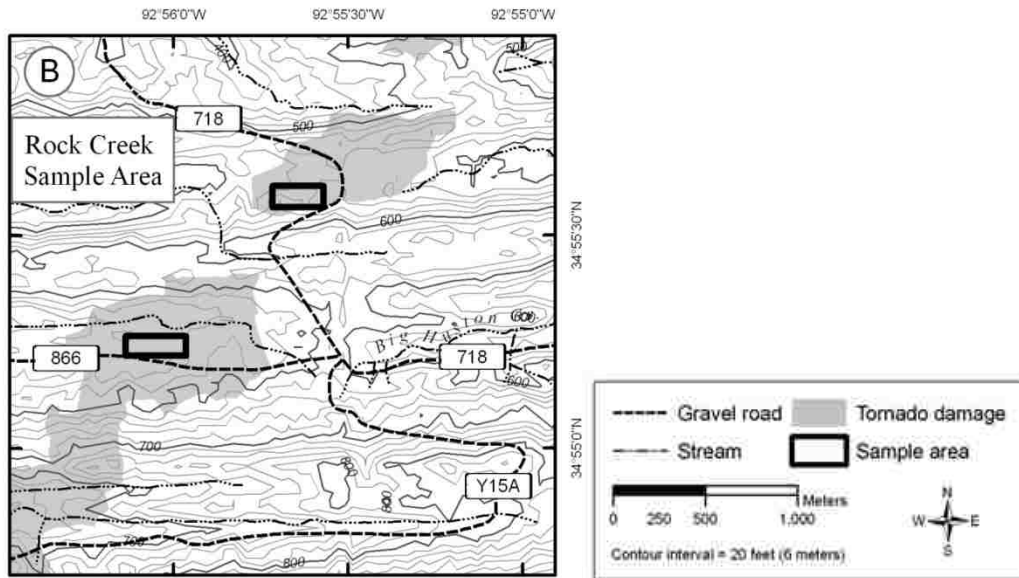


**Figure 2.9** Map location of areas that were sampled using transects for the Rock Creek blowdown area. Figure from Phillips et al., 2008b.

For the Rock Creek Tornado Blowdown area the exact spatial location of sampled treethrows were not collected. However, from previously published maps I was able to determine the approximate areas that were sampled (Figure 2.10) (Phillips et al., 2008a).



**Figure 2.10** Aerial view of the Rock Creek Tornado Blowdown Site. Imagery courtesy of Bing Maps through ArcMap.

Each transect was 5 meters wide from each side of a randomly selected placement of a centerline (10 meters wide total) and with varying width according to the extent of localized extreme damage. All treethrows that had any part of the trunk within the transect were included in the study. NAC-1 had 15 samples, NAC-2 had 9, RC-1 had 12, RC-2 only 3, and RC-3 had 6 uprooted trees. Since the blowdown consisted of only shortleaf pine, tree type was not included as a study parameter for this site. The following field data were collected for the 45 downed trees in the Rock Creek blowdown area:

- 1) Diameter at breast height
- 2) Wad and pit dimensions (width, thickness, height, area, volume)
- 3) Presence or absence of unweathered mined bedrock

The following geospatial data was collected for the Rock Creek blowdown site:

- 1) Underlying bedrock
- 2) Soil mapping unit
- 3) Mean stand DBH

Mean wad and pit dimensions were recorded from the average of multiple measurements using either a folding ruler or measuring tape. DBH was recorded using a dendrometer diameter tape. As done in the 2011 Alum Creek Experimental Forest, the

number of measurements taken in the field depended upon the complexity of the geometry of the wad and pit. These measurements were averaged and used to estimate the surface area and volume of disturbed soil. The presence of unweathered bedrock disturbed by the tree roots was confirmed by sight. Those appearing “fresh” or lacking in weathered or rounded surfaces were counted as mined bedrock. Geologic and soil geospatial data was obtained from the same sources as used for the Alum Creek Experimental Forest. Mean stand DBH was calculated by taking the mean of all DBH data available for each stand from USDA-FS data (2008).

### C. Mena Blowdown Area

Two transects were used (named MBA and MBB) at the Mena Blowdown Area. For both transects, the starting point of the centerline was randomly chosen. The centerline was oriented so that it would cross, perpendicular to the evident tornado path, beginning in an area of mild to moderate damage through the center of severe damage, so that a sample of all levels of damage could be included in the dataset. The beginning and end points of each centerline was recorded with a global positioning receiver. MBA was comprised of two subtransects – one parallel to the path of the tornado and the other subtransect perpendicular to the path. MBB also used two subtransects but both were perpendicular to the path of the tornado. Figure 2.11 is a hypothetical graphical representation of the sampling path taken. Unfortunately, time limitations restricted the full width of transect MBB.

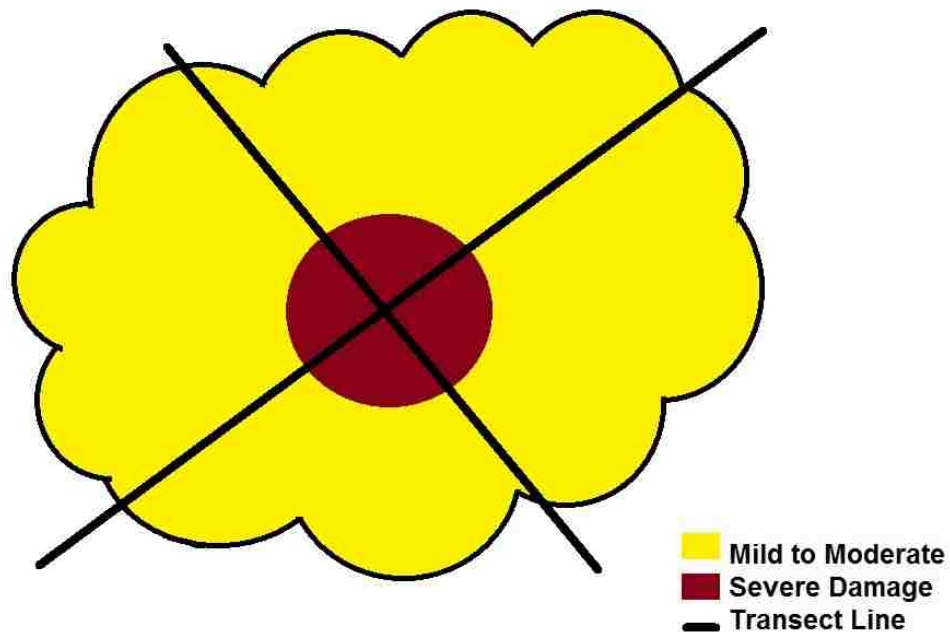


**Figure 2.11** Drawn hypothetical example of transects for MBA.

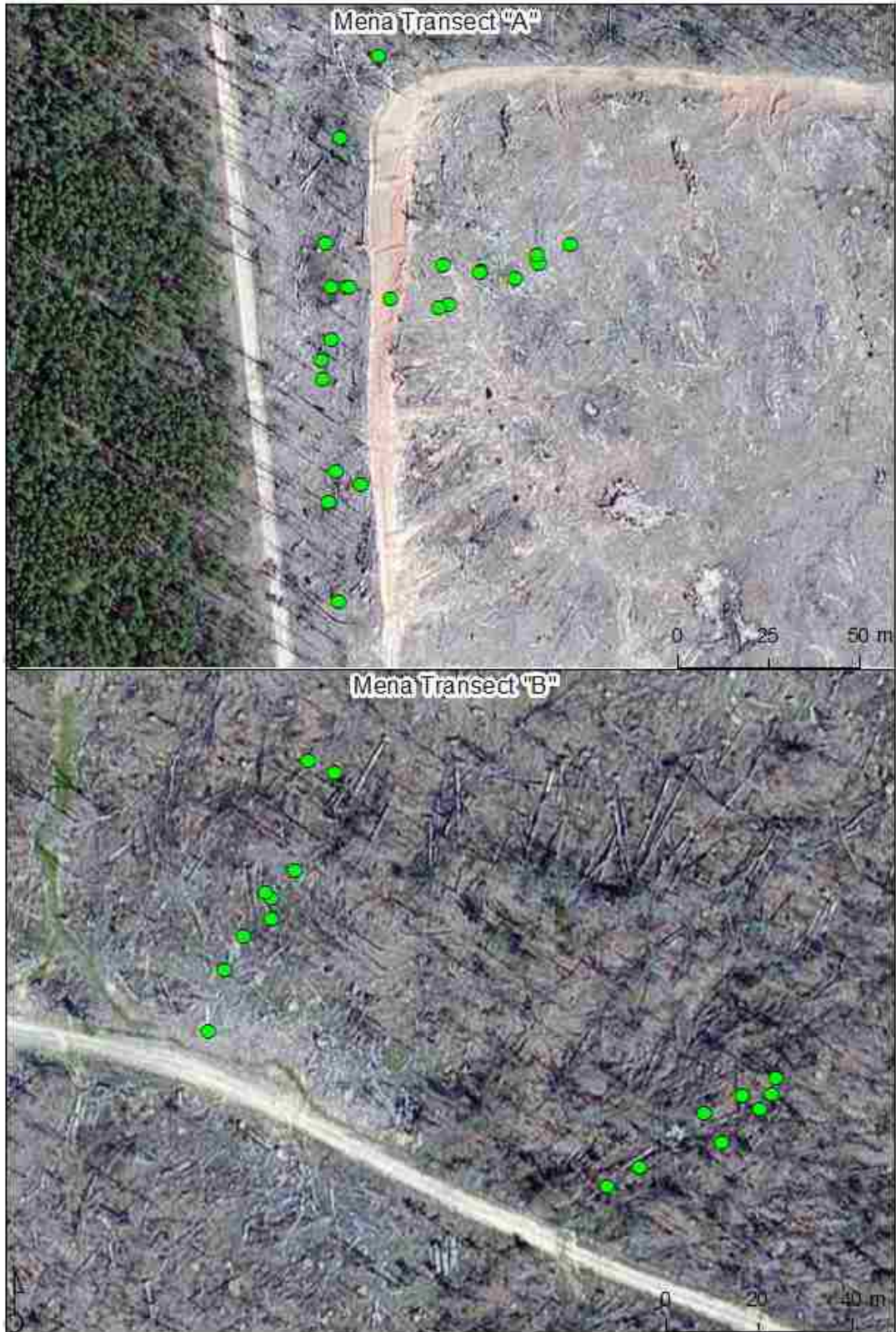


**Figure 2.12** Aerial view of the Mena Tornado Blowdown site transects. Imagery courtesy of Bing Maps for ArcMap.

Those rootwads located within 5m of the transect centerline were included within the study, making the width of each transect a total of 10m. Due to the fact that tree type in the blowdown area was composed of only shortleaf pine, tree type was not included as a parameter for this site. The following data were collected for the fifty-two downed trees in the Mena Tornado Blowdown area are:

- 1) DBH
- 2) Wad dimensions (width, thickness, height, area, volume)
- 3) Soil type
- 4) Presence or absence of unweathered mined bedrock

In addition, bedrock type or parent material was recorded from visual analysis or through utilization of a soil auger in the pit for each sample. Just as done with the Alum Creek Experimental Forest, a GIS was employed to aide in forming a complete idea of the importance of factors that determine the location of hotspots. The following data was collected for the sampled locations within the Mena Blowdown site:

- 1) Slope
- 2) Aspect
- 3) Soil mapping unit
- 4) Underlying bedrock
- 5) Mean stand DBH

Soil type was classified in the field by a USDA-FS soil staff member (2009). Soil mapping units were taken from the NRCS online SSURGO database (2011). There were some differences between the classification information provided by the soil scientist and the online database of mapping units as can be seen in the base data maps following. But, this is to be expected considering the high degree of soil variability over small areas within the forest (Phillips and Marion, 2005). Site aspect, slope, and geology data were likewise gathered from the same sources as in the Alum Creek area analysis.

Maps showing the unaltered geospatial data to be used in the mapping process can be found in Appendix A.

## Chapter Three

### Methodology

#### I. Statistical determination of variables correlated to bedrock mining

Again, the goals of this study are the following:

3. To determine the abiotic and biotic factors that are highly correlated with the potential for bedrock mining found in tree throws
4. To map areas highly likely to experience bedrock mining by means of tree throw

To ascertain areas within each of the three study areas that are highly likely to experience bedrock mining by means of tree throw in west-central Arkansas it was necessary to organize the acquired data. This was also completed to aid in the investigation of the second goal of this study - to map areas highly likely to experience bedrock mining by means of tree throw. First, topographic and tree location data sets were developed using existing data sets or location data acquired in the field. Next, the data for each study area were separated into two groups depending on whether bedrock mining was present or absent, and each variable was plotted on a graph to show the frequency of occurrence in the presence or absence of mined bedrock in tree throws.

Pearson's correlation and Fisher's Exact Test were used to provide an understanding of the relationship between variables and between variables and the presence or absence of mined bedrock. The Pearson's correlation indicates the linear strength of the relationship between two variables by giving a number within the range of -1 to +1. The resulting correlation number represents a perfectly inverse linear relationship at -1, no relationship at 0, and a linear relationship at +1. SPSS, the statistical software, automatically generates the associated p-values for each Pearson's R value, which were used to set thresholds for entry into the logistic regression model. Relatively strong P-values were accepted for testing primarily due to the low occurrence of statistically significant P-values in this study. The approach of accepting relatively strong P-values is further justified by a review of the literature concerning factors that control the occurrence of bedrock mining.

Fisher's Exact Test is a chi-square statistic that was used within this analysis because it allows for the testing of categorical data. Generally displayed as a contingency table, the chi-square test compares the observed count in each cell to the hypothesized/expected count to test the hypothesis of "no association" between the rows and columns. Fisher's Exact test was applied to all three sites for all categorical variables over the more commonly applied Pearson's Chi-square test in order to avoid the test's assumption that each item has an expected frequency of five or more. A relatively high P-value indicates a stronger association between the factor in question and bedrock presence. It is important to point out that the chi-Squared Fisher's Exact Test is nonparametric. Nonparametric procedures do not require that the study populations have a normal distribution or make any variance assumptions about the sample populations (IBM Corporation, 2011). Nonparametric tests are less powerful than parametric tests but



they have the advantage of being able to be applied to categorical data – which is necessary in the case of this study.

## **II. Modeling factors using binary logistic regression**

To satisfy the first goal of this study, testing for multicollinearity was followed by modeling the relevant factors using binary logistic regression. Multicollinearity should be avoided in modeling. It is the result of strong correlations among pairs of predictor variables in regression analysis. Multicollinearity furthermore inflates the variances of parameter estimates and provides undesirable repetition of results. To test for this, collinearity diagnostics were performed in SPSS, providing tolerance and variance inflation factors (VIF) for each explanatory variable. High tolerance values indicate high multicollinearity in the model. In less robust models, such as those produced in this study, tolerance values above 2.5 would cause concern of high model multicollinearity (personal correspondence with Dr. Arne Bathke of the Advanced Statistics Laboratory at the University of Kentucky, 01/18/2011). To apply collinearity testing to the categorical variables, each variable was transformed into a set of dummy numerical variables.

Binary logistic regression was used to predict the occurrence of mined bedrock. Logistic regression is useful for this analysis because it attempts to fit a model that describes the relationship between a dependent variable (presence/absence of bedrock mining) and a set of independent variables (Van Den Eeckhaut et al., 2006). Logistic regression allows for the prediction of how explanatory variables can affect a dichotomous outcome. The test is considered “binary” because the logistic regression analysis assesses the predominance of selected factors on a dichotomous outcome, in this case as presence or absence (Anderson, 1982). The dependent variable in question, presence/absence, is discrete and not continuous so therefore logistic regression is the most appropriate test.

The application of logistic regression techniques have been used extensively in the prediction of landslide events (Ayalew and Yamagishi, 2005, Dai and Lee, 2002, Dai and Lee, 2003, Duman et al., 2006, Ohlmacher and Davis, 2003). For example, Ayalew and Yamagishi (2005) examined the relative importance of seven variables, including proximity to roads to study anthropogenic forcing, in landslide formation on the coast of Japan. Likewise, Dai and Lee (2002) used multiple logistic regression to map areas outside of Hong Kong that would be of very low, low, moderate, or high relative susceptibility to land sliding based on several topographic factors. In the USA, Ohlmacher and Davis (2003) also used logistic regression to determine that, for the Atchison area of Kansas, slope and geology are the best predictor variables for evaluating landslide hazard areas. Van Den Eeckhaut et al. (2006) used logistic regression to create a landslide susceptibility map in Belgium using low, moderate, high, and very high classes of susceptibility.

The reason for the extensive application of logistic regression modeling is that it “fits” the odds ratio of explanatory variables to a regression function, forming a set of odds of an event happening or not happening. The odds described here are essentially the rates of the proportions for the two possible outcomes for each sample, 0 or 1, absence or presence of bedrock mining activity. Logistic regression allows for explanatory variables

to describe how the probability of an event occurring (1) or not occurring (0) depends upon these explanatory variables. For example, in this study I am interested in the presence (1) or absence (0) of bedrock mining activity.

Given that there are only two possible outcomes (or response categories), 0 or 1, absence or presence, it must be that the outcome or response probability ( $p$ ) is  $0 \leq p \leq 1$  and that logistic regression models the outcome or response in terms of some explanatory variable(s). The logistic regression method uses the log odds (as in **logistic** regression) in the place of simple odds commonly seen in straightforward linear regression. Using the natural logarithm transforms this to produce the statistical model for logistic regression:

$$\log\left(\frac{p}{1-p}\right) = \beta_0 + \beta_1 x \quad \text{Equation [3.1]}$$

Where  $p$  is the binomial proportion and  $x$  is the explanatory variable.  $\beta_0$  and  $\beta_1$  are the parameters of the logistic regression model.

The equation used to describe the logistic regression is:

$$\text{Mined bedrock present} = \frac{e^{(\alpha + \beta_1 x_1 + \beta_2 x_2 + \dots + \beta_i x_i)}}{1 + e^{(\alpha + \beta_1 x_1 + \beta_2 x_2 + \dots + \beta_i x_i)}} \quad \text{Equation [3.2]}$$

Where  $\alpha$  = the constant of the derived equation and  $\beta$  = the coefficient of the predictor variables. Several of the possible explanatory variables are categorical as opposed to only quantitative variables. Part of the power behind this method is that it allows categorical and/or numerical variables to predict any sort of categorical phenomenon by “dummy coding” the categorical variables (King, 2008)!

For this study, variable selection within SPSS 20.0 was performed using the “Forward Stepwise (Conditional)” method as use by Ozdemir (2011), Van Den Eeckhaut et al. (2006), Ayalew and Yamagishi (2005), and Dai and Lee (2002). In this method, each variable is *added* one at a time, step-by-step into the model. The operator is able to set the entry threshold  $p$ -value (with presence) for acceptance into model testing (IBM Corporation, 2011). Likewise, the operator is also required to set a threshold for removal from the modeling process. Variables that do not have a high enough likelihood-ratio statistic, based on conditions set by the operator, are removed. Due to the differences at each site, different entry and removal thresholds were accepted based on the Pearson’s correlation values and Fishers’ correlation coefficients. In other words, the Forward Stepwise (conditional) method allowed me to accept relatively high  $p$ -values into the modeling process. I chose to use models that included a constant term.

Several tests are performed on each of the steps of the stepwise logistic regression. The likelihood ratio (-2 Log likelihood) is used to compare the how each of the steps compare (UCLA, 2012). Generally, the smaller the -2 Log likelihood, the better the model. The Cox & Snell  $R^2$  is can be interpreted like a more commonly understood  $R^2$  of multiple regression. The Nagelkerke  $R^2$  is much like the Cox & Snell  $R^2$  but does not range from 0 to 1 (UCLA, 2012).

The binary logistic regression results are explained by the following parameters: the logit coefficient (B), significance (Sig.), and the odds ratio. The significance is  $p \leq 0.05$ . The “B” column in each of the regression results sections is the logit coefficient or

the estimated logistic regression coefficient(s) for the model. One can understand this value as the change in the average value of the dependent variable (odds of presence) from a unit of change in the independent variables. For example, given an increase of one unit of a given variable, if the “B” value for the example variable is -0.035 then the odds would be expected to decrease by 0.035 units when all other variables are held constant in the model (UCLA, 2011). These logit coefficients are what form the coefficient value, or weights, for the terms in each particular site’s regression equation. It is these logit coefficients that will be used in the mapping process discussed later. Those variables not included in the model did not improve the overall goodness of fit. Or, in other words, the explanatory variable in question did not make a significant contribution to the predictive portion of the model (IBM Corporation, 2011).

Next, in each of the tables the standard errors of the individual regression coefficients are listed. “Sig.”, or the significance, is the two-tailed *p*-value of the coefficients. Per the definition of a *p*-value, if the “Sig.” value for a given variable is 0.999 then one can conclude that if another random sampling of the area (Alum Creek Experimental Forest or one of the two tornado blowdown areas) the sampling difference would be smaller than observed in the actual samples taken 99.9% of the time and larger than actually observed in 0.01% of cases (UCLA, 2011).

Finally, the odds ratio (OR) can be described as:

$$\frac{\text{Probability of positive mined bedrock}}{\text{Probability of no mined bedrock}} \quad \text{Equation [3.3]}$$

And

$$\text{Probability} = \frac{\text{Odds}}{1+\text{Odds}} \quad \text{Equation [3.4]}$$

(Sweet and Grace-Martin, 1998). This ratio denotes how many times greater the odds of positive mined bedrock are for each one unit increase in the independent variable (whichever factor being examined) (Sweet and Grace-Martin, 1998). To clarify this, an example is useful. So, given an odds ratio of 0.013, the odds of bedrock being mined is decreased by a factor of 0.013 if the explanatory variable (named variable) is compared to some other explanatory variable in the same category (like comparing two types of bedrock), when the other variables in the model are controlled. On the other hand, if the odds ratio is >1, the odds will increase likewise by that factor. In other words, if the odds ratio is greater than one the probability of bedrock mining is increased and if the odds ratio is less than one the odds of bedrock mining activity occurring is decreased.

Separate models were developed for each study location. The reasoning for this is that the forcing mechanisms, tornado blowdowns or cycle-of-life events are fundamentally different between sites, and are likely to be controlled by different variables.

Once again, Pearson’s Correlation was used to examine the following variables:

- 1) Wad dimensions (width, height, thickness, area, and volume)
- 2) DBH
- 3) Slope<sup>#</sup>
- 4) Decay Class\*

Fisher's Exact test was applied to the following variables:

- 1) Type of fall (Cross slope, downslope, upslope)\*
- 2) Position on slope (ridge, mid-slope, etc.)\*
- 3) Aspect<sup>#</sup>
- 4) Soil mapping unit
- 5) Underlying bedrock
- 6) Tree type\*

<sup>#</sup>. indicates that the variable was only tested for the Alum Creek Experimental Forest and Mena Tornado Blowdown sites

\* indicates that the variable was only tested for the Alum Creek Experimental Forest

### **III. Geospatial Data Compilation**

The location data gathered in the field from all samples were loaded into an ARCInfo point type shapefile. This includes the following data for the Alum Creek Experimental Forest:

- 1) Latitude and longitude
- 2) Type of Fall (Cross slope, downslope, upslope)
- 3) Position on slope (ridge, mid-slope, etc.)
- 4) Diameter at breast height
- 5) Decay class
- 6) Slope angle
- 7) Tree type (conifer or hardwood)
- 8) Underlying geology
- 9) Soil mapping unit
- 10) Presence or absence of bedrock in rootwad
  - a. Type of bedrock if present
  - b. Estimation of percent out of 100 of bedrock in wad
- 11) Wad dimensions (length, width, height, area, volume)
- 12) Mean Stand DBH

For the Rock Creek tornado blowdown area the exact spatial location of sampled tree throws were not collected. However, from previously published maps I was able to determine the approximate areas that were sampled (Phillips et al., 2008a). Due to this, data that was capable of being gathered and displayed using the GIS was not useful in the statistical analysis. For this site data gathered in the field from all samples were loaded into an ARCInfo point type shapefile. This includes the following data:

- 1) Slope angle
- 2) Mean stand DBH
- 3) Wad dimensions
- 4) Soil mapping unit
- 5) Presence or absence of bedrock in rootwad
  - a. Type of bedrock if present
- 6) Underlying geology

For the Mena tornado blowdown area the location data gathered in the field and into an ARCInfo point type shapefile included:

- 1) Latitude and Longitude
- 2) Slope angle
- 3) Diameter at breast height
- 4) Tree type (conifer or hardwood)
- 5) Underlying geology
- 6) Soil mapping unit
- 7) Presence or absence of bedrock in rootwad
  - a. Type of bedrock if present
- 8) Wad dimensions (length, width, height, area, volume)

Base imagery was provided by ArcGIS Online map services, which is a built-in feature of the ArcMap program (ESRI, 2012). Elevation raster data retrieved from the National Elevation Dataset courtesy of the U.S. Geological Survey for both the Polk county and Saline and Perry county areas at the 1/3 arc second (10 m) scales. From this elevation data, aspect for both study sites was calculated using the Spatial Analyst extension in ArcMap. Similarly, because slope data was not collected in the field at the blowdown site, slope was also calculated using the Spatial Analyst extension in ArcMap for both transects, MBA and MBB. Soil data was gathered from National Resources Conservation Service, Soil Survey Staff (2011) and geology data was also available through the USGS data repository (USGS, 1993). Stand-scale DBH data was retrieved from employees at the Southern Research Station in Arkansas (Marion, 2012). Each of these variables was then joined to the original field data shapefile to create a geospatial dataset.

#### **IV. GIS Analysis**

To map future or potential areas of bedrock mining, each independent variable in the binary logistic regression model was then transferred for use in the GIS. The statistical analyses indicate the strength of association between the topographic, environmental, and tree specific variables with the presence of mined bedrock. Base map imagery varied between sites and within maps for the same sites based on scale and aesthetics. The method adopted in this study is similar to the method used by Ayalew and Yamagishi (2005).

Raster data was first classified and then converted to a polygon feature class. Point data, that which was gathered in the field, was left unaltered. The data acquired in the field will be joined with a soil, geology, DBH, elevation, slope, and aspect layer. From these analyses a map of “odds” was generated using ArcMap software. Equation coefficients, or logit coefficient in the tables for each site’s model, will be used in the mapping process. The logistic regression results allowed for three even breaks to be placed into the histograms of each of the applicable variables. These three groups represent the odds as high, medium, and low classes. In the case of any binary groupings, two classes of high and low odds were then mapped. Modified equal intervals have been

chosen as the preferred methodology because it allows for streamlined translation among variables, with breaks grounded in actual field data, as well as easier map interpretation. The intervals are termed “modified” because the equal intervals are chosen based on actual data points – not the full range of values possible. For example, slope angle in the Alum Creek Experimental Forest area ranges from 0 to 60 degrees. However, all data acquired there was taken within the range of 0 to 30 degrees. Therefore breaks at the 10 and 20 degree levels would equally break up the range of the actual data points. As is commonly the case in scientific studies, extrapolation is often necessary as complete data may not be possible to obtain or is completely impractical to attempt. As such, a degree of uncertainty is inherent in the data extrapolation used within this methodology but is limited by the fact that outliers and extreme values will rest within either a “high” or “low” odds defined area.

Using this methodology, for the Alum Creek Experimental Forest site, the approximate area of the Rock Creek Tornado Blowdown area, and the Mena Tornado Blowdown area a separate map for each variable with low, medium, and high odds (if applicable) was created. Extrapolated odds from the cycle-of-life uprooting events in the Alum Creek Experimental Forest were mapped for other areas of the Ouachita Mountains, including the location of the Mena and Rock Creek Tornado Blowdowns. Having this information is interesting because it allows one to answer the question, “What if the tornado had not traversed this area; where would the cycle-of-life tree throws mine bedrock in this area?”

## Chapter Four

### Results

The data collected in the field and from online sources for the Alum Creek Experimental Forest, the Rock Creek Tornado Blowdown, and Mena Tornado Blowdown sample areas are in appendices B, C, and D. These tables include all observed values and characteristics as well as the calculations for root wad surface area and volume.

47 treethrows were sampled in the Alum Creek Experimental Forest, 45 in the Rock Creek Tornado Blowdown area, and 51 in the Mena Tornado Blowdown area. Mined bedrock was found to be present in the majority, 88, of the aggregate (all sites) sampled tree throws with 55 or 38.4% lacking mined bedrock (Figure 4.1). For the cycle-of-life uprooting events of the Alum Creek Experimental Forest, 26 or 55% of the samples displayed bedrock with the slight minority, 21 or 45%, showing no mined bedrock. Altogether the tornado blowdown sites had nearly double the number of samples exhibiting mined bedrock, 62 or 65%, than those without unweathered mined bedrock, 34 or 35%. The Rock Creek blowdown showed an overwhelming majority of mined bedrock in 38 of the samples taken with only 7 samples showing none. In the blowdown area from the year 2009, the majority of treethrows exhibited no visible mined bedrock at 27 or 53% samples with the slight minority, 24 or 47%, having mined unweathered bedrock.

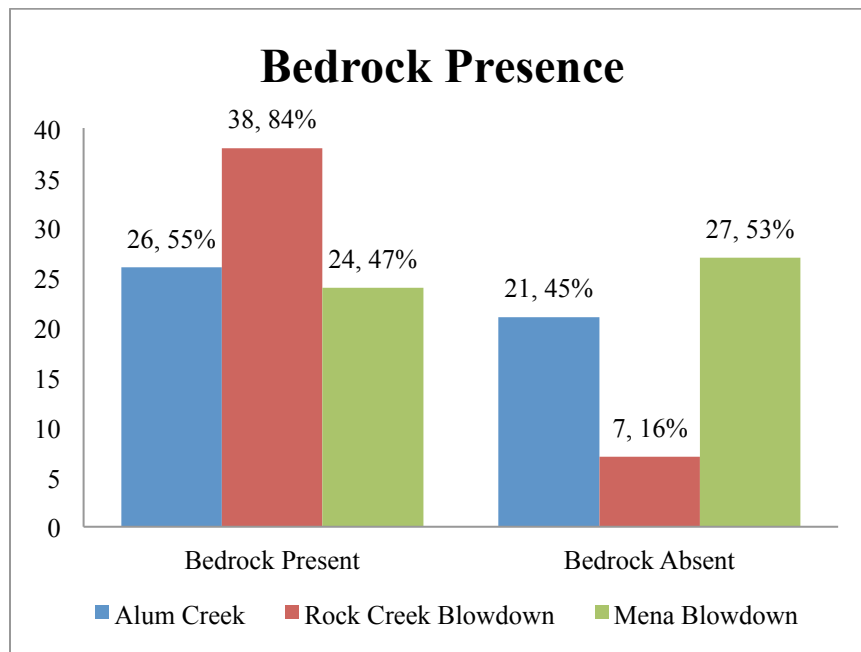


**Figure 4.1** Bedrock presence versus absence for all sites.

## I. Alum Creek Experimental Forest

For the 47 cycle-of-life uprooting events of the Alum Creek Experimental Forest, 26 of the samples displayed bedrock with the slight minority, 21, showing no mined bedrock. Bedrock mining is more common than rare in all variables at this site. The mean and range of values for all wad measurements is higher in the set of samples that contained mined bedrock (Figures 4.2-4.3 with further statistics in table 4.1). Decay class, seen in figure 4.5, and slope angle, in figure matched this pattern (see Figures 4.5 and 4.6). Most samples acquired were in the decay class “3” to “6” range. Contrary to what was expected, DBH values were lower for the samples with bedrock present than those without (Figure 4.4). Conifers and those trees whose type could not be determined showed a slight tendency for mining activity (Figure 4.8). Samples taken from areas of shale and sandstone bedrock types both favored mining bedrock, with the difference being a bit larger for sandstone than shale (Figure 4.9).

The majority of samples were taken from the Carnasaw-Townley-Pirum and the Carnasaw-Pirum-Clebit general soil map units (Figure 4.10). The Carnasaw-Townley-Pirum and Clebit-Carnasaw-Pirum map units demonstrated a modest inclination for mining activity. Moreover, the Carnasaw-Pirum-Clebit map unit presented a strong disposition for mining bedrock. The two samples taken from the Zafra-Leadvale and Ceda gravelly loam mapping units showed no mined bedrock. Likewise, the Carnasaw-Pirum-Townley map unit showed a preference for samples not mining. These soil mapping units count and presence/absence of bedrock data can be seen in figure 4.10 following.

However, because soil mapping unit data had so many categories it was further simplified by primary component unit (most abundant unit in a sample) (Table 4.1). For the Alum Experimental Forest four primary component units were identified; the Carnasaw, Ceda, Clebit, and Zafra. Their depth to bedrock ranged from shallow to very deep. The deep Carnasaw series showed a slight tendency to mine bedrock more often than not and was most commonly found with 40 samples. The shallow Clebit series mined bedrock more often than not and was found in 5 samples and the very deep Ceda and moderately deep Zafra were both found in 1 sample each, neither of which had mined bedrock.

Treethrows with South, West, Northeast, and Eastern aspects, in decreasing order, have the highest frequency of bedrock mining with the South showing quadruple the number of mined versus unmined samples (Figure 4.11). Alternately, the Southeast, Southwest, and Northern aspects were less likely to mine bedrock, in order of their likelihood of mining from greatest to least. From a crosstabulation of decay class and aspect (Figure 4.6), it appears as though some weather event or other forcing agent may have potentially caused a clustering of uprooting events on the southern and western aspects. Perhaps the southern and western aspects received the brunt of high winds or the load of a heavy ice storm compared to the northern and eastern aspects.

As far as type of fall is concerned (Figure 4.12), cross-slope falls had equal chances of uprooting mined bedrock or not. Downslope falls showed nearly twice as many positive samples and negative. On the other hand, upslope falls displayed a small



tendency for not mining bedrock. A large number of unknown positions on slope for the Alum Creek Experimental Forest unfortunately occurred during the collection process. Position on slope data can be seen in figure 4.13 following. Uprooted wads near the top, but not at the ridge of the slope, mined no bedrock. Ridgetop, flat, and midslope sites presented a predilection for mining activity, whereas sites occurring at the bottom of a slope had equal chances of uprooting mined bedrock or not.

For all boxplot figures, the term “unbooked” maximums and minimums refers to those points outside the minimum and maximum whiskers, in other words outliers!

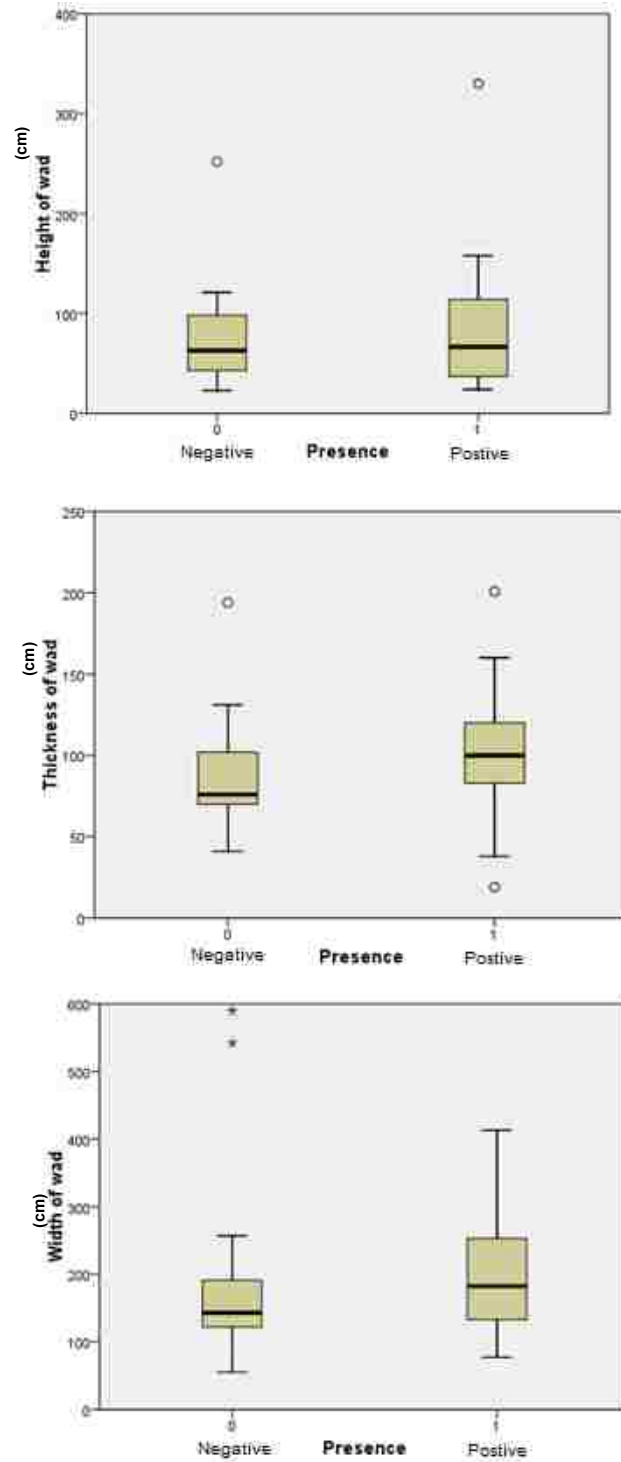


**Figure 4.2** Boxplots showing the unbooked minimum value, first quartile, median, third quartile, and unbooked maximum value of the wad dimensions gathered in the field (units centimeters) within the Alum Creek Experimental Forest. Circles denote outliers, values that do not fall in the inner fences, and stars denote extreme outlier values found in the dataset.

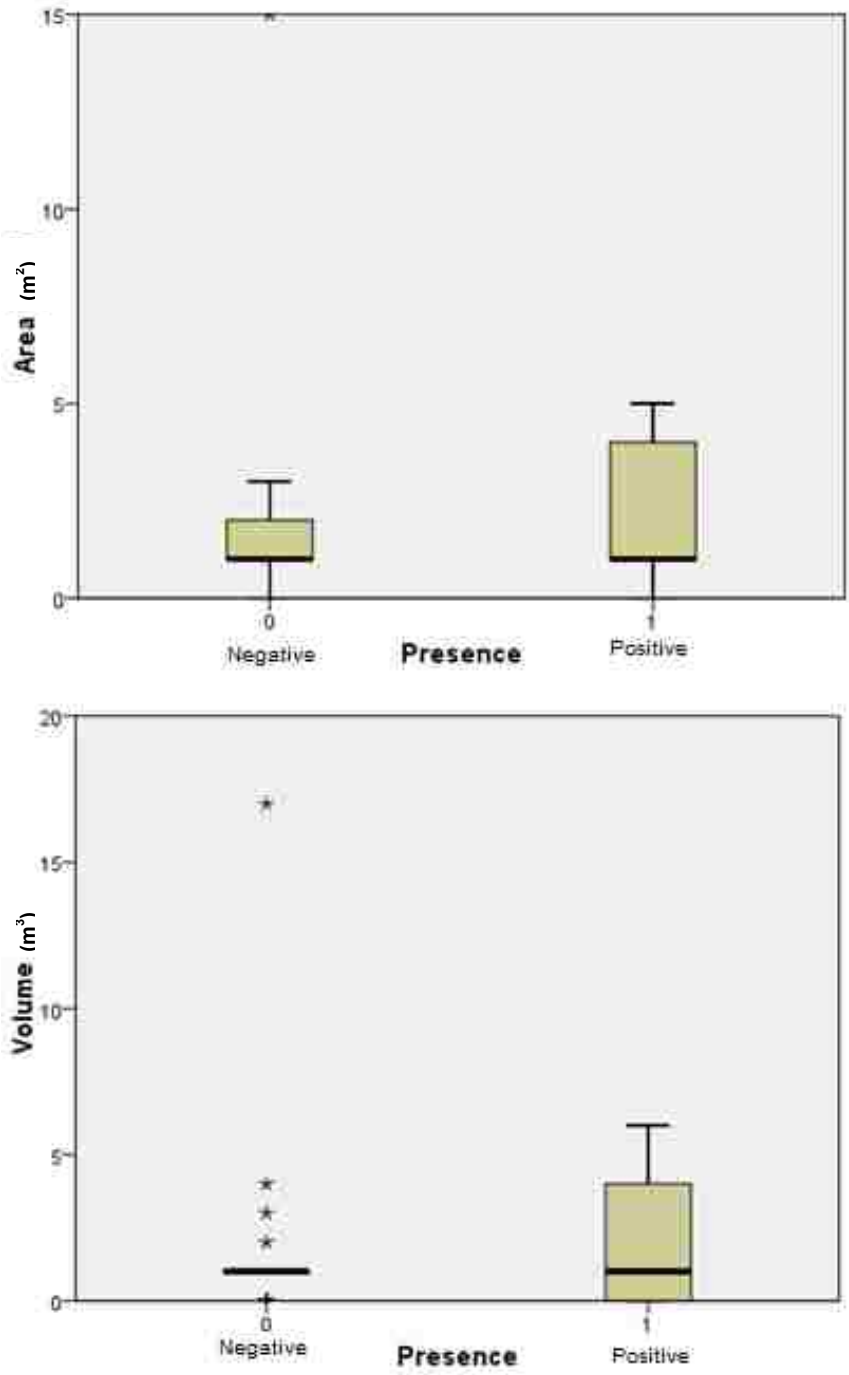


**Figure 4.3** Boxplots showing the unbooked minimum value, first quartile, median, third quartile, and unbooked maximum value of the wad dimensions calculated from wad dimensions gathered in the field within the Alum Creek Experimental Forest. Stars denote extreme outlier values. Area and volume units in square meters.

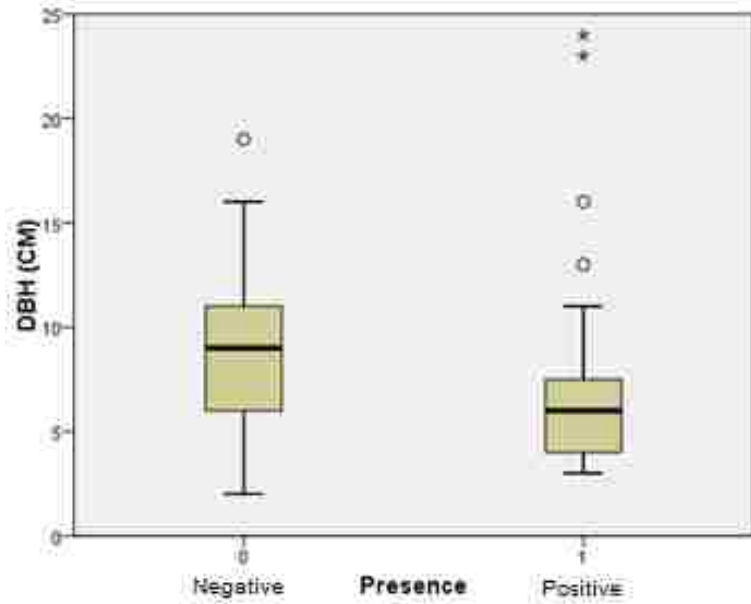


**Figure 4.4** Boxplot showing the unbooked minimum value, first quartile, median, third quartile, and unbooked maximum value of the diameter at breast height gathered in the field within the Alum Creek Experimental Forest. Circles denote outliers, values that do not fall in the inner fences, and stars denote extreme outlier values.

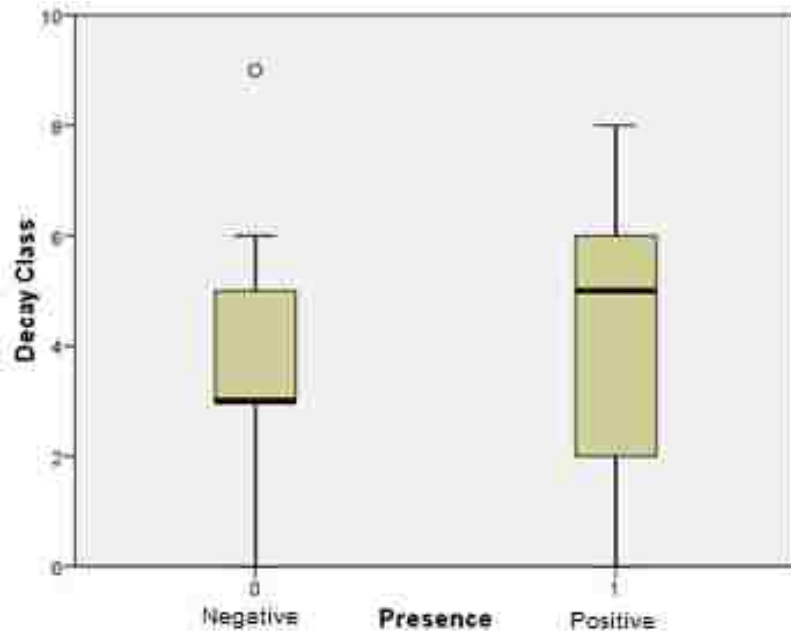


**Figure 4.5** Boxplot showing the unbooked minimum value, first quartile, median, third quartile, and unbooked maximum value of the decay class classification gathered in the field within the Alum Creek Experimental Forest. Circles denote outliers, or values that do not fall in the inner fences.

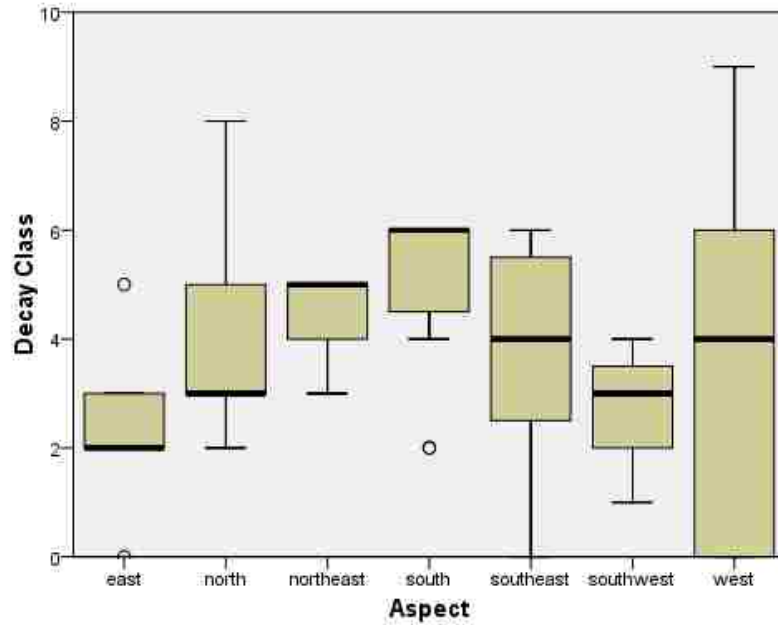


**Figure 4.6** Boxplot showing the unbooked minimum value, first quartile, median, third quartile, and unbooked maximum value of decay class classification gathered in the field in comparison to the aspect on which they were discovered in the Alum Creek Experimental Forest. Circles denote outliers, or values that do not fall in the inner fences.

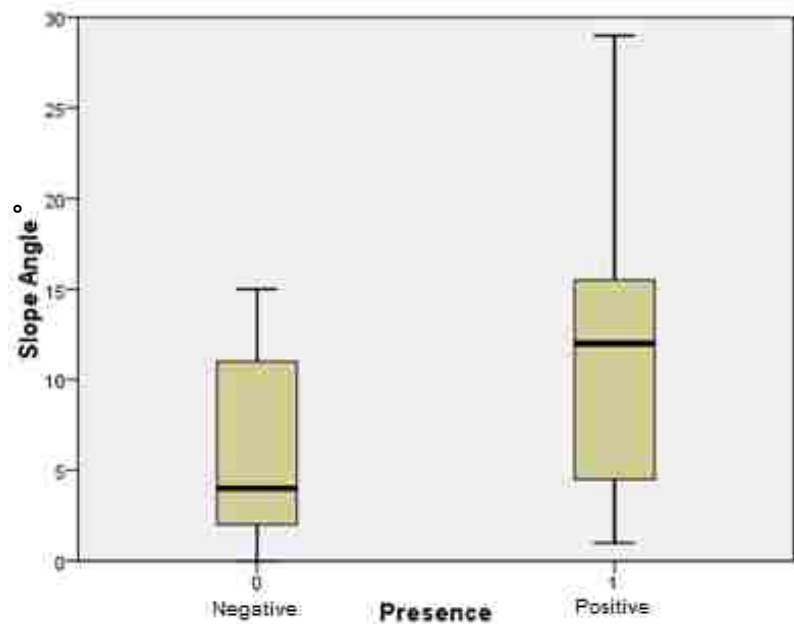


**Figure 4.7** Boxplot showing the unbooked minimum value, first quartile, median, third quartile, and unbooked maximum value of the slope angle calculated in the field (units degrees) in the Alum Creek Experimental Forest.

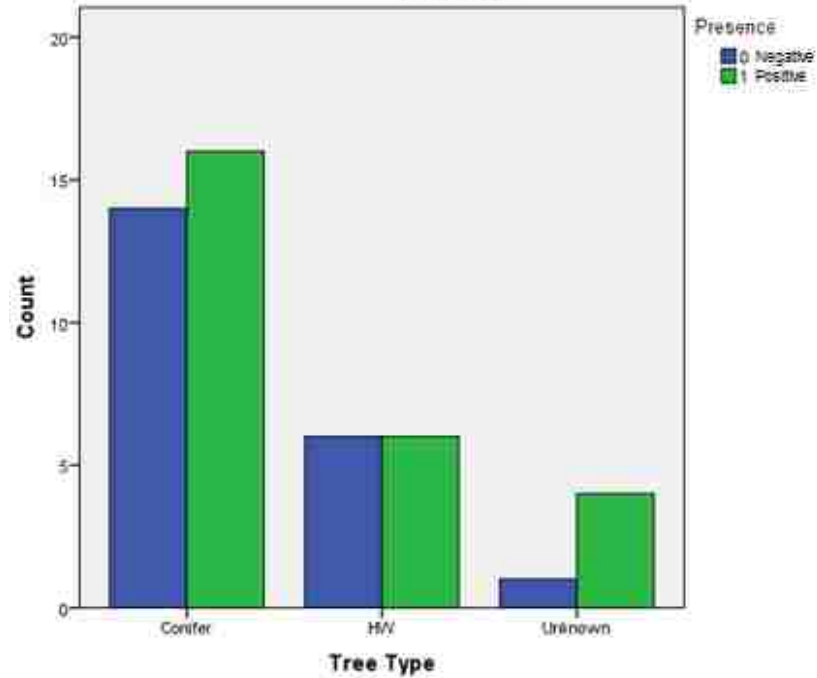


**Figure 4.8** Count of tree type data sampled in the field. “0” denotes the absence of mined bedrock found and ‘1” denotes presence in the Alum Creek Experimental Forest.

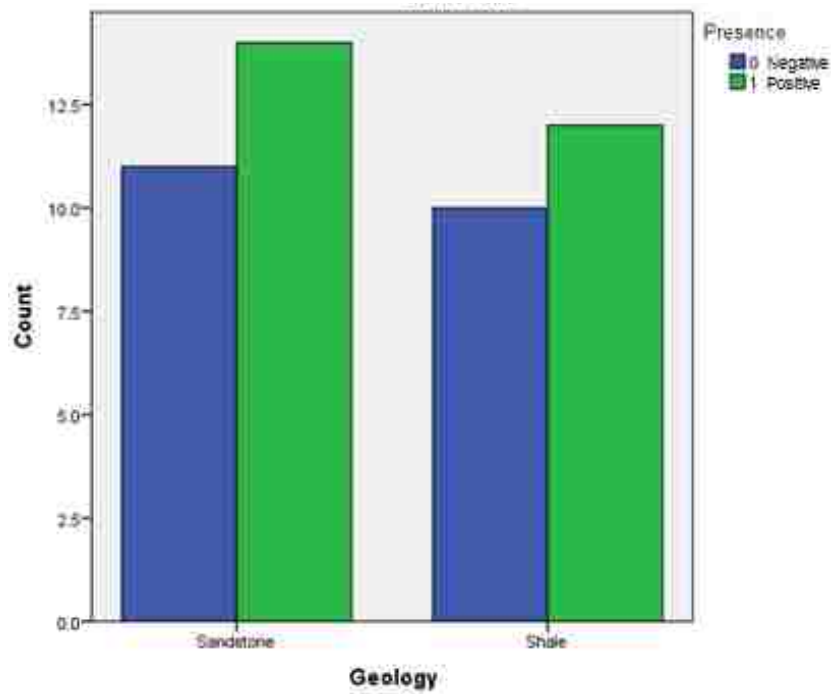


**Figure 4.9** Count of geology data sampled in the field. “0” denotes the absence of mined bedrock found and ‘1” denotes presence in the Alum Creek Experimental Forest.

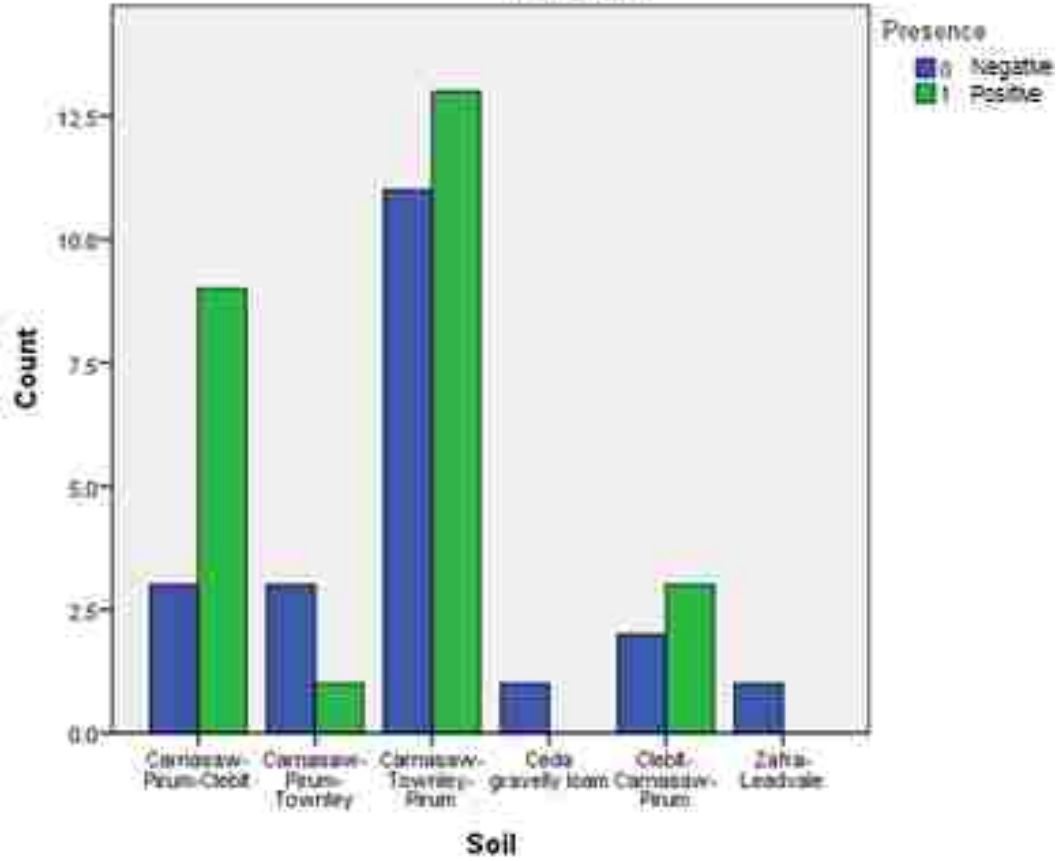


**Figure 4.10** Count of soil data gathered using a GIS. “0” denotes the absence of mined bedrock found and ‘1’ denotes presence in the Alum Creek Experimental Forest.

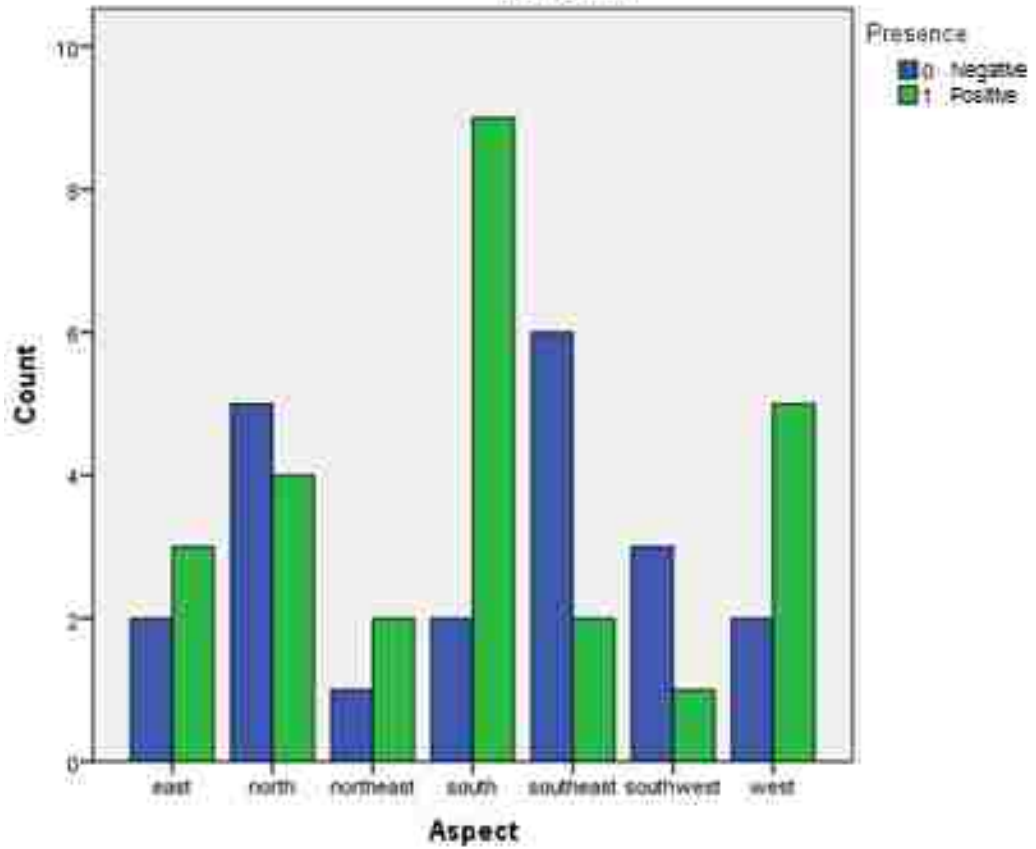


**Figure 4.11** Count of aspect data gathered using a DEM in a GIS. “0” denotes the absence of mined bedrock found and “1” denotes presence in the Alum Creek Experimental Forest.



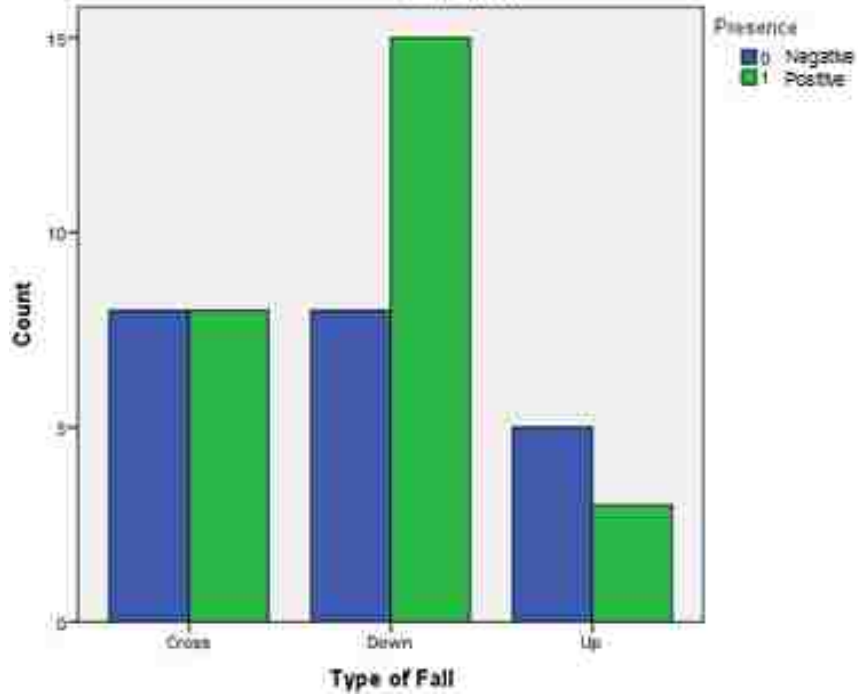


**Figure 4.12** Count of type of fall data sampled in the field. “0” denotes the absence of mined bedrock found and ‘1’ denotes presence in the Alum Creek Experimental Forest.

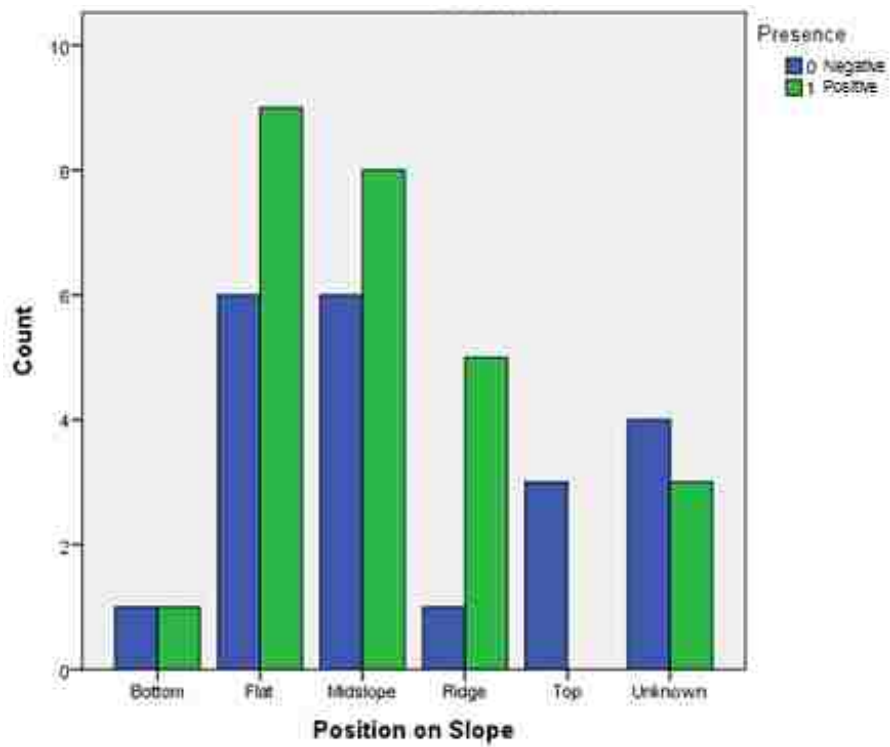


**Figure 4.13** Count of position on slope data sampled in the field. “0” denotes the absence of mined bedrock found and ‘1’ denotes presence in the Alum Creek Experimental Forest.

Table 4.1 further describes the numerical data (below). The degrees of freedom varied by the availability of data.

**Table 4.1** Descriptive statistics of numerical data in the Alum Creek Experimental Forest. DBH, height, width, and thickness of wad in cm. Area in m<sup>2</sup> and volume in m<sup>3</sup>. Slope in degrees.

|                         | N  | Minimum | Maximum | Mean   | Percentiles |      |
|-------------------------|----|---------|---------|--------|-------------|------|
|                         |    |         |         |        | 25th        | 75th |
| <b>DBH</b>              | 40 | 2       | 24      | 8.15   | 4           | 10.5 |
| <b>Slope</b>            | 44 | 0       | 29      | 8.89   | 2.25        | 14   |
| <b>Height of wad</b>    | 47 | 23      | 330     | 80.72  | 113         | 242  |
| <b>Width of wad</b>     | 47 | 55      | 590     | 195.13 | 70          | 113  |
| <b>Thickness of wad</b> | 46 | 19      | 201     | 93.83  | 38          | 103  |
| <b>Area of wad</b>      | 47 | 0       | 15      | 1.87   | 1           | 3    |
| <b>Volume of wad</b>    | 47 | 0       | 17      | 1.91   | 0           | 3    |

The correlation analysis for the Alum Creek Experimental Forest found that no factors had a (Bonferroni corrected) significant relationship with the presence of mined bedrock (Table 4.2). However, the continuous variables most highly correlated with bedrock mining (Presence) are slope angle, wad thickness, DBH, and decay class. Interestingly, decay class had a relatively high correlation with wad height and volume as well as with DBH.

**Table 4.2** Pearson's probabilities from treethrows within the Alum Creek Experimental Forest samples.

|                        |                     | Presence | DBH (CM) | Height of wad | Width of wad | Thickness of wad | Area (m <sup>2</sup> ) | Volume | Slope Angle | Decay Class |
|------------------------|---------------------|----------|----------|---------------|--------------|------------------|------------------------|--------|-------------|-------------|
| Presence               | Pearson Correlation | 1        | -.101    | .086          | .038         | .181             | .006                   | .034   | .345        | .067        |
|                        | Sig. (2-tailed)     |          | .534     | .565          | .801         | .228             | .969                   | .820   | .022        | .656        |
|                        | N                   | 47       | 40       | 47            | 47           | 46               | 47                     | 47     | 44          | 47          |
| DBH (CM)               | Pearson Correlation | -.101    | 1        | .559          | .053         | .157             | .242                   | .226   | -.163       | -.282       |
|                        | Sig. (2-tailed)     | .534     |          | .000          | .746         | .332             | .132                   | .161   | .329        | .078        |
|                        | N                   | 40       | 40       | 40            | 40           | 40               | 40                     | 40     | 38          | 40          |
| Height of wad          | Pearson Correlation | .086     | .559     | 1             | .397         | .269             | .785                   | .778   | -.117       | -.305       |
|                        | Sig. (2-tailed)     | .565     | .000     |               | .006         | .071             | .000                   | .000   | .450        | .037        |
|                        | N                   | 47       | 40       | 47            | 47           | 46               | 47                     | 47     | 44          | 47          |
| Width of wad           | Pearson Correlation | .038     | .053     | .397          | 1            | .270             | .763                   | .721   | -.071       | -.192       |
|                        | Sig. (2-tailed)     | .801     | .746     | .006          |              | .070             | .000                   | .000   | .646        | .196        |
|                        | N                   | 47       | 40       | 47            | 47           | 46               | 47                     | 47     | 44          | 47          |
| Thickness of wad       | Pearson Correlation | .181     | .157     | .269          | .270         | 1                | .269                   | .407   | -.114       | .093        |
|                        | Sig. (2-tailed)     | .228     | .332     | .071          | .070         |                  | .071                   | .005   | .467        | .540        |
|                        | N                   | 46       | 40       | 46            | 46           | 46               | 46                     | 46     | 43          | 46          |
| Area (m <sup>2</sup> ) | Pearson Correlation | .006     | .242     | .785          | .763         | .269             | 1                      | .971   | -.154       | -.282       |
|                        | Sig. (2-tailed)     | .969     | .132     | .000          | .000         | .071             |                        | .000   | .319        | .055        |
|                        | N                   | 47       | 40       | 47            | 47           | 46               | 47                     | 47     | 44          | 47          |
| Volume                 | Pearson Correlation | .034     | .226     | .778          | .721         | .407             | .971                   | 1      | -.129       | -.286       |
|                        | Sig. (2-tailed)     | .820     | .161     | .000          | .000         | .005             | .000                   |        | .404        | .051        |
|                        | N                   | 47       | 40       | 47            | 47           | 46               | 47                     | 47     | 44          | 47          |
| Slope Angle            | Pearson Correlation | .345     | -.163    | -.117         | -.071        | -.114            | -.154                  | -.129  | 1           | .222        |
|                        | Sig. (2-tailed)     | .022     | .329     | .450          | .646         | .467             | .319                   | .404   |             | .148        |
|                        | N                   | 44       | 38       | 44            | 44           | 43               | 44                     | 44     | 44          | 44          |
| Decay Class            | Pearson Correlation | .067     | -.282    | -.305         | -.192        | .093             | -.282                  | -.286  | .222        | 1           |
|                        | Sig. (2-tailed)     | .656     | .078     | .037          | .196         | .540             | .055                   | .051   | .148        |             |
|                        | N                   | 47       | 40       | 47            | 47           | 46               | 47                     | 47     | 44          | 47          |

Fisher's Exact test revealed that, again, none of the variables for the Alum Creek Experimental Forest site had a  $p$ -value above the Bonferonni corrected  $\alpha = 0.006$  threshold to have a statistically significant relationship with the presence of mined bedrock (Table 4.3). However, Aspect did display a relatively high P-value.

**Table 4.3** Results of Fisher's Exact Test for the Alum Creek Experimental Forest. An observed  $P$ -value of  $\leq 0.05$  indicates that a statistically significant association between the factor in question and bedrock presence

| <b>Alum Creek Experimental Forest</b> |                    |
|---------------------------------------|--------------------|
|                                       | <b>Probability</b> |
| Aspect                                | 0.176              |
| Position on Slope                     | 0.284              |
| Soil Mapping Unit                     | 0.316              |
| Tree Type                             | 0.492              |
| Type of Fall                          | 0.346              |
| Underlying Bedrock                    | 0.920              |

#### **A. Constructing the Model**

VIF values greater than 2.5 were removed from modeling with the exception of wad volume (Appendix B). This value was maintained in modeling to retain some measurement of the predicting strength of rooting volume, as this was identified as being an important predictor of bedrock mining (Stokes et al., 1996; Fourcaud et al., 2008). Another round of collinearity testing indicated that stepwise logistic regression could be undertaken (Table 4.4).

**Table 4.4** Second round of collinearity testing for the Alum Experimental Forest.

|                    | <b>Collinearity Statistics</b> |       |
|--------------------|--------------------------------|-------|
|                    | Tolerance                      | VIF   |
| Volume             | .781                           | 1.281 |
| Slope Angle        | .763                           | 1.310 |
| Decay Class        | .781                           | 1.280 |
| Soil Mapping Unit  | .647                           | 1.545 |
| Aspect             | .756                           | 1.323 |
| Tree Type          | .809                           | 1.237 |
| Underlying Geology | .651                           | 1.536 |
| Type of Fall       | .791                           | 1.265 |
| Position on Slope  | .827                           | 1.209 |

After variables that were highly correlated with the dependant variable (presence/absence of bedrock mining) the forward stepwise (conditional) binary logistic regression was completed in SPSS. The threshold entry probability value for stepwise testing for this site was set at 0.3 and the removal value was set at 0.35. Significance testing of the logistic regression model showed that the model was statistically significant at the  $\leq 0.05$  level (Table E.2). Furthermore, the model summary showed a discernible reduction in the -2 log likelihood in the stepwise procedure from step 1 to step 5 (Table E.3). Both  $R^2$  values increased from step 1 to step 5 (Table E.3).

**Table 4.5** Model summary for the Alum Experimental Forest.

| -2 Log likelihood | Cox & Snell<br>R Square | Nagelkerke<br>R Square |
|-------------------|-------------------------|------------------------|
| 11.51             | .658                    | .880                   |

**Table 4.6** Forward Stepwise (Conditional) output for the Alum Experimental Forest

|                          | (B)<br>Logit<br>Coefficient | Sig.      | Exp(B)<br>Odds Ratio |
|--------------------------|-----------------------------|-----------|----------------------|
| Slope Angle              | .520                        | .066      | 1.683                |
| Decay Class              | 6.630                       | .100      | 757.798              |
| <i>Aspect</i>            |                             | .813      |                      |
| East                     | -29.685                     | .998      | .000                 |
| North                    | -55.535                     | .996      | .000                 |
| Northeast                | -43.284                     | .999      | .000                 |
| South                    | -48.247                     | .997      | .000                 |
| Southeast                | -55.971                     | .996      | .000                 |
| Southwest                | -50.457                     | .997      | .000                 |
| Sandstone                | 11.849                      | .077      | 139983.315           |
| <i>Position on Slope</i> |                             | .744      |                      |
| Bottom Portion           | 19.130                      | .858      | 203344642.677        |
| Flat Area                | 24.826                      | .118      | 60482448846.677      |
| Midslope                 | 10.305                      | .228      | 29878.934            |
| Ridge                    | .465                        | .936      | 1.591                |
| Top Portion              | -83.237                     | .997      | .000                 |
| Constant                 | 5.839                       | 11665.068 | 1.000                |

As step 5 of the forward stepwise binary logistic regression had the best model it was accepted as the model for the Alum Creek Experimental Forest (Table 4.6).Western

and northwestern aspect positions and Unknown positions on slope were not included within the model, meaning that their predictive value did not strengthen the “fit” of the model in comparison to the constant only model.

## **II. Rock Creek Tornado Blowdown**

The Rock Creek Tornado Blowdown site showed an overwhelming majority of mined bedrock in 38 (84.4%) of the samples taken with only 7 (15.6%) of samples showing none. Bedrock mining was dominant across all variables at this site. Of the wad dimensions collected in the field, the range of values for width and height for those samples with and without mined bedrock were nearly equal, and the means slightly higher in both cases for those with a positive presence (Figures 4.14 and 4.15 and further statistics seen in Table 4.7). This pattern follows for calculated wad area. To the contrary, wad thickness range was much smaller for negative presence than positive but, showed a marginally larger mean (Figure 4.14). However, wad volume range for positive presence was much larger than negative and demonstrated a faintly larger mean. Tree DBH was greater and had a slightly larger range for positive mined bedrock presence than negative (Figure 4.16).

Of the four geology types on which samples were taken, as can be seen following in figure 4.17, sandstone, sandstone and quartz, shale, shale and sandstone, all but sandstone and quartz type exhibited a preference for mining bedrock. However, the small number of samples warrants further investigation to determine if this is in fact the case. In fact, those samples with sandstone were represented by a 100% chance of mining bedrock and the shale type seemed to be at least five times more likely to mine unweathered bedrock than to not.

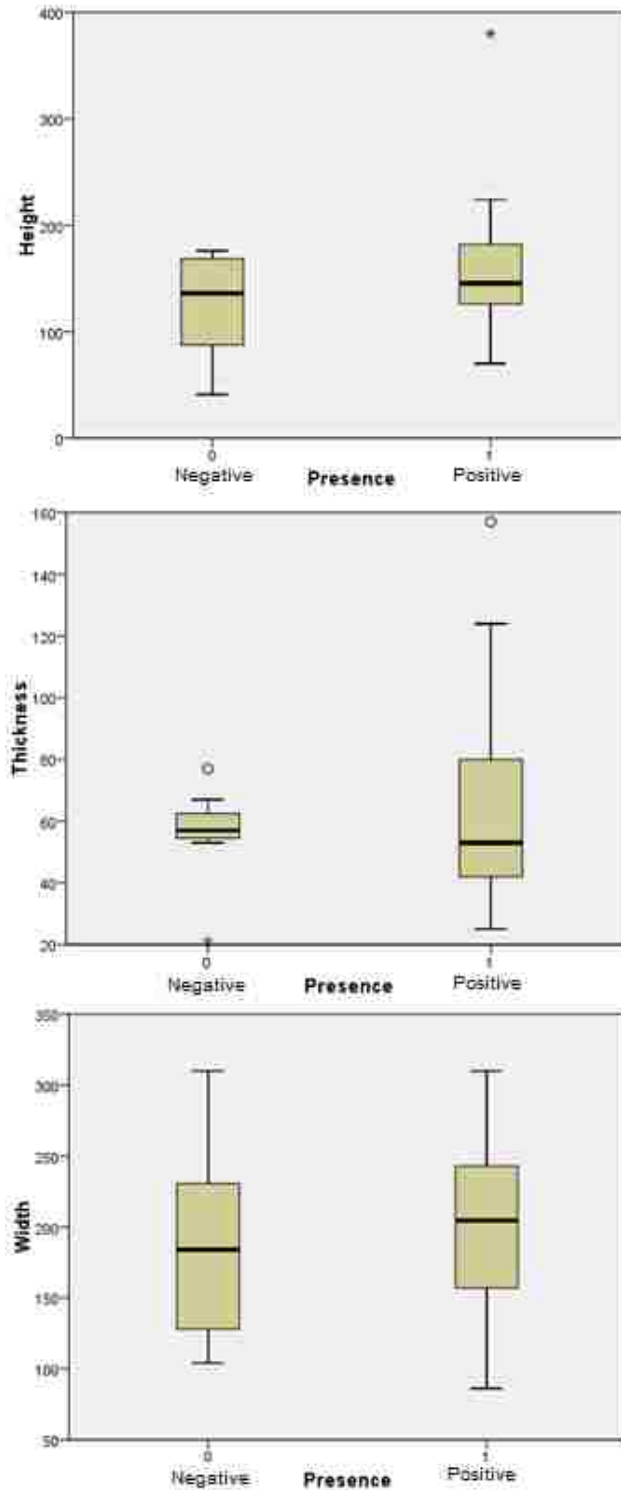


**Figure 4.14** Boxplots showing the unbooked minimum value, first quartile, median, third quartile, and unbooked maximum value of the wad dimensions gathered in the field (units centimeters) within the Rock Creek Tornado Blowdown site. Circles denote outliers, or values that do not fall in the inner fences.

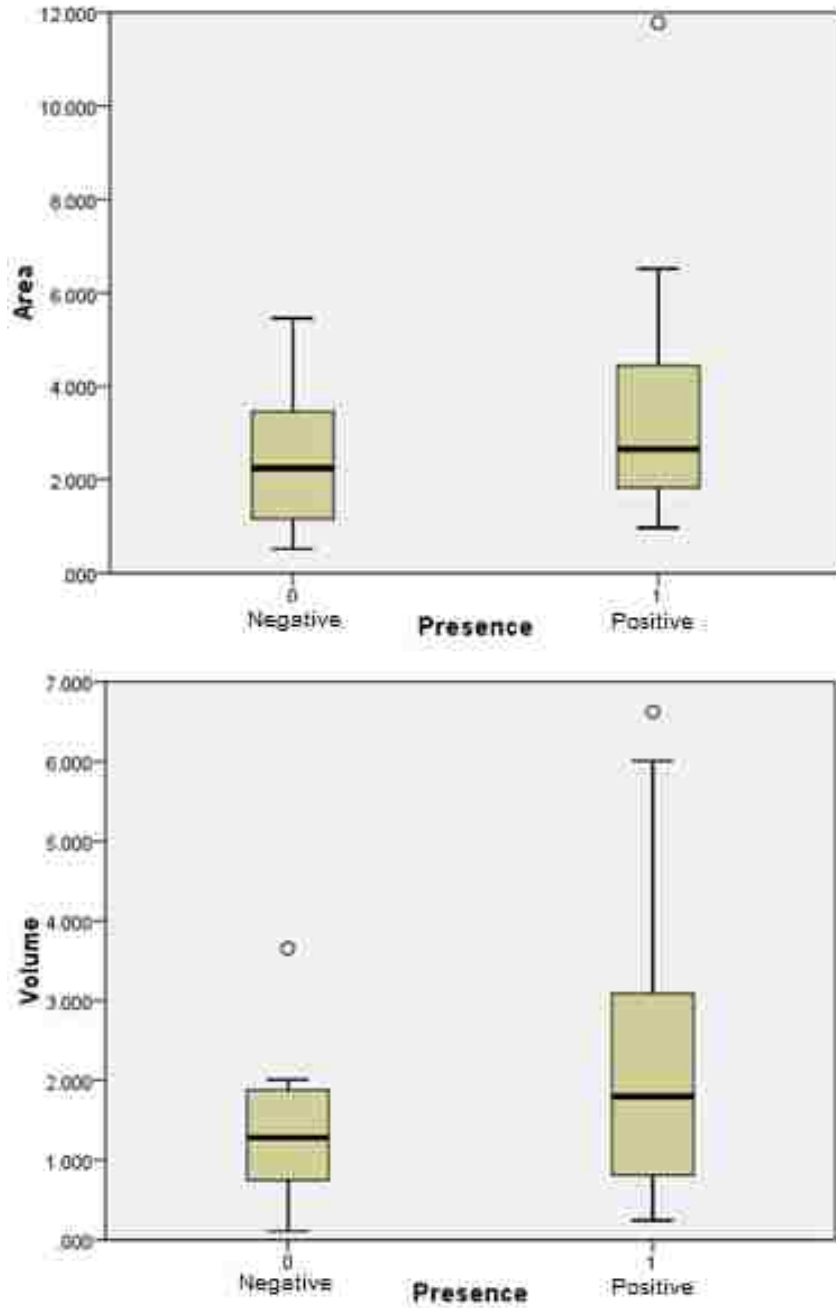


**Figure 4.15** Boxplot showing the unbooked minimum value, first quartile, median, third quartile, and unbooked maximum value of the wad dimensions calculated from wad dimensions gathered in the field within the Rock Creek Tornado Blowdown site. Circles denote outliers, or values that do not fall in the inner fences. Area and volume units in square meters.





**Figure 4.16** Boxplot showing the unbooked minimum value, first quartile, median, third quartile, and unbooked maximum value of the diameter at breast height gathered in the field (units centimeters) within the Rock Creek Tornado Blowdown site. Circles denote outliers, or values that do not fall in the inner fences.

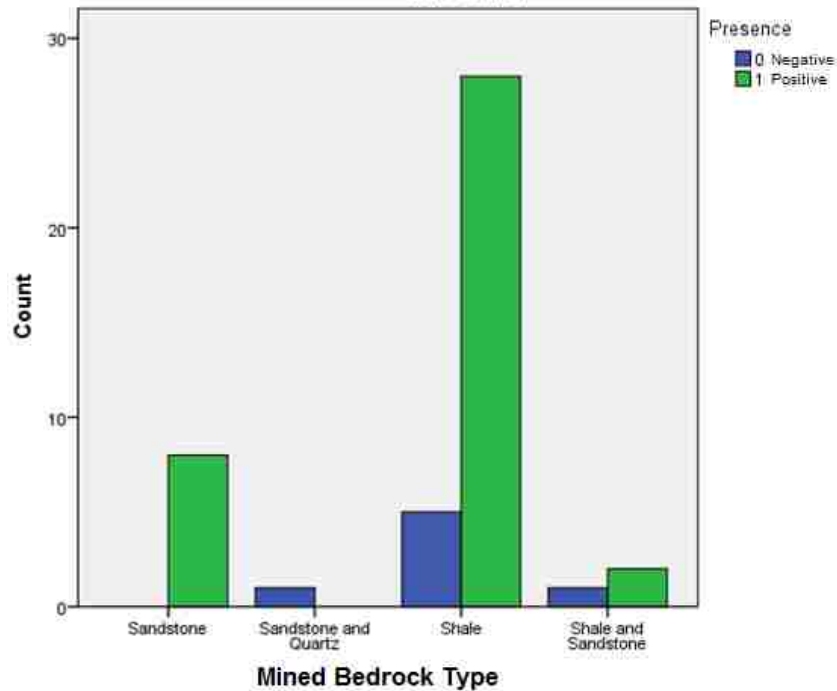


**Figure 4.17** Count of geology data sampled in the field. “0” denotes the absence of mined bedrock found and ‘1’ denotes presence for samples within the Rock Creek Tornado Blowdown site.

Table 4.7 further describes the numerical data (see below).

**Table 4.7** Descriptive statistics of numerical data for samples within the Rock Creek Tornado Blowdown site. DBH, height, width, and thickness of wad in cm. Area in m<sup>2</sup> and volume in m<sup>3</sup>. Slope in degrees.

|                         | Percentiles |         |        |       |       |
|-------------------------|-------------|---------|--------|-------|-------|
|                         | Minimum     | Maximum | Mean   | 25th  | 75th  |
| <b>DBH</b>              | 16          | 53      | 34.13  | 28    | 37.5  |
| <b>Height of wad</b>    | 41          | 380     | 150.91 | 124.5 | 177.5 |
| <b>Width of wad</b>     | 86          | 310     | 198    | 151.5 | 237   |
| <b>Thickness of wad</b> | 21          | 157     | 62     | 42    | 77    |
| <b>Area of wad</b>      | 0.52        | 11.78   | 3.18   | 1.62  | 4.33  |
| <b>Volume of wad</b>    | 0.109       | 6.625   | 2.06   | 0.8   | 2.91  |

The correlation analysis for the Rock Creek Tornado Blowdown found a great number of significant relationships between variables (Table 4.8). However, none of the variables were significantly correlated with bedrock mining at the Bonferroni corrected  $\alpha = 0.008$ . Of the continuous variables examined, DBH had the highest correlation with bedrock mining. Wad height, volume, and area also had relatively high P-values correlated with Presence.

**Table 4.8** Pearson's probabilities for datapoints within the Rock Creek Tornado Blowdown site.

|           |                     | Presence | DBH  | Width | Height | Thickness | Area | Volume |
|-----------|---------------------|----------|------|-------|--------|-----------|------|--------|
| Presence  | Pearson Correlation | 1        | .333 | .072  | .215   | .104      | .147 | .164   |
|           | Sig. (2-tailed)     |          | .026 | .637  | .157   | .495      | .336 | .282   |
|           | N                   | 45       | 45   | 45    | 45     | 45        | 45   | 45     |
| DBH       | Pearson Correlation | .333     | 1    | .663  | .637   | .521      | .694 | .776   |
|           | Sig. (2-tailed)     | .026     |      | .000  | .000   | .000      | .000 | .000   |
|           | N                   | 45       | 45   | 45    | 45     | 45        | 45   | 45     |
| Width     | Pearson Correlation | .072     | .663 | 1     | .594   | .170      | .827 | .715   |
|           | Sig. (2-tailed)     | .637     | .000 |       | .000   | .263      | .000 | .000   |
|           | N                   | 45       | 45   | 45    | 45     | 45        | 45   | 45     |
| Height    | Pearson Correlation | .215     | .637 | .594  | 1      | .216      | .922 | .767   |
|           | Sig. (2-tailed)     | .157     | .000 | .000  |        | .154      | .000 | .000   |
|           | N                   | 45       | 45   | 45    | 45     | 45        | 45   | 45     |
| Thickness | Pearson Correlation | .104     | .521 | .170  | .216   | 1         | .167 | .651   |
|           | Sig. (2-tailed)     | .495     | .000 | .263  | .154   |           | .272 | .000   |
|           | N                   | 45       | 45   | 45    | 45     | 45        | 45   | 45     |
| Area      | Pearson Correlation | .147     | .694 | .827  | .922   | .167      | 1    | .816   |
|           | Sig. (2-tailed)     | .336     | .000 | .000  | .000   | .272      |      | .000   |
|           | N                   | 45       | 45   | 45    | 45     | 45        | 45   | 45     |
| Volume    | Pearson Correlation | .164     | .776 | .715  | .767   | .651      | .816 | 1      |
|           | Sig. (2-tailed)     | .282     | .000 | .000  | .000   | .000      | .000 |        |
|           | N                   | 45       | 45   | 45    | 45     | 45        | 45   | 45     |

Fisher’s Exact test revealed that the only categorical variable tested, Underlying bedrock, had a p-value above the  $\alpha = 0.05$  threshold to have a statistically significant relationship with the presence of mined bedrock (Table 4.9).

**Table 4.9** Fisher’s Exact Test results for the Rock Creek Tornado Blowdown site. An observed *P*-value of  $\leq 0.05$  indicates that a statistically significant association between the factor in question and bedrock presence for datapoints within the Rock Creek Tornado Blowdown site.

| <b>Rock Creek Tornado Blowdown</b> |                    |
|------------------------------------|--------------------|
|                                    | <b>Probability</b> |
| Underlying Bedrock                 | 0.054              |

### A. Constructing the model

Due to the limited number of variables capable of being tested for the Rock Creek Tornado Blowdown area, higher VIF values were accepted (Table E.5). The lowest VIF values were therefore accepted into a second round of collinearity testing (Table 4.10). This round of testing indicated that stepwise logistic regression could be undertaken (Table 4.10).

**Table 4.10** Second round of collinearity testing for the Rock Creek Tornado Blowdown

|                    | Collinearity |       |
|--------------------|--------------|-------|
|                    | Tolerance    | VIF   |
| DBH                | .719         | 1.391 |
| Thickness          | .729         | 1.373 |
| Underlying Geology | .985         | 1.016 |

After variables that were highly correlated with the dependant variable (presence/absence of bedrock mining) were identified, the forward stepwise (conditional) binary logistic regression was completed in SPSS. The threshold entry probability value for stepwise testing for this site was set at 0.2 and the removal value was set at 0.25. Significance testing of the logistic regression model showed that the model was statistically significant at the  $\leq 0.05$  level (Table E.6). Furthermore, the model summary showed a discernible reduction in the -2 log likelihood in the stepwise procedure from step 1 to step 5 (Table 4.11). Both  $R^2$  values increase from step 1 to step 5 (Table 4.11).

**Table 4.11** Model Summary for the Rock Creek Tornado Blowdown.

| -2 Log likelihood | Cox & Snell R Square | Nagelkerke R Square |
|-------------------|----------------------|---------------------|
| 26.331            | .244                 | .421                |

**Table 4.12** Forward Stepwise (Conditional) output for the Rock Creek Tornado Blowdown area.

|                           | (B)<br>Logit<br>Coefficient | Sig. | Exp(B)<br>Odds Ratio |
|---------------------------|-----------------------------|------|----------------------|
| DBH                       | .391                        | .017 | 1.479                |
| <i>Underlying Geology</i> |                             | .098 |                      |
| Sandstone                 | 5.879                       | .035 | 357.463              |
| Shale                     | 4.451                       | .042 | 85.710               |
| Thickness                 | -.052                       | .109 | .949                 |
| Constant                  | -11.577                     | .020 | .000                 |

As step 3 of the forward stepwise binary logistic regression had the best model it was accepted as the model for the Rock Creek Tornado Blowdown (Table 4.12). The sandstone and shale and the sandstone and quartz underlying geology were not included within the model, meaning that their predictive value did not strengthen the “fit” of the model in comparison to the constant only model.

### III. Mena Tornado Blowdown

In the Mena blowdown area, the majority of treethrows exhibited no mined bedrock at 27 (53%) samples with the slight minority, 24 (47%), having mined unweathered bedrock. Bedrock mining presence was slightly more variable across factors for this site compared to the other two sites. Wad dimension measurements were similar pattern to the other tornado blowdown site (Figures 4.18 – 4.19). That is, thickness means actually *larger* in negative presence rootwads than in positive presence wads while height and width means of positive wads remained larger than the negative bedrock presence wads. Furthermore, both wad area and volume range and means were larger for positive than negative presence (Figure 4.19). DBH mean, as seen in figure 4.20, was additionally larger in the positive presence group of wads. However, contrary to initial considerations, slope angle was slightly higher in those samples without mined bedrock than those with a positive presence (Figure 4.21).

Figure 4.22 shows that hardwood trees were somewhat more likely to uproot unweathered bedrock than pines and those unidentified trees. Of the bedrock types seen in figure 4.24, all categories containing shale mined bedrock much more often than not. However, the other geology types, alluvium and sandstone, much less often mined bedrock than not. The Southwest, Southeast, and Western aspects did not mine bedrock more often than they did (Figure 4.25). The samples taken on the Southern positions, the direction from which the tornado came showed positive mined bedrock presence in approximately 50% more samples than negative presence.

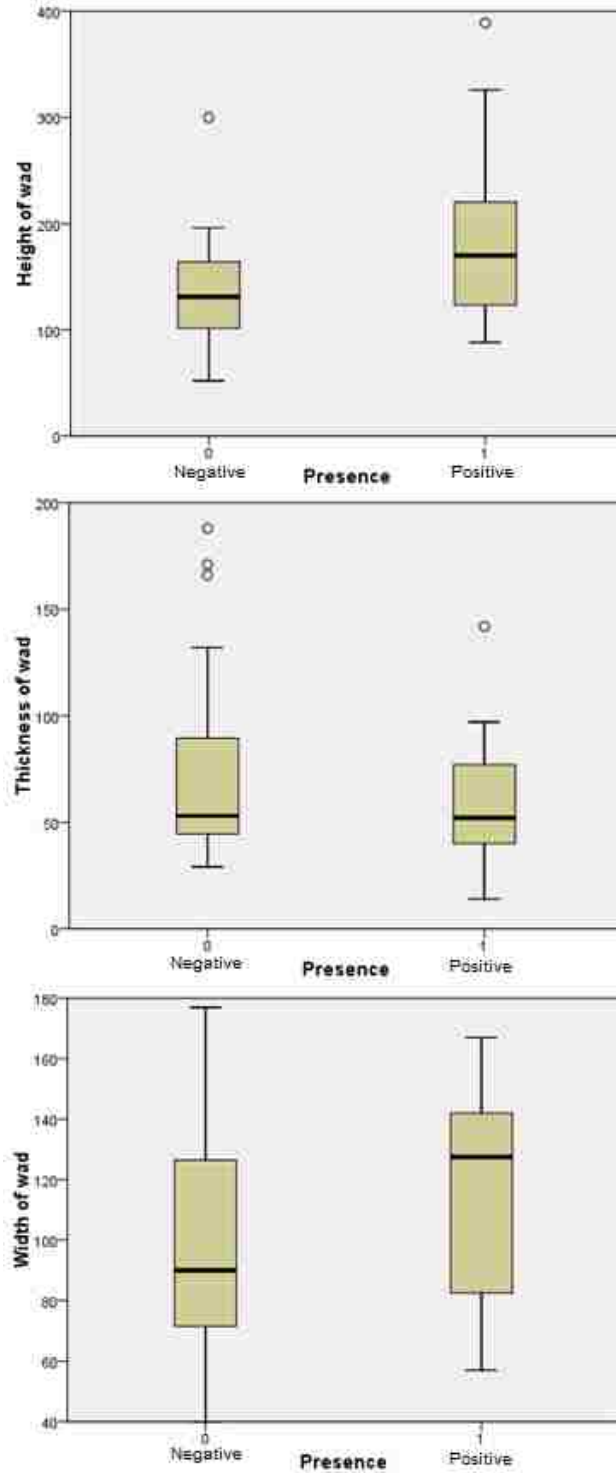


**Figure 4.18** Boxplots showing the unbooked minimum value, first quartile, median, third quartile, and unbooked maximum value of the wad dimensions gathered in the field (units centimeters) for samples within the Mena Tornado Blowdown site. Circles denote outliers, or values that do not fall in the inner fences.

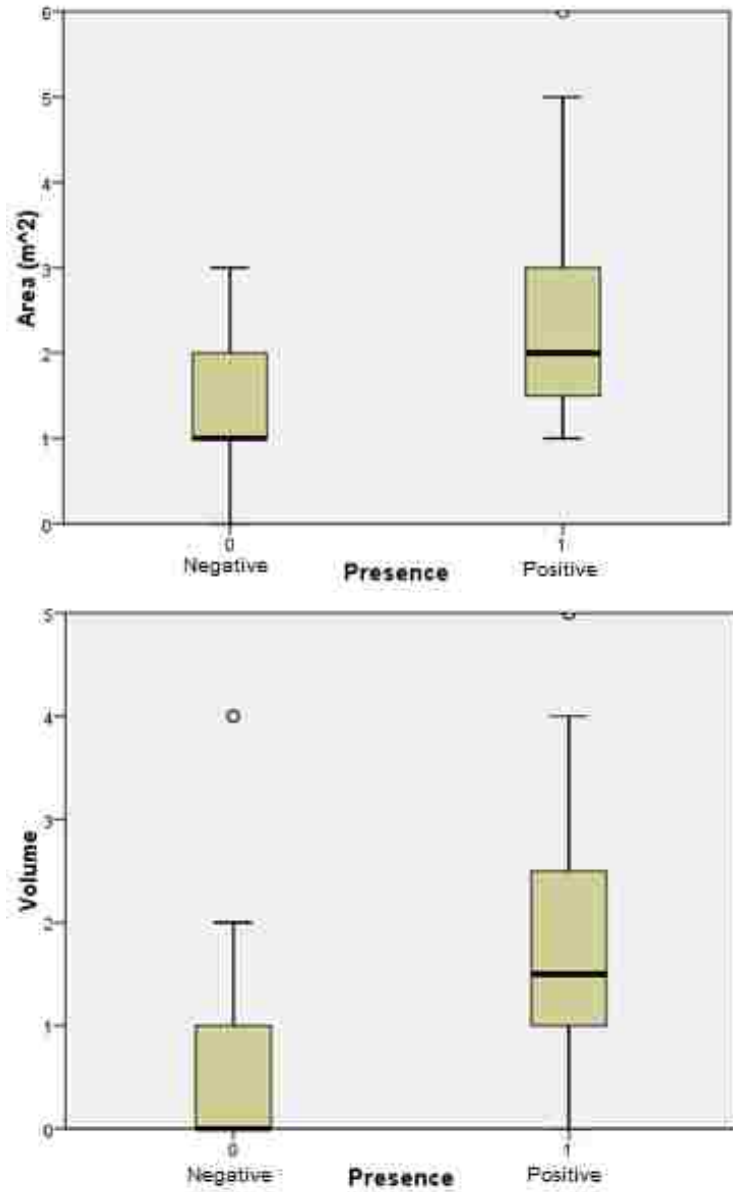


**Figure 4.19** Boxplots showing the unbooked minimum value, first quartile, median, third quartile, and unbooked maximum value of the wad dimensions calculated from wad dimensions gathered in the field within the Mena Tornado Blowdown site. Circles denote outliers, or values that do not fall in the inner fences. Area and volume units in square meters.



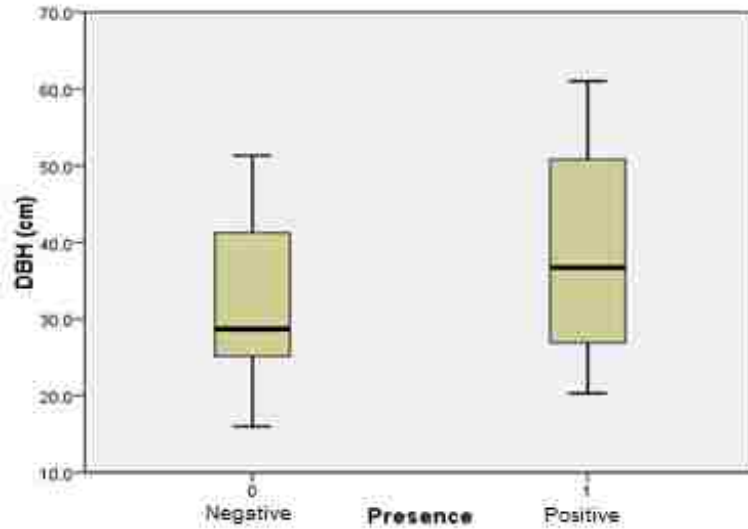


**Figure 4.20** Boxplot showing the unbooked minimum value, first quartile, median, third quartile, and unbooked maximum value of the diameter at breast height gathered in the field (units centimeters) for samples within the Mena Tornado Blowdown site.

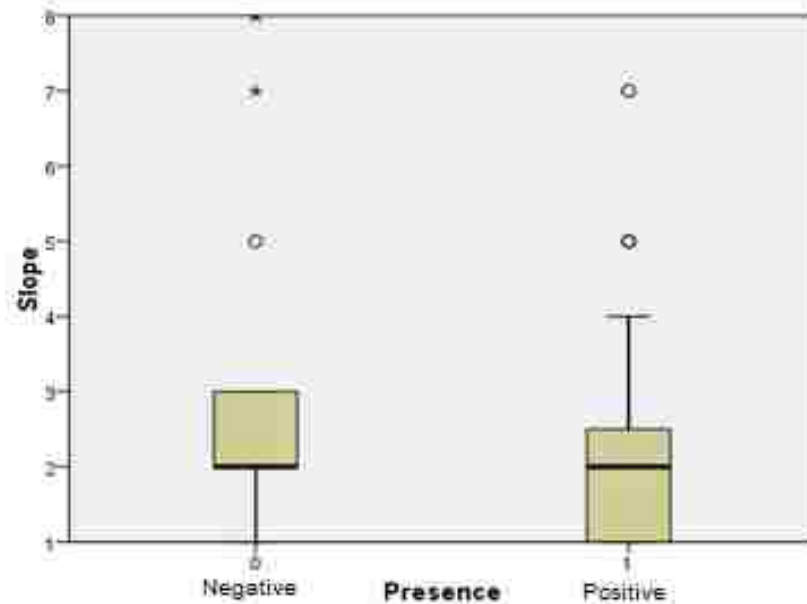


**Figure 4.21** Boxplot showing the unbooked minimum value, first quartile, median, third quartile, and unbooked maximum value of the slope angle calculated using a DEM in a GIS (units degrees) for samples within the Mena Tornado Blowdown site. Circles denote outliers, or values that do not fall in the inner fences, and stars denote extreme outlier values found in the dataset.

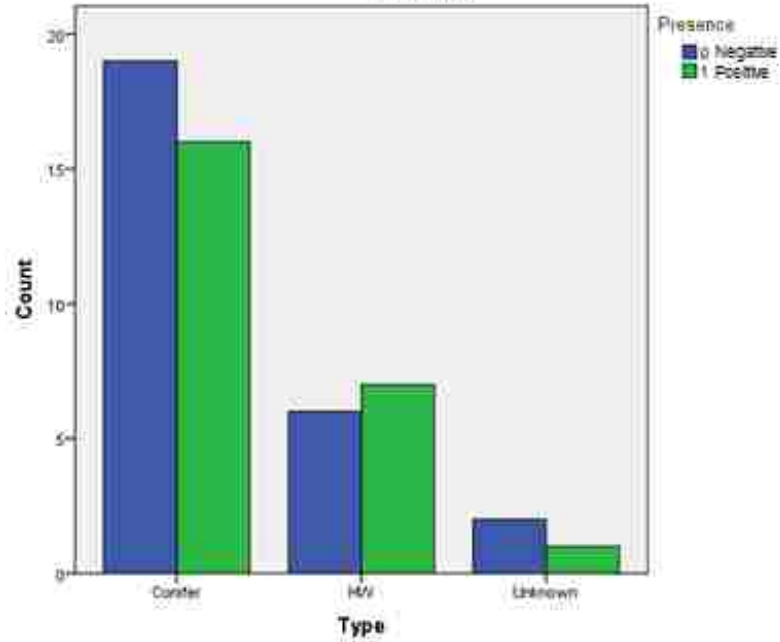


**Figure 4.22** Count of tree type data sampled in the field. “0” denotes the absence of mined bedrock found and ‘1’ denotes presence for samples within the Mena Tornado Blowdown site.

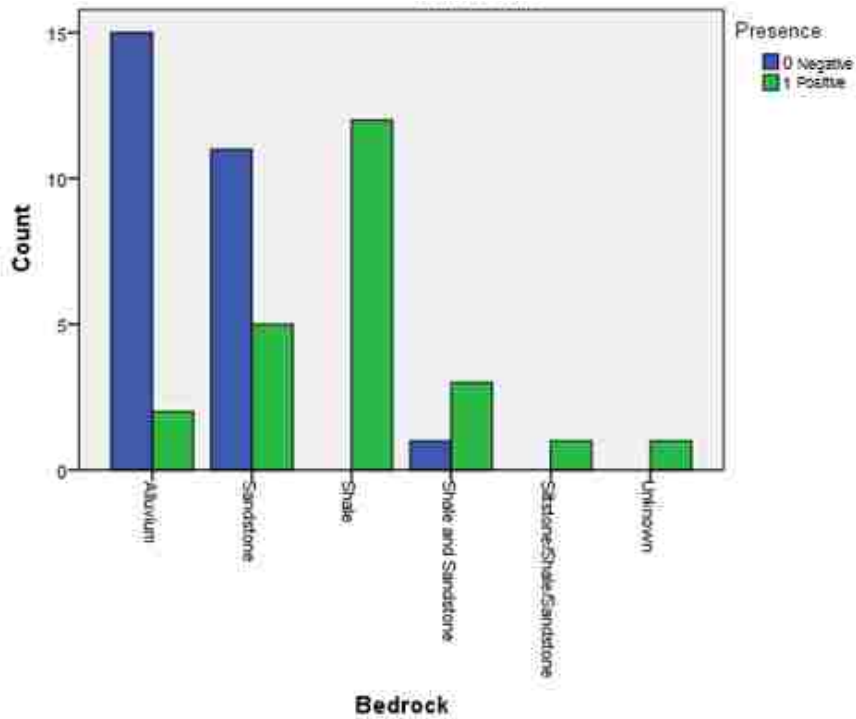


**Figure 4.23** Count of geology data sampled in the field. “0” denotes the absence of mined bedrock found and ‘1’ denotes presence for samples within the Mena Tornado Blowdown site.

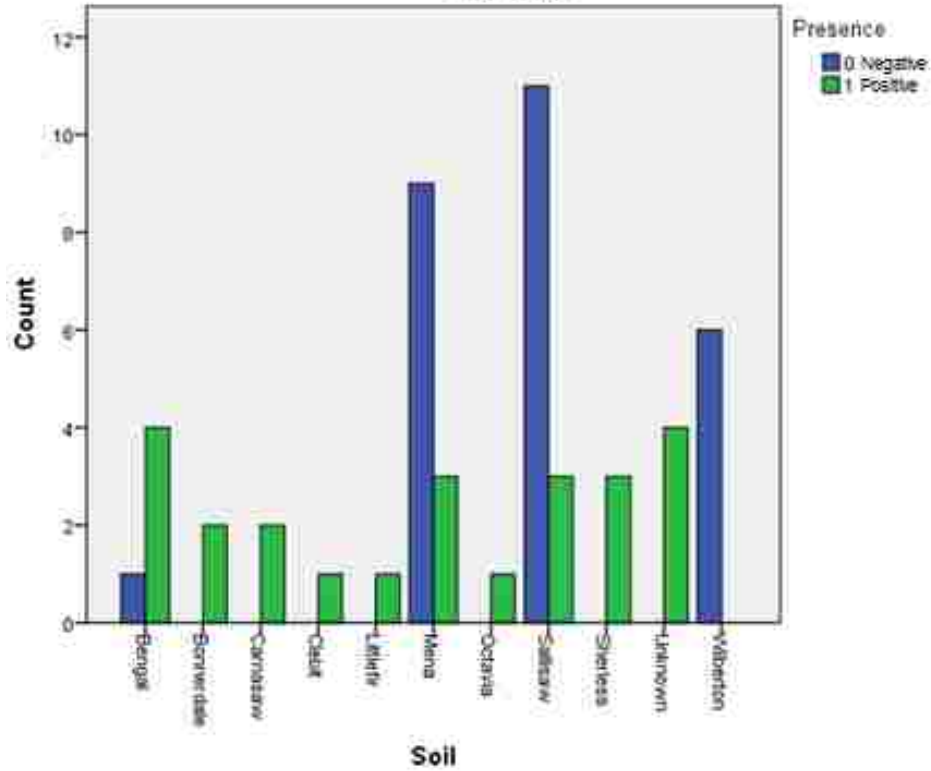


**Figure 4.24** Count of soil data sampled in the field. “0” denotes the absence of mined bedrock found and ‘1’ denotes presence for samples within the Mena Tornado Blowdown site.

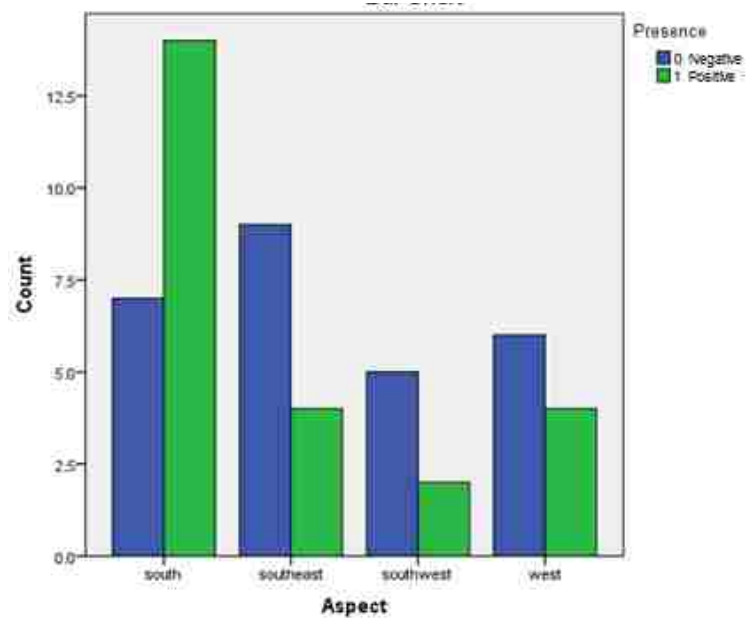


**Figure 4.25** Count of aspect data sampled in the field. “0” denotes the absence of mined bedrock found and ‘1’ denotes presence for samples within the Mena Tornado Blowdown site.

**Table 4.13** Descriptive statistics of numerical data for samples within the Mena Tornado Blowdown site. DBH, height, width, and thickness of wad in cm. Area in m<sup>2</sup> and volume in m<sup>3</sup>. Slope in degrees.

|                         | Percentiles |         |        |      |      |
|-------------------------|-------------|---------|--------|------|------|
|                         | Minimum     | Maximum | Mean   | 25th | 75th |
| <b>DBH</b>              | 16          | 61      | 35.653 | 25.4 | 45.2 |
| <b>Slope</b>            | 1           | 8       | 2.47   | 1    | 3    |
| <b>Height of wad</b>    | 52          | 389     | 158.69 | 114  | 186  |
| <b>Width of wad</b>     | 40          | 177     | 106.06 | 75   | 133  |
| <b>Thickness of wad</b> | 14          | 188     | 66.45  | 42   | 84   |
| <b>Area of wad</b>      | 0           | 6       | 1.8    | 1    | 2    |
| <b>Volume of wad</b>    | 0           | 5       | 1.2    | 0    | 2    |

Much like the other sample sites, the bivariate correlation of the parameters examined at the Mena Tornado Blowdown area displayed a great number of significant relationships between variables (Tables 4.14 and 4.15). The relationship of bedrock presence and other parameters was found to be significant for wad area and height. DBH and wad volume had a relatively high P-value correlated with Presence. Interestingly, DBH was highly correlated with all wad measurements and relatively highly correlated with bedrock mining and slope angle. In addition, slope angle was highly correlated with wad thickness and volume and relatively highly correlated with width of wad.

**Table 4.14** Pearson's probabilities for samples within the Mena Tornado Blowdown site

|           |                     | Presence | Slope | DBH  | Height | Width | Thickness | Volume | Area |
|-----------|---------------------|----------|-------|------|--------|-------|-----------|--------|------|
| Presence  | Pearson Correlation | 1        | -.176 | .258 | .395   | .208  | -.179     | .339   | .543 |
|           | Sig. (2-tailed)     |          | .217  | .067 | .004   | .142  | .209      | .015   | .000 |
|           | N                   | 51       | 51    | 51   | 51     | 51    | 51        | 51     | 51   |
| Slope     | Pearson Correlation | -.176    | 1     | .247 | -.049  | .281  | .500      | .496   | .137 |
|           | Sig. (2-tailed)     | .217     |       | .081 | .735   | .046  | .000      | .000   | .337 |
|           | N                   | 51       | 51    | 51   | 51     | 51    | 51        | 51     | 51   |
| DBH       | Pearson Correlation | .258     | .247  | 1    | .628   | .582  | .417      | .524   | .586 |
|           | Sig. (2-tailed)     | .067     | .081  |      | .000   | .000  | .002      | .000   | .000 |
|           | N                   | 51       | 51    | 51   | 51     | 51    | 51        | 51     | 51   |
| Height    | Pearson Correlation | .395     | -.049 | .628 | 1      | .577  | .231      | .443   | .765 |
|           | Sig. (2-tailed)     | .004     | .735  | .000 |        | .000  | .102      | .001   | .000 |
|           | N                   | 51       | 51    | 51   | 51     | 51    | 51        | 51     | 51   |
| Width     | Pearson Correlation | .208     | .281  | .582 | .577   | 1     | .339      | .565   | .708 |
|           | Sig. (2-tailed)     | .142     | .046  | .000 | .000   |       | .015      | .000   | .000 |
|           | N                   | 51       | 51    | 51   | 51     | 51    | 51        | 51     | 51   |
| Thickness | Pearson Correlation | -.179    | .500  | .417 | .231   | .339  | 1         | .558   | .146 |
|           | Sig. (2-tailed)     | .209     | .000  | .002 | .102   | .015  |           | .000   | .307 |
|           | N                   | 51       | 51    | 51   | 51     | 51    | 51        | 51     | 51   |
| Volume    | Pearson Correlation | .339     | .496  | .524 | .443   | .565  | .558      | 1      | .746 |
|           | Sig. (2-tailed)     | .015     | .000  | .000 | .001   | .000  | .000      |        | .000 |
|           | N                   | 51       | 51    | 51   | 51     | 51    | 51        | 51     | 51   |
| Area      | Pearson Correlation | .543     | .137  | .586 | .765   | .708  | .146      | .746   | 1    |
|           | Sig. (2-tailed)     | .000     | .337  | .000 | .000   | .000  | .307      | .000   |      |
|           | N                   | 51       | 51    | 51   | 51     | 51    | 51        | 51     | 51   |

Fisher’s Exact test revealed (Table 4.15) that soil mapping unit and underlying bedrock have a statistically significant relationship with the presence of mined bedrock. The remaining variable, aspect, did not have a *p*-value below the 0.05 threshold for significance.

**Table 4.15** An observed *P*-value of  $\leq 0.05$  indicates that a statistically significant association between the factor in question and bedrock presence for samples within the Mena Tornado Blowdown site.

*Fisher's Exact Test*

| <b>Mena Tornado Blowdown</b> |                    |
|------------------------------|--------------------|
|                              | <b>Probability</b> |
| Aspect                       | 0.128              |
| Soil Mapping Unit            | 0.000              |
| Underlying Bedrock           | 0.000              |

#### A. Constructing the Model

VIF values greater than 2.5 were removed from modeling with the exception of wad height (Table E.9). This value was maintained in modeling to retain some measurement of the predicting strength of rooting, as this was identified as being an important predictor of bedrock mining (Stokes et al., 1996; Fourcaud et al., 2008). Another round of collinearity testing indicated that stepwise logistic regression could be undertaken (Table 4.16).

**Table 4.16** Second round of collinearity testing for the Mena Tornado Blowdown.

|                    | Collinearity Statistics |       |
|--------------------|-------------------------|-------|
|                    | Tolerance               | VIF   |
| Slope Angle        | .704                    | 1.420 |
| DBH                | .647                    | 1.545 |
| Height             | .638                    | 1.566 |
| Underlying Geology | .796                    | 1.256 |
| Soil Mapping Unit  | .894                    | 1.119 |
| Aspect             | .716                    | 1.397 |

After variables that were highly correlated with the dependant variable were identified (presence/absence of bedrock mining), the forward stepwise (conditional) binary logistic regression was completed in SPSS. The threshold entry probability value for stepwise testing for this site was set at 0.16 and the removal value was set at 0.18 because these levels allowed relatively significant variables to be modeled. Significance testing of the logistic regression model showed that the model was statistically significant

at the  $\leq 0.05$  level (Table E.10). Furthermore, the model summary showed a discernible reduction in the -2 log likelihood in the stepwise procedure from step 1 to step 5 (Table 4.17). Both  $R^2$  values increase from step 1 to step 5 (Table 4.17 and E.11).

**Table 4.17** Model summary for the Mena Tornado Blowdown.

| -2 Log likelihood | Cox & Snell R Square | Nagelkerke R Square |
|-------------------|----------------------|---------------------|
| 17.664            | .645                 | .861                |

**Table 4.18** Forward Stepwise (Conditional) output for the Mena Tornado Blowdown.

|                           | (B)<br>Logit<br>Coefficient | Sig.  | Exp(B)<br>Odds Ratio   |
|---------------------------|-----------------------------|-------|------------------------|
| <i>Underlying Geology</i> |                             | 1.000 |                        |
| Alluvium                  | -3.273                      | 1.000 | .038                   |
| Mixture                   | 39.132                      | 1.000 | 98845516734319100.000  |
| Sandstone                 | -1.323                      | 1.000 | .266                   |
| Shale                     | 19.442                      | 1.000 | 277705021.587          |
| Sandstone and Shale       | 16.717                      | 1.000 | 18201097.996           |
| <i>Soil Mapping Unit</i>  |                             | 1.000 |                        |
| Bengal                    | 21.092                      | 1.000 | 1446476641.122         |
| Bengal/Bismarck/Nashoba   | -19.990                     | 1.000 | .000                   |
| Bonnerdale                | 41.295                      | .999  | 859286504221049000.000 |
| Carnasaw                  | 39.489                      | .999  | 141158779674581000.000 |
| Clebit                    | 19.690                      | 1.000 | 355937088.100          |
| Littlefir                 | 19.006                      | .999  | 179497215.738          |
| Mena                      | 19.690                      | 1.000 | 355937088.100          |
| Octavia                   | 17.548                      | 1.000 | 41767818.778           |
| Sallisaw                  | 39.001                      | .999  | 86659645020933500.000  |
| Sherless                  | 39.132                      | .999  | 98845470925528900.000  |
| Constant                  | -17.929                     | 1.000 | .000                   |

As step 2 of the forward stepwise binary logistic regression had the best model it was accepted as the model for the Mena Tornado Blowdown (Table 4.18). The Wilberton and unknown soil mapping units were not included within the model, meaning that their predictive value did not strengthen the “fit” of the model in comparison to the constant only model.

## IV. Map Creation

Using the logit coefficients (B) for each of the sites, maps were created to predict “hotspot” areas of bedrock mining.

### A. Maps for the Alum Creek Experimental Forest

47 samples were used, including 26 presence points and 21 absence points in the creation of bedrock mining “hotspot” maps for the Alum Creek Experimental Forest. Logit coefficients from the logistic regression model were used in the creation of “hotspot” prediction maps (Table 4.19).

**Table 4.19** Logit Coefficients (B) for the Alum Experimental Forest hotspot mapping.

|                    |        | <i>Aspect</i>    |         | <i>Position on Slope</i> |         |
|--------------------|--------|------------------|---------|--------------------------|---------|
| <b>Slope Angle</b> | .520   | <b>Southeast</b> | -55.971 | <b>Top Portion</b>       | -83.237 |
| <b>Decay Class</b> | 6.630  | <b>North</b>     | -55.535 | <b>Ridge</b>             | .465    |
| <b>Sandstone</b>   | 11.849 | <b>Southwest</b> | -50.457 | <b>Midslope</b>          | 10.305  |
| <b>Constant</b>    | 5.839  | <b>South</b>     | -48.247 | <b>Bottom Portion</b>    | 19.130  |
|                    |        | <b>Northeast</b> | -43.284 | <b>Flat Area</b>         | 24.826  |
|                    |        | <b>East</b>      | -29.685 |                          |         |

For the Slope Angle maps, the actual range of all slope angle values ranged from 0 to 60 degrees but the actual data points from which predictive extrapolation were could be used were within the range of 0 to 30 degrees. Modified equal intervals were chosen as the preferred methodology for the slope angle variable because it allowed for streamlined translation among variables, with breaks grounded in actual field data, as well as easier map interpretation. The intervals are termed “modified” because the equal intervals are chosen based on actual data points – not the full range of values possible. Therefore breaks were placed in the histogram of the slope angle map at the 10 and 20 degree levels to equally break up the range of the actual data points. The “low” odds of mining bedrock show a range of 0 to 9.67 degrees, “medium” odds represented 9.67 to 19.34 degrees angle and “high” odds represent 19.34 and greater degree.

Several aspect positions displayed a negative relationship with bedrock mining. Only the western and northwestern aspects were not included in the model for this site. The eastern aspect was assigned “medium” odds of mining due to the natural break in the range of the logit coefficients.

The case-by-case nature of wad dimensions made mapping of these variables impossible. DBH has been considered as a proxy for wad dimensions but, the work of Phillips and Marion in this area rejects that notion (2005). They found that, in fact, DBH and wad dimensions have a complex relationship that is affected by environmental setting as well as by the size of the tree. In much the same way position on slope cannot currently be accurately mapped. Therefore, if this model was to be used in the field, only ground-truthing could produce reliable results.



The previously mapped positively and negatively correlated variables in the logistic regression equation were combined to produce a map containing highest and lowest odds of bedrock mining activity for the Alum Creek Experimental Forest area. The areas of highest odds were located on shale bedrock and had a slope angle of 19.34 degrees and higher, and were coincidentally on the western or northwestern aspects (as the other aspects were assigned low or medium odds). The areas of lowest odds had the lowest category of slope angle, 0 to 10 degrees and were on the southeast, north, southwest, south, or northeastern aspect.

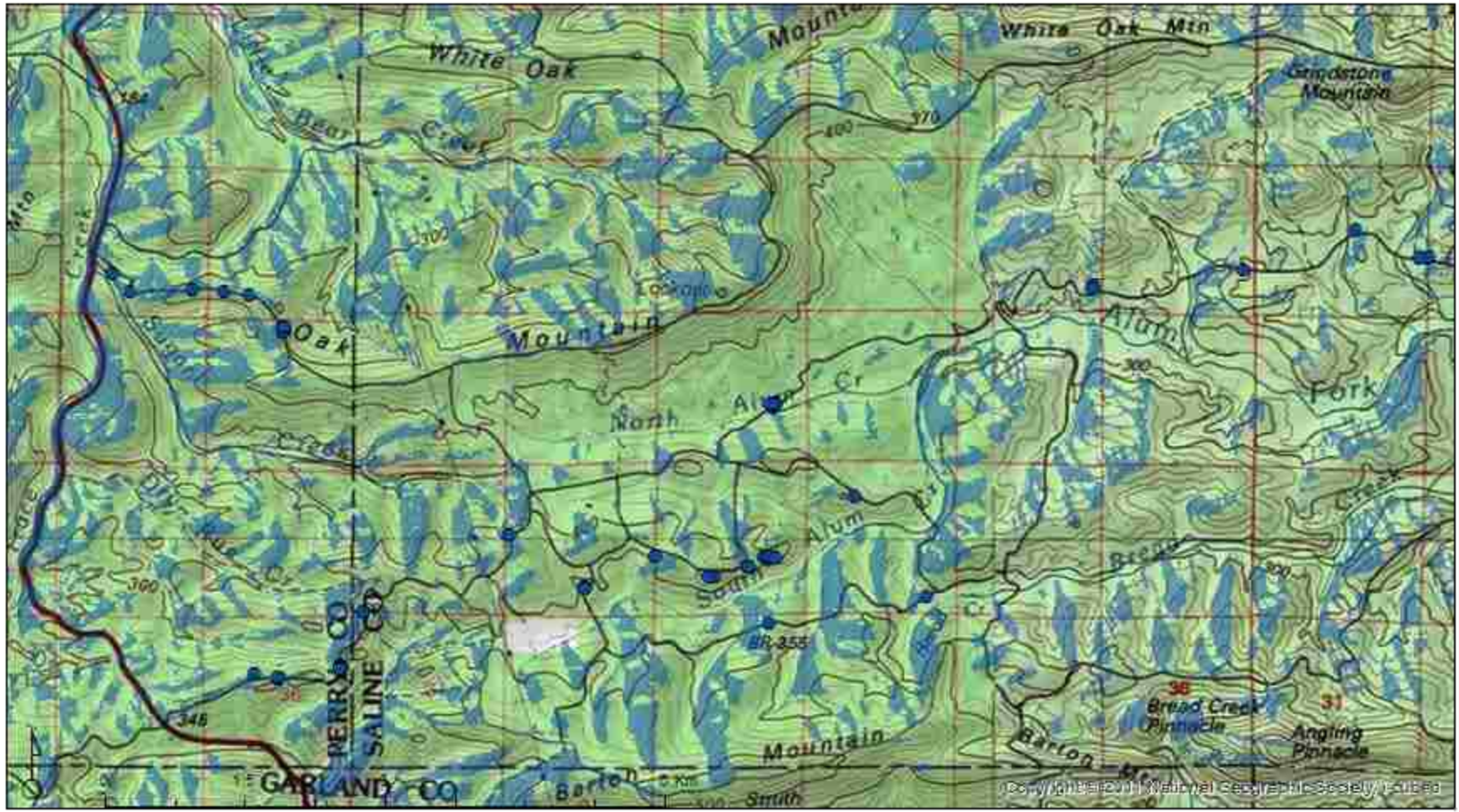
# Alum Creek Experimental Forest

## Aspect

Not included in the model

- Sample Locations
- West Northwest

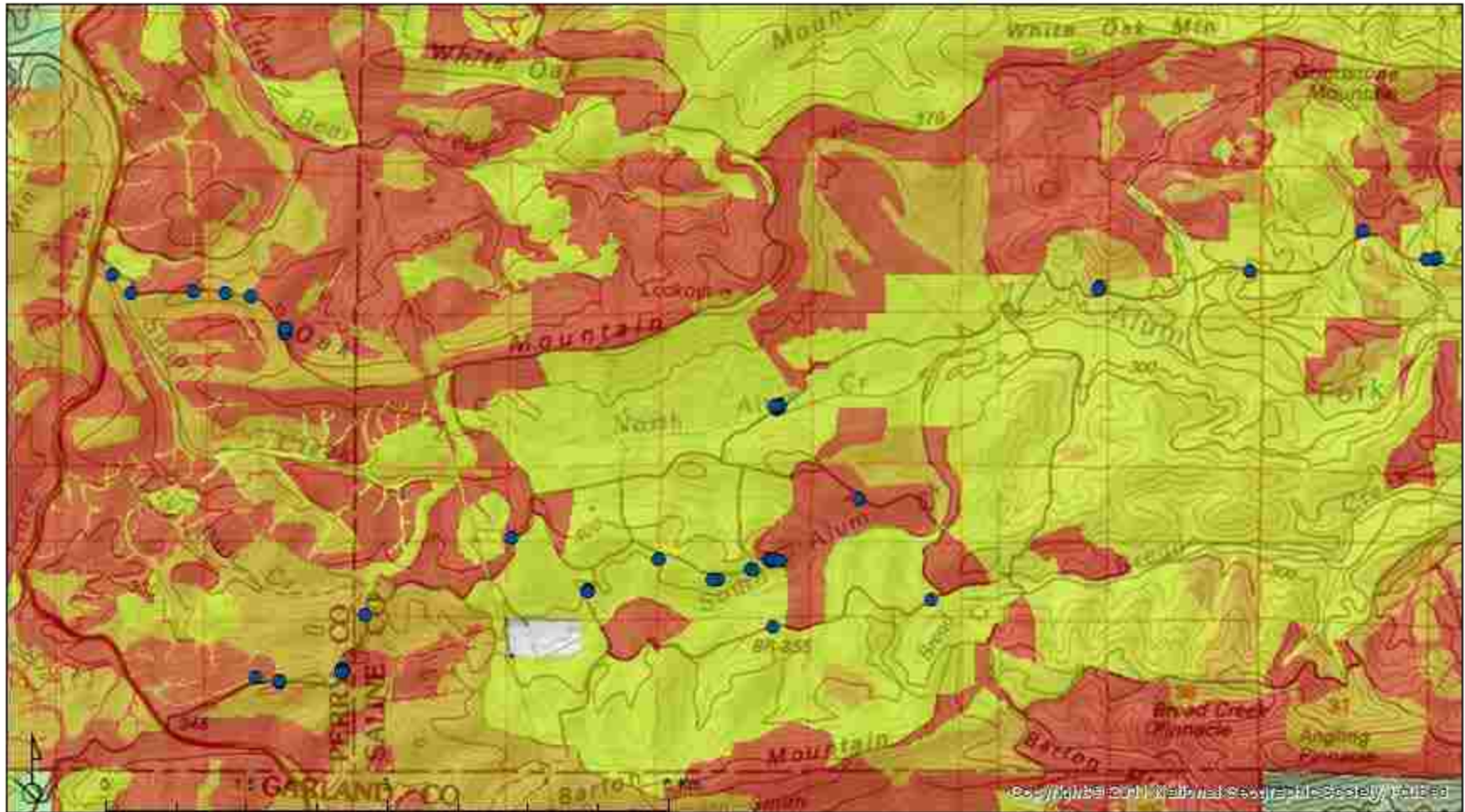
69



Copyright © 2011 National Geographic Society, Inc.

# Alum Creek Experimental Forest

Diameter at Breast Height

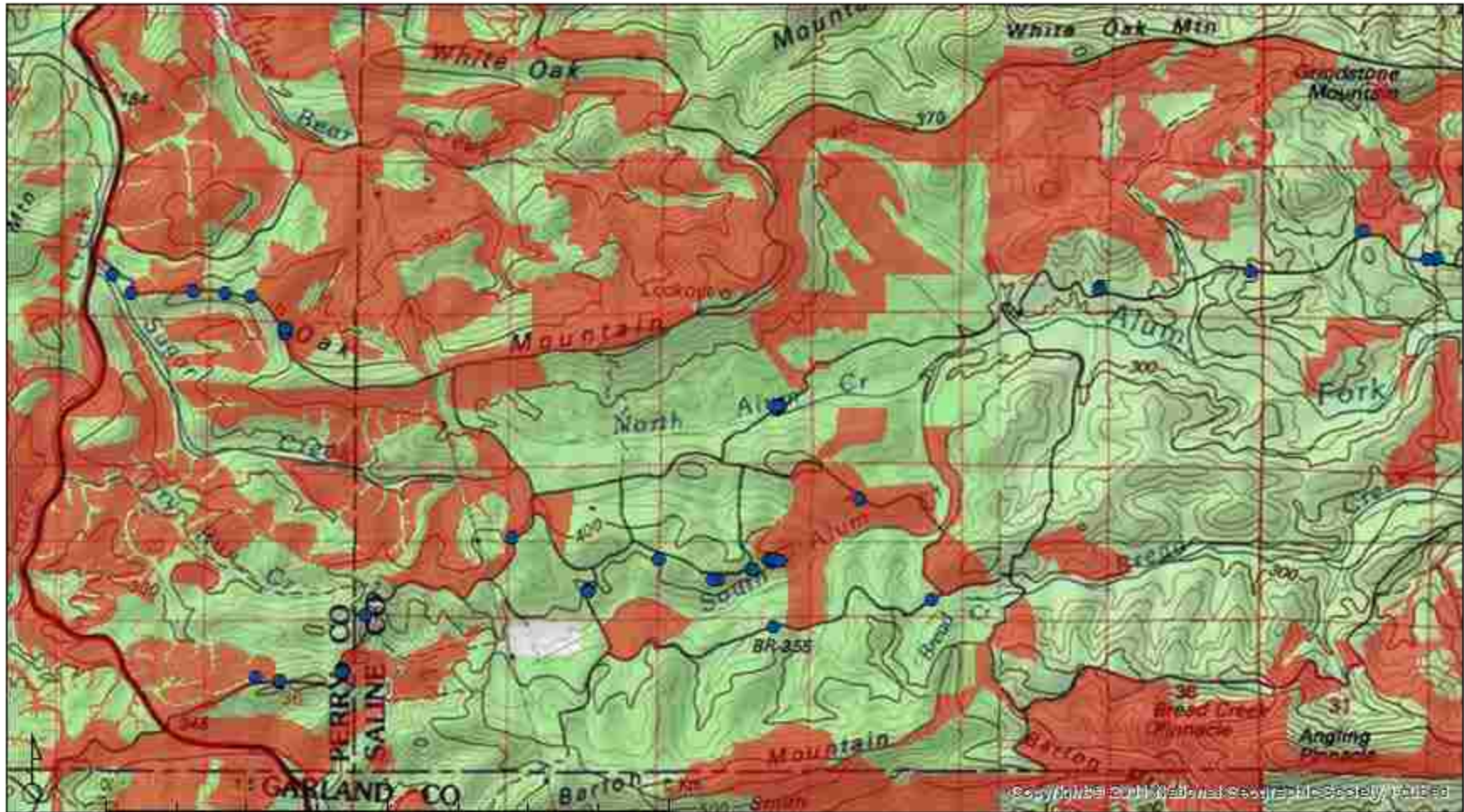


# Alum Creek Experimental Forest

## Odds of Bedrock Mining

Mean Diameter at Breast Height

- Sample Locations
- High Odds 7.8 - 15 in.

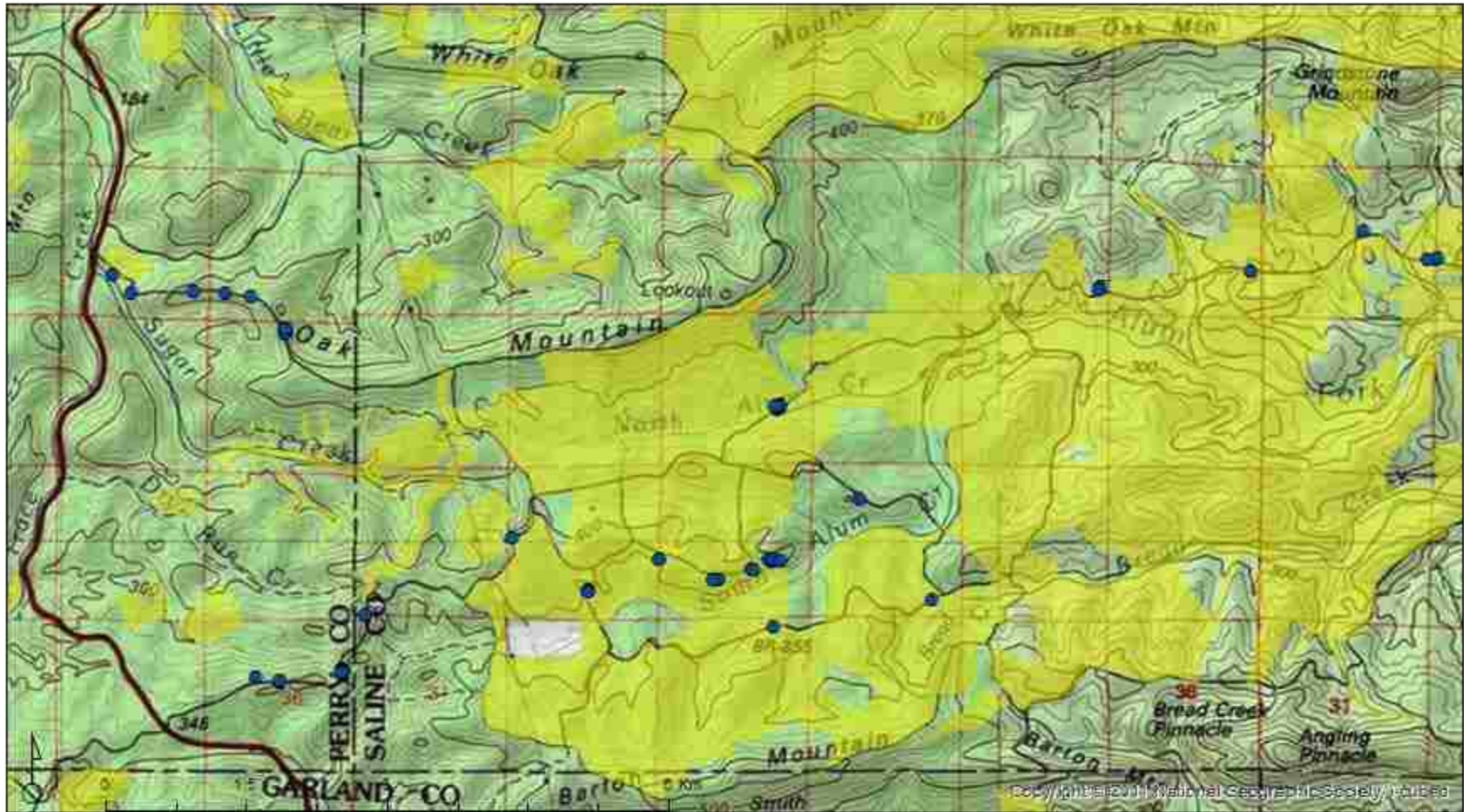


# Alum Creek Experimental Forest

Diameter at Breast Height

● Sample Locations

Low Odds 0 - 3.9 in.

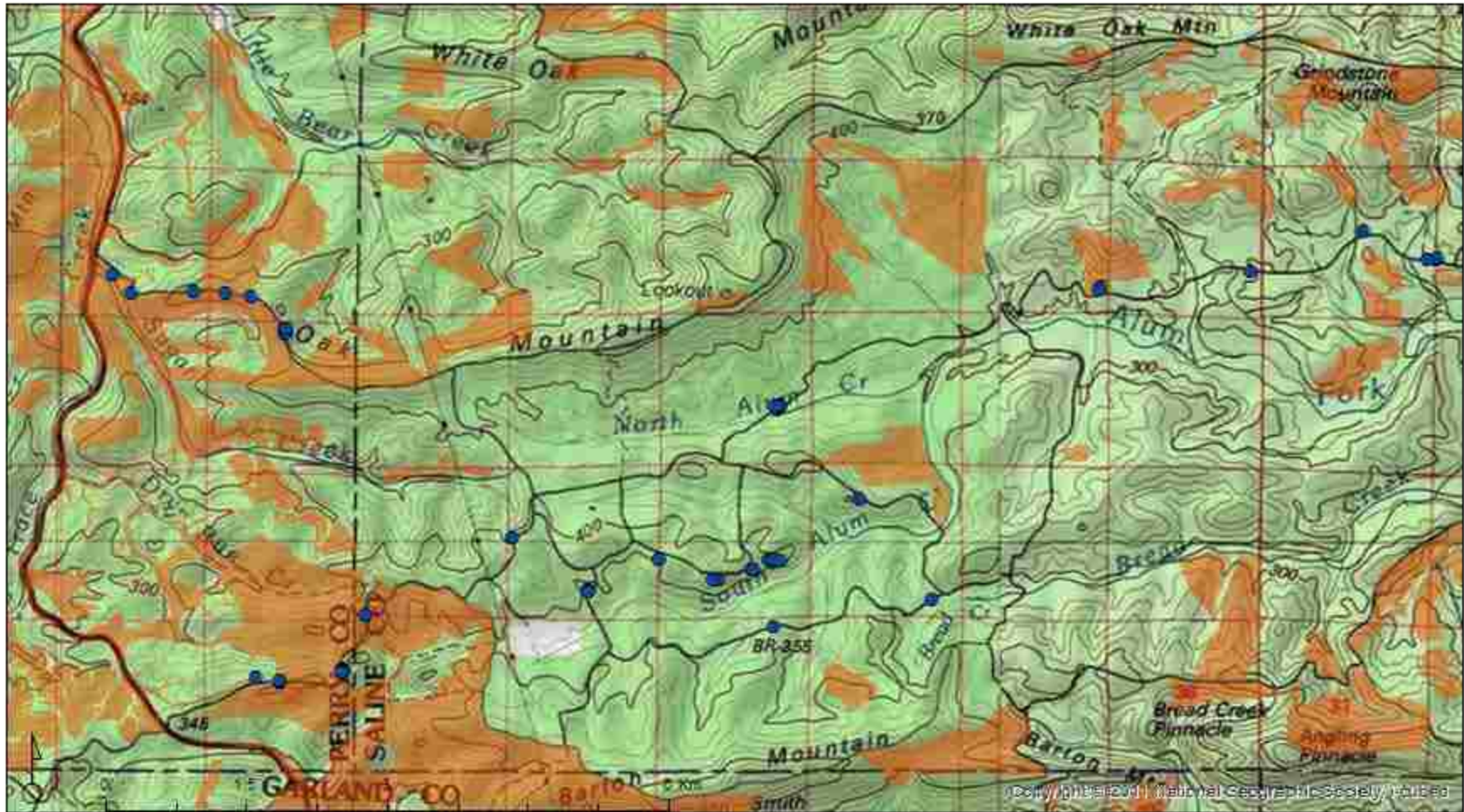


# Alum Creek Experimental Forest

Diameter at Breast Height

● Sample Locations

Medium Odds 3.9 - 7.8 in.



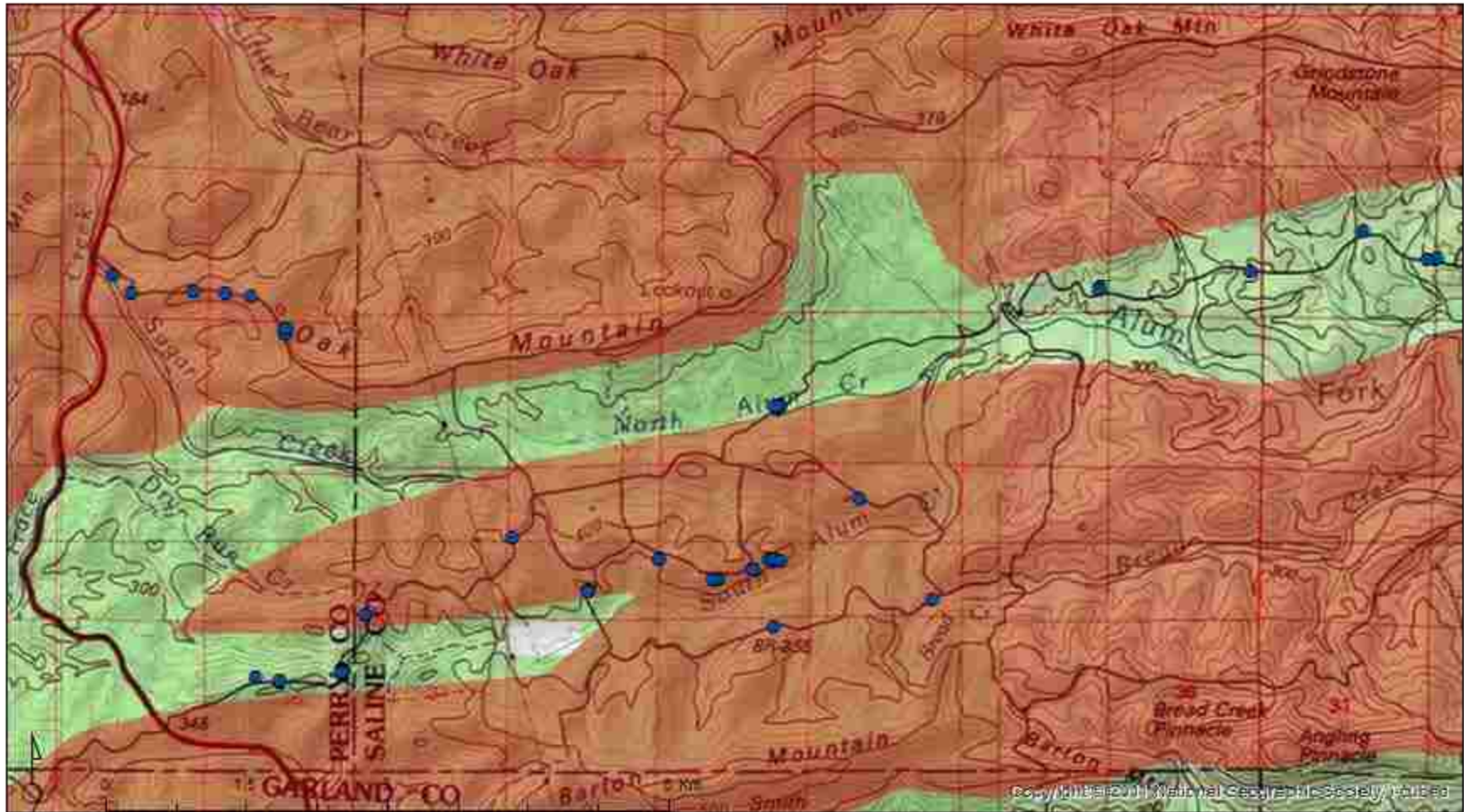
# Alum Creek Experimental Forest

## Underlying Geology

High Odds

● Sample Locations

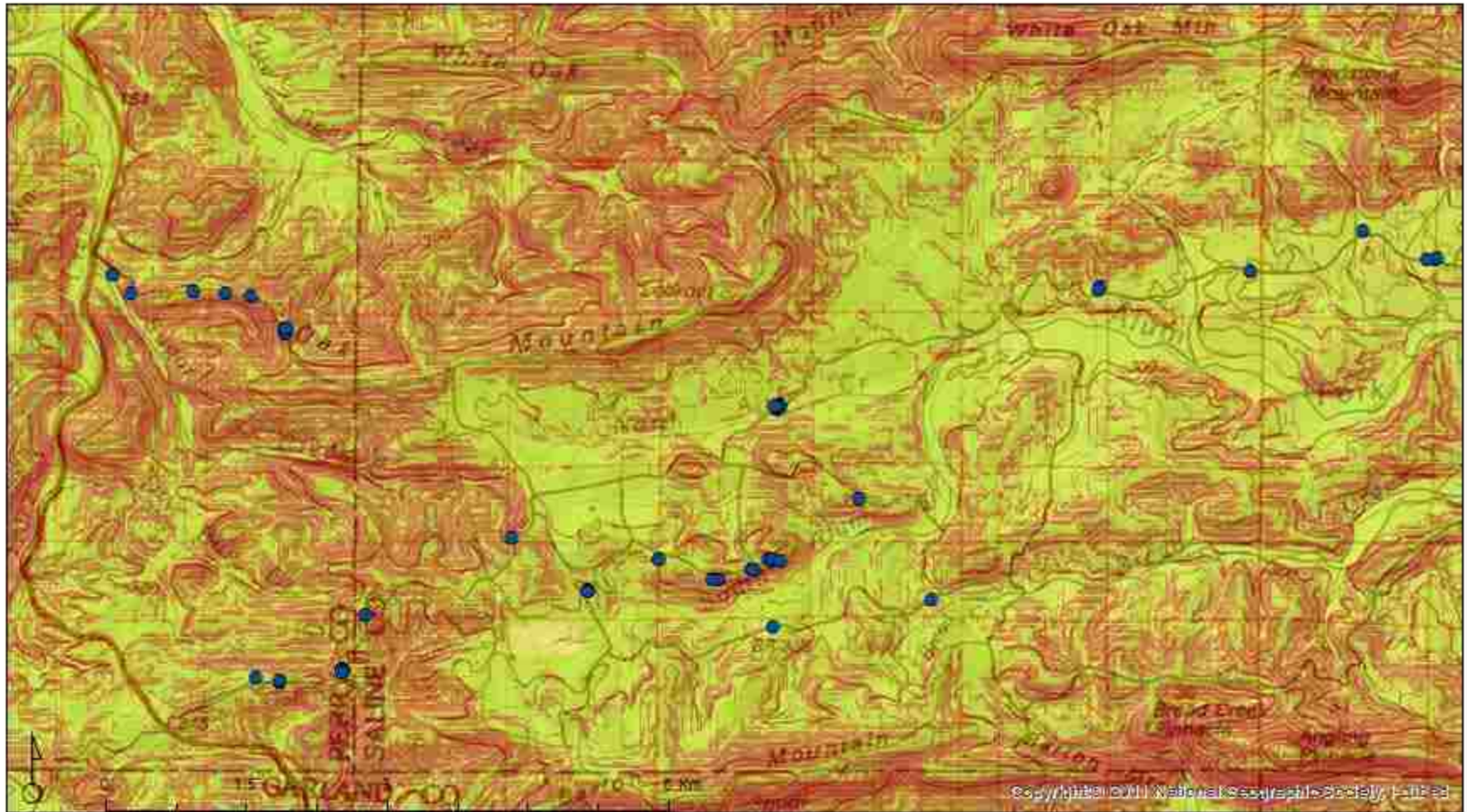
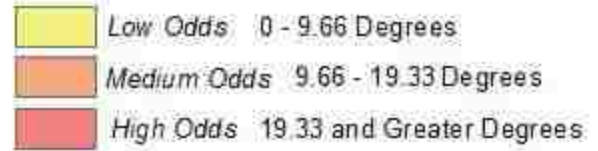
■ Sandstone



# Alum Creek Experimental Forest

Slope Angle

● Sample Locations



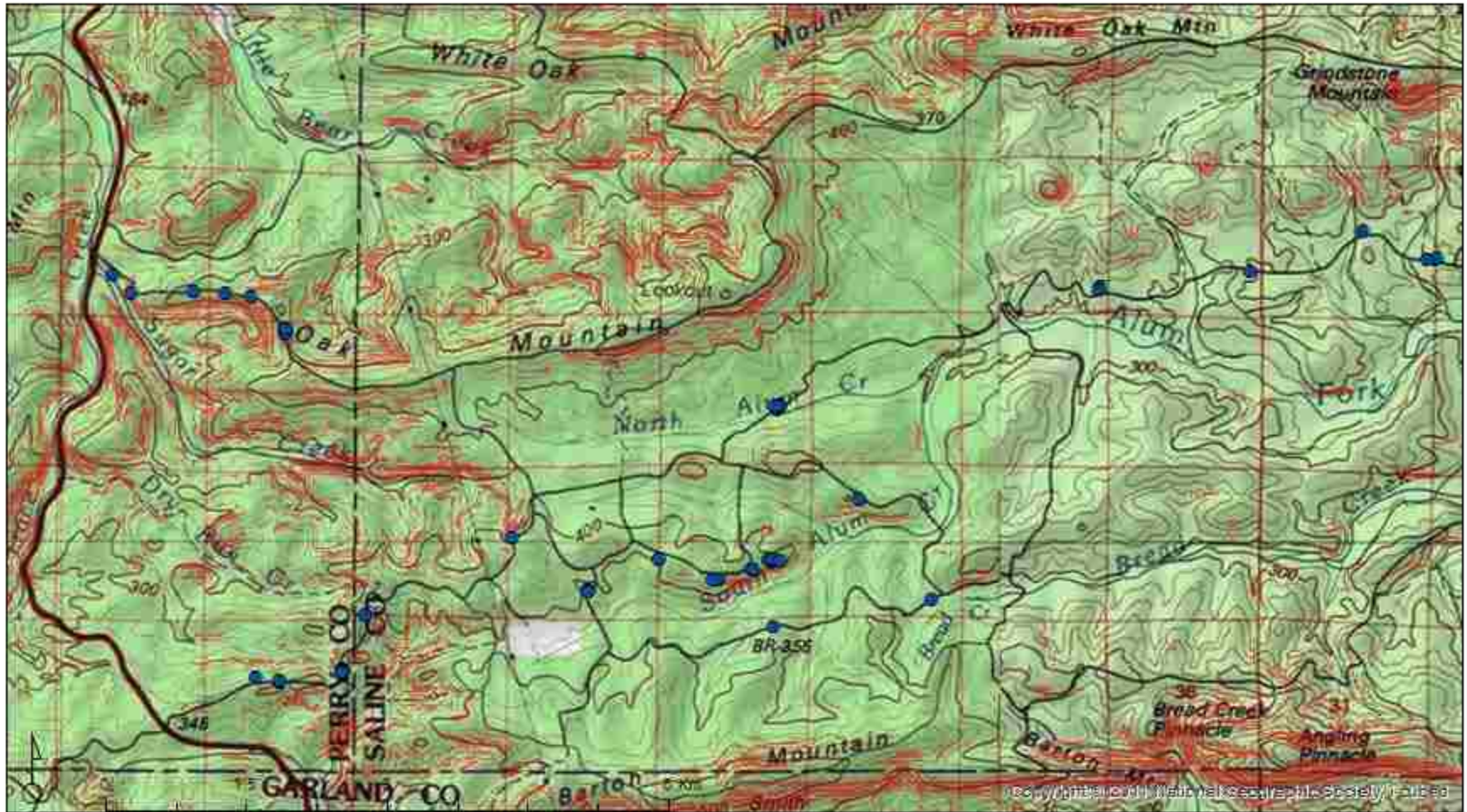


# Alum Creek Experimental Forest

Slope Angle

● Sample Locations

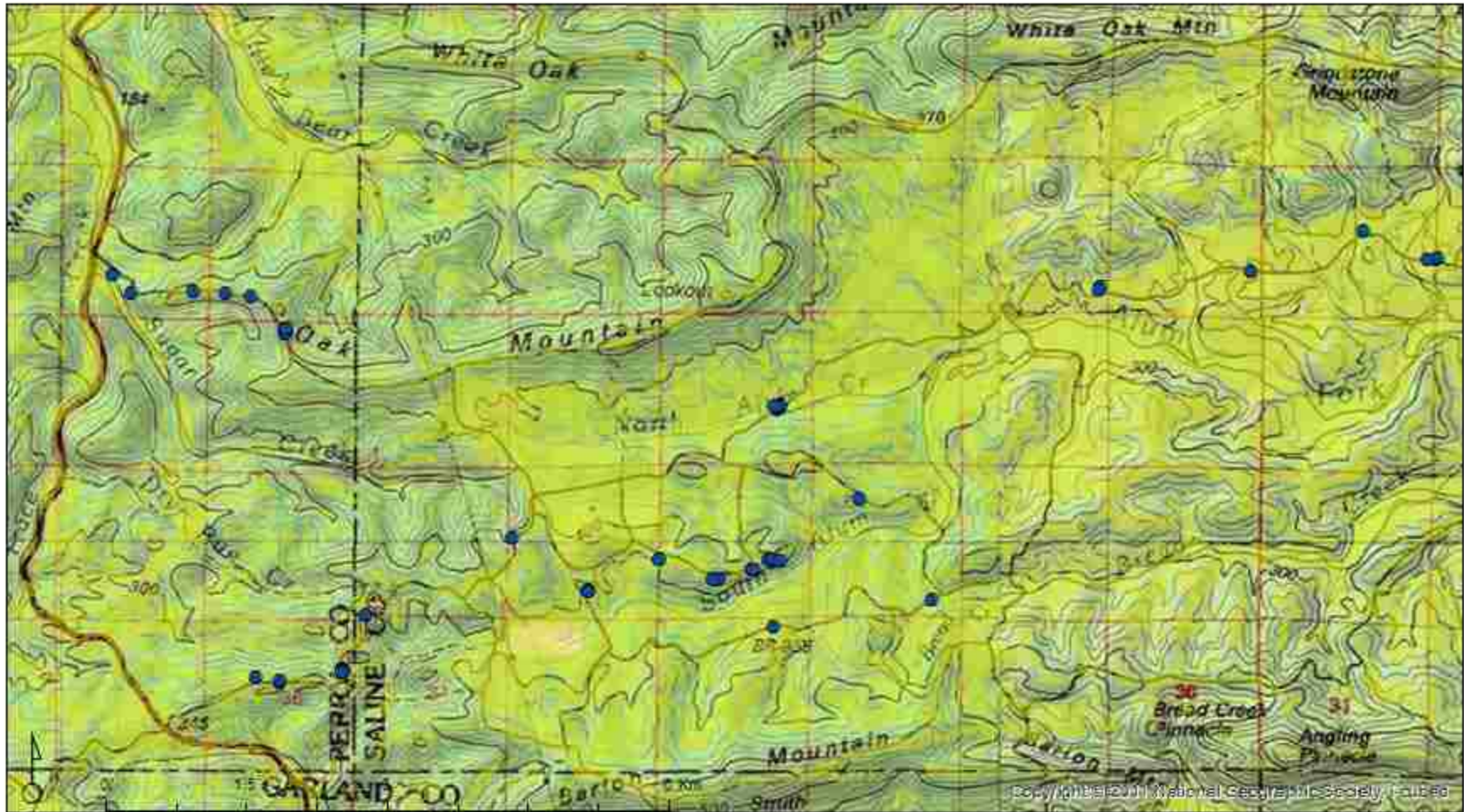
High Odds: 19.33 and Greater Degrees



# Alum Creek Experimental Forest

## Slope Angle

● Sample Locations    Low Odds 0 - 9.66 Degrees



# Alum Creek Experimental Forest

Slope Angle

● Sample Locations

Medium Odds: 9.66 - 19.33 Degrees



# Alum Creek Experimental Forest Highest Odds

- High Odds
- Alum Experimental Forest Data Locations



# Alum Creek Experimental Forest

## Lowest Odds

- Low Odds
- Alum Experimental Forest Data Locations



## B. Maps for the Rock Creek Tornado Blowdown area

For the Rock Creek Tornado Blowdown area the exact spatial location of sampled tree throws were not collected. However, from previously published maps I was able to determine the approximate areas that were sampled (Figure 2.9) (Phillips et al., 2008b). Table 4.20 lists the logit coefficients that were used for mapping odds of bedrock mining for this site.

**Table 4.20** Logit Coefficients (B) for the Rock Creek Tornado Blowdown.

|                  |         | <i>Underlying Geology</i> |       |
|------------------|---------|---------------------------|-------|
| <b>DBH</b>       | .391    | <b>Sandstone</b>          | 5.879 |
| <b>Thickness</b> | -.052   | <b>Shale</b>              | 4.451 |
| <b>Constant</b>  | -11.577 |                           |       |

During the map making process it was determined that available geologic maps of the study areas was too coarse in scale to be useful for this type of fine scale mapping. The extensive folding and faulting of the stratigraphy of the Ouachita Mountain chain is most likely the reasoning for this coarseness as the creation of a detailed geologic map would be nearly impossible. Therefore, due to the ineffective nature of available data, maps were not produced for the odds of the underlying bedrock variables.

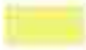


Three equal interval groups of odds of bedrock mining were created for stand mean DBH data. Low odds of mining bedrock showed a range of 0 to 4 (mean) inches in diameter. Medium odds represented 4to 8 inches and high odds were represented by a range of 8 to 12 (mean) inches in diameter. The northern study area within the Rock Creek Tornado Blowdown site was found to have high odds of bedrock mining based on DBH and the southern area within the site had low odds of mining. Again, the case-by-case nature of wad dimensions made mapping of these variables impossible.

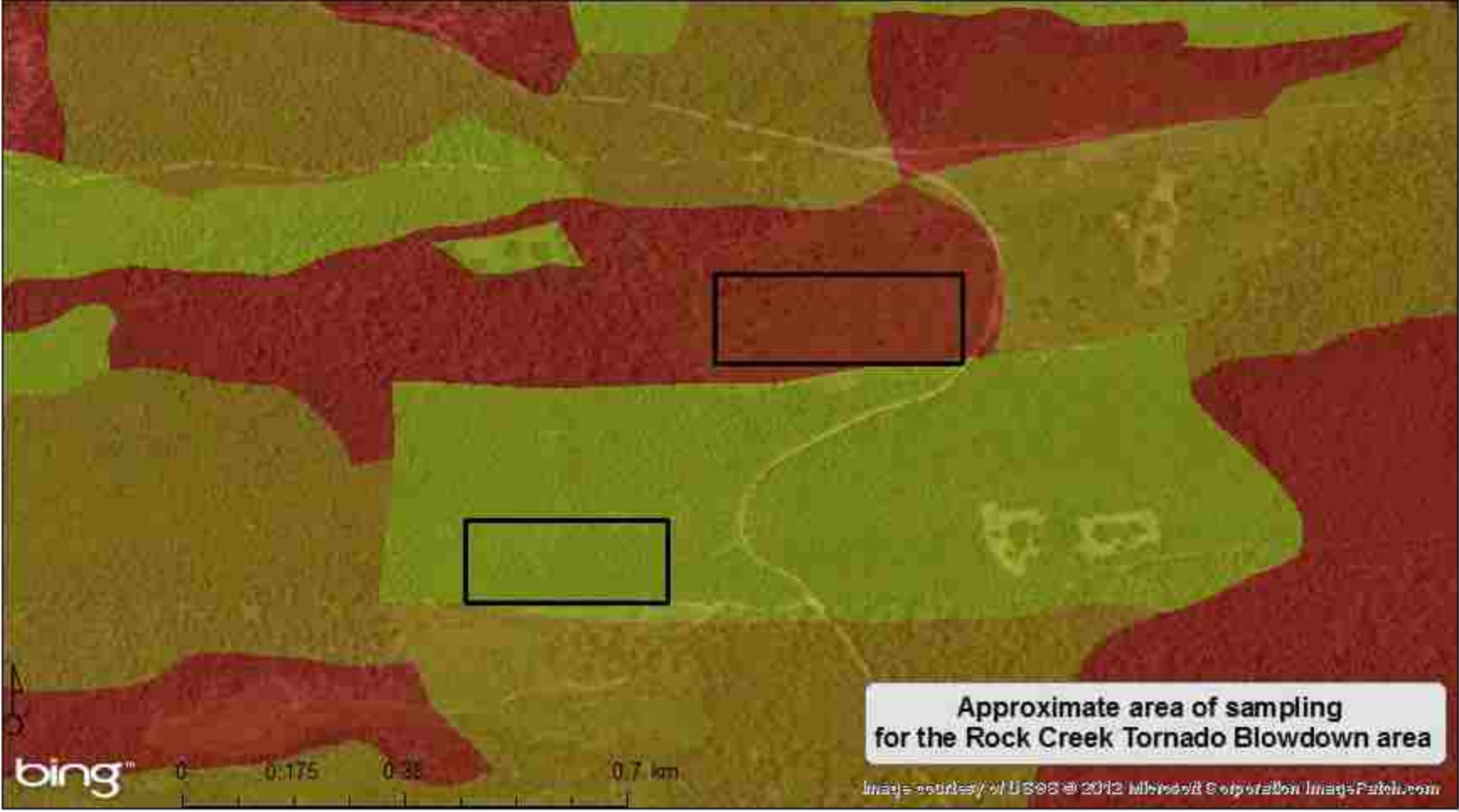
The “highest” and “lowest” odds of bedrock mining calculated for the cycle-of-life uprootings of the Alum Creek Experimental Forest were applied to create a map of extrapolated odds for the Rock Creek Tornado Blowdown area to show areas of potential non-tornado forced uprooting caused bedrock mining activity. For this map, the areas of highest odds were located on shale bedrock and had a slope angle of 19.34 degrees and higher, were located on sandstone, and coincidentally on the western or northwestern aspects (as the other aspects were assigned low or medium odds). The areas of lowest odds had the lowest category of slope angle, 0 to 10 degrees and were on the southeast, north, southwest, south, or northeastern aspect, and were coincidentally on shale bedrock (as this was the only other geologic type represented in the study area). Also, for the creation of this map, bedrock type was not helpful in creating the map of extrapolated odds because sandstone bedrock underlies the entire area. The areas of highest odds were located on shale bedrock and had a slope angle of 19.34 degrees and higher and were coincidentally on the western or northwestern aspects (as the other aspects were assigned low or medium odds).

# Rock Creek Tornado Blowdown

## Odds of Bedrock Mining

Diameter at Breast Height

|   |        |                |
|---|--------|----------------|
|  | Low    | 0.0 - 4.0 in.  |
|  | Medium | 4.0 - 8.0 in.  |
|  | High   | 8.0 - 12.0 in. |

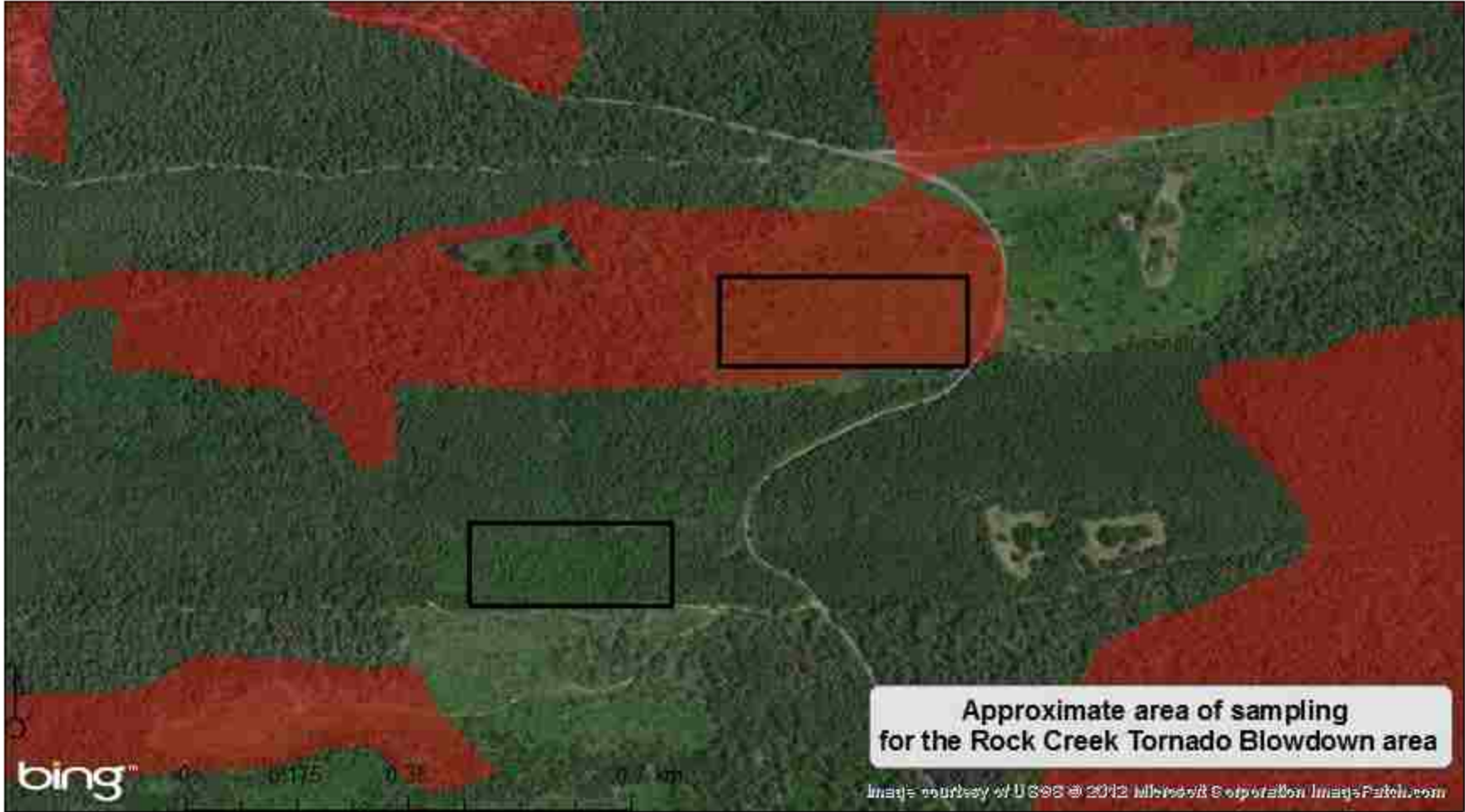


# Rock Creek Tornado Blowdown

Odds of Bedrock Mining  
Diameter at Breast Height

High 8.0 - 12.0 in.

83



Approximate area of sampling  
for the Rock Creek Tornado Blowdown area

Image courtesy of USGS © 2012 Microsoft Corporation ImagePatch.com



# Rock Creek Tornado Blowdown

Odds of Bedrock Mining  
Diameter at Breast Height

Low 0.0 - 4.0 in.

84



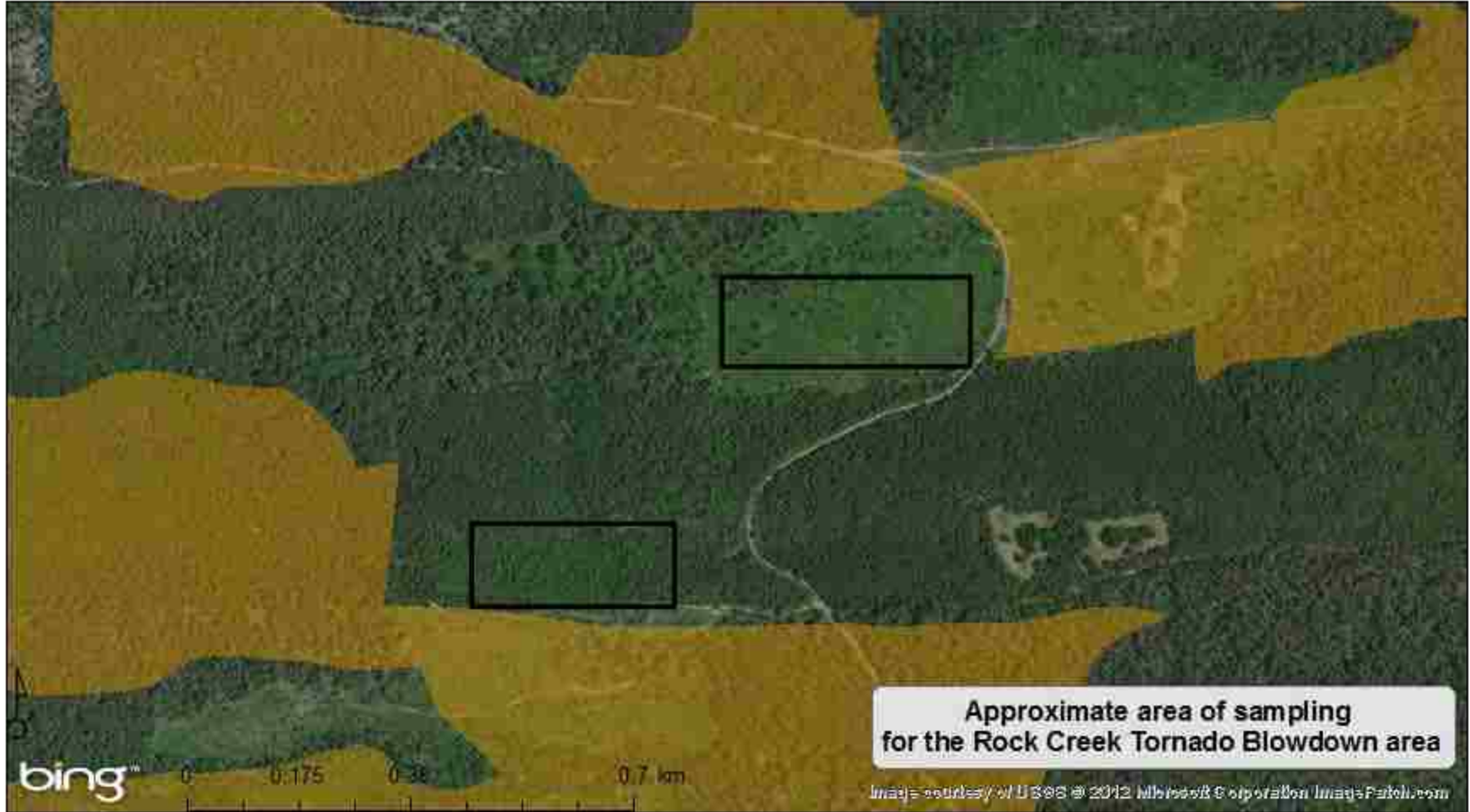
# Rock Creek Tornado Blowdown

Odds of Bedrock Mining

Diameter at Breast Height

Medium 4.0 - 8.0 in.

85

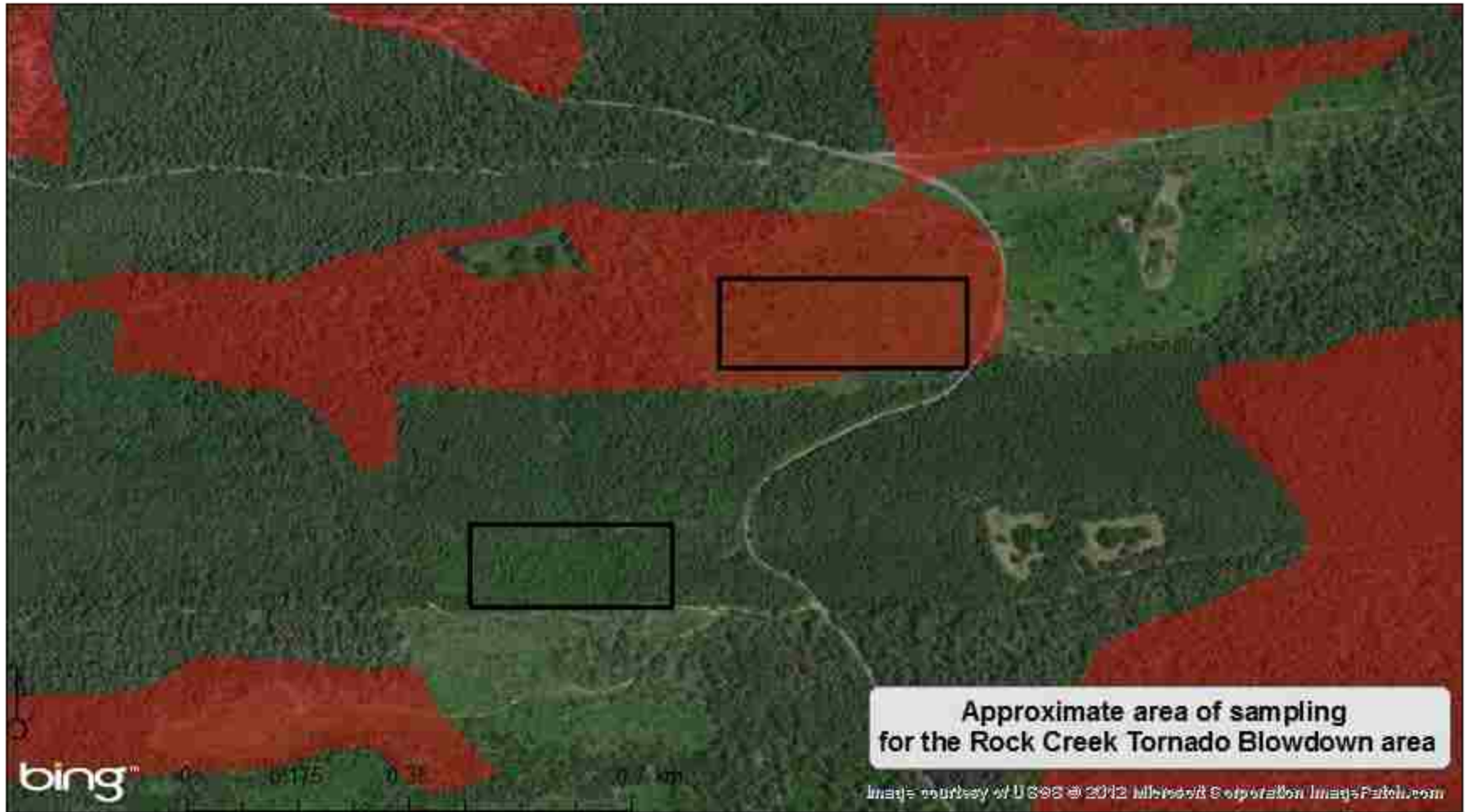


# Rock Creek Tornado Blowdown

Highest Odds

 High Odds

98



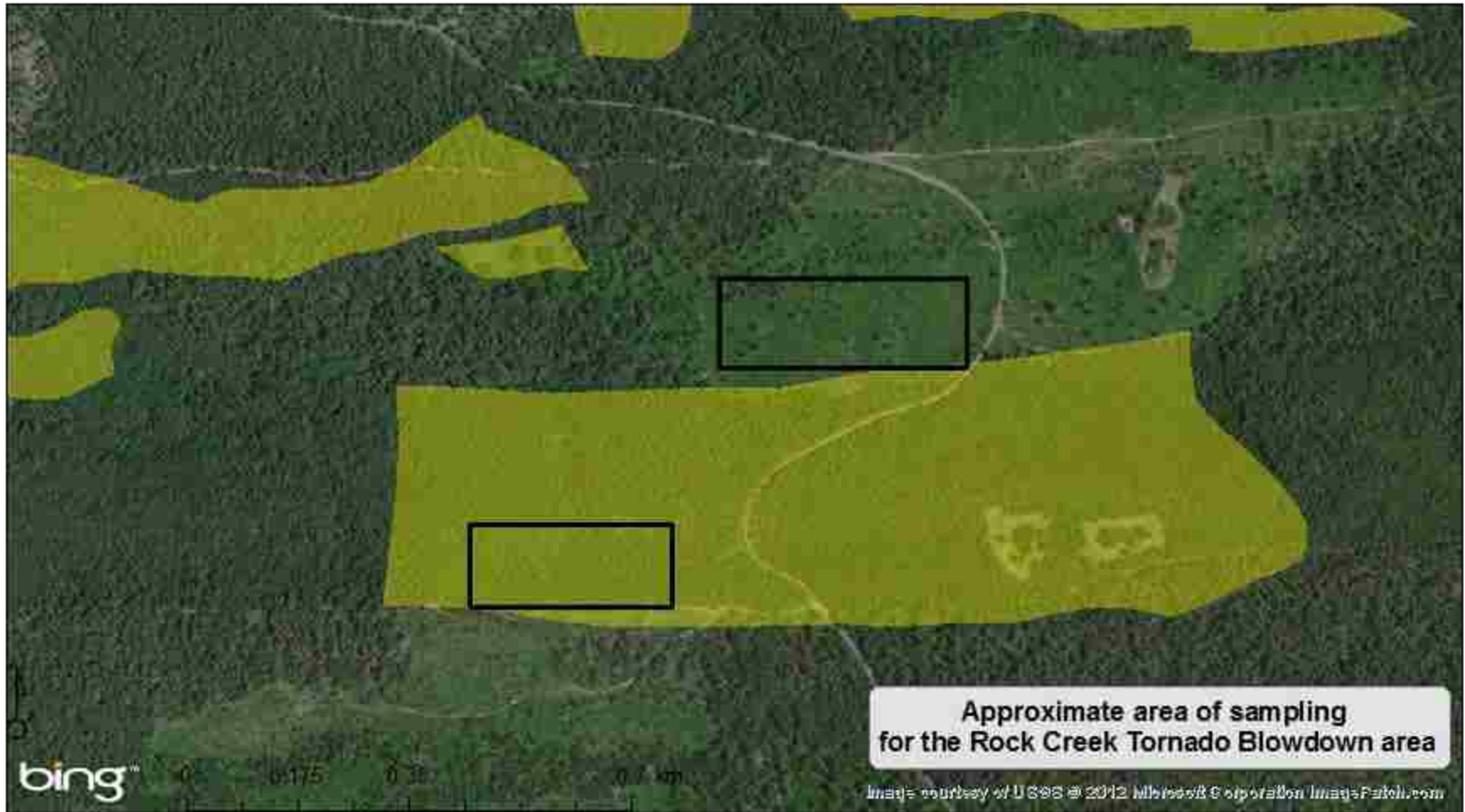
Approximate area of sampling  
for the Rock Creek Tornado Blowdown area

Image courtesy of USGS © 2012 Microsoft Corporation ImagePatch.com

# Rock Creek Tornado Blowdown


Lowest Odds

 Low Odds

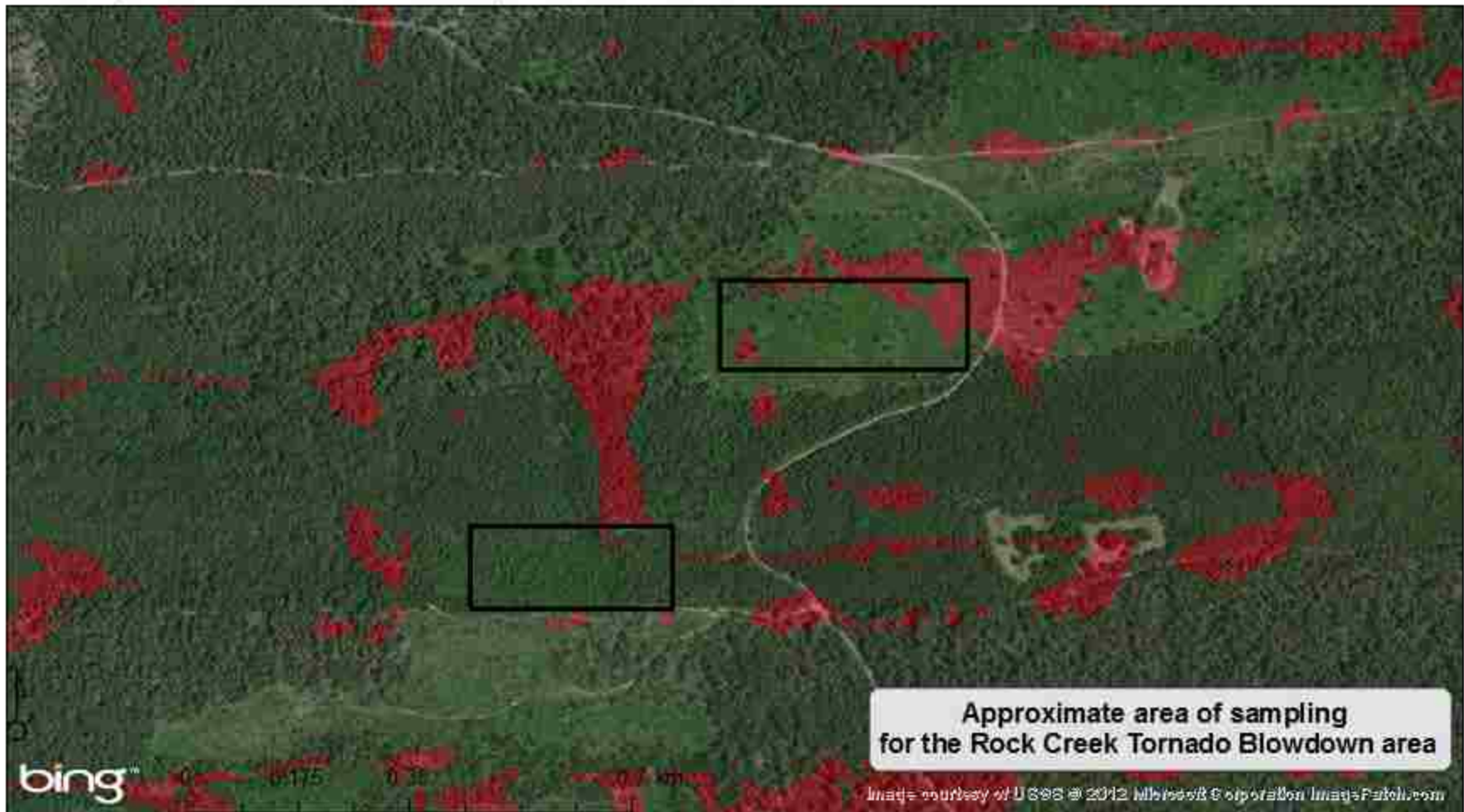


## Rock Creek Tornado Blowdown

### High Odds of Bedrock Mining

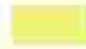
 Highest Odds

Extrapolated Odds from the Alum Creek Experimental Forest Model

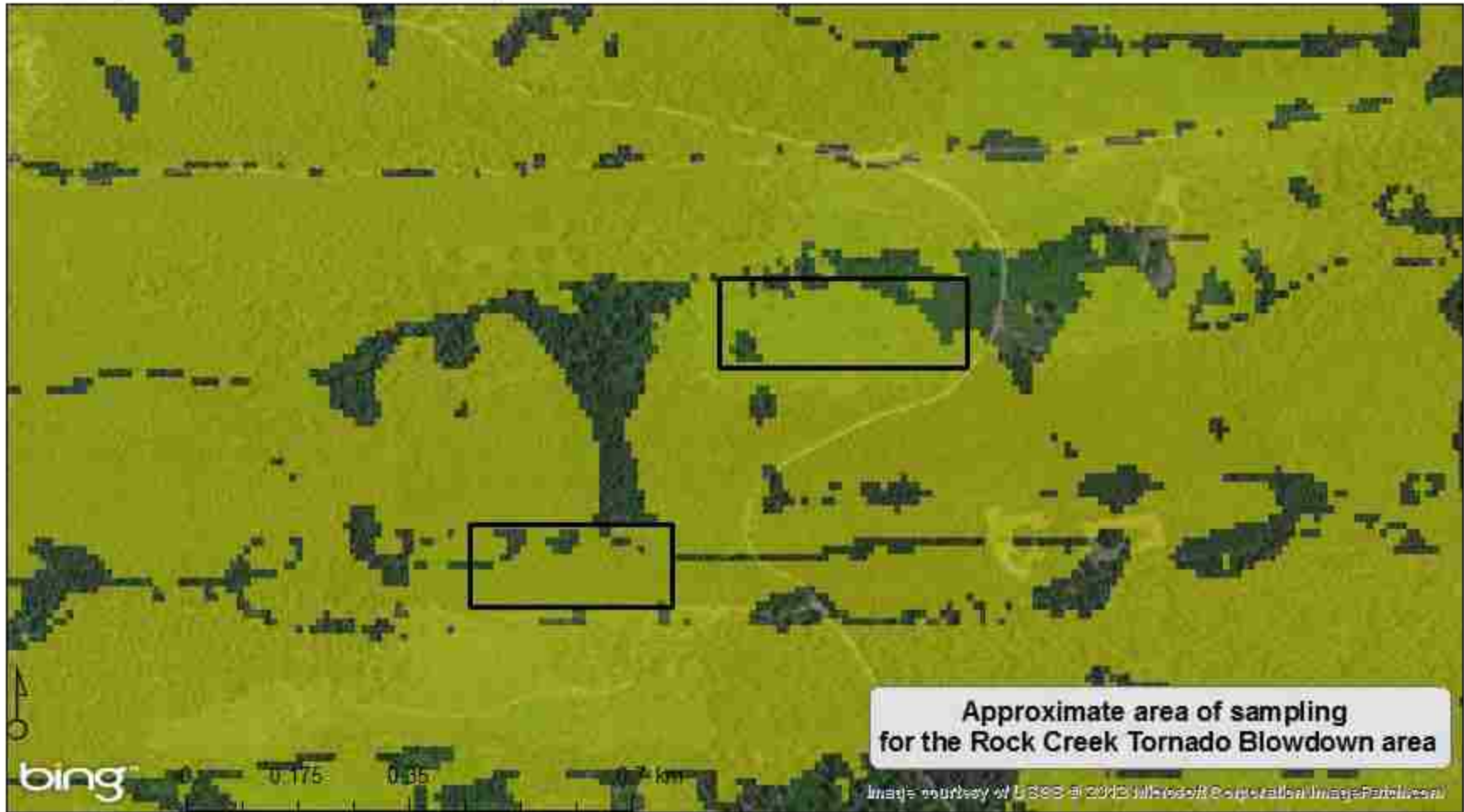


# Rock Creek Tornado Blowdown

## Low Odds of Bedrock Mining

 Lowest Odds

Extrapolated Odds from the Alum Creek Experimental Forest Model



### C. Maps for the Mena Tornado Blowdown transects

51 samples were used, including 24 presence points and 27 absence points in the creation of bedrock mining “hotspot” maps for the Mena Tornado Blowdown transects. Table 4.21 lists the logit coefficients that were used for mapping odds of bedrock mining for this site. Map creation for the Mena Tornado Blowdown transects preceded in the same manner as the map creation for the Alum Creek Experimental Forest and the Rock Creek Tornado Blowdown.

**Table 4.21** Logit Coefficients (B) for the Mena Tornado Blowdown.

| <i>Underlying Geology</i>  |         | <i>Soil Mapping Unit</i>       |         |
|----------------------------|---------|--------------------------------|---------|
| <b>Alluvium</b>            | -3.273  | <b>Bengal/Bismarck/Nashoba</b> | -19.990 |
| <b>Sandstone</b>           | -1.323  | <b>Octavia</b>                 | 17.548  |
| <b>Sandstone and Shale</b> | 16.717  | <b>Littlefir</b>               | 19.006  |
| <b>Shale</b>               | 19.442  | <b>Clebit</b>                  | 19.690  |
| <b>Mixture</b>             | 39.132  | <b>Mena</b>                    | 19.690  |
| <b>Constant</b>            | -17.929 | <b>Bengal</b>                  | 21.092  |
|                            |         | <b>Sallisaw</b>                | 39.001  |
|                            |         | <b>Sherless</b>                | 39.132  |
|                            |         | <b>Carnasaw</b>                | 39.489  |
|                            |         | <b>Bonnerdale</b>              | 41.295  |

The Mena Tornado Blowdown model is that the accepted variables have many categories. Therefore I deemed negative logit coefficients to have low odds and then split the positive logit coefficients into medium and high odds at their natural breaks. The sandstone and shale geology, shale, mixture of rock types had a positive effect on the odds of bedrock mining. The alluvium and sandstone geology were considered to have low odds, the sandstone and shale and the shale only bedrock type to have medium odds, and the mixture to have high odds. Whereas, areas with alluvium and sandstone had lowered odds. Of the soil mapping units only the Bengal/Biskarck/Nashoba had a negative effect on mining odds and so this soil unit was classified as having “low odds.” The high number of categories in this

The “highest” and “lowest” odds of bedrock mining calculated for the cycle-of-life uprootings of the Alum Creek Experimental Forest were applied to create a map of extrapolated odds for the Mena Tornado Blowdown area to show areas of potential non-tornado forced uprooting caused bedrock mining activity. The areas of highest odds were located on shale bedrock and had a slope angle of 19.34 degrees and higher and were coincidentally on the western or northwestern aspects (as the other aspects were assigned low or medium odds). The areas of lowest odds had the lowest category of slope angle, 0 to 10 degrees and were on the southeast, north, southwest, south, or northeastern aspect, and were on shale bedrock.

# Mena Tornado Blowdown Area

## Odds of Bedrock Mining

Underlying Geology

● Mena Data Samples

Low Odds Sandstone  
High Odds Shale  
No Information





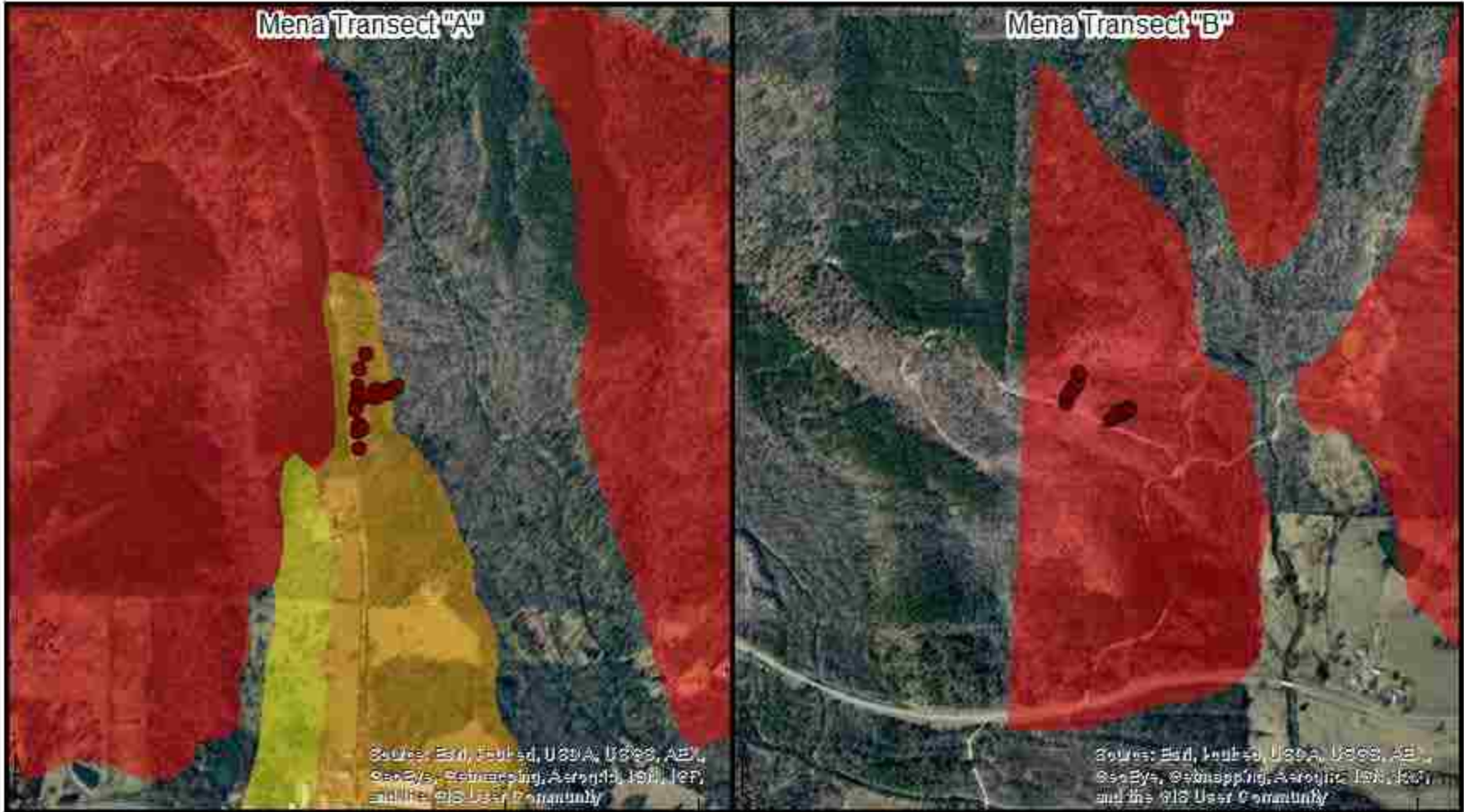
# Mena Tornado Blowdown Area

## Odds of Bedrock Mining

Soil Mapping Unit

Mena Data Samples

- Low Odds Bengal/Biskarck/Nashoba
- Medium Odds Octavia, Littlefir, Clebit, Mena, Bengal
- High Odds Sallisaw, Sherless, Camasaw, Bonnderdale

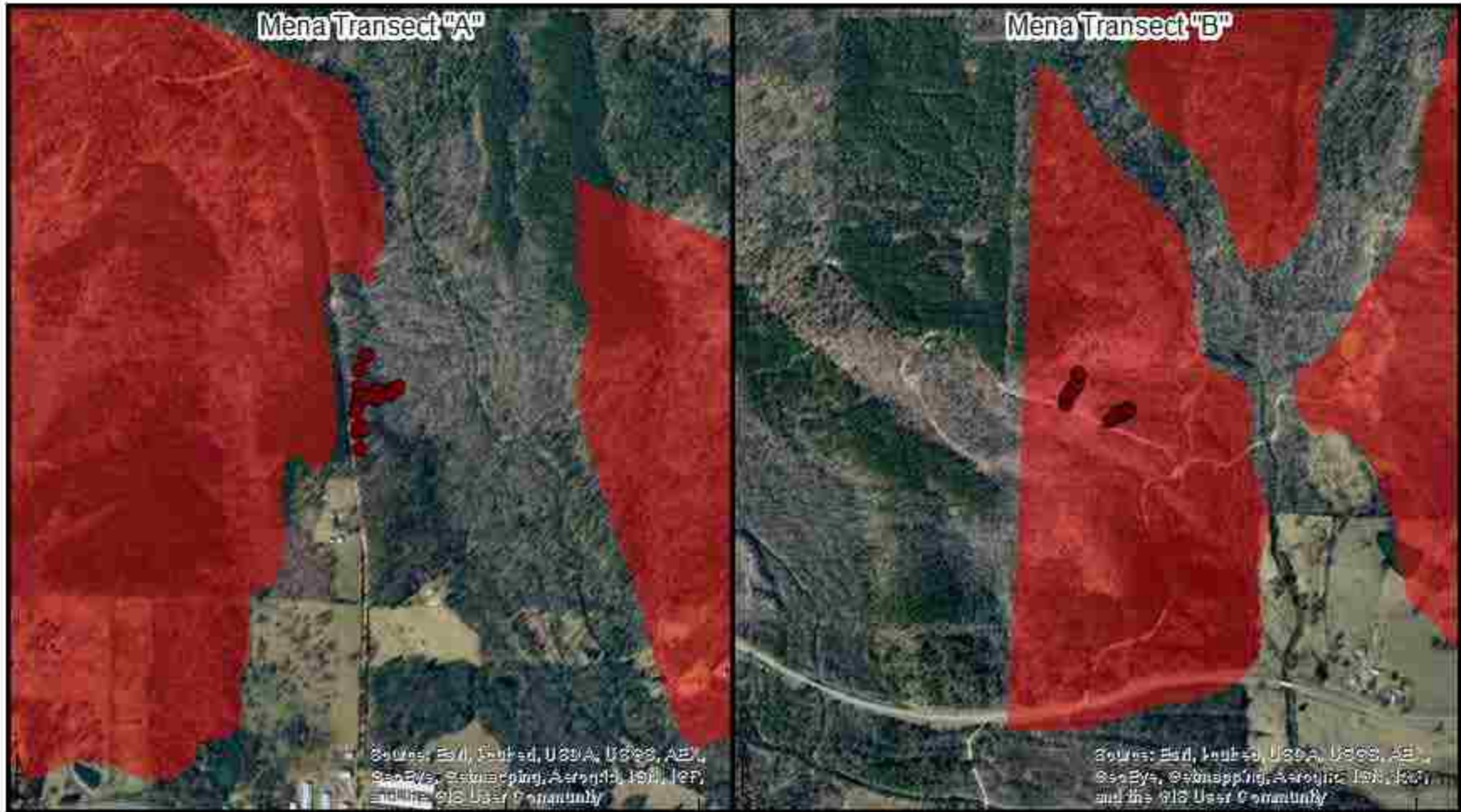


# Mena Tornado Blowdown Area

Highest Odds

● Mena Data Samples

■ High Odds

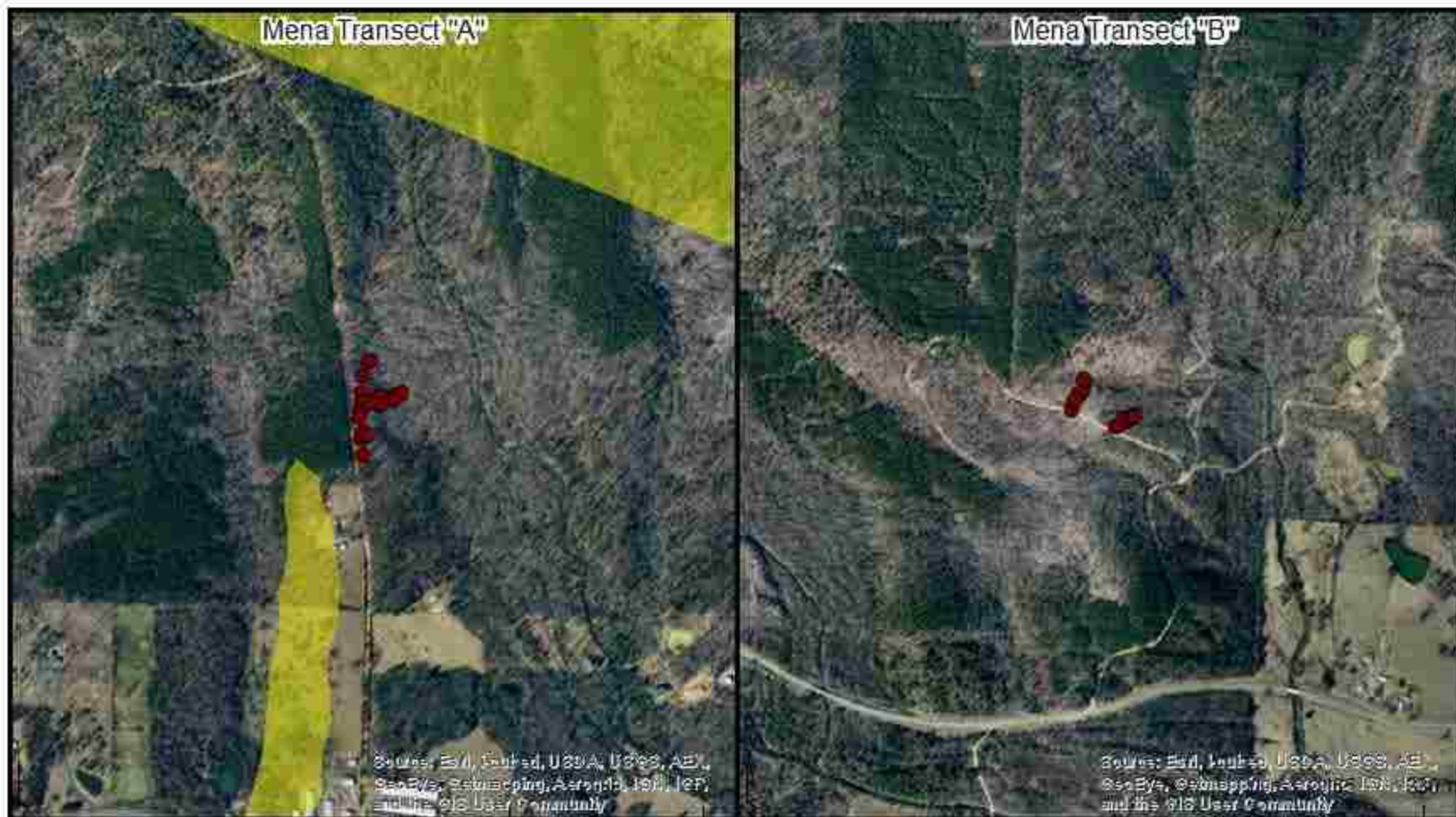


# Mena Tornado Blowdown Area

Lowest Odds

● Mena Data Samples

Low Odds

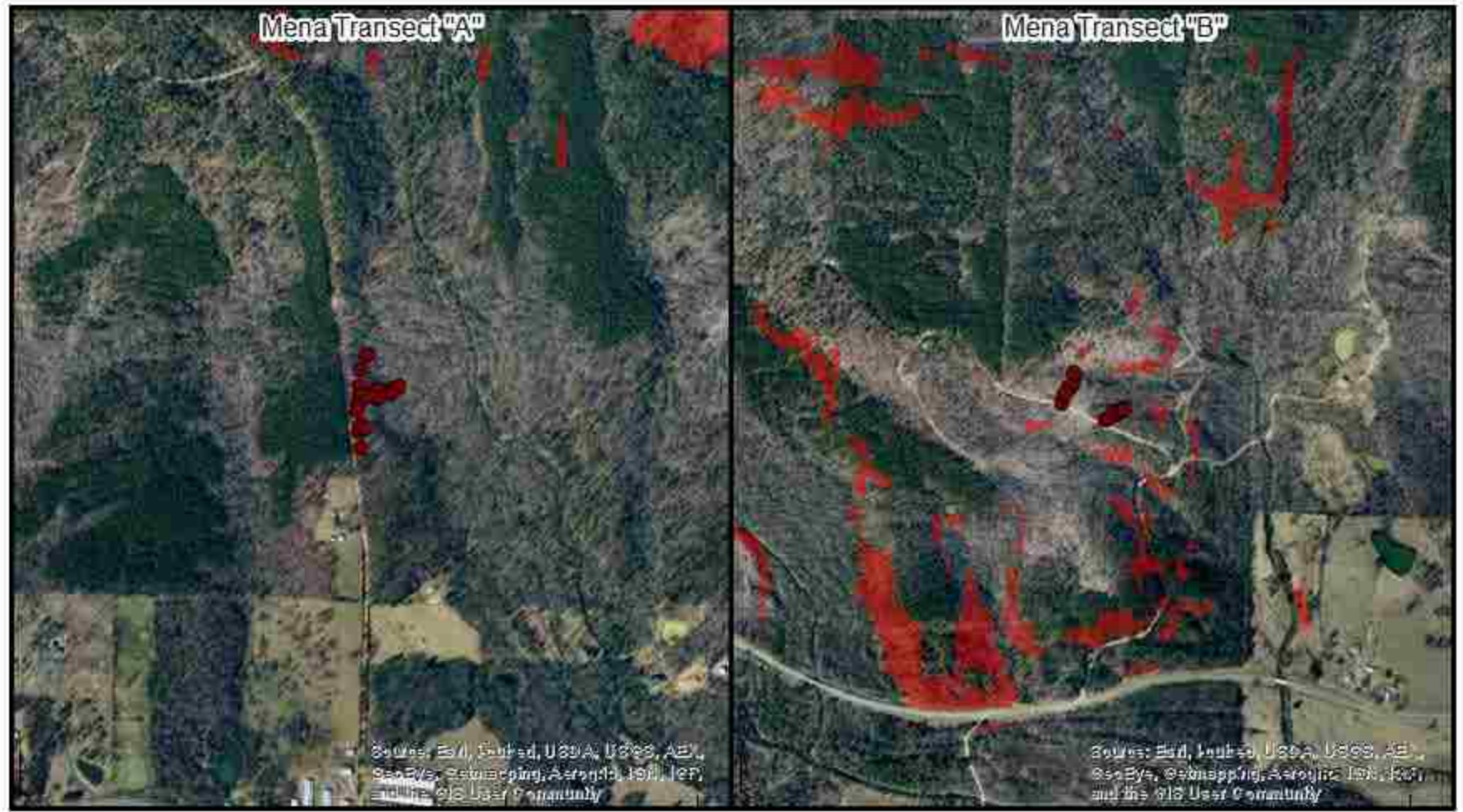


# Mena Tornado Blowdown Area

## Odds of Bedrock Mining

Extrapolated Odds from the Alum Creek Experimental Forest Model

- Mena Data Samples
- Highest Odds



## Mena Tornado Blowdown Area Odds of Bedrock Mining

- Mena Data Samples
- Lowest Odds

Extrapolated Odds from the Alum Creek Experimental Forest Model



## **Chapter Five**

### **Discussion**

Overall, bedrock mining occurs slightly more often than not in tree uprooting events within the Ouachita mountain forest. It was expected at the beginning of this project that the differing forcing mechanism of turnover (tornado versus so-called cycle-of-life uprootings) would cause variation in the importance of predictive parameters. The intense force of energy from the blast of a tornado seems likely to displace the majority of the root mass and surrounding soil plate along with any bedrock the roots had worked their way into for all trees in an affected area. By contrast, cycle-of-life uprootings can occur at vastly differing times, allowing for a greater variance in wad diameter from soil and fragment displacement over time, weathering of less-resistant bedrock fragments into smaller, less readily identifiable as fresh bedrock pieces, and even incomplete initial uprooting. Additionally, cycle-of-life uprootings involve mainly individual and rarely a few grafted trees while windthrown uprootings can experience the domino effect in which larger trees fall over and consequently uproot neighboring trees with their impact (Schaetzl et al., 1989b). Therefore I have separated the discussion into two groups: the cycle-of-life uprootings and the tornado blowdowns.

#### **I. Alum Creek Experimental Forest**

Local and temporal contingencies seem to be especially important for the cycle-of-life treethrows because the conditions surrounding and causing their upheaval can vary widely, which is reflected in the complex model for the Alum Creek Experimental forest. Even though a great number of parameters were examined for the cycle-of-life model and many were found to not strengthen the model, the relationship between bedrock mining and these parameters remained quite complicated.

Type of fall and position on slope were recorded only for samples within the Alum Creek Experimental Forest. As far as type of fall is concerned, cross-slope falls had equal chances of uprooting mined bedrock or not. Downslope falls showed nearly twice as many positive presence samples as negative. On the other hand, upslope falls displayed a meager tendency to not mine bedrock. One reason for this could be, although it has not been proven, the uneven distribution of root mass that trees often adopt when on an uneven surface. In cases like this, roots on the lower portion of the slope may grow to a longer and wider reach to support the upslope weight of the tree without digging in too deep to bedrock. Similarly roots on the upslope side could grow deeper into the soil for added stability, and cause downslope falls to mine more bedrock.

Position on slope was included in the logistic regression model for the Alum Creek site. An examination of the relationship between position on slope and bedrock mining proved to be enlightening. Ridgetop, flat, and midslope sites mined bedrock more often than not (Figure 2.8). Uprooted wads on the top portion of the slope mined no

bedrock and samples at the bottom portion of the slope presented even chances of mining activity or none at all.

It was expected that the exposed ridges would experience higher rates of disturbance and have shallower soils leading to greater rates of mining activity (Ruel, 2000; Shure et al., 2006). Ridge sites in the model do exhibit slightly increased odds of mining activity. The absence of bedrock mining found in treethrows near the top but not at the ridge of slopes was entirely unanticipated due to the relatively long duration and intensity of exposure to weather. Both the ridge and top portion of the slope mined only sandstone bedrock so bedrock type does not appear to be the determining factor behind this unusual occurrence (Figure 5.1). Furthermore, there is not a significant relationship between underlying geology and position on slope (Table 4.2). Wad thickness is only very slightly lower for the top portion of the slope samples so rooting depth is unlikely to be the reason (Figure 5.2). It is possible that this is simply the result of sparse data. Three samples were found on the top portion of a slope – two of which were in a compound fall (samples 5a and 5b).

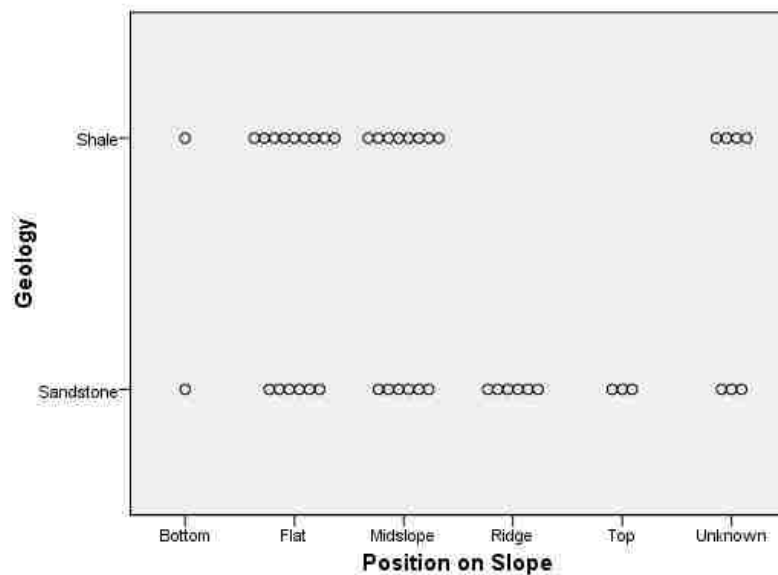


**Figure 5.1** Dot plot of underlying geology and position on slope for the Alum Creek Experimental Forest site.

A possible explanation for the prevalence of bedrock mining in flat areas is that they are also likely to experience disturbance in the form of water logging – generating possible greater instability for trees in flat areas. Flat areas, bottom portion of the slope, and the midslope showed an increase in the probability of bedrock being mined. The uncertainty about the multi-faceted relationship of position on slope and bedrock mining presence suggest that it may have been more beneficial to have had a reduced number of classes of positions on slope. For example, the ridge and top portion of slope positions are often similar in soil moisture content and geology in this geographic area so they could have been grouped together. Likewise, flat areas and the bottom portion of slope

are similar in geology and often in soil moisture content. Furthermore, the small dataset cannot give a robust explanation or enhance understanding of the relationship between these variables so future work should consider expanding upon this research area.

Aspect was included in the site's model; however western and northwestern aspects did not have a strong enough predictive value to strengthen the fit of the model. All other aspect positions had a negative influence on the odds of bedrock mining. Wind damage is the leading cause of abiotic damage to trees (Sellier et al., 2005). Foster (1988) observed that aspect serves as a major control on the intensity of wind-forced uprooting and stand damage. The wind roses for the western and eastern portions of the Ouachita National Forest show that the most frequent winds originate out of the south and southwest (Figure 5.2). If the aspect of a location bears the brunt of the prevailing wind or storm tracks, one can see a clear connection between aspect and the susceptibility of a tree to ice or wind damage (LaFon and Speer, 2002; Bragg et al., 2003; Warillowand Mou, 2004; Stueve et al., 2007). However, no treethrows were found on the northwestern slopes, where the average wind speeds are quite high. The high prevalence of bedrock mining on the southern, eastern, northeastern, and western aspects correlates well with the speed and frequency of winds out of those directions (Figure 4.11 and 5.2). Likewise, the rarity of bedrock mining on the southeastern, southwestern, and northern slopes correlates well with the relatively low speed and infrequent winds originating out of the southeast, southwest, and north (Figure 4.11 and 5.2).

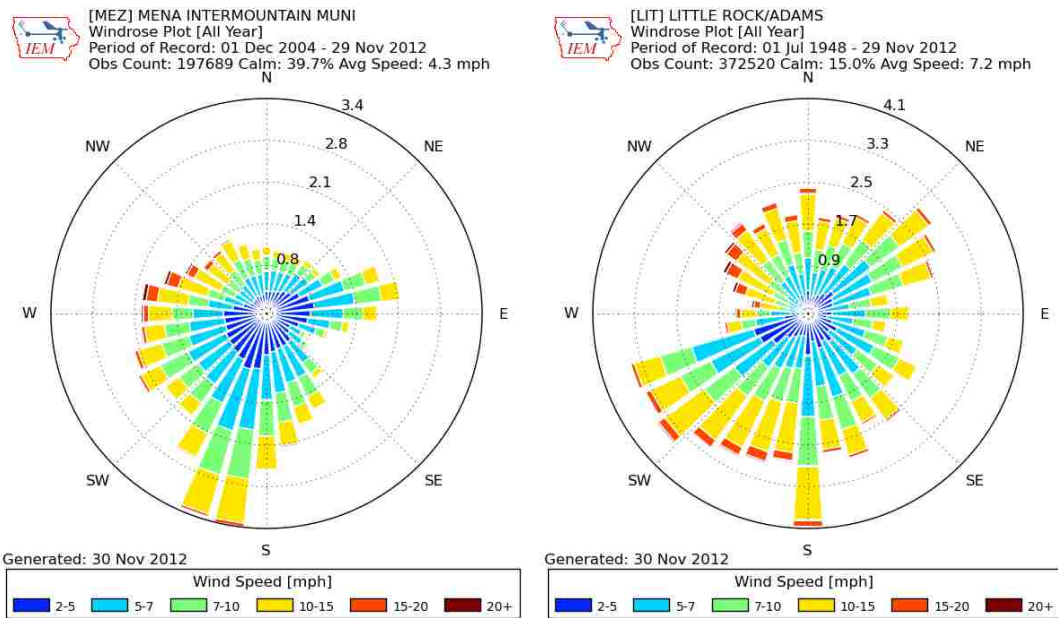


**Figure 5.2** Wind roses showing the speed and primary direction of the winds (year-round) for the western (left) and eastern (right) Ouachita National Forest area (Iowa State University, 2012).

There is also the idea that aspect position is related to the soil moisture content. Aspects with a reduced heat load and shorter sun exposure should be expected to retain soil moisture for longer periods, increasing the chances of them falling over. To examine if this was the case I calculated the direct insolation for the Alum Creek Experimental



Forest site area using the Solar Radiation toolset within the Spatial Analyst toolbar in ArcMap. This tool utilized the same 1/3 arc-second (30 m) resolution elevation data that was used in prior analysis (USGS, 2011). I set the tool to examine the entirety of 2011 to find the total direct insolation which is the sum of the direct insolation from the track of the sun across the sky overhead (Esri, 2012). The higher the direct insolation value, the more sun the spot receives (Figure 5.3). I then used Pearson's correlation to examine the relationship between bedrock mining presence and the direct insolation value. The relationship was found to be insignificant at a value of 0.896. This suggests that insolation is not a good predictor of bedrock mining. But, future studies should more explicitly determine this relationship with a research design tailored to specifically study insolation instead of it being considered as only a secondary part of aspect as it was in this study.

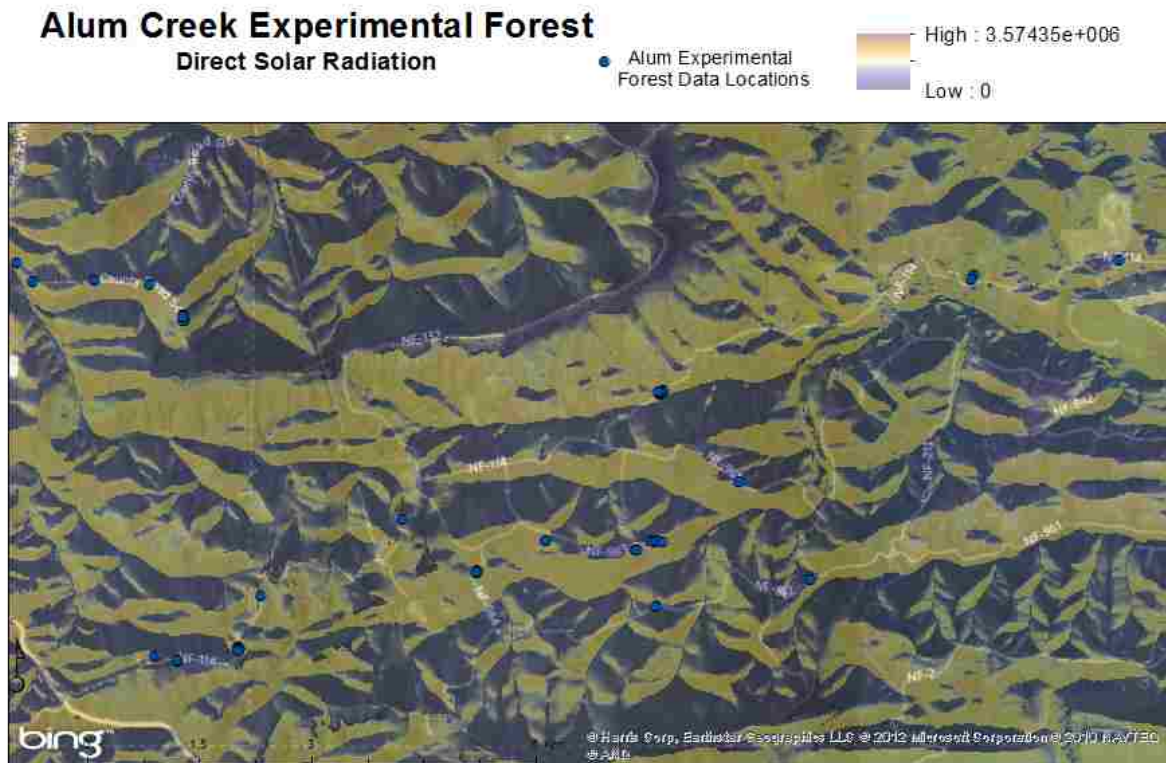


**Figure 5.3** Direct insolation map for the Alum Creek Experimental forest area.

Slope angle was found to be positively correlated with presence of fresh bedrock in uprooted wads for the cycle-of-life uprootings. This result corresponds with Norman et al.'s (1995) finding of a positive relationship between pit depth and slope steepness, that rooting is habitually deeper on steeper slopes, allowing for increased mining activity. Ulanova (2000) also confirmed this relationship, through a review of the literature that as slope increases the percentage of surface area coverage of wind throw disturbances also increases. If pit dimensions had been logged as wad dimensions were, these results would gain reliability.

For this study, decay class was utilized as a proxy parameter for estimated time in situ since a sampled tree had initially uprooted for the Alum Creek Experimental Forest site. In the case of the tornado blowdown sites, decay class data was not gathered as the time since uprooting was known. The mean and range of values for decay class were higher in the set of samples that tested positively for mined bedrock, meaning that slightly older trees more often contained bedrock fragments. Most samples acquired were in the decay class “3” to “6” range.

It was expected that there would be a positive relationship between the time an uprooted tree has been in situ and disintegration of the root wad. In temperate areas like the Ouachita National Forest, felled boles will likely linger, decaying for a relatively long period, perhaps upward of a century for the largest woody debris (Onega and Eickmeier, 1991; Muller, 2003; Busing, 2005). Over time the soil wad attached to the roots will break down, returning the soil to the ground surface, flowing down slope, or refilling the original pit, adding to soil heterogeneity (Lutz, 1960; Phillips and Marion, 2006). When slopes are steep, bare sediment and rock fragments are greatly affected by the processes of erosion (Norman et al., 1995). Gallaway et al. (2009) found that the oldest wads on the steepest slopes maintained the least measurable amount of mined bedrock due to processes of disintegration and eventual transport away from the root wad.

However, these expectations were incorrect for the cycle-of-life samples. Decay class actually exhibited a moderately strong positive effect on bedrock mining within the site’s model. It is possible that the gradual wasting of the soil surrounding the bedrock fragments in wads allowed them to be identified more easily than in less decayed boles. This would suggest that a more thorough examination of wads should be undertaken in future studies.

At this site, hardwood trees had equal chances of uprooting mined bedrock or not. But, conifers (and those trees whose type was unable to be determined) had a slight preference for mining activity. Conceivably, the reason for the slight mining preference of these conifers is the characteristically deeply trenched tap root architecture found in the short-left pine of this area. Conifers overall displayed an overall deeper mean and range of rooting depth than hardwoods (Figure 5.4). Later-successional species, such as high wood strength deciduous varieties, were found by Peterson (2007) to be more wind-firm than their earlier-successional softwood neighbors. At the beginning of this study a question was posed; if conifers have weaker roots in general than deciduous tree types but have deeper tap-root architecture, which root characteristic is the most important for bedrock mining? The results suggest that, all other factors being equal, the deep tap-root structure is more important for predicting bedrock mining in cycle-of-life uprooting events.

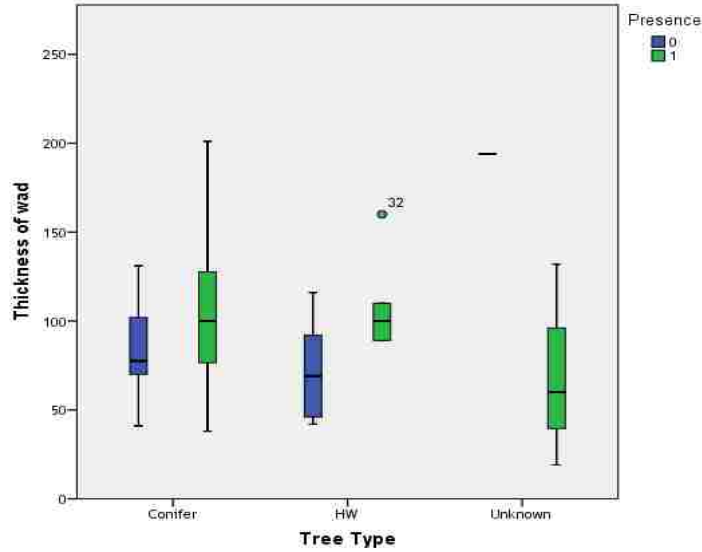


**Figure 5.4** Boxplot of tree type, thickness of wad, and presence of bedrock mining.

In the beginning it was anticipated that tree diameter would have a considerable impact on uprooting and bedrock mining activity as multiple previous studies established that greater tree size (stem mass or DBH) yields increased toppling and the size of the resulting pit-mound system (Peterson, 2007; Nicholl et al., 2006; Webb, 1989). With a higher chance of uprooting, rather than snapping or simply rotting in place, one can expect a higher probability of the occurrence of bedrock mining. Additionally a larger pit-mound system is often due to increased wad dimensions – meaning that the tree’s roots have penetrated further into the surrounding soil, regolith, and bedrock.

Unexpectedly for the Alum Creek Experimental Forest cycle-of-life uprootings, trees that had positive identification of mined bedrock were on average, smaller than those trees that did not mine bedrock. Perhaps, simply, these larger trees have been able to grow to such a size because they first sprouted on areas of thicker soil than their smaller counterparts, disallowing mining activity and interaction with the bedrock interface altogether. Wad dimensions of samples that mined bedrock were slightly larger than those that did not. An evaluation of the correlation coefficient (R) of wad dimensions with DBH determined that all R values were low positive values. DBH and height of wad was 0.56, DBH and width was 0.07, DBH and thickness was 0.15, DBH and area was 0.24, and DBH and volume was 0.25. This suggests that there is a weak correlation between tree size and rooting as well as wad, pit, and mound dimensions. The contradictory nature of the relationship between tree size, wad dimensions, and bedrock mining warrants further investigation in future studies.

A review of the literature suggested that root penetration into bedrock is more likely to occur in shale than in sandstone as weathering was more rapid in the shale layers of the area (Phillips et al., 2008a). Therefore it was anticipated that bedrock mining would more often occur in areas with shale bedrock than those with sandstone. However, samples taken from areas of shale and sandstone bedrock types both mined bedrock more

often than not (Figure 4.9). Treethrows on sandstone actually had a higher rate of mining than shale sites. For the site's logistic regression model, sandstone was positively correlated with mining activity and shale underlying geology was not included in the model.

One possible explanation for the prevalence of sandstone bedrock fragments in uprooted wads is the visual method used to acquire presence or absence evidence. Confirmation by sight alone could cause oversight of shale bedrock in rootwads as shale can weather quite rapidly once unearthed compared to sandstone, causing relatively fresh shale bedrock to appear to be hill slope or soil fragment material. Phillips et al. (2008b) found at the dam site analyzed, that the extent of weathering was directly related to rock strength. Figure 5.5 demonstrates that shale bedrock was rarely found within any pit-mounds older than a decay class "6," while sandstone bedrock was found in the oldest classes. Sandstone bedrock was found in half of all decay class "6" or greater samples.

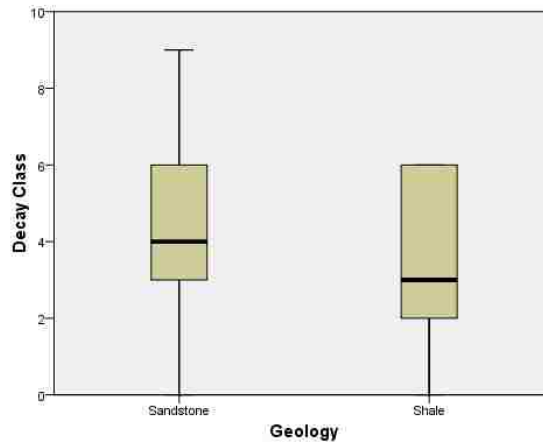


**Figure 5.5** Boxplot of the decay classification with the geology found in sample mounds within the Alum Creek Experimental Forest, Arkansas.

This begs the question, is the rate of weathering of fresh shale bedrock fragments measurably faster than that of sandstone? Shale is perhaps the most easily weathered of sedimentary rocks in this area and often weathers by physical disintegration (Phillips et al., 2005). In their study of regolith evolution in the Ouachita Mountains, Phillips et al. found that concentrations of shale fragments were greatly reduced above the C horizon (2005). They determined that this was due to the rapid chemical and physical weathering occurring within the forest soils. Future studies should determine how this faster rate of weathering can affect nutrient flux and the overall state of forest soils.

Binkley and Giardina (1998) found that trees can substantially alter soils within just a few generations. Soils that allow for sufficient rooting depth and dissemination allow root systems to transfer stress to the surrounding soil when disturbed, inhibiting toppling (Stokes et al., 1996). Likewise, in the Ouachita Mountains, Phillips et al. (2005) found that the local spatial variability in regolith thickness was directly associated with the influence of trees through root action and tree/stump rot followed by infilling of soil.

Soil mapping units were not included in the model for the cycle-of-life uprootings. However, Pearson’s correlation between underlying geology and soil mapping unit classes was highly statistically significant ( $\alpha=0.001$ ). So, even though the soil mapping unit parameter was not included in the model, sandstone bedrock was and so the soil types that are located on sandstone bedrock should likewise increase the odds of finding mined bedrock (Figure 5.6).

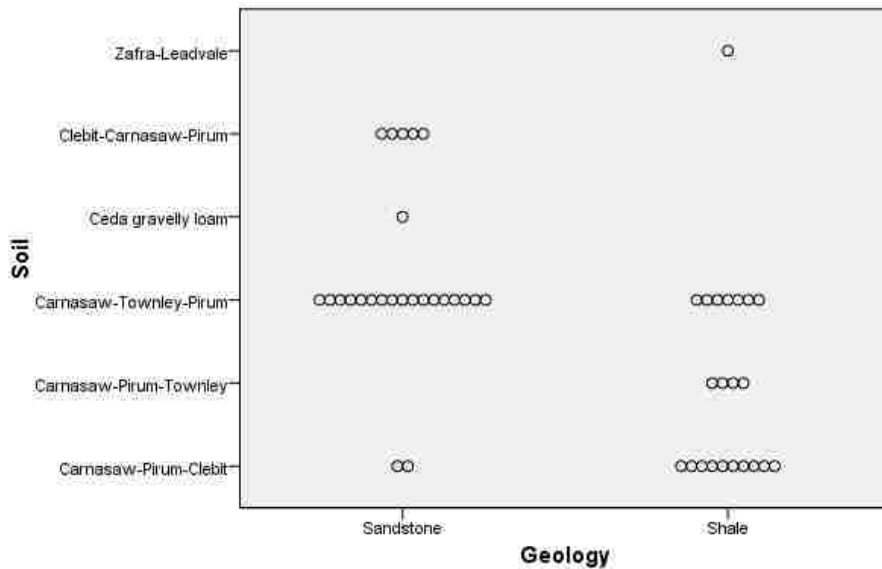


**Figure 5.6** Dot plot of underlying geology and soil mapping units for the Alum Creek Experimental Forest site.

## II. Rock Creek and Mena Tornado Blowdown

The forcing mechanism that causes the treethrow event seems to intrinsically change the relationship between the abiotic and biotic factors that control bedrock mining. The reason for the difference in the positive or negative odds is likely due to a combination of local and specific forcing mechanism strength contingency. The Rock Creek Tornado blowdown site showed an overwhelming majority of mined bedrock in 38 (84.4%) of the samples taken with only 7 (15.6%) of samples showing none. The tornado responsible for the forest damage at the Rock Creek was a strong F3 on the Fujita scale (National Weather Service, 2007). In the Mena blowdown area, the majority of treethrows exhibited no mined bedrock at 27 (53%) samples with the slight minority, 24 (47%), having mined unweathered bedrock. The tornado that caused the damage to the forest outside of Mena, Arkansas was rated as a relatively weak F1 on the Fujita scale (NCDC, 2011).

Unlike the Alum Creek Experimental Forest site, the Mena Tornado blowdown area expressed a greater likelihood of mining bedrock in northern or western aspects with freshly mined bedrock presence. This supplies an example of the difference that

uprooting forcing mechanism can cause in the relative importance of variables. The difference in aspect importance reflects the north-to-south path of the tornado event. The long track type of the tornados that caused the damage of the Rock Creek blowdown sites moved from a southwest to northeastern direction. However, the Rock Creek Tornado blowdown site was not examined for the influence of aspect as location data for individual samples was not recorded. If the southern and eastern aspect grouping had reflected a positive correlation to bedrock mining it would have strengthened the assumption of the powerful effect of differing forcing mechanisms. Aspect position was not included in either of the tornado blowdowns' models.

Slope angle was also not included in the Mena Tornado blowdown's model. The negative correlation between slope angle and bedrock mining activity for the Mena Tornado Blowdown site is likely due to the relatively flat terrain, which greatly reduces the slope range sampled. If slope angle data was gathered for the Rock Creek Tornado Blowdown site, would the relationship of slope angle and bedrock mining still be negative?

Due to the homogeneity of species within the blowdown sites, tree type was not deemed an appropriate variable for evaluation in the statistical modeling process. If the blowdowns had knocked over hardwoods, a more productive discussion could have been produced. Future work should undertake the assessment of the relationship between tree type, forcing mechanism, and the potential for bedrock mining. Similar methodology, using logistic regression, could be applied to determine the relative importance of various tree specific characteristics such as root and crown structure, wood strength, and type on odds of mining bedrock when uprooted by tornado winds, ice storms, or any other forcing mechanism.

It was expected that the larger a tree is in DBH that the deeper and more penetrating its roots would penetrate down to bedrock. For both sites, tree DBH had a greater median value and a slightly larger range for positive mined bedrock presence than for negative. DBH values for both sites were remarkably similar (Figure 5.7).

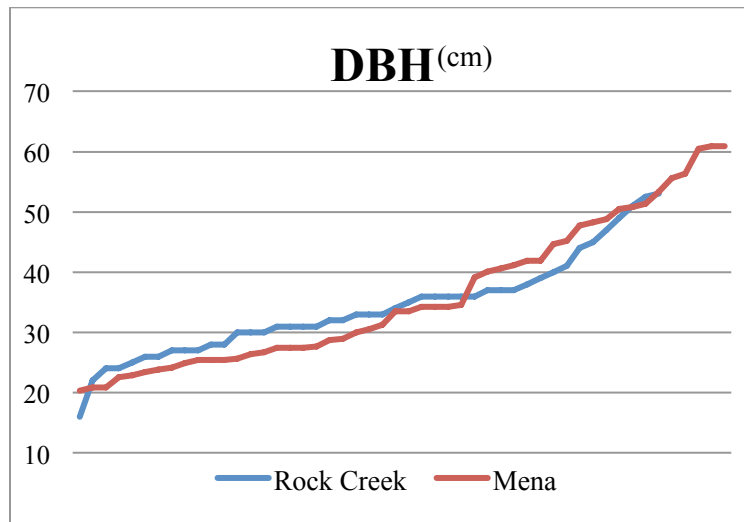


Figure 5.7 Graph of DBH values for both tornado blowdown sites.

Some interesting differences and similarities in the wad dimensions of both tornado blowdown areas were found (Table 5.1). Only the Rock Creek site had a wad dimension, thickness, in its model. Mean thickness is similar for both areas and were both negatively correlated with mined bedrock presence. Coincidentally, increased wad thickness slightly decreased the model's odds of bedrock mining for the Rock Creek site. Presumably this is due to the increased anchorage strength that a deep root structure would impart upon a tree against the force of the wind. Or, as thickness can also serve in this case as a proxy for soil thickness, albeit slightly a weak one, it could be that thinner wads caused by thinner soils would be more likely to have mined bedrock. Wad height, width, area, and volume are smaller for the Mena site than the Rock Creek.

**Table 5.1** Mean values of wad dimensions recorded at each of the tornado blowdown study sites

| Mean Values                   | Rock Creek | Mena   |
|-------------------------------|------------|--------|
| <i>Height (cm)</i>            | 150.91     | 106.06 |
| <i>Width (cm)</i>             | 198        | 158.69 |
| <i>Thickness (cm)</i>         | 62         | 66.45  |
| <i>Area (m<sup>2</sup>)</i>   | 3.18       | 1.8    |
| <i>Volume (m<sup>3</sup>)</i> | 2.06       | 1.2    |

Rooting depth for the smaller diameter and rooting area trees at the Mena site is actually, on average, deeper than the larger diameter and rooting area trees of the Rock Creek site (Figure 5.8). The shallower roots of the larger Rock Creek could occur due to many things such root crowding or competition, locally shallow depths to the bedrock interface, etc. However, it is clear that this reduced rooting depth should have an increased affect on the vulnerability of uprooting (Stokes et al., 1996; Fourcaud et al., 2008). It is possible that these differences account for some of the dissimilarity between the sites' rate of bedrock mining.

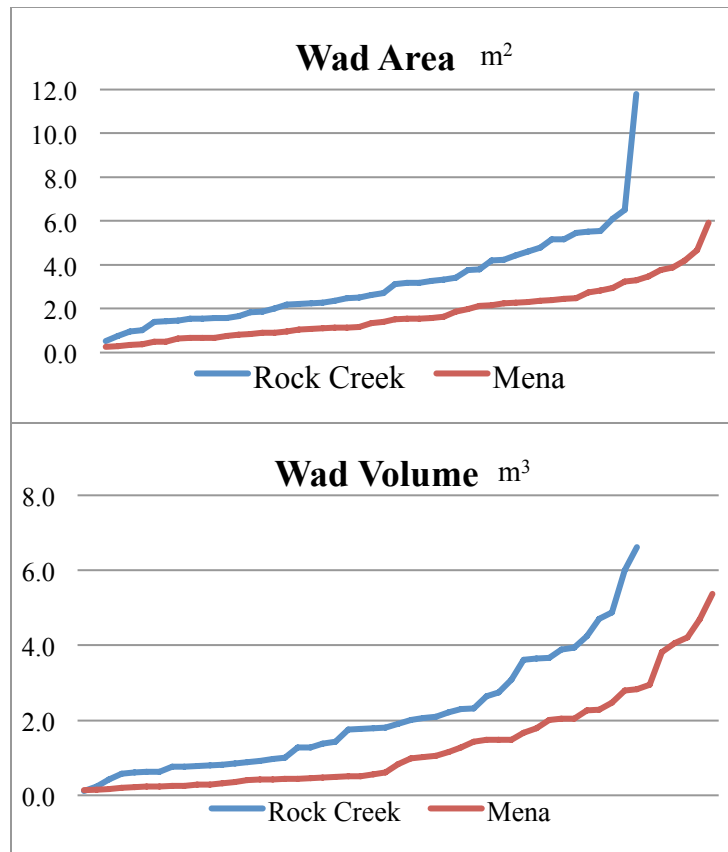


**Figure 5.8** Comparison of wad area and volume for the tornado blowdown sites.

Of the four geology types on which samples were taken at the Rock Creek Tornado Blowdown site, sandstone, sandstone and quartz, shale, shale and sandstone, all but sandstone and quartz type exhibited a preference for mining bedrock (this type was finally not included in the model). In fact, the samples with sandstone were represented by a 100% chance of mining bedrock and the shale type seemed to be at least five times more likely to mine unweathered bedrock than to not. For the Mena site, all categories containing shale mined bedrock much more often than not. However, the other geology types, alluvium and sandstone, much less often mined bedrock than not.

Logic suggests that coherent, structurally sound bedrock is likely to be more resistant to bedrock mining by root action than friable, fragile, bedrock varieties. However, the findings from the tornado blowdown areas complicate this notion. At the Mena site underlying sandstone geology presented as highly indicative of bedrock mining. Yet, at the Rock Creek Tornado Blowdown site shale bedrock was also positively correlated with mining activity; although the odds were approximately four times less. One possible explanation for this is the violent force by which the trees were uprooted simultaneously by the F3 tornado at the Rock Creek site, forcibly unearthing all material surrounding the root shafts, leading to a high prevalence of mined unweathered bedrock found within this site; only 7 of the 38 samples were absent of bedrock



fragments. It is conceivable that the lower winds speeds of the F1 tornado at the Mena site allowed the trees to strain in place longer before uprooting. Withstanding an increased duration of time against the forces of the winds the attachments of the roots to the bedrock surrounding them could have been gradually loosed as compared to the sudden ripping of a strong F3 tornado at the Rock Creek site. Another explanation for this difference could lie in the varied and non-homogenous stratigraphy of the Ouachita Mountains where sandstone caps the underlying shale layer with many layers containing varying amounts of shale and sandstone (Haley et al., 1979).

Both sandstone and shale underlying bedrock increased the odds of bedrock mining at the Rock Creek site (Appendix B). The sandstone and shale and the sandstone and quartz underlying geology were not included within the model, as they did not improve the fit of the model for the Rock Creek site. The Mena Tornado Blowdown site was distinct in that it had many areas of alluvial soils, which tend to have increased depth to bedrock as compared to other soils – it is not surprising that the odds of mining were reduced by alluvium parent material. Shale, a mixture of bedrock types, and sandstone and shale underlying bedrock all increased the odds for the Mena blowdown (Table 4.18). As only one sample exhibited the mixture geology type this relationship is questionable.

Soil data was not utilized or recorded for the Rock Creek Tornado Blowdown site. As location data was also not recorded for this study area, soil GIS maps were not able to be applied to this research. However, soil data was collected for the Mena Tornado Blowdown site (Figure 4.24). The Wilberton and unknown soil mapping units were not included within Mena Tornado Blowdown model, meaning that their predictive value did not strengthen the “fit” of the model in comparison to the constant only model. However, all but the mixed Bengal/Bismarck/Nashoba group increased the odds of bedrock mining. This occurrence could be due to the overall higher likelihood of positive bedrock mining for each group.

Pearson’s correlation between underlying geology and soil mapping unit classes was not significant for the Mena site ( $\alpha=0.125$ ). This is most likely the reason that both the underlying geology and soil mapping unit parameters were included in the site’s model – unlike the highly significant relationship of the two parameters that the Alum Creek site in which only the underlying geology parameter was included in the model. The dissimilar results for the two sites reaffirm the assertion by Phillips and Marion (2005) that a high degree of soil variability over small areas exists within the Ouachita National Forest. Accordingly, soil mapping unit may be so locally variable that its use as a predictive parameter for identifying bedrock mining hotspots may be limited.

If soil data had been collected for the Rock Creek Tornado Blowdown site it would have been interesting to explore if this parameter was affected by the tornado forcing mechanism in the same way. The great importance of soil mapping unit in the Mena model suggests that the concept should be studied further to see if there is any commonality across samples created by the same forcing mechanism.

### **III. Mapping Results**

Maps of highest and lowest odds were produced for the models in all three sites. In addition, the highest and lowest odds of bedrock mining from the Alum Creek Experimental forest cycle-of-life model were mapped onto the two tornado blowdown areas. In the case of the Alum Creek Experimental Forest and the Mena tornado blowdown sites, the breadth of highest odds is much more restricted than the areas of lowest odds. This is obviously due to the parameters in each site's model but, having a smaller area of study presents a much more manageable amount of data for any future analyses on areas of bedrock hotspots. The highest and lowest odds maps for the Rock Creek tornado blowdown site could be more restricted in area if forest stand plots were smaller, as highest and lowest odds areas were limited by mean stand DBH data, but ultimately on-the-ground sampling could overcome this problem.

Mapping of the cycle-of-life odds was a successful endeavor as these and the extrapolated odds maps could be put to practical use by researchers to delineate areas of high/low bedrock mining potential within many areas of the Ouachita National forest. While the tornado blowdown maps and associated odds could be used to determine the effect of similar force storms in the area.

The low resolution of the available geologic geospatial data made this a mostly ineffective parameter for the mapping portion of this project. Likewise, the differences between the information provided by the soil surveyor and the online database of mapping units as can be caused mapping problems for the Mena tornado site. But, this is to be expected considering the high degree of soil variability over small areas within the forest – making proper mapping of this parameter nearly impossible (Phillips and Marion, 2005). It may therefore be more practical for future studies to rely solely on available geospatial data or solely on expert opinion – otherwise extensive ground-truthing may be necessary to better understand the relationship between soil characteristics and bedrock mining hotspots.

The primary impetus for the translation and utilization of these results is the medium on which their display is confined. Without the size constraints inherent in the publication of this thesis, the mapping products could be utilized in a more effective, efficient, and engaging format. A more appropriate medium would be a digital file or software program that could allow for the input of probability values over a base map. This would allow for multiple view scales and added levels of detail. Nevertheless, researchers may be able to use these maps to determine areas for further research on bedrock mining process in a more efficient way.

### **IV. Suggestions for Future Studies**

Based on the results of this study, there are several recommendations for the future direction of research. The next step in this area of would be to complete a comparative study of several cycle-of-life and several tornado blowdown sites to strengthen or reassess the ideas herein about the importance of topographic, tree specific,

geologic, and soil characteristics. For this to be the most effective it would be imperative that the same variables be collected at all sites to allow for a balanced examination and discussion of the variables that affect bedrock mining in treethrow.

Future work should also answer how the differing weathering rates of sandstone and shale can impact local soil characteristics, nutrient flux, and patterns of soil turnover. Furthermore, subsequent studies could undertake the assessment of the relationship between soil type, forcing mechanism, and the potential for bedrock mining. However, the utilization of similar methodology would most likely necessitate grouping of soil types, as the number of soils in a small area can be quite numerous, in order to avoid overparameterization and overall weakening of the produced model. Or, conversely, certain soil characteristics could be chosen as explanatory variables in lieu of the application of copious individual soil types.

To form a more complete picture of the topographic factors influencing uprooting and bedrock mining activity, soil thickness data could have been collected for each sample. Definitive measurements for depth to bedrock would have been instrumental in determining if those trees sampled had actually penetrated through the soil horizons and into the regolith and bedrock interface to allow for actual mining activity. Soils, and their corresponding characteristics, within the Ouachita Mountain Range tend to be highly locally variable with individual trees acting as a primary source of variation (Phillips and Marion, 2006). If the depth to regolith or the bedrock interface is locally quite deep then mining of fresh bedrock would not be possible by tree roots in that location. In support of this, Humphreys and Wilkinson (2007) describe how very thick soils have only limited soil production as the depth acts as a barrier to weathering of underlying bedrock.

## Chapter Six

### Conclusion

This study endeavored to determine the abiotic and biotic factors that are highly correlated with the rate of bedrock mining activity found in treethrows, and to geographically assign those areas of high odds (hotspots) for mining activity within the Ouachita National Forest. Logistic regression modeling was employed to assign areas highly likely to experience bedrock detachment by means of uprooting within the three study areas. From the logistic regression models maps were generated to fulfill the second goal of this study, to geographically assign areas highly likely to experience bedrock detachment.

Importantly, the calculated site specific logistic regression models suggest that topographic factors, tree specific characteristics, as well as the local geology and soil characteristics all have a significant effect upon the probability of bedrock mining activity throughout the Ouachita National Forest, Arkansas. Observations taken from cycle-of-life uprootings and tornado blowdown events also granted the possibility to analyze the affect that the differing forcing mechanisms have upon the relative importance of the abiotic and biotic variables in the appearance of bedrock mining activity.

Given the varied relative importance of controls on the prevalence of bedrock mining, even within a defined and similar study area as the Ouachita National Forest, overall generalizations are difficult to make. The complex results of this study strongly support Phillips' assertion that "landscape evolution has irreducible elements of contingency and path-dependency (2006)." While certain parameters are constant (depending upon scale), geology, slope position, aspect, and angle, tree type, soil characteristics to name a few. Other parameters are naturally stochastic like rooting dimensions, local weather patterns, type and strength of uprooting forcing mechanisms. The unpredictable nature of these factors further complicates generalizations and reductions.

Local and temporal contingencies seem to be especially important for the cycle-of-life treethrows because the conditions surrounding and causing their upheaval can vary widely, which is reflected in the complex model for the Alum Creek Experimental forest. Even though a great number of parameters were examined for the cycle-of-life model and many were found to not strengthen the model, the relationship between bedrock mining and these parameters remained quite complicated. On the other hand, a tornado event indiscriminately uproots trees so one might expect that local contingencies are minimized. However, as this study shows, even high magnitude events are affected by local contingencies.

The results suggest that the impact of trees on the bedrock interface involves more than the simple relationship of the tree and the bedrock itself; the circumstances of the actual uprooting event and the timing of the event are significant. The forcing mechanism that causes the treethrow event intrinsically changes the relationship between the abiotic

and biotic factors that control bedrock mining. For each site evaluated underlying bedrock type was found to be significant in identifying hotspot areas; this warrants further study. The potential for cycle-of-life uprootings to exhibit bedrock mining was heavily influenced by topographic characteristics (slope angle, aspect, and position on slope). Flat areas, the bottom portion, and midslope areas with potentially greater moisture content increased the likelihood of bedrock mining as expected. Slope angle also displayed its relationship to mining activity as expected.

Slope aspect was expected to be important in predicting mining hotspots and the expected windward/leeward relationship did, for the most part, correlate well with bedrock mining. Deviations likely reflect the contingency present in local weather events (e.g. ice storms and high winds). In the Alum Creek Experimental Forest site, the trees' state of decay had a positive influence on the odds of finding mined bedrock in the wads. Such is not the case of the tornado blowdown sites, as presumably all treethrows have been in situ for the same duration of time and were all uprooted by the same mechanism.

The Rock Creek site, hit by a powerful F3 tornado, exhibited increased odds of mining for larger diameter trees on areas of sandstone and shale bedrock. However, against predictions for this site, thicker, deeper, roots meant that the likelihood of mining was decreased. A degree of contingency is present in the underlying geology parameters for the tornado blowdown sites. While both shale and sandstone increase the odds of mining in the Rock Creek site, sandstone geology decreased odds at the Mena blowdown, which was hit by a weaker F1 tornado. For the Mena site, all categories containing shale mined bedrock much more often than not. The reason for the difference in the positive or negative odds is likely due to a combination of local and specific forcing mechanism strength contingency. Tree type was not able to be studied for these sites because both tornados hit shortleaf pine stands. All but the Bengal/Bismarck/Nashoba soil mapping unit increased the likelihood of bedrock mining.

Albeit a powerful methodology, care should be taken in the selection of explanatory variables. None of the statistical procedures outlined in this study has the ability to determine whether any given factor has a measurable influence on the phenomenon in question – in fact an underlying assumption of the methodology is that all factors included in the study do in fact affect the odds of the phenomenon. Additional complementary studies in similar environments are needed to better understand the importance of the abiotic and biotic factors on bedrock mining and treethrow. The maps produced for the greatest odds of bedrock mining should be tested for validity through boots-on-the-ground sampling. However, the consideration of further efforts in this area of study should keep in mind the complexity that local and temporal contingency brought to this study and that adding more parameters may not strengthen a model due to these. As Phillips wisely said in his 2006 paper, “historical and spatial contingencies are and must be engaged on their own terms – that is, the contingencies cannot be subsumed under global laws by simply collecting more and better data or constructing more involved models.”

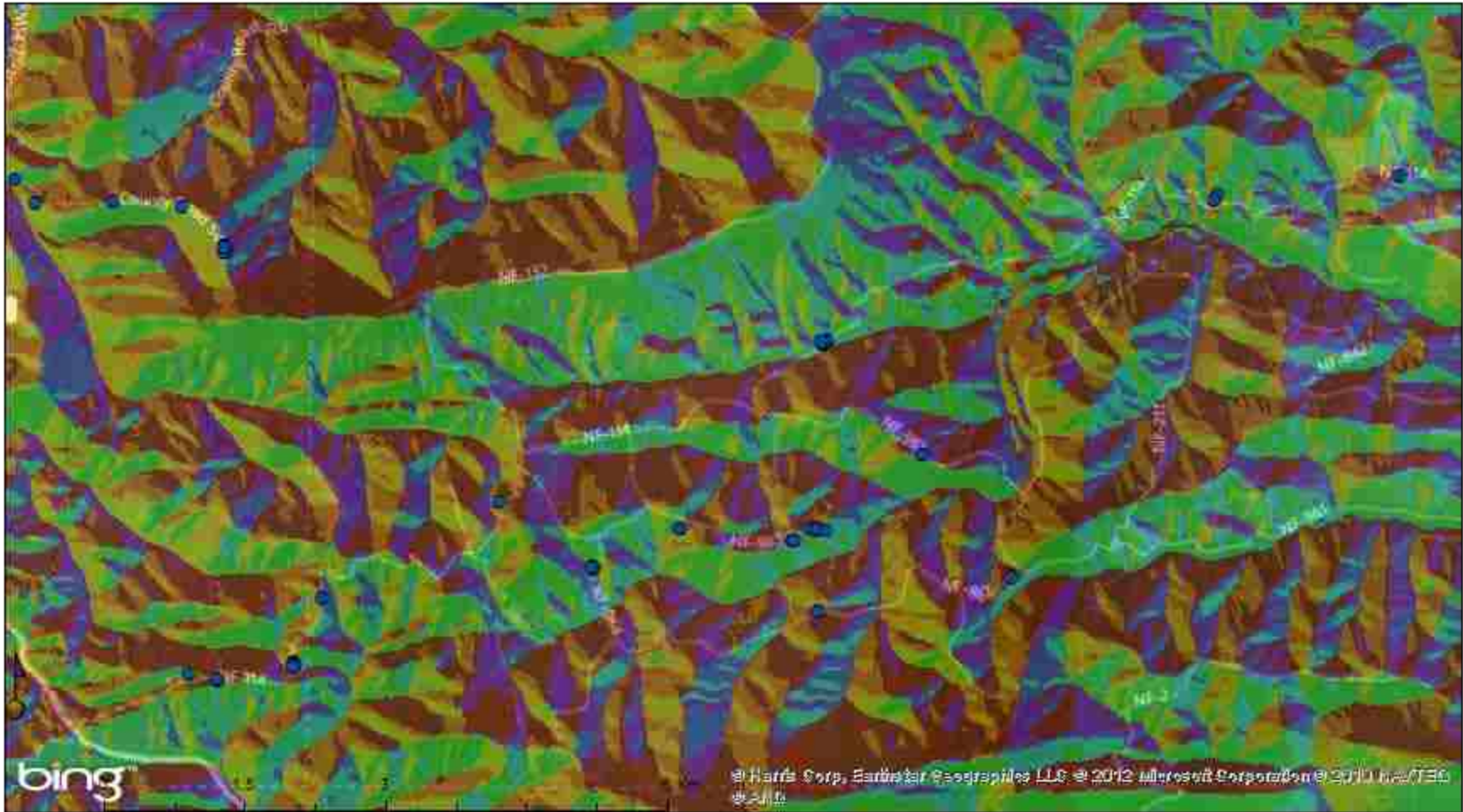
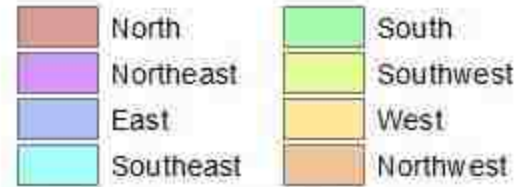
The methodology employed in this study could be eventually adopted for use in identifying hotspots of other biogeomorphic phenomena in any variety of environmental

settings. The flexibility of the statistical procedures to adopt any assortment of potentially influential factors offers a powerful tool for researchers. Moreover, the ease of mapping the best predictor factors further boosts the spatial predictive power of the methodology.

**Appendix A**  
**Unaltered Geospatial Data**

# Alum Creek Experimental Forest Aspect

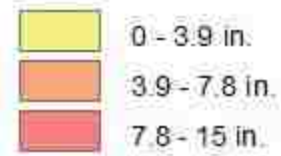
● Alum Experimental Forest Data Locations





# Alum Creek Experimental Forest Diameter at Breast Height

• Alum Experimental Forest Data Locations



# Alum Creek Experimental Forest

## Sample Locations

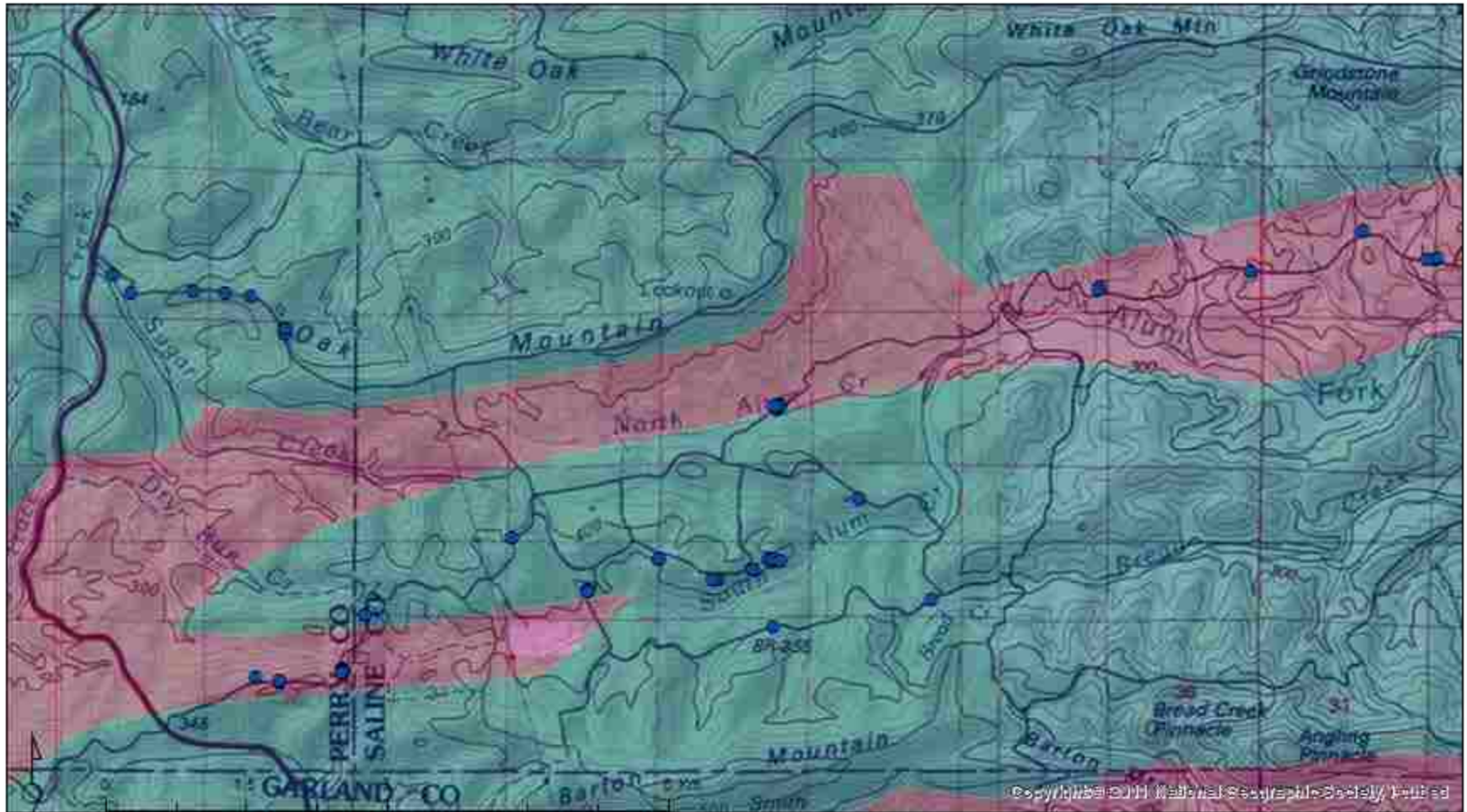
Decay Class



# Alum Creek Experimental Forest

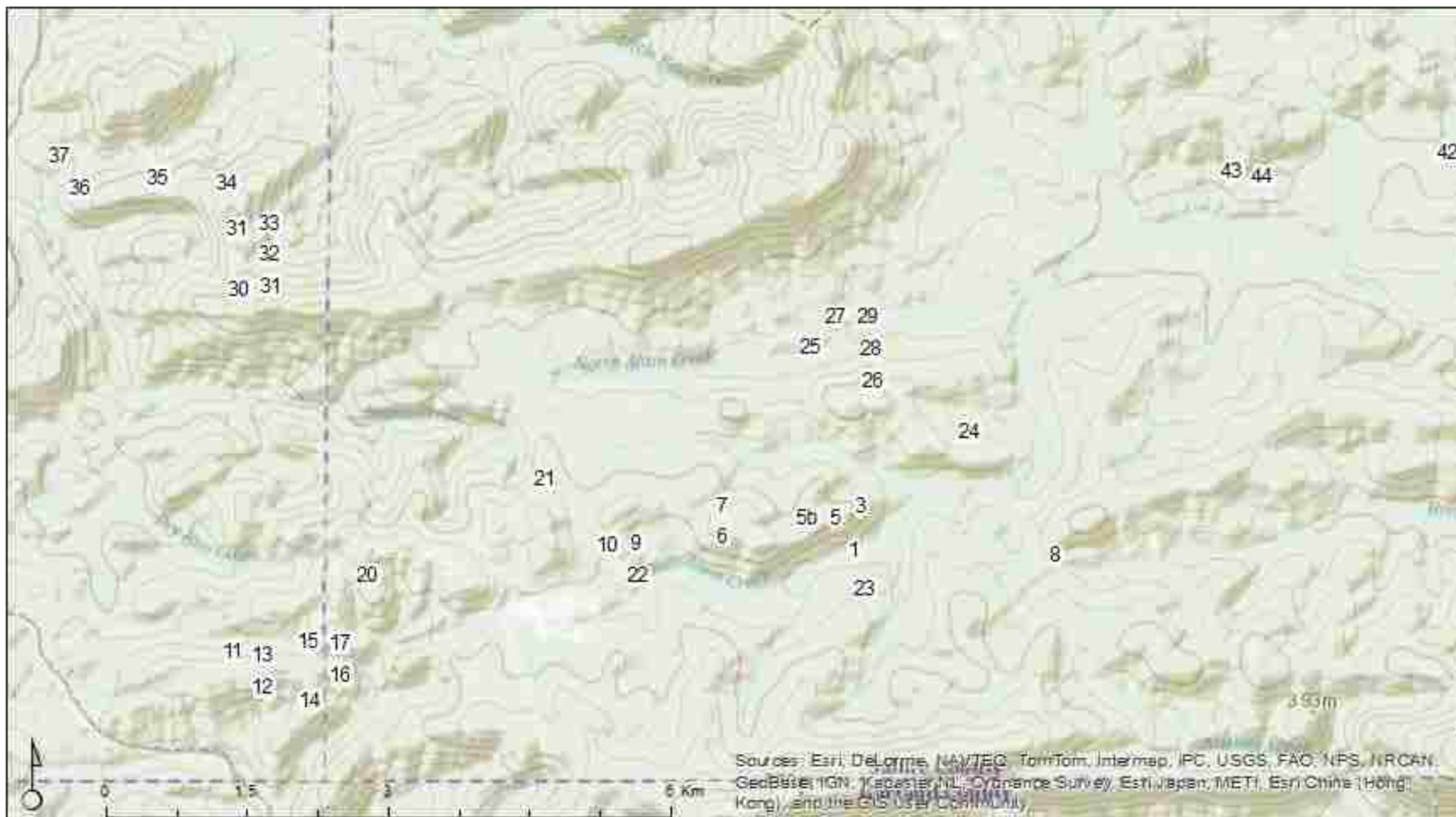
## Underlying Geology

- Sample Locations
- Sandstone
- Shale



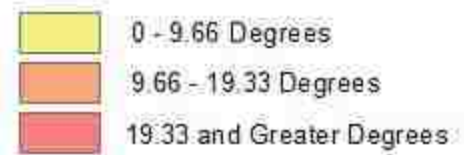
# Alum Creek Experimental Forest

## Sample Locations



# Alum Creek Experimental Forest Slope Angle

● Alum Experimental Forest Data Locations



# Alum Creek Experimental Forest Soil Mapping Unit

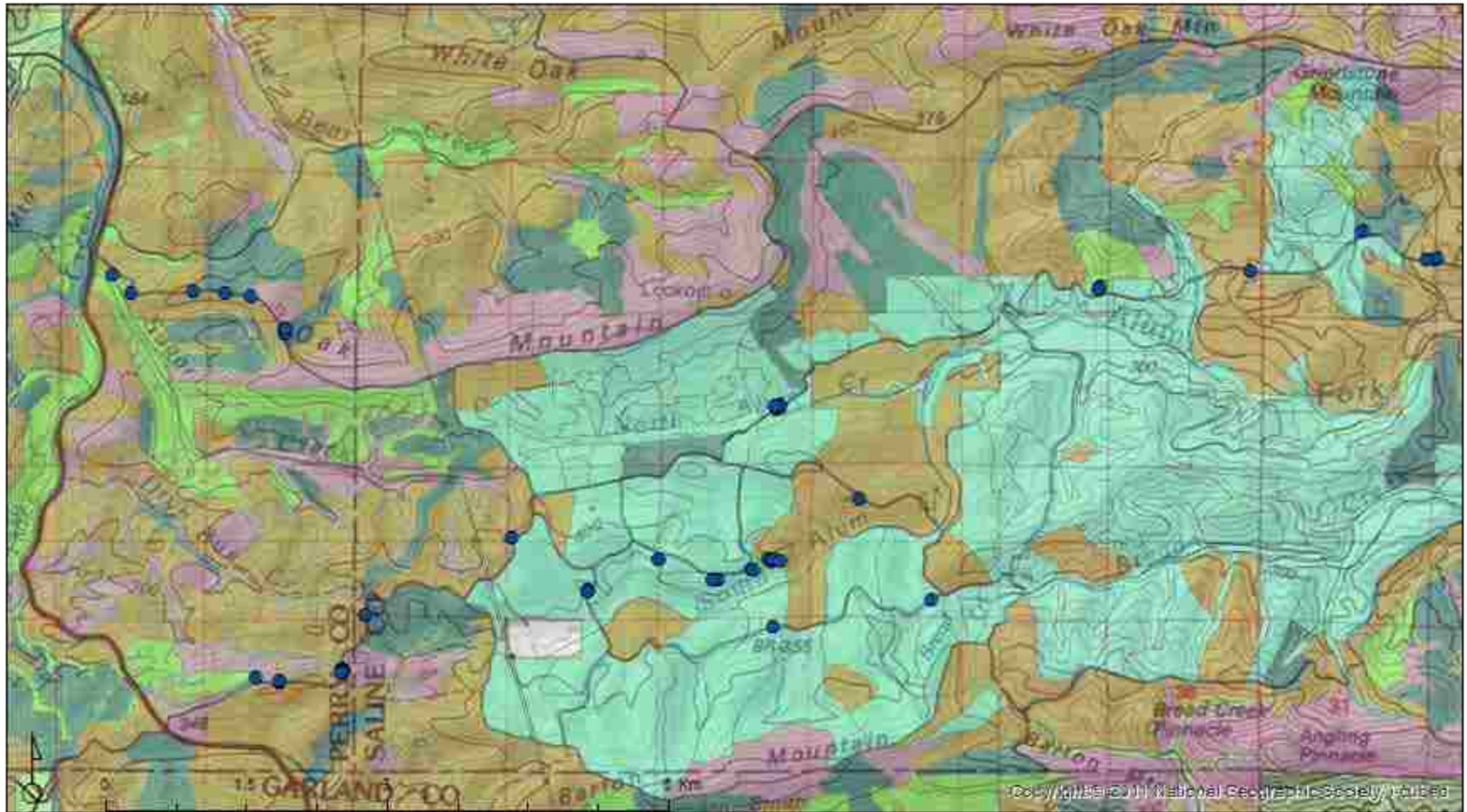
● Alum Experimental Forest Data Locations

|                                     |                                  |
|-------------------------------------|----------------------------------|
| Carnasa w-Pirum-Townley association | Sherwood fine sandy loam         |
| Carnasa w-Townley-Pirum (steep)     | Carnasa w-Pirum association      |
| Zabra-Leadville complex             | Carnasa w-Pirum-Clebit (rolling) |
| Carnasa w-Pirum-Clebit (very steep) | Carnasa w-Pirum-Clebit (steep)   |
| Ceda gravelly loam                  |                                  |

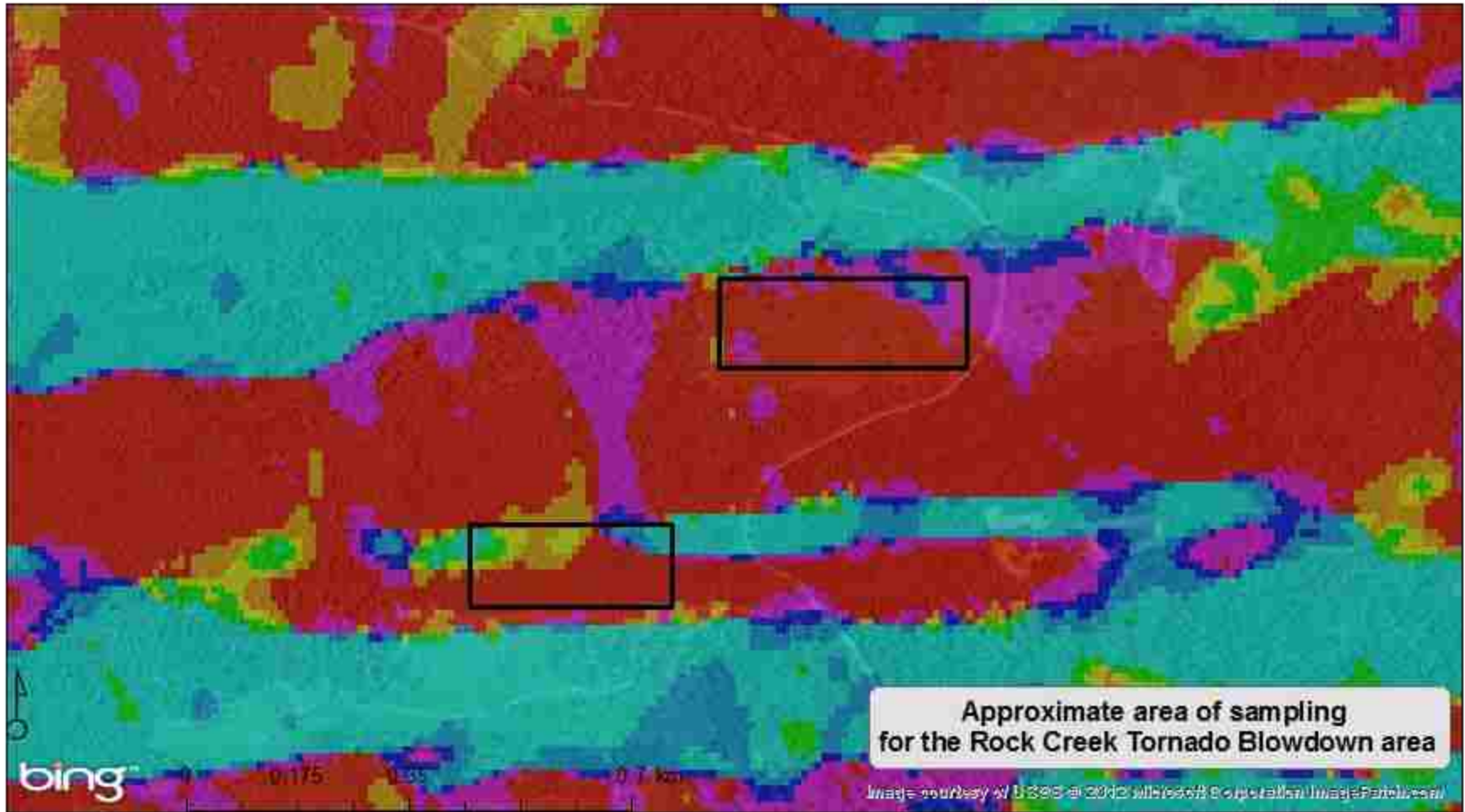
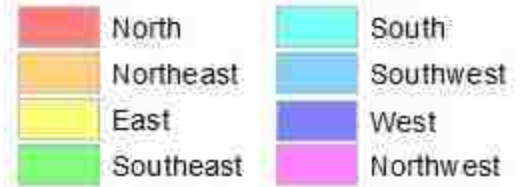


# Alum Creek Experimental Forest

## Tree Type



# Rock Creek Tornado Blowdown Aspect





# Rock Creek Tornado Blowdown

Mean Stand  
Diameter at Breast Height

Forest Stands  
DBH Values in Inches

124



Approximate area of sampling  
for the Rock Creek Tornado Blowdown area

bing

Image courtesy of USGS © 2012 Microsoft Corporation ImagePatch.com

# Rock Creek Tornado Blowdown

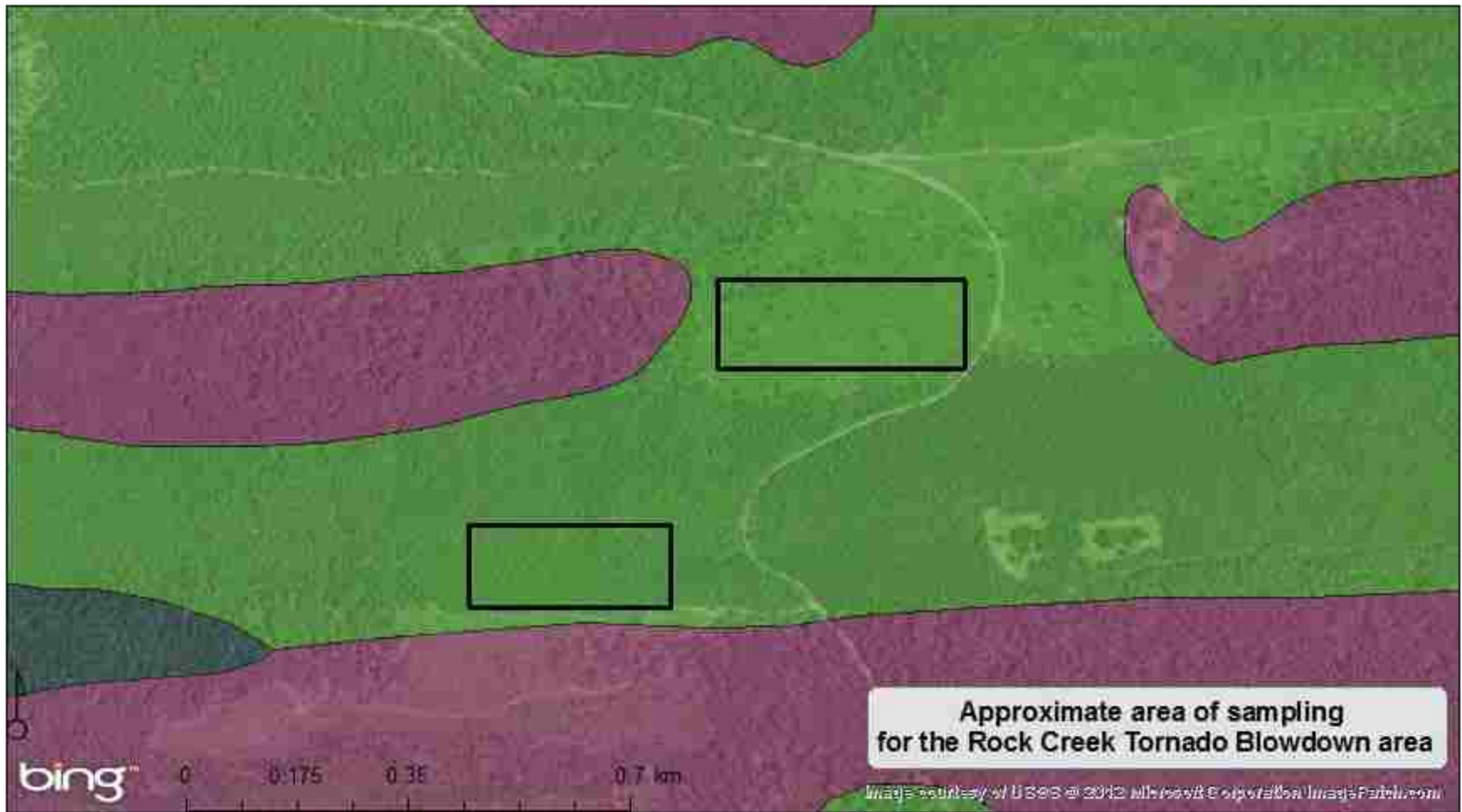
## Underlying Geology

 Sandstone



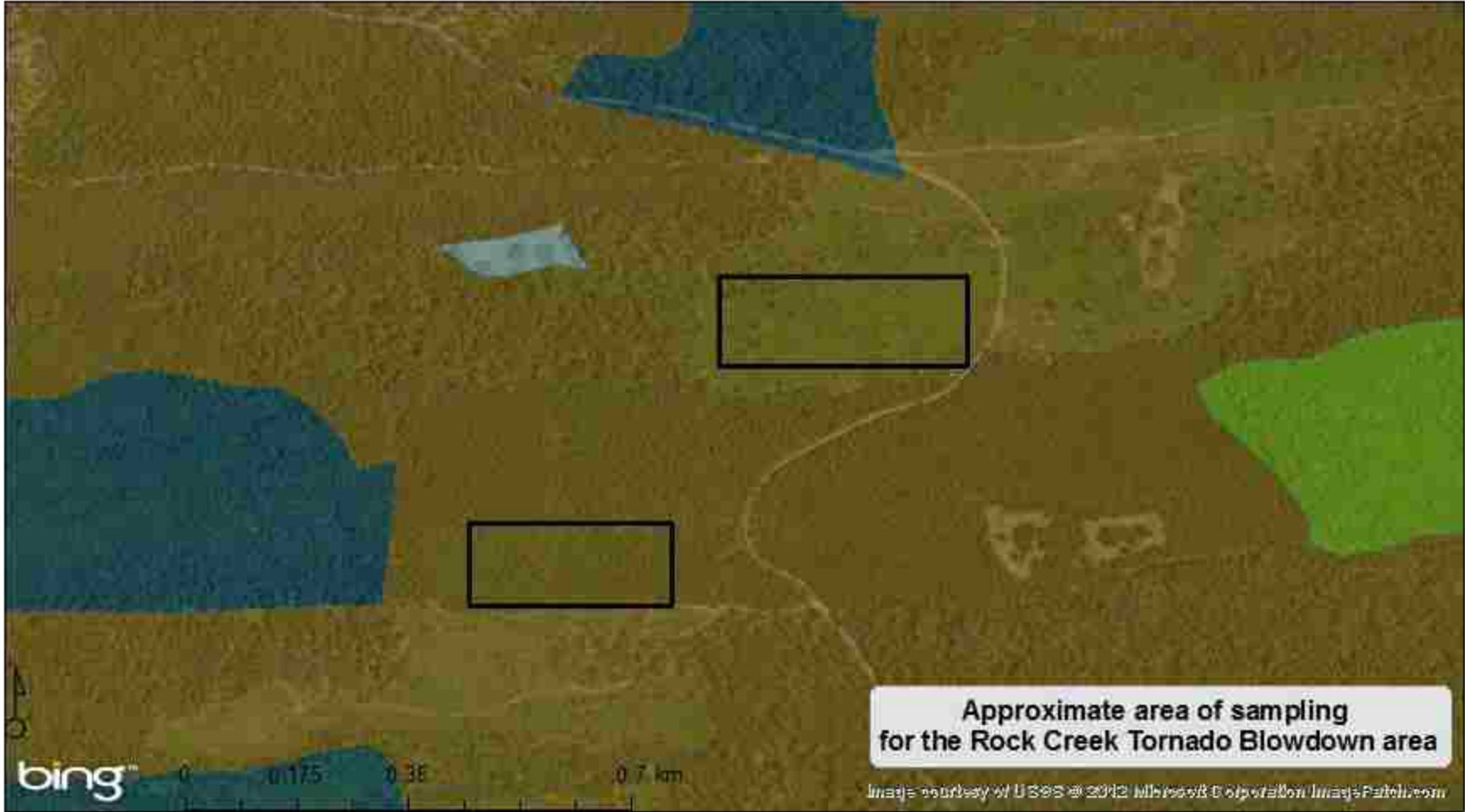
# Rock Creek Tornado Blowdown Soil Mapping Unit

- Camasaw-Pirum
- Camasaw-Pirum-Clebit (rolling)
- Camasaw-Pirum-Clebit (steep)



# Rock Creek Tornado Blowdown

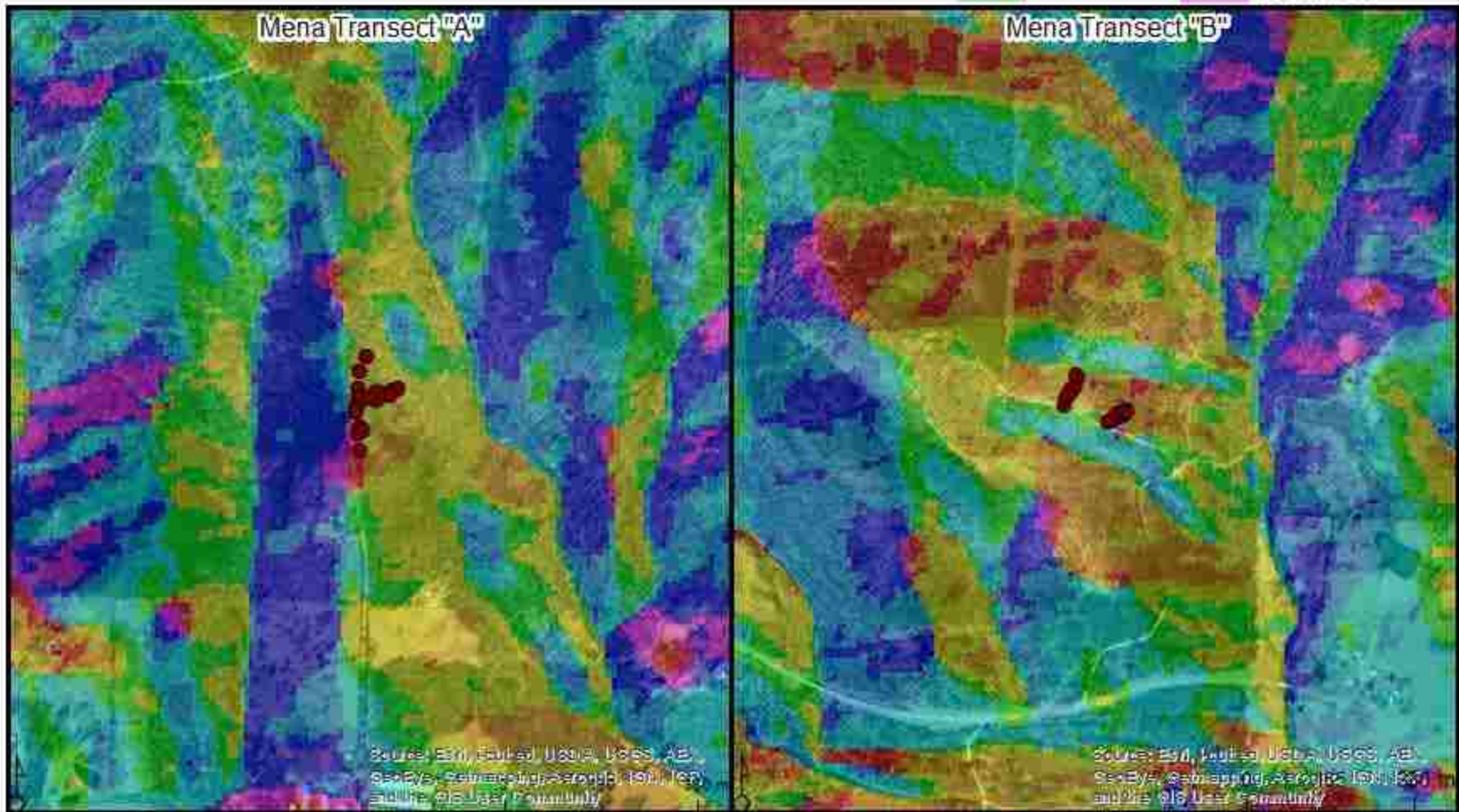
Tree Type



# Mena Tornado Blowdown Area

Aspect

● Mena Blow down Data Samples



# Mena Tornado Blowdown Area

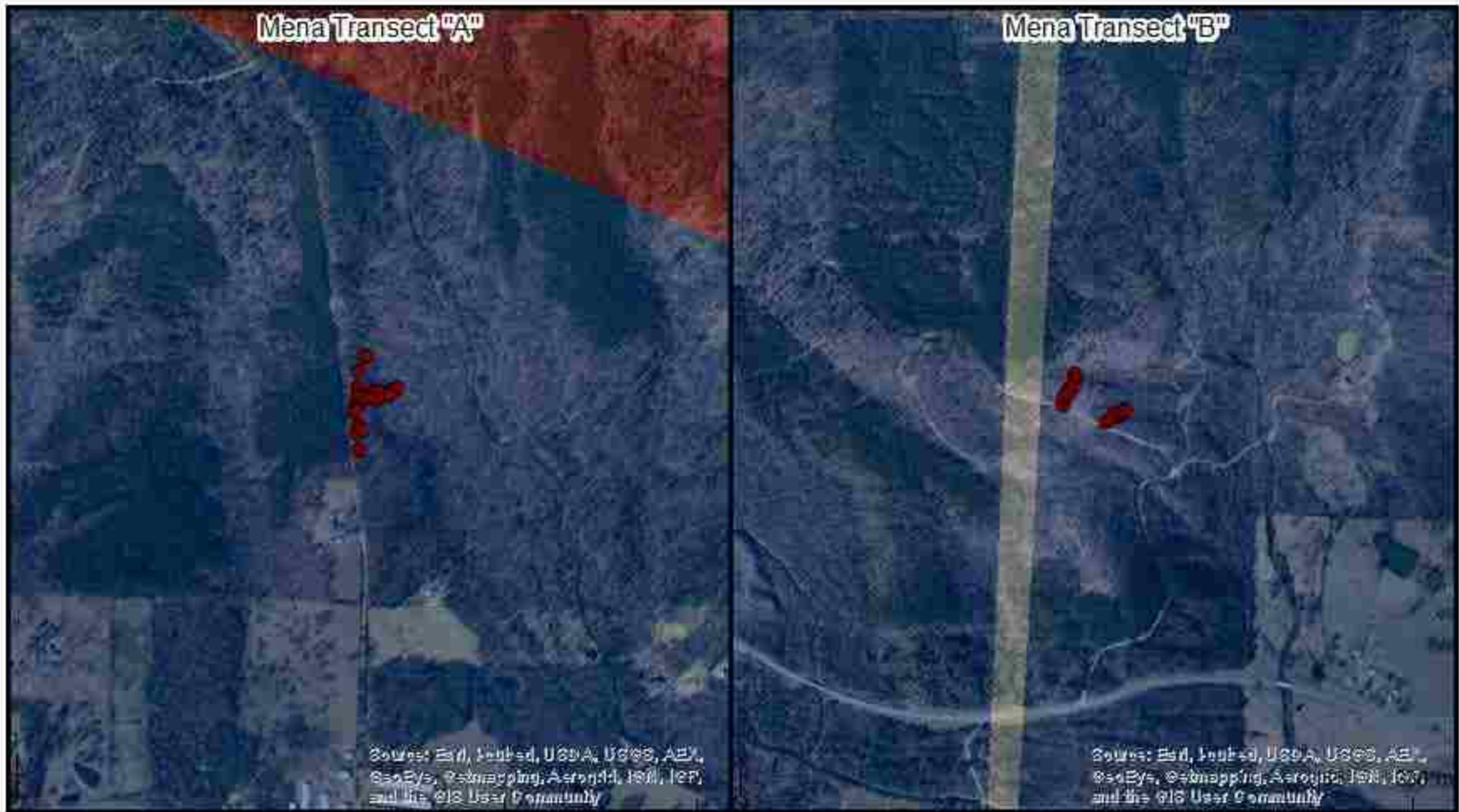
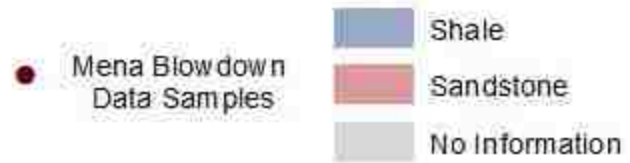
## Diameter at Breast Height

- Mena Blow down Data Samples
- Stand Mean DBH



# Mena Tornado Blowdown Area

## Underlying Geology



# Mena Tornado Blowdown Area

## Slope Angle



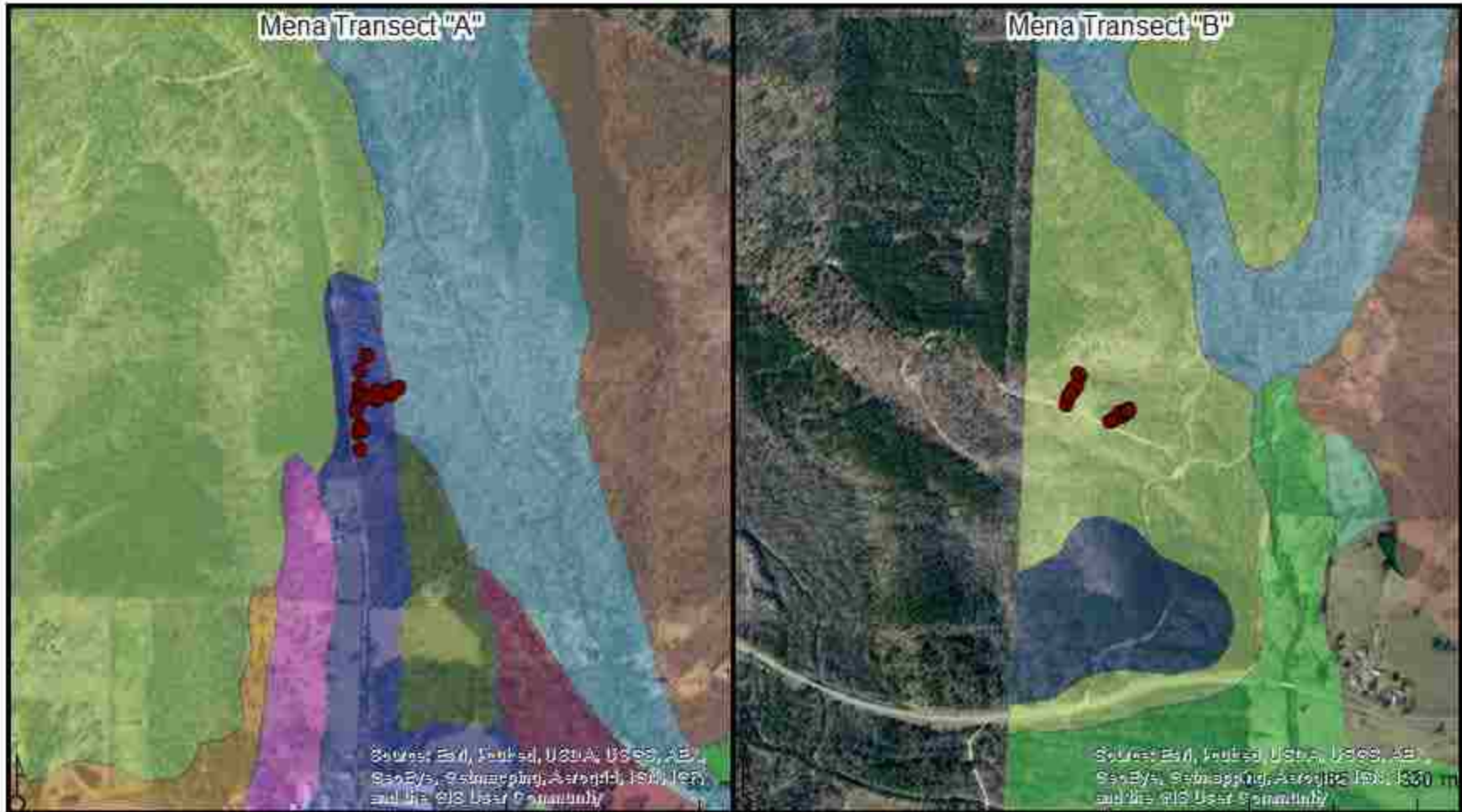


# Mena Tornado Blowdown Area

## Soil Mapping Unit

● Mena Blow down Data Samples

|   |   |   |
|---|---|---|
|  Mena gravelly sily loam |  Kenn-Ceda       |  Kenn gravelly fine sandy loam     |
|  Mena silt loam          |  Wetsaw loam     |  Sherless-Littlefir (1-8% slope)   |
|  Mazam silt loam         |  Cupco silt loam |  Sherless-Littlefir (8-15% slope)  |
|  Nashoba-Bismarck        |   |  Sherless-Littlefir (15-35% slope) |

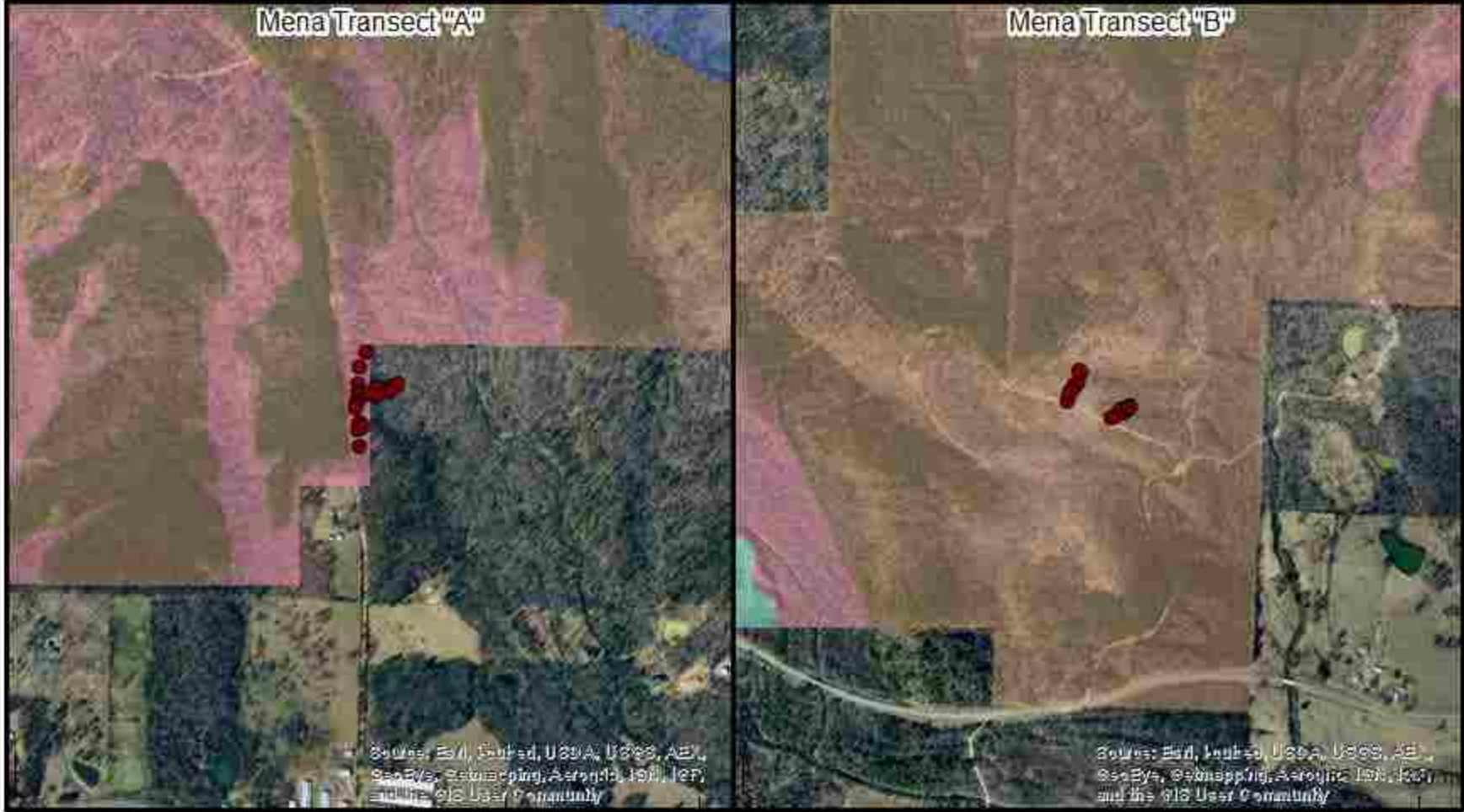


# Mena Tornado Blowdown Area

## Tree Type

● Mena Blow down Data Samples

- Hardwood
- Conifer
- No Data
- Conifer Dominant



## Appendix B

### Alum Creek Experimental Forest Data

#### Wad Dimensions

| Tree | Height | Width  | Thickness | Area  | Volume |
|------|--------|--------|-----------|-------|--------|
| 1    | 54.61  | 126.49 | 66.55     | 0.69  | 0.46   |
| 2a   | 47.63  | 138.43 | 102.45    | 0.66  | 0.68   |
| 2b   | 29.63  | 134.62 | 69.85     | 0.40  | 0.28   |
| 3    | 38.10  | 193.04 |           | 0.74  | 0.00   |
| 4    | 330.20 | 142.67 | 135.33    | 4.71  | 6.38   |
| 5a   | 30.48  | 113.67 | 52.32     | 0.35  | 0.18   |
| 5b   | 26.92  | 134.62 | 75.57     | 0.36  | 0.27   |
| 6    | 34.71  | 206.38 | 132.08    | 0.72  | 0.95   |
| 7    | 42.55  | 163.07 | 193.89    | 0.69  | 1.35   |
| 8    | 103.29 | 258.33 | 141.67    | 2.67  | 3.78   |
| 9    | 81.28  | 181.67 | 110.91    | 1.48  | 1.64   |
| 10   | 57.15  | 541.67 | 46.14     | 3.10  | 1.43   |
| 11   | 148.75 | 253.00 | 141.60    | 3.76  | 5.33   |
| 12   | 104.14 | 144.15 | 41.91     | 1.50  | 0.63   |
| 13   | 22.54  | 93.35  | 69.85     | 0.21  | 0.15   |
| 14   | 44.70  | 287.50 | 201.00    | 1.29  | 2.58   |
| 15a  | 35.56  | 129.54 | 82.80     | 0.46  | 0.38   |
| 15b  | 24.45  | 124.46 | 45.97     | 0.30  | 0.14   |
| 16   | 39.12  | 178.65 | 120.02    | 0.70  | 0.84   |
| 17   | 37.34  | 190.00 | 85.09     | 0.71  | 0.60   |
| 18a  | 31.21  | 132.59 | 107.95    | 0.41  | 0.45   |
| 18b  | 77.79  | 131.23 | 19.05     | 1.02  | 0.19   |
| 19   | 103.63 | 413.00 | 109.73    | 4.28  | 4.70   |
| 20   | 33.02  | 165.10 | 70.10     | 0.55  | 0.38   |
| 21   | 36.07  | 116.21 | 59.69     | 0.42  | 0.25   |
| 22   | 49.78  | 257.33 | 92.46     | 1.28  | 1.18   |
| 23   | 146.30 | 241.67 | 105.41    | 3.54  | 3.73   |
| 24   | 114.30 | 320.67 | 99.91     | 3.67  | 3.66   |
| 25   | 121.29 | 233.33 | 131.45    | 2.83  | 3.72   |
| 26   | 251.67 | 590.00 | 111.76    | 14.85 | 16.59  |
| 27   | 99.91  | 55.00  | 99.06     | 0.55  | 0.54   |

### Wad Dimensions - Continued

|           |        |        |        |      |      |
|-----------|--------|--------|--------|------|------|
| <b>28</b> | 158.33 | 261.67 | 92.08  | 4.14 | 3.81 |
| <b>29</b> | 62.65  | 119    | 68.33  | 0.75 | 0.51 |
| <b>30</b> | 80     | 191.33 | 120    | 1.53 | 1.84 |
| <b>31</b> | 103.33 | 150    | 88.75  | 1.55 | 1.38 |
| <b>32</b> | 48.75  | 166.67 | 97.5   | 0.81 | 0.79 |
| <b>33</b> | 85.5   | 122.25 | 74.5   | 1.05 | 0.78 |
| <b>34</b> | 90     | 183.33 | 100    | 1.65 | 1.65 |
| <b>35</b> | 79     | 151.33 | 86     | 1.2  | 1.03 |
| <b>36</b> | 115.75 | 235    | 159.5  | 2.72 | 4.34 |
| <b>37</b> | 98.21  | 107.53 | 70.49  | 1.06 | 0.74 |
| <b>38</b> | 56.73  | 141.39 | 78.74  | 0.8  | 0.63 |
| <b>39</b> | 84.46  | 143.09 | 41.28  | 1.21 | 0.5  |
| <b>40</b> | 103.12 | 243.84 | 116.33 | 2.51 | 2.93 |
| <b>41</b> | 43.18  | 187.96 | 73.66  | 0.81 | 0.6  |
| <b>42</b> | 145    | 298.33 | 89.33  | 4.33 | 3.86 |
| <b>43</b> | 41.33  | 77     | 38     | 0.32 | 0.12 |

### Tree Specific Characteristics

| Tree      | Tree Type | DBH (CM) | Decay Class | Presence |
|-----------|-----------|----------|-------------|----------|
| <b>1</b>  | Conifer   | 5.53     | 5           | 1        |
| <b>2a</b> | Conifer   | x        | 5           | 0        |
| <b>2b</b> | Conifer   | x        | 4           | 0        |
| <b>3</b>  | Unknown   | x        | 8           | 1        |
| <b>4</b>  | Conifer   | 23.68    | 4           | 1        |
| <b>5a</b> | Conifer   | 4.34     | 6           | 0        |
| <b>5b</b> | Conifer   | x        | 6           | 0        |
| <b>6</b>  | Unknown   | x        | 0           | 1        |
| <b>7</b>  | Unknown   | x        | 9           | 0        |
| <b>8</b>  | Conifer   | 5.13     | 4           | 1        |
| <b>9</b>  | Conifer   | 5.92     | 5           | 1        |
| <b>10</b> | HW        | 6.32     | 4           | 0        |
| <b>11</b> | Conifer   | 7.30     | 4           | 1        |
| <b>12</b> | HW        | 5.53     | 3           | 0        |

**Tree Specific Characteristics - Continued**

|            |         |       |   |   |
|------------|---------|-------|---|---|
| <b>13</b>  | HW      | 2.37  | 3 | 0 |
| <b>14</b>  | Conifer | 3.75  | 6 | 1 |
| <b>15a</b> | Conifer | 3.16  | 6 | 1 |
| <b>15b</b> | Conifer | 2.76  | 6 | 1 |
| <b>16</b>  | Conifer | 3.95  | 6 | 1 |
| <b>17</b>  | Conifer | 3.55  | 6 | 1 |
| <b>18a</b> | HW      | 3.16  | 5 | 1 |
| <b>18b</b> | Unknown | x     | 6 | 1 |
| <b>19</b>  | HW      | 7.89  | 2 | 1 |
| <b>20</b>  | Conifer | 3.35  | 5 | 1 |
| <b>21</b>  | Unknown | 3.16  | 0 | 1 |
| <b>22</b>  | HW      | 9.08  | 3 | 0 |
| <b>23</b>  | Conifer | 3.95  | 3 | 1 |
| <b>24</b>  | Conifer | 6.32  | 3 | 1 |
| <b>25</b>  | Conifer | 5.53  | 3 | 0 |
| <b>26</b>  | Conifer | 7.5   | 2 | 0 |
| <b>27</b>  | Conifer | 4.54  | 3 | 0 |
| <b>28</b>  | HW      | 7.1   | 0 | 1 |
| <b>29</b>  | HW      | 7.89  | 0 | 0 |
| <b>30</b>  | Conifer | 8.68  | 6 | 0 |
| <b>31</b>  | HW      | 10.66 | 6 | 1 |
| <b>32</b>  | Conifer | 7.1   | 6 | 1 |
| <b>33</b>  | Conifer | 15.79 | 3 | 0 |
| <b>34</b>  | Conifer | 13.03 | 1 | 1 |
| <b>35</b>  | Conifer | 9.08  | 5 | 0 |
| <b>36</b>  | HW      | 15.79 | 0 | 1 |
| <b>37</b>  | Conifer | 11.45 | 3 | 0 |
| <b>38</b>  | Conifer | 11.45 | 3 | 0 |
| <b>39</b>  | Conifer | 11.84 | 2 | 0 |
| <b>40</b>  | HW      | 18.95 | 4 | 0 |
| <b>41</b>  | Conifer | 8.68  | 3 | 0 |
| <b>42</b>  | HW      | 22.89 | 2 | 1 |
| <b>43</b>  | Conifer | 7.5   | 5 | 1 |

| <b>Tree</b> | <b>Geology</b> | <b>Soil</b>            |
|-------------|----------------|------------------------|
| <b>1</b>    | Sandstone      | Carnasaw-Townley-Pirum |
| <b>2a</b>   | Sandstone      | Carnasaw-Townley-Pirum |
| <b>2b</b>   | Sandstone      | Carnasaw-Townley-Pirum |
| <b>3</b>    | Sandstone      | Carnasaw-Townley-Pirum |
| <b>4</b>    | Sandstone      | Carnasaw-Townley-Pirum |
| <b>5a</b>   | Sandstone      | Carnasaw-Townley-Pirum |
| <b>5b</b>   | Sandstone      | Carnasaw-Townley-Pirum |
| <b>6</b>    | Sandstone      | Carnasaw-Townley-Pirum |
| <b>7</b>    | Sandstone      | Carnasaw-Townley-Pirum |
| <b>8</b>    | Sandstone      | Carnasaw-Townley-Pirum |
| <b>9</b>    | Sandstone      | Carnasaw-Townley-Pirum |
| <b>10</b>   | Sandstone      | Carnasaw-Townley-Pirum |
| <b>11</b>   | Shale          | Carnasaw-Pirum-Clebit  |
| <b>12</b>   | Shale          | Carnasaw-Pirum-Clebit  |
| <b>13</b>   | Shale          | Carnasaw-Pirum-Clebit  |
| <b>14</b>   | Shale          | Carnasaw-Pirum-Clebit  |
| <b>15a</b>  | Shale          | Carnasaw-Pirum-Clebit  |
| <b>15b</b>  | Shale          | Carnasaw-Pirum-Clebit  |
| <b>16</b>   | Shale          | Carnasaw-Pirum-Clebit  |
| <b>17</b>   | Shale          | Carnasaw-Pirum-Clebit  |
| <b>18a</b>  | Shale          | Carnasaw-Pirum-Clebit  |
| <b>18b</b>  | Shale          | Carnasaw-Pirum-Clebit  |
| <b>19</b>   | Shale          | Carnasaw-Townley-Pirum |
| <b>20</b>   | Sandstone      | Carnasaw-Townley-Pirum |
| <b>21</b>   | Sandstone      | Carnasaw-Townley-Pirum |
| <b>22</b>   | Sandstone      | Carnasaw-Townley-Pirum |
| <b>23</b>   | Sandstone      | Carnasaw-Townley-Pirum |
| <b>24</b>   | Sandstone      | Carnasaw-Townley-Pirum |
| <b>25</b>   | Shale          | Carnasaw-Townley-Pirum |
| <b>26</b>   | Shale          | Carnasaw-Townley-Pirum |
| <b>27</b>   | Shale          | Carnasaw-Townley-Pirum |
| <b>28</b>   | Shale          | Carnasaw-Townley-Pirum |
| <b>29</b>   | Shale          | Carnasaw-Townley-Pirum |
| <b>30</b>   | Sandstone      | Clebit-Carnasaw-Pirum  |
| <b>31</b>   | Sandstone      | Clebit-Carnasaw-Pirum  |
| <b>32</b>   | Sandstone      | Clebit-Carnasaw-Pirum  |

| <b>Tree</b> | <b>Geology</b> | <b>Soil - Continued</b> |
|-------------|----------------|-------------------------|
| 33          | Sandstone      | Clebit-Carnasaw-Pirum   |
| 34          | Sandstone      | Clebit-Carnasaw-Pirum   |
| 35          | Sandstone      | Carnasaw-Pirum-Clebit   |
| 36          | Sandstone      | Carnasaw-Pirum-Clebit   |
| 37          | Sandstone      | Ceda gravelly loam      |
| 38          | Shale          | Carnasaw-Pirum-Townley  |
| 39          | Shale          | Carnasaw-Pirum-Townley  |
| 40          | Shale          | Carnasaw-Pirum-Townley  |
| 41          | Shale          | Zafra-Leadvale          |
| 42          | Shale          | Carnasaw-Pirum-Townley  |
| 43          | Shale          | Carnasaw-Townley-Pirum  |

#### Topographic Factors

| <b>Tree</b> | <b>Aspect</b> | <b>Type of Fall</b> | <b>Position on Slope</b> | <b>Slope Angle</b> |
|-------------|---------------|---------------------|--------------------------|--------------------|
| 1           | northeast     | Down                | Ridge                    | x                  |
| 2a          | northeast     | Cross               | Flat                     | 2                  |
| 2b          | southeast     | Cross               | Flat                     | 2                  |
| 3           | north         | Cross               | Ridge                    | 3                  |
| 4           | south         | Up                  | Ridge                    | 12                 |
| 5a          | southeast     | Down                | Top                      | 14                 |
| 5b          | southeast     | Down                | Top                      | 14                 |
| 6           | west          | Down                | Midslope                 | x                  |
| 7           | west          | Down                | Midslope                 | 9                  |
| 8           | north         | Cross               | Midslope                 | 1                  |
| 9           | south         | Down                | Ridge                    | 11                 |
| 10          | southeast     | Cross               | Midslope                 | 4                  |
| 11          | west          | Cross               | Midslope                 | 2.5                |
| 12          | north         | Down                | Midslope                 | 14                 |
| 13          | north         | Down                | Bottom                   | 14                 |
| 14          | south         | Down                | Midslope                 | 15                 |
| 15a         | south         | Down                | Unknown                  | 13                 |
| 15b         | south         | Down                | Unknown                  | 13                 |
| 16          | south         | Down                | Midslope                 | x                  |

**Topographic Factors - Continued**

|            |           |       |          |     |
|------------|-----------|-------|----------|-----|
| <b>17</b>  | south     | Cross | Flat     | 21  |
| <b>18a</b> | south     | Down  | Flat     | 22  |
| <b>18b</b> | south     | Down  | Flat     | 22  |
| <b>19</b>  | southeast | Down  | Flat     | 29  |
| <b>20</b>  | east      | Cross | Flat     | 5   |
| <b>21</b>  | west      | Down  | Ridge    | 16  |
| <b>22</b>  | southeast | Cross | Unknown  | 6   |
| <b>23</b>  | north     | Cross | Bottom   | 17  |
| <b>24</b>  | northeast | Up    | Flat     | 4   |
| <b>25</b>  | north     | Cross | Flat     | 2.5 |
| <b>26</b>  | east      | Cross | Unknown  | 3   |
| <b>27</b>  | east      | Cross | Unknown  | 1   |
| <b>28</b>  | east      | Down  | Flat     | 5   |
| <b>29</b>  | southeast | Cross | Flat     | 3.5 |
| <b>30</b>  | west      | Down  | Top      | 11  |
| <b>31</b>  | west      | Down  | Midslope | 13  |
| <b>32</b>  | north     | Down  | Flat     | 6   |
| <b>33</b>  | north     | Down  | Midslope | 15  |
| <b>34</b>  | southwest | Up    | Flat     | 1.5 |
| <b>35</b>  | north     | Down  | Ridge    | 3   |
| <b>36</b>  | west      | Cross | Unknown  | 2   |
| <b>37</b>  | southwest | Up    | Unknown  | 2   |
| <b>38</b>  | south     | Up    | Flat     | 4   |
| <b>39</b>  | south     | Up    | Midslope | 1   |
| <b>40</b>  | southwest | Up    | Midslope | 9   |
| <b>41</b>  | southwest | Up    | Flat     | 0   |
| <b>42</b>  | east      | Cross | Midslope | 11  |
| <b>43</b>  | southeast | Down  | Midslope | 12  |



## Appendix C

### Rock Creek Tornado Blowdown Area Data

#### Wad Dimensions and Underlying Geology

| Presence | Width | Height | Thickness | Area | Volume | Geology              |
|----------|-------|--------|-----------|------|--------|----------------------|
| 1        | 86    | 120    | 41        | 1.03 | 0.42   | Sandstone            |
| 1        | 216   | 174    | 48        | 3.76 | 1.80   | Sandstone            |
| 0        | 230   | 136    | 56        | 3.13 | 1.75   | Shale                |
| 1        | 156   | 89     | 44        | 1.39 | 0.61   | Shale                |
| 1        | 170   | 133    | 39        | 2.26 | 0.88   | Shale                |
| 1        | 113   | 162    | 34        | 1.83 | 0.62   | Shale                |
| 1        | 157   | 172    | 51        | 2.70 | 1.38   | Shale                |
| 1        | 122   | 127    | 49        | 1.55 | 0.76   | Shale                |
| 1        | 244   | 182    | 52        | 4.44 | 2.31   | Shale                |
| 0        | 310   | 176    | 67        | 5.46 | 3.66   | Shale                |
| 0        | 130   | 173    | 57        | 2.25 | 1.28   | Shale                |
| 0        | 231   | 164    | 53        | 3.79 | 2.01   | Shale and Sandstone  |
| 1        | 115   | 128    | 66        | 1.47 | 0.97   | Sandstone            |
| 1        | 310   | 179    | 71        | 5.55 | 3.94   | Sandstone            |
| 1        | 113   | 126    | 60        | 1.42 | 0.85   | Sandstone            |
| 0        | 126   | 125    | 58        | 1.58 | 0.91   | Shale                |
| 1        | 196   | 95     | 41        | 1.86 | 0.76   | Shale                |
| 1        | 220   | 119    | 30        | 2.62 | 0.79   | Shale                |
| 1        | 117   | 83     | 25        | 0.97 | 0.24   | Shale                |
| 1        | 167   | 133    | 45        | 2.22 | 1.00   | Shale                |
| 1        | 225   | 70     | 40        | 1.58 | 0.63   | Sandstone            |
| 0        | 184   | 41     | 77        | 0.75 | 0.58   | Sandstone and Quartz |
| 1        | 199   | 124    | 32        | 2.47 | 0.79   | Shale                |
| 1        | 280   | 218    | 80        | 6.10 | 4.88   | Shale and Sandstone  |
| 1        | 260   | 162    | 87        | 4.21 | 3.66   | Shale and Sandstone  |
| 1        | 229   | 139    | 66        | 3.18 | 2.10   | Shale                |
| 1        | 167   | 120    | 64        | 2.00 | 1.28   | Shale                |

**Wad Dimensions and Underlying Geology - Continued**

|   |     |     |     |       |      |           |
|---|-----|-----|-----|-------|------|-----------|
| 1 | 166 | 132 | 101 | 2.19  | 2.21 | Sandstone |
| 1 | 180 | 92  | 49  | 1.66  | 0.81 | Shale     |
| 1 | 116 | 133 | 124 | 1.54  | 1.91 | Shale     |
| 1 | 272 | 190 | 70  | 5.17  | 3.62 | Shale     |
| 1 | 230 | 142 | 81  | 3.27  | 2.65 | Shale     |
| 1 | 147 | 161 | 97  | 2.37  | 2.3  | Shale     |
| 1 | 195 | 128 | 71  | 2.5   | 1.77 | Shale     |
| 1 | 214 | 149 | 97  | 3.19  | 3.09 | Shale     |
| 1 | 262 | 210 | 77  | 5.5   | 4.24 | Shale     |
| 1 | 211 | 200 | 157 | 4.22  | 6.63 | Shale     |
| 1 | 243 | 190 | 102 | 4.62  | 4.71 | Shale     |
| 1 | 230 | 224 | 40  | 5.15  | 2.06 | Shale     |
| 1 | 199 | 172 | 42  | 3.42  | 1.44 | Shale     |
| 1 | 252 | 190 | 81  | 4.79  | 3.88 | Shale     |
| 0 | 104 | 50  | 21  | 0.52  | 0.11 | Shale     |
| 1 | 210 | 158 | 54  | 3.32  | 1.79 | Shale     |
| 1 | 296 | 220 | 42  | 6.51  | 2.74 | Shale     |
| 1 | 310 | 380 | 51  | 11.78 | 6.01 | Sandstone |

## Appendix D

### Mena Tornado Blowdown Area Data

#### Rootwad Dimensions

| Tree          | Height | Width | Thickness | Area | Volume |
|---------------|--------|-------|-----------|------|--------|
| <b>MBA001</b> | 170    | 161   | 65        | 2.74 | 1.78   |
| <b>MBA003</b> | 122    | 114   | 44        | 1.39 | 0.61   |
| <b>MBA004</b> | 102    | 159   | 91        | 1.62 | 1.48   |
| <b>MBA005</b> | 233.5  | 166   | 73        | 3.88 | 2.83   |
| <b>MBA006</b> | 52     | 96    | 88        | 0.50 | 0.44   |
| <b>MBA007</b> | 59     | 43    | 101       | 0.25 | 0.26   |
| <b>MBA008</b> | 231    | 127   | 84        | 2.93 | 2.46   |
| <b>MBA009</b> | 181    | 117   | 60        | 2.12 | 1.27   |
| <b>MBA010</b> | 120.5  | 128   | 132.5     | 1.54 | 2.04   |
| <b>MBA011</b> | 150    | 144   | 49        | 2.16 | 1.06   |
| <b>MBA012</b> | 190    | 125   | 171       | 2.38 | 4.06   |
| <b>MBA013</b> | 198    | 167   | 142       | 3.31 | 4.70   |
| <b>MBA014</b> | 182    | 156   | 71        | 2.84 | 2.02   |
| <b>MBA015</b> | 193    | 116   | 188       | 2.24 | 4.21   |
| <b>MBA020</b> | 196    | 177   | 110       | 2.27 | 1.02   |
| <b>MBA021</b> | 151    | 88    | 63        | 0.76 | 0.26   |
| <b>MBA022</b> | 177    | 128   | 45        | 0.39 | 0.17   |
| <b>MBA023</b> | 112    | 68    | 34        | 1.55 | 1.43   |
| <b>MBA024</b> | 64     | 61    | 43        | 1.07 | 0.49   |
| <b>MBA025</b> | 121    | 128   | 92        | 3.24 | 5.38   |
| <b>MBA026</b> | 164    | 65    | 46        | 1.05 | 0.15   |
| <b>MBA027</b> | 300    | 108   | 166       | 0.66 | 0.23   |
| <b>MBA028</b> | 163    | 64.33 | 14        | 1.86 | 1.49   |
| <b>MBA029</b> | 114    | 58    | 35        | 1.97 | 1.16   |
| <b>MBA050</b> | 143    | 130   | 80        | 3.47 | 3.82   |
| <b>MBA051</b> | 148    | 133   | 59        | 1.33 | 0.84   |
| <b>MBB001</b> | 389    | 152   | 50        | 5.91 | 2.96   |
| <b>MBB002</b> | 326    | 129   | 54        | 4.21 | 2.27   |
| <b>MBB003</b> | 125    | 88    | 42        | 1.10 | 0.46   |
| <b>MBB004</b> | 295    | 158   | 49        | 4.66 | 2.28   |

**Rootwad Dimensions - Continued**

|               |     |       |       |      |      |
|---------------|-----|-------|-------|------|------|
| <b>MBB005</b> | 180 | 133   | 70    | 2.39 | 1.68 |
| <b>MBB006</b> | 170 | 146   | 40    | 2.48 | 0.99 |
| <b>MBB007</b> | 115 | 83    | 33    | 0.96 | 0.32 |
| <b>MBB008</b> | 177 | 138   | 21    | 2.44 | 0.51 |
| <b>MBB009</b> | 287 | 131.5 | 74    | 3.77 | 2.79 |
| <b>MBB010</b> | 210 | 110   | 88.33 | 2.31 | 2.04 |
| <b>MBB011</b> | 186 | 82    | 97    | 1.53 | 1.48 |
| <b>MBB013</b> | 121 | 60    | 56    | 1.16 | 0.56 |
| <b>MBB014</b> | 143 | 81    | 48    | 0.34 | 0.22 |
| <b>MBB015</b> | 69  | 40    | 50    | 0.28 | 0.14 |
| <b>MBB016</b> | 87  | 93    | 29    | 0.81 | 0.24 |
| <b>MBB017</b> | 132 | 87    | 35    | 1.15 | 0.4  |
| <b>MBB018</b> | 132 | 86    | 37.5  | 1.14 | 0.43 |
| <b>MBB019</b> | 108 | 63    | 53    | 0.68 | 0.36 |
| <b>MBB020</b> | 121 | 54    | 44    | 0.65 | 0.29 |
| <b>MBB021</b> | 88  | 57.33 | 40    | 0.51 | 0.2  |
| <b>MBB022</b> | 131 | 63.67 | 34    | 0.83 | 0.28 |
| <b>MBB023</b> | 170 | 92    | 33    | 1.56 | 0.52 |
| <b>MBB024</b> | 91  | 75    | 70    | 0.68 | 0.48 |
| <b>MBB025</b> | 101 | 90    | 46    | 0.91 | 0.42 |
| <b>MBB026</b> | 102 | 89    | 49    | 0.91 | 0.45 |

### Topographic Data

| <b>Tree</b>   | <b>Bedrock</b>      | <b>Soil Series</b>    | <b>Aspect</b> | <b>Slope</b> | <b>DBH</b> |
|---------------|---------------------|-----------------------|---------------|--------------|------------|
| <b>MBA001</b> | Shale               | Bengal                | Southwest     | 4.55         | 41.15      |
| <b>MBA003</b> | Alluvium            | Mena                  | South         | 5.02         | 28.96      |
| <b>MBA004</b> | Alluvium            | Mena                  | West          | 3.00         | 50.55      |
| <b>MBA005</b> | Shale               | Mena                  | West          | 2.50         | 53.34      |
| <b>MBA006</b> | Alluvium            | Mena                  | West          | 2.50         | 41.91      |
| <b>MBA007</b> | Alluvium            | Mena                  | West          | 2.50         | 27.43      |
| <b>MBA008</b> | Shale               | Mena                  | West          | 2.24         | 48.26      |
| <b>MBA009</b> | Alluvium            | Mena                  | West          | 1.80         | 26.67      |
| <b>MBA010</b> | Alluvium            | Mena                  | West          | 1.98         | 47.75      |
| <b>MBA011</b> | Alluvium            | Mena                  | Southwest     | 4.99         | 41.91      |
| <b>MBA012</b> | Alluvium            | Mena                  | Southwest     | 7.33         | 51.31      |
| <b>MBA013</b> | Shale               | Octavia               | Southwest     | 7.00         | 60.96      |
| <b>MBA014</b> | Alluvium            | Mena                  | Southwest     | 7.50         | 50.80      |
| <b>MBA015</b> | Alluvium            | Wilberton             | West          | 8.00         | 40.64      |
| <b>MBA020</b> | Alluvium            | Wilberton             | South         | 1.65         | 16.00      |
| <b>MBA021</b> | Alluvium            | Wilberton             | South         | 2.13         | 34.29      |
| <b>MBA022</b> | Alluvium            | Wilberton             | Southwest     | 2.13         | 48.77      |
| <b>MBA023</b> | Alluvium            | Wilberton             | Southeast     | 2.75         | 20.83      |
| <b>MBA024</b> | Alluvium            | Mena                  | Southwest     | 2.75         | 23.37      |
| <b>MBA025</b> | Shale and Sandstone | Unknown               | West          | 4.02         | 22.86      |
| <b>MBA026</b> | Shale               | Bengal                | West          | 2.43         | 29.97      |
| <b>MBA027</b> | Sandstone           | Sallisaw              | South         | 1.35         | 34.54      |
| <b>MBA028</b> | Shale               | Bengal                | South         | 1.65         | 20.32      |
| <b>MBA029</b> | Sandstone           | Sherless              | South         | 2.80         | 20.83      |
| <b>MBA050</b> | Shale and Sandstone | Bengal                | Southeast     | 2.30         | 33.53      |
| <b>MBA051</b> | Alluvium            | Wilberton             | Southeast     | 2.30         | 34.29      |
| <b>MBB001</b> | Shale               | Carnasaw              | South         | 1.65         | 60.96      |
| <b>MBB002</b> | Shale               | Sherless              | South         | 0.57         | 60.45      |
| <b>MBB003</b> | Shale               | Sherless and Carnasaw | South         | 0.57         | 33.53      |
| <b>MBB004</b> | Sandstone           | Unknown               | South         | 0.58         | 45.21      |
| <b>MBB005</b> | Sandstone           | Carnasaw              | South         | 1.12         | 40.13      |

**Topographic Data – Continued**

|               |                     |                         |           |      |       |
|---------------|---------------------|-------------------------|-----------|------|-------|
| <b>MBB006</b> | Shale               | Littlefir               | South     | 1.12 | 34.29 |
| <b>MBB007</b> | Mixture             | Clebit                  | South     | 1.05 | 25.65 |
| <b>MBB008</b> | Shale               | Bonnerdale              | Southeast | 1.05 | 26.42 |
| <b>MBB009</b> | Alluvium            | Bonnerdale              | Southeast | 0.75 | 56.39 |
| <b>MBB010</b> | Shale and Sandstone | Unknown                 | South     | 0.75 | 55.63 |
| <b>MBB011</b> | Shale               | Sallisaw                | South     | 0.58 | 44.7  |
| <b>MBB013</b> | Sandstone           | Sallisaw                | South     | 2.78 | 39.12 |
| <b>MBB014</b> | Sandstone           | Sallisaw                | South     | 2.79 | 31.24 |
| <b>MBB015</b> | Sandstone           | Sallisaw                | South     | 2    | 27.43 |
| <b>MBB016</b> | Sandstone           | Sallisaw                | South     | 2    | 22.61 |
| <b>MBB017</b> | Sandstone           | Sallisaw                | Southeast | 2    | 30.48 |
| <b>MBB018</b> | Sandstone           | Sallisaw                | Southeast | 2    | 24.13 |
| <b>MBB019</b> | Sandstone           | Sallisaw                | Southeast | 2    | 27.69 |
| <b>MBB020</b> | Sandstone           | Sallisaw                | Southeast | 2    | 28.7  |
| <b>MBB021</b> | Sandstone           | Sallisaw                | Southeast | 0.7  | 25.4  |
| <b>MBB022</b> | Sandstone           | Sallisaw                | Southeast | 0.7  | 24.89 |
| <b>MBB023</b> | Unknown             | Unknown                 | South     | 1.64 | 27.43 |
| <b>MBB024</b> | Sandstone           | Sallisaw                | South     | 1.64 | 25.4  |
| <b>MBB025</b> | Sandstone           | Sallisaw                | Southeast | 0.56 | 23.88 |
| <b>MBB026</b> | Shale and Sandstone | Bengal/Bismarck/Nashoba | Southeast | 0.56 | 25.4  |

## Appendix E

### Other Statistical Data

**Table E.1** First round of collinearity testing for the Alum Creek Experimental Forest.

|                    | Collinearity Statistics |        |
|--------------------|-------------------------|--------|
|                    | Tolerance               | VIF    |
| Height             | .215                    | 4.644  |
| Width              | .243                    | 4.111  |
| Thickness          | .253                    | 3.946  |
| Area               | .013                    | 77.350 |
| Volume             | .015                    | 67.376 |
| Slope Angle        | .515                    | 1.942  |
| Decay Class        | .490                    | 2.041  |
| Soil Mapping Unit  | .598                    | 1.672  |
| Aspect             | .605                    | 1.653  |
| Tree Type          | .460                    | 2.172  |
| Underlying Geology | .590                    | 1.696  |
| Type of Fall       | .719                    | 1.391  |
| Position on Slope  | .706                    | 1.417  |

**Table E.2** Chi-square testing of the binary logistic regression model for the Alum Creek Experimental Forest.

|        |       | Chi-square | df | Sig. |
|--------|-------|------------|----|------|
| Step 1 | Step  | 4.889      | 1  | .027 |
|        | Block | 4.889      | 1  | .027 |
|        | Model | 4.889      | 1  | .027 |
| Step 2 | Step  | 7.363      | 5  | .195 |
|        | Block | 12.252     | 6  | .057 |
|        | Model | 12.252     | 6  | .057 |
| Step 3 | Step  | 2.881      | 1  | .090 |
|        | Block | 15.133     | 7  | .034 |
|        | Model | 15.133     | 7  | .034 |
| Step 4 | Step  | 14.612     | 6  | .024 |
|        | Block | 29.745     | 13 | .005 |
|        | Model | 29.745     | 13 | .005 |
| Step 5 | Step  | 11.002     | 1  | .001 |
|        | Block | 40.747     | 14 | .000 |
|        | Model | 40.747     | 14 | .000 |

**Table E.3** Model summary for the Alum Creek Experimental Forest.

| Step | -2 Log likelihood | Cox & Snell R Square | Nagelkerke R Square |
|------|-------------------|----------------------|---------------------|
| 1    | 47.368            | .121                 | .162                |
| 2    | 40.006            | .276                 | .369                |
| 3    | 37.124            | .328                 | .440                |
| 4    | 22.513            | .543                 | .727                |
| 5    | 11.51             | .658                 | .880                |



**Table E.4** Forward Stepwise (Conditional) output for the Alum Creek Experimental Forest

**Variables in the Equation**

|        | Logit Coefficient        | Sig.    | Odds Ratio |                 |
|--------|--------------------------|---------|------------|-----------------|
| Step 1 | Slope Angle              | .118    | .043       | 1.125           |
|        | Constant                 | -.785   | .176       | .456            |
| Step 2 | Slope Angle              | .194    | .028       | 1.214           |
|        | <i>Position on Slope</i> |         | .789       |                 |
|        | Bottom Portion           | -1.592  | .395       | .203            |
|        | Flat Area                | .976    | .372       | 2.654           |
|        | Midslope                 | -.097   | .931       | .907            |
|        | Ridge                    | .665    | .666       | 1.944           |
|        | Top Portion              | -22.243 | .999       | .000            |
|        | Constant                 | -1.414  | .151       | .243            |
| Step 3 | Slope Angle              | .226    | .017       | 1.253           |
|        | Sandstone                | 1.483   | .107       | 4.405           |
|        | <i>Position on Slope</i> |         | .779       |                 |
|        | Bottom Portion           | -1.917  | .345       | .147            |
|        | Flat Area                | 1.170   | .310       | 3.221           |
|        | Midslope                 | .036    | .975       | 1.036           |
|        | Ridge                    | -.181   | .912       | .834            |
|        | Top Portion              | -23.224 | .999       | .000            |
|        | Constant                 | -2.324  | .054       | .098            |
| Step 4 | Slope Angle              | .306    | .032       | 1.358           |
|        | Aspect                   |         | .639       |                 |
|        | East                     | -19.937 | .999       | .000            |
|        | North                    | -24.230 | .999       | .000            |
|        | Northeast                | -3.197  | 1.000      | .041            |
|        | South                    | -20.711 | .999       | .000            |
|        | Southeast                | -23.450 | .999       | .000            |
|        | Southwest                | -23.095 | .999       | .000            |
|        | Sandstone                | 3.097   | .046       | 22.123          |
|        | <i>Position on Slope</i> |         | .720       |                 |
|        | Bottom Portion           | .488    | .870       | 1.628           |
|        | Flat Area                | 2.629   | .103       | 13.857          |
|        | Midslope                 | 1.238   | .424       | 3.449           |
|        | Ridge                    | .074    | .982       | 1.077           |
|        | Top Portion              | -44.050 | .999       | .000            |
|        | Constant                 | 17.450  | .999       | 37875245.625    |
| Step 5 | Slope Angle              | .520    | .066       | 1.683           |
|        | DecayClass               | 6.630   | .100       | 757.798         |
|        | Aspect                   |         | .813       |                 |
|        | East                     | -29.685 | .998       | .000            |
|        | North                    | -55.535 | .996       | .000            |
|        | Northeast                | -43.284 | .999       | .000            |
|        | South                    | -48.247 | .997       | .000            |
|        | Southeast                | -55.971 | .996       | .000            |
|        | Southwest                | -50.457 | .997       | .000            |
|        | Sandstone                | 11.849  | .077       | 139983.315      |
|        | <i>Position on Slope</i> |         | .744       |                 |
|        | Bottom Portion           | 19.130  | .858       | 203344642.677   |
|        | Flat Area                | 24.826  | .118       | 60482448846.677 |
|        | Midslope                 | 10.305  | .228       | 29878.934       |
|        | Ridge                    | .465    | .936       | 1.591           |
|        | Top Portion              | -83.237 | .997       | .000            |
|        | Constant                 | 5.839   | 11665.068  | 1.000           |

**Table E.5** First round of collinearity testing for the Rock Creek Tornado Blowdown.

|                    | Collinearity |        |
|--------------------|--------------|--------|
|                    | Tolerance    | VIF    |
| DBH                | .321         | 3.113  |
| Width              | .104         | 9.632  |
| Height             | .051         | 19.750 |
| Thickness          | .140         | 7.160  |
| Area               | .018         | 54.214 |
| Volume             | .055         | 18.093 |
| Underlying Geology | .842         | 1.187  |

**Table E.6** Chi-square testing of the binary logistic regression model for the Rock Creek Tornado Blowdown area.

|        |       | Chi-square | df | Sig. |
|--------|-------|------------|----|------|
| Step 1 | Step  | 6.092      | 1  | .014 |
|        | Block | 6.092      | 1  | .014 |
|        | Model | 6.092      | 1  | .014 |
| Step 2 | Step  | 3.650      | 2  | .161 |
|        | Block | 9.742      | 3  | .021 |
|        | Model | 9.742      | 3  | .021 |
| Step 3 | Step  | 2.827      | 1  | .093 |
|        | Block | 12.569     | 4  | .014 |
|        | Model | 12.569     | 4  | .014 |

**Table E.7** Model Summary for the Rock Creek Tornado Blowdown.

| Step | -2 Log likelihood | Cox & Snell R Square | Nagelkerke R Square |
|------|-------------------|----------------------|---------------------|
| 1    | 32.808            | .127                 | .219                |
| 2    | 29.158            | .195                 | .336                |
| 3    | 26.331            | .244                 | .421                |

**Table E.8** Forward Stepwise (Conditional) output for the Rock Creek Tornado Blowdown area.

|        |                           | Logit Coefficient | Sig. | Odds Ratio |
|--------|---------------------------|-------------------|------|------------|
| Step 1 | DBH                       | .162              | .039 | 1.176      |
|        | Constant                  | -3.374            | .149 | .034       |
| Step 2 | DBH                       | .224              | .017 | 1.251      |
|        | <i>Underlying Geology</i> |                   | .171 |            |
|        | Sandstone                 | 4.010             | .070 | 55.125     |
|        | Shale                     | 3.528             | .074 | 34.049     |
|        | Constant                  | -8.576            | .035 | .000       |
| Step 3 | DBH                       | .391              | .017 | 1.479      |
|        | <i>Underlying Geology</i> |                   | .098 |            |
|        | Sandstone                 | 5.879             | .035 | 357.463    |
|        | Shale                     | 4.451             | .042 | 85.710     |
|        | Thickness                 | -.052             | .109 | .949       |
|        | Constant                  | -11.577           | .020 | .000       |

**Table E.9** First round of collinearity testing for the Mena Tornado Blowdown.

|                    | Collinearity Statistics |        |
|--------------------|-------------------------|--------|
|                    | Tolerance               | VIF    |
| Slope Angle        | .484                    | 2.066  |
| DBH                | .453                    | 2.208  |
| Width              | .197                    | 5.084  |
| Height             | .371                    | 2.696  |
| Thickness          | .265                    | 3.770  |
| Area               | .073                    | 13.723 |
| Volume             | .106                    | 9.428  |
| Underlying Geology | .592                    | 1.689  |
| Soil Mapping Unit  | .780                    | 1.282  |
| Aspect             | .571                    | 1.750  |

**Table E.10** Chi-square testing of the binary logistic regression model for the Mena Tornado Blowdown.

|        |       | Chi-square | df | Sig. |
|--------|-------|------------|----|------|
| Step 1 | Step  | 33.836     | 5  | .000 |
|        | Block | 33.836     | 5  | .000 |
|        | Model | 33.836     | 5  | .000 |
| Step 2 | Step  | 19.025     | 10 | .040 |
|        | Block | 52.860     | 15 | .000 |
|        | Model | 52.860     | 15 | .000 |

**Table E.11** Model summary for the Mena Tornado Blowdown.

| Step | -2 Log likelihood | Cox & Snell R Square | Nagelkerke R Square |
|------|-------------------|----------------------|---------------------|
| 1    | 36.689            | .485                 | .647                |
| 2    | 17.664            | .645                 | .861                |

**Table E.12** Forward Stepwise (Conditional) output for the Mena Tornado Blowdown.

|                                  | Logit Coefficient | Sig.  | Odds Ratio             |
|----------------------------------|-------------------|-------|------------------------|
| Step 1 <i>Underlying Geology</i> |                   | .388  |                        |
| Alluvium                         | -23.218           | 1.000 | .000                   |
| Mixture                          | .000              | 1.000 | 1.000                  |
| Sandstone                        | -21.991           | 1.000 | .000                   |
| Shale                            | .000              | 1.000 | 1.000                  |
| Sandstone and Shale              | -20.104           | 1.000 | .000                   |
| Constant                         | 21.203            | 1.000 | 1615476537.305         |
| Step 2 <i>Underlying Geology</i> |                   | 1.000 |                        |
| Alluvium                         | -3.273            | 1.000 | .038                   |
| Mixture                          | 39.132            | 1.000 | 98845516734319100.000  |
| Sandstone                        | -1.323            | 1.000 | .266                   |
| Shale                            | 19.442            | 1.000 | 277705021.587          |
| Sandstone and Shale              | 16.717            | 1.000 | 18201097.996           |
| <i>Soil Mapping Unit</i>         |                   | 1.000 |                        |
| Bengal                           | 21.092            | 1.000 | 1446476641.122         |
| Bengal/Bismarck/Nashoba          | -19.990           | 1.000 | .000                   |
| Bonnerdale                       | 41.295            | .999  | 859286504221049000.000 |
| Carnasaw                         | 39.489            | .999  | 141158779674581000.000 |
| Clebit                           | 19.690            | 1.000 | 355937088.100          |
| Littlefir                        | 19.006            | .999  | 179497215.738          |
| Mena                             | 19.690            | 1.000 | 355937088.100          |
| Octavia                          | 17.548            | 1.000 | 41767818.778           |
| Sallisaw                         | 39.001            | .999  | 86659645020933500.000  |
| Sherless                         | 39.132            | .999  | 98845470925528900.000  |
| Constant                         | -17.929           | 1.000 | .000                   |

## Bibliography

*Maps throughout this thesis were created using ArcGIS® software by Esri. ArcGIS® and ArcMap™ are the intellectual property of Esri and are used herein under license. Copyright © Esri. All rights reserved. For more information about Esri® software, please visit [www.esri.com](http://www.esri.com).*

*Base imagery citations can be found at the bottom of each map created.*

Adams, M.B., Loughry, L., Plaughter, L., 2004. Experimental Forests and Ranges of the USDA Forest Service. Gen. Tech. Rep. NE-321. Newtown Square, PA: U.S. Department of Agriculture, Forest Service, Northeastern Research Station.

Anderson, J.A., 1982. Logistic discrimination, In: P.R. Krishnaiah and L.N. Kanal, (Ed.s), Handbook of Statistics, Elsevier, Volume 2, pp. 169-191.

Arkansas Geological Survey, 2007. Stratigraphic Summary of the Arkansas Valley and Ouachita Mountains. [http://www.geology.ar.gov/geology/strat\\_arvalley\\_ouachitamtn.htm](http://www.geology.ar.gov/geology/strat_arvalley_ouachitamtn.htm) Accessed August 17, 2011.

Arthur, M., Paratley, R., and Blankenship, B. 1998. Single and repeated fires affect survival and regeneration of woody and herbaceous species in an oak-pine forest. Journal of the Torrey Botanical Society, 125, 3.

Ayalew, L. and Yamagishi, H. 2005 The application of GIS-based logistic regression or landslide susceptibility mapping in the Kakuda-Yahiko Mountains, Central Japan. Geomorphology, 65, 15-31.

Bellingham, P.J., Tanner, E.V.J., 2000. The influence of topography on tree growth, mortality, and recruitment in a tropical montane forest. Biotropica, 32, 378-384.

Binkley, D., Giardina, C., 1998. Why do tree species affect soils? The Warp and Woof of tree-soil interactions. Biogeochemistry, 42, 89-106.

Boettcher, S.E., Kalisz, P.J., 1990. Single-Tree Influence on Soil Properties in the Mountains of Eastern Kentucky. Ecology, 71, 4, 1365-1372.

Bragg, D.C., Shelton, M.G., and Zeide, B., 2003. Impacts of ice storms on forests in the southern United States. Forest Ecology and Management, 186, 99-123.

Burns, R.M. and Honkala, B.H., 1990. Agriculture Handbook 654: Silvics of North America. Washington, DC: United States Department of Agriculture Forestry Service. [http://www.na.fs.fed.us/spfo/pubs/silvics\\_manual/table\\_of\\_contents.htm](http://www.na.fs.fed.us/spfo/pubs/silvics_manual/table_of_contents.htm) Accessed December 21, 2011.

Busing, R.T. 2005. Tree mortality, canopy turnover, and woody detritus in old cove forests of the Southern Appalachians. Ecology, 86, 73-84.

- Carbin, G., 2011. Severe Weather Database Files (1990-Mena). Norman, Oklahoma: United States. NOAA's National Weather Service.  
<http://www.spc.noaa.gov/wcm/index.html#data> Assessed December 21, 2011.
- Crook, M.J. and Ennos, A.R. 1996. The anchorage mechanics of deep rooted larch, *Larix europea* x *L japonica*. *Journal of Experimental Botany*, 47, 303, 1509-1517.
- Dahal, R.K., Hasegawa, S., Nonomura, A., Yamanaka, M., Dhakal, S., Paudyal, P. 2008. Predictive modeling of rainfall-induced landslide hazard in the Lesser Himalaya of Nepal based on weights-of-evidence. *Geomorphology*, 102, 496-510.
- Dai, F.C. and Lee, C.F. 2002. Landslide characteristics and slope instability modeling using GIS, Lantau Island, Hong Kong. *Geomorphology*, 42, 213-228.
- Dupuy, L.; Fourcaud, T.; and Stokes, A., 2005. A numerical investigation into the influence of soil type and root architecture on tree anchorage. *Plant and Soil*, 278, 119–134.
- Ennos, A.R., 1997. Wind as an ecological factor. *Trends in Ecology and Evolution*, 12: 108-111.
- Esri. 2012. How solar radiation is calculated. Assessed on October 20, 2012.  
[http://help.arcgis.com/en/arcgisdesktop/10.0/help/index.html#/How\\_solar\\_radiation\\_is\\_calculated/009z000000tm000000/](http://help.arcgis.com/en/arcgisdesktop/10.0/help/index.html#/How_solar_radiation_is_calculated/009z000000tm000000/)
- Falinski, J.B., 1978. Uprooted trees, their distribution and influence on the primeval forest biotope. *Vegetatio*, 38, 175–83.
- Foster, D.R., 1988. Species and stand response to catastrophic wind in central New England, USA. *Journal of Ecology*, 76, 135-151.
- Fourcaud, T.; Nan, J.; Zhang, ZQ.; and Stokes, A., 2008. Understanding the Impact of Root Morphology on Overturning Mechanisms: A Modelling Approach. *Annals of Botany*, 101, 1267–1280.
- Gabet, E.J. and Mudd, S.M., 2010. Bedrock erosion by root fracture and treethrow: A coupled biogeomorphic model to explore the humped soil production function and the persistence of hillslope soils. *Journal of Geophysical Research-Earth Surface*, 115, 1-14.
- Gabet, E.J., Reichman, O.J., Seabloom, E.W., 2003. The Effects of Bioturbation on Soil Processes and Sediment Transport. *Annual Review of Earth and Planet Sciences*, 31, 249-273.
- Gallaway J., Martin Y., and Johnson E., Mena. Sediment transport due to tree root throw: integrating tree population dynamics, wildfire and geomorphic response. *Earth Surface Processes and Landforms*, 34, 1255-1269.
- Genet, M., Stokes, A., Fourcaud, T. Norris, J.E., 2010. The influence of plant diversity on slope stability in a moist evergreen deciduous forest. *Ecological Engineering*, 36, 3, 265-275.

- Gholz, H.L., Wedin, D.A., Smitherman, S.M., Harmon, M.E., Partons, W.J., 2000. Long-term dynamics of pine and hardwood litter in contrasting environments: toward a global model of decomposition. *Global Change Biology*, 6, 751-765.
- Gilbert, N., Johnson, S., Gleeson, S., Blankenship, B., and Arthur, M. 2003. Effects of prescribed fire on physiology and growth of *Acer rubrum* and *Quercus* spp. Seedlings in an oak-pine forest on the Cumberland Plateau, KY. *Journal of the Torrey Botanical Society*, 130, 4, 253-264.
- Gritzner, M.L., Marcus, W.A., Aspinall, R. Custer, S.G. 2010. Assessing landslide potential using GIS, soil wetness modeling and topographic attributes, Payette River Idaho. *Geomorphology*, 371, 149-165.
- Gross, K.L., Maruca, D., Pregitzer, K.S., 1992. Seedling Growth and Root Morphology of Plants with Different Life-Histories. *New Phytologist*, 120, 4, 535-542.
- Haley, B.R., Stone, C.G., Viele, G.W., 1979. A Guidebook to the Second Geological Excursion on Lake Ouachita. State of Arkansas, Arkansas Geological Commission.
- Haley, G.J. and Woods, J.A., 1979. SOIL SURVEY OF Saline County, Arkansas. Soil Conservation Service, USDA
- Hart, J.L., Grissino-Myer, H.D., Mena. Gap-scale disturbance processes in secondary hardwood stands on the Cumberland Plateau, Tennessee, USA. *Plant Ecology*, 201, 131-146.
- Hedrick, L.; Bukenhofer, GA; Montague, WG; Pell, WF; and Guldin, JM., 2007. Shortleaf pine-bluestem restoration in the Ouachita National Forest. In: Kabrick, John M.; Dey, Daniel C.; Gwaze, David, (Ed,s) Shortleaf pine restoration and ecology in the Ozarks: proceedings of a symposium; Rock Creek November 7-9; Springfield, MO. General Technical Report NRS-P-15. Newtown Square, PA: U.S. Department of Agriculture, Forest Service, Northern Research Station, 206-213.
- Heimsath, A.M., Dietrich, W.E., Nishiizumi, K., Finkel, R.C., 1997. The soil production function and landscape equilibrium. *Nature*, 388, 358-361.
- Iowa State University of Science and Technology. 2012. Custom Wind Rose for the Mount Ida – Automated Surface Observing System Network – Federal Aviation Administration. Accessed on October 18, 2012. [http://mesonet.agron.iastate.edu/sites/site.php?station=MWT&network=AR\\_ASOS](http://mesonet.agron.iastate.edu/sites/site.php?station=MWT&network=AR_ASOS)
- Jenny, H. 1941. *Factors of Soil Formation: A System of Quantitative Pedology*. Dover Publications, New York, NY.
- Kelleman, M., Tackaberry, R., 1993. Disturbance and tree species coexistence in tropical riparian forest fragments. *Global Ecology and Biogeography Letters*, 3, 1-9.
- King, J. E., 2008. Binary logistic regression. In J. W. Osborne (Ed.s), *Best practices in quantitative methods*. Sage Publications, Thousand Oaks, CA, 358–384.



- Lafon, C.W. and Speer, J.H., 2002. Using dendrochronology to identify major ice storm events in oak forests of southwestern Virginia. *Climate Research*, 20, 41-54.
- Lafon, C.W., 2004. Ice-storm disturbance and long-term forest dynamics in the Adirondack Mountains. *Journal of Vegetation Science*, 15, 267-276.
- Lenart, M.T., Falk, D.A., Scatena, F.N., Osterkamp, W.R., 2010. Estimating soil turnover rate from tree uprooting during hurricanes in Puerto Rico. *Forest Ecology and Management*, 259, 1076–1084.
- Lorimer, C.G., White, A.S., 2003. Scale and frequency of natural disturbances in the northeastern US: Implications for early successional forest habitats and regional age distributions. *Forest Ecology and Management*, 185, 41-64.
- Lorimer, C.G., White, A.S., 2003. Scale and frequency of natural disturbances in the northeastern US: Implications for early successional forest habitats and regional age distributions. *Forest Ecology and Management*, 185, 41-64.
- Lutz, H.J., 1960. Movement of rocks by uprooting of forest trees. *American Journal of Science*, 258, 752-756.
- Lutz, H.J., and Griswold, F.S., 1939. The influence of tree roots on soil morphology. *American Journal of Science*, 237, 289-400.
- Mayer, H. (1987) Wind-Induced Tree Sways, *Trees*, 1, 195-206
- Mehta, C.R. and Patel, N.R. 2010. IBM SPSS Exact Tests. Assessed online on July 8, 2012 at [http://www.sussex.ac.uk/its/pdfs/SPSS\\_Exact\\_Tests\\_19.pdf](http://www.sussex.ac.uk/its/pdfs/SPSS_Exact_Tests_19.pdf)
- Muller, R.N., 2003. Landscape patterns of change in coarse woody debris accumulation in an old-growth deciduous forest on the Cumberland Plateau, Southeastern Kentucky. *Canadian Journal of Forestry Research*, 33, 763-769.
- National Climate Data Center, 2011. Event Record Details. <http://www4.ncdc.noaa.gov/cgi-win/wwcgi.dll?wwevent~ShowEvent~756147> and <http://www4.ncdc.noaa.gov/cgi-win/wwcgi.dll?wwevent~ShowEvent~756066> Accessed August 18, 2011.
- National Weather Service, 2007. Severe weather on Nov 27 2005 (damage surveys). Date <http://www.srh.noaa.gov/lzk/html/surveys112705yr.htm> Assessed December 21, 2011.
- National Weather Service, Mena. 1971 – 2000 Normals. <http://www.srh.noaa.gov/lzk/clinorms.php?site=003> Accessed August 16, 2011.
- National Weather Service, Mena. The Tornado Outbreak of April 9th, Mena. 2011. [http://www.srh.noaa.gov/shv/events/select.php?date=0409Mena\\_1](http://www.srh.noaa.gov/shv/events/select.php?date=0409Mena_1) Accessed August 18.
- Nicholl, BC. and Ray, D. (1996) Adaptive growth of tree root systems in response to wind action and site conditions. *Tree Physiology* 16, 891-898.

- Nicoll, B.C., Achim, A., Mochan, S., Gardiner, B.A., 2005. Does steep terrain influence tree stability? A field investigation. *Canadian Journal of Forestry Research*, 35, 2360-2367.
- Nicoll, BC.; Gardiner, BA.; Rayner,B.; and Peace, AJ., Rock Creek. Anchorage of coniferous trees in relation to species, soil type, and rooting depth *Canadian Journal of Forestry Research*, 36, 1871–1883.
- Nicoll, BC.; Gardiner, BA.; Rayner,B.; and Peace, AJ., Rock Creek. Anchorage of coniferous trees in relation to species, soil type, and rooting depth. *Canadian Journal of Forestry Research*, 36, 1871–1883.
- Norman, S.A., Schaetzl, R.J., Small, T.W. 1995. Effects of slope angle on mass movement by tree uprooting. *Geomorphology*, 14, 19-27.
- Onega, T.L., Eickmeier, W.G., 1991. Woody detritus inputs and decomposition kinetics in a southern temperate deciduous forest. *Bulletin of the Torrey Botanical Club*, 118, 52-57.
- Ozdemir, A. 2011. Using a binary logistic regression method and GIS for evaluating and mapping the groundwater spring potential in the Sultan Mountains (Aksehir, Turkey). *Journal of Hydrology*, 405, 123-136.
- Peterson, C.J., 2007. Consistent influence of tree diameter and species on damage in nine eastern North America tornado blowdowns. *Forest Ecology and Management*, 250: 96-108.
- Peterson, M.S., Rigby J.K., Hintze, L.F., 1973. *Historical geology of North America*. Dubuque, Iowa, W.C. Brown Co.
- Phillips J.D., Marion D.A., 2004. Pedological memory in forest soil development. *Forest Ecology and Management*, 188, 363-380.
- Phillips, J.D. 2006. Evolutionary geomorphology: thresholds and nonlinearity in landform response to environmental change. *Hydrology and Earth Systems Science*, 10, 731-742.
- Phillips, J.D., Luckow, K., Marion, D.A., and Adams, K.R., 2005. Rock fragment distribution and regolith evolution in the Ouachita Mountains, Arkansas, USA. *Earth Surface Processes and Landforms*, 30, 429-442.
- Phillips, J.D., Marion, D.A., 2005. Biomechanical effects, lithological variations, and local pedodiversity in some forest soils of Arkansas. *Geoderma*, 124, 73–89.
- Phillips, J.D., Marion, D.A., Rock Creek. 2006. Biomechanical effects of trees on soil and regolith: beyond treethrow. *Annals of the Association of American Geographers*, 96, 2, 233-247.

- Phillips, J.D., Marion, D.A., Turkington, A.V. 2008a. Pedologic and Geomorphic Impacts Of a Tornado Blowdown Event In a Mixed Pine-Hardwood Forest. *Catena*, 75, 278-287.
- Phillips, J.D., Turkington, A.V., Marion, D.A., 2008b. Weathering and vegetation effects in early stages of soil formation. *Catena*, 72, 21-28.
- Rentch, J.S., 2010. Relationship between treefall direction, slope-aspect, and wind in eight old-growth oak stands in the Central Hardwood Forest, USA. *Journal of the Torrey Botanical Society*, 137, 391-400.
- Richards, H.G., 1953. *Record of the Rocks: The Geological Story of Eastern North America*. New York, Ronald Press Co.
- Robert, A., 2003. Simulation of the effect of topography and tree falls on stand dynamics and stand structure in tropical forests. *Ecological Modeling*, 167, 287-303.
- Roering, J.J., Marshall, J., Booth, A.M., Mort, M., Qusheng, J., 2010. Evidence for biotic controls on topography and soil production. *Earth and Planetary Science Letters*, 298, 183-190.
- Ruel, J.C., 2000. Factors influencing windthrow in balsam fir forests: From landscape studies to individual tree studies. *Forest Ecology and Management*, 135, 169-178.
- Šamonil, P., Král, K., Hort, L. 2010. The role of tree uprooting in soil formation: A critical literature review. *Geoderma*, 157, 65-79.
- Schaetzl, R.J., Burns, S.F., Johnson, D.L, Small, T.W., 1989a. Tree uprooting: Review of impacts on forest ecology. *Vegetatio*, 79, 165-176.
- Schaetzl, R.J., Follmer, L.R., 1990. Longevity of treethrow microtopography: Implications for mass wasting. *Geomorphology*, 3, 113-123.
- Schaetzl, R.J., Johnson, D.L., Burns, S.F., Small, T.W., 1989b. Tree uprooting: Review of terminology, process, and environmental implications. *Canadian Journal of Forestry Research*, 19, 1-11.
- Sellier, D., Fourcaud, T., Lac, P., 2005. A finite element model for investigating effects of aerial architecture on tree oscillations. *Tree Physiology*, 26, 799–806.
- Shure, D.J., Phillips, D.L., Bostick, P.E., Rock Creek. Gap size and succession in cutover southern Appalachian forests: An 18 year study of vegetation dynamics. *Plant Ecology*, 185, 299-318.
- Small, T.W., Schaetzl, R.J., Brixie, J.M., 1990. Redistribution and mixing of soil gravels by tree uprooting. *Professional Geographer*, 42, 4, 445-457.
- Soil Survey Staff, Natural Resources Conservation Service, United States Department of Agriculture. Soil Survey Geographic (SSURGO) Database for [Arkansas]. <http://soildatamart.nrcs.usda.gov> . Accessed September, 2011.

Soil Survey Staff. Natural Resources Conservation Service, United States Department of Agriculture. 1982. Web Soil Survey of Perry County, Arkansas. <http://soildatamart.nrcs.usda.gov/manuscripts/AR105/0/Perry.pdf> Assessed September 29, 2011.

Soil Survey Staff. Natural Resources Conservation Service, United States Department of Agriculture, 2003. Web Soil Survey of Polk County, Arkansas. <http://soildatamart.nrcs.usda.gov/Manuscripts/AR113/0/polkcounty.pdf> Assessed August 19, 2011.

Soil Survey Staff. Natural Resources Conservation Service, United States Department of Agriculture. 1979. Web Soil Survey of Saline County, Arkansas. Web Soil Survey. Assessed September 29, 2011. [http://soils.usda.gov/survey/online\\_surveys/arkansas/AR125/saline.pdf](http://soils.usda.gov/survey/online_surveys/arkansas/AR125/saline.pdf)

Southern Research Station, USDA. 2008. Alum Creek Experimental Forest. <http://www.srs.fs.usda.gov/4159/ACEF.html> Accessed August 18, 2011.

Spetich, M.A., Liechty, H.O., Stanturf, J.A., Marion, D.A., Luckow, K., Meier, C.E., Guldin, J.M., 2002. Coarse woody debris of a preresoration shortleaf pine-bluestem forest. In: Outcalt K. W. (Eds) Proceedings of the 11th Southern Silvicultural Research Conference. General Technical Report SRS-GTR-48. Asheville, NC: USDA Forest Service, Southern Research Station. 615-619.

Stearn, C.W., Carroll, R.L., Clark, T.H., 1979. Geological evolution of North America. New York, Wiley.

Stevens, V., 1997. The ecological role of coarse woody debris: an overview of the ecological importance of CWD in B.C. forests. B.C. Ministry of Forests, Research Branch, Victoria, B.C. Work Paper 30.

Stokes, A., Atger, C., Bengough, A.G., Fourcaud, T., Sidle, R.C., Mena. Desirable plant root traits for protecting natural and engineer slopes against landslides. *Plant and Soil*, 324, 1-30.

Stokes, A., Ball, J., Fitter, A.H., Brain, P., Coutts, M.P., 1996. An Experimental Investigation of the Resistance of Model Root Systems to Uprooting. *Annals of Botany* 78, 415-421.

Stokes, A., Mattheck, C., 1996. Variation of wood strength in tree roots. *Journal of Experimental Botany*, 47, 298, 693-699.

Stout, B.B. 1956. Studies of the root systems of deciduous trees. *Black Rock Forest Bulletin*, 15. Harvard University, Cambridge, MA.

Stueve, K.M., Lafon, C.W., and Isaacs, R.E., 2007. Spatial patterns of ice storm disturbance on a forested landscape in the Appalachian Mountains, Virginia. *Area*, 39, 1, 20-30.

- Sweet S.A., Grace-Martin, K., 1998. Chapter 8: Multivariate Analysis with Logistic Regression In, *Data analysis with SPSS: A First Course in Applied Statistics*. Boston, MA, Allyn & Bacon.  
<http://www.colorado.edu/ibs/pop/jyoung/socy3301/assignments/week11.pdf> Accessed on December 2, 2011 at
- The Nature Conservancy, 2003. Ouachita Mountains Ecoregional Assessment: December 2003. Assessed online August 5, 2012 at  
[http://www.nature.org/ourinitiatives/regions/northamerica/unitedstates/oklahoma/explore/ouachita\\_mts-1.pdf](http://www.nature.org/ourinitiatives/regions/northamerica/unitedstates/oklahoma/explore/ouachita_mts-1.pdf)
- UCLA: Academic Technology Services, Statistical Consulting Group. Annotated SPSS Output: Multinomial Logistic Regression. 2012.  
<http://www.ats.ucla.edu/stat/spss/output/mlogit.htm> Assessed January 10, 2012.
- Ulanova, N.G., 2000. The effects of windthrow on forests at different spatial scales: a review. *Forest Ecology and Management*, 135, 1-3, 155-167.
- United States Department of Agriculture – Forest Service, Northeastern Research Station. 2003. Experimental Forests and ranges of the USDA Forest Service. General Technical Report NE-321 Revised.
- United States Department of Agriculture – Forest Service. 2008. West and Eastern Forest stand data polygon, “FSVegSpR08.” Supplied by Dr. Daniel Marion, USFS Southern Research Station.
- United States Department of Agriculture, 2005. Revised Land and Resource Management Plan: Ouachita National Forest, Arkansas and Oklahoma.  
[http://www.fs.usda.gov/Internet/FSE\\_DOCUMENTS/fsm9\\_039609.pdf](http://www.fs.usda.gov/Internet/FSE_DOCUMENTS/fsm9_039609.pdf) Accessed August 16, 2011.
- United States Geological Survey Staff, United States Geological Survey. 1993. Geologic Map of Arkansas.  
[http://www.geology.ar.gov/sms\\_maps/Geologic%20Map%20of%20Arkansas%201993%20\(34x52\).pdf](http://www.geology.ar.gov/sms_maps/Geologic%20Map%20of%20Arkansas%201993%20(34x52).pdf). Accessed September, 2011.
- Van Den Eeckhaut, M., Vanwalleghem, T., Poesen, J., Govers, G., Verstraeten, G., Vandekerckhove, L. 2006. Prediction of landslide susceptibility using rare events logistic regression: A case-study in the Flemish Ardennes (Belgium). *Geomorphology*, 76, 392-410.
- Warillow, M., and Mou, P., 1999. Ice storm damage to forest tree species in the ridge and valley region of southwestern Virginia. *Journal of the Torrey Botanical Society*, 126, 2, 147-158.
- Webb, S.L., 1989. Windstorm Consequences in Two Forests, Itasca State Park, Minnesota. *Ecology*, 70, 4, 1167-1118.
- Whitsed, R., Corner, R., Cook, S. 2011. A model to predict ordinal suitability using sparse and uncertain data. *Applied Geography*, 32, 401-408.

Wilford, G.E., Wall, J.R.D., 1965. Karst topography in Sarawak. *Journal of Tropical Geography*, 21, 44–70.

Young, T.P., Hubbell, S.P., 1991. Crown asymmetry, treefalls and repeat disturbance of broad-leaved forest gaps. *Ecology*, 72, 1464-1471.

## VITA

### Stephanie Marie Houck

#### Date and Place of Birth

June 3<sup>rd</sup>, 1987  
MacDill Air Force Base, Florida

#### Educational Institutions

University of Kentucky  
Lexington, KY  
Bachelor of Arts in Geography and Classics, minor in History, 2009

#### Professional Positions

|            |   |
|------------|---|
| 2012       | University of Kentucky, College of Agriculture, Biosystems and Agricultural Engineering Department, Technical |
| 2010       | United States Environmental Protection Agency, Program Analyst  |
| 2009, 2011 | Copperhead Road Geosciences, Research Assistant   |

#### Scholastic and Professional Honors

|           |   |
|-----------|---|
| 2010-2012 | Graduate Student Support, Teaching Assistantship, University of Kentucky      |
| 2009      | Graduated Magna Cum Laude, with Departmental Honors in Geography and Classics |
| 2008      | University of Kentucky Undergraduate Research Grant (\$2,000)                 |
| 2008      | Student Skills Development Grant (\$2,000)                                    |
| 2005-2009 | Governor's Scholars Program Presidential Academic Scholarship                 |